Electrokinetic-enhanced migration of solutes for improved bioremediation in heterogeneous granular porous media

Richard T. Gill

In partial fulfilment for the degree of

Doctor of Philosophy

Department of Civil and Structural Engineering

University of Sheffield

January 2016

Abstract

Contaminated land is a global problem. Where it presents an unacceptable risk to receptors such as human health or ecosystems, remediation actions must be taken. Current remediation technologies can be ineffective due to mass transfer limitations. A typical scenario where these limitations control remediation efficacy is a physically heterogeneous aquifer where hydraulic conductivity (K) varies spatially. Under these conditions remediation is limited by solute migration across K boundaries. This thesis couples two remediation technologies, *in situ* bioremediation and electrokinetics (EK), to overcome the mass transfer limitations presented by physically heterogeneous settings. Bioremediation is the transformation of contaminants into less harmful substances by microorganisms; and electrokinetics (EK) is the application of a direct current to initiate certain transport processes independent of K. Where bioremediation is limited due to the influence of physical heterogeneity, EK transport processes could be applied to initiate an additional flux of solutes across K boundaries. This thesis investigates the influence of physical heterogeneity on EK migration of an amendment designed to enhance bioremediation.

The research presented herein advances the current state of knowledge for EK-BIO applications both at the fundamental level and field-scale using laboratory and desk based studies respectively. Laboratory apparatus was designed and built to accommodate physical heterogeneity, electrokinetic transport of solutes and contaminant biodegradation. Broadly, two types of EK experiment were conducted. Firstly, EK amendment migration under abiotic conditions on different arrangements of physical heterogeneity. Secondly, experiments in the same laboratory setup that introduced contaminant and microbial variables. From these experiments a conceptual framework is developed that describes the influence of physical heterogeneity on the EK transport of an amendment. It relates the spatial change in material properties associated with physical

heterogeneity with aspects of EK application, such as the voltage gradient, and observes the implications for amendment transport. For example a layered contrast in material type generated a non-uniform electric field when direct current was applied, this led to non-uniform EK transport of the amendment relative to homogeneous settings. When contaminant and microbial variables were introduced to the experimental setup a greater understanding of EK-BIO applications to physically heterogeneous settings was gained. These experiments highlight and discuss the technical issues applying EK to enhance bioremediation by amendment addition versus contaminant removal by EK induced pore fluid movement.

Desk based studies included a review of EK-BIO literature and a sustainability assessment that considered EK-BIO at the field scale. The review summarises the practical aspects of the technology in applications to natural environments. It notes that numerous limitations exist to EK-BIO applications in these settings but that there are many different implementation methods that can mitigate these effects. The sustainability assessment compares EK-BIO with conventional remediation technologies against specific criteria for a complex site contaminated with BTEX and MTBE. EK-BIO compares well to other technologies however characteristics of the site will determine the potential sustainability benefits of applying EK.

Acknowledgements

There are many people without whom I could not have completed this work. I'd like to extend my wholehearted thanks to:

- My supervisors Steve Thornton, Mike Harbottle and Jonathan Smith for their guidance and encouragement and for giving me the opportunity to work on something so rewarding;
- The funding body, EPSRC and Shell Global Solutions for financial support during the project;
- The technical staff at Kroto, Andrew Fairburn and Gabi Kakonyi for their support in the lab and brightening up the long days;
- The technical staff in the Civil Engineering workshops specifically Paul Blackbourn and Don Jenkins for building the bench-scale rigs and putting up with what must have seemed like endless pestering;
- The Soil and Groundwater team at Shell Global Solutions, Rijswijk for making me feel welcome during the internship;
- My colleagues at the Groundwater Protection and Restoration Group for their good humour, support and friendship;
- My dear friends Mike and Chloë who have been there since day one of my undergraduate degree;
- My parents, Jan and Steve, and brother, Michael for their endless support;
- Finally, Rachel, who has been there for all the ups and downs.

Table of Contents

List of Figures

List of Tables

Nomenclature

T	Absolute temperature	K
ρ_b	Bulk mass density	g/mL
C_i	Concentration of solute, i	g/m^3
I	Current density	$C/s\text{-}m^2$
ε	Dielectric constant	-
J_i^D	Diffusion mass flux	$mg/m^2\text{-}s$
x	Distance	m
D_i^*	Effective diffusion coefficient	m^2/s
σ*	Effective electrical conductivity	S/m
u_i^*	Effective ionic mobility of solute, i	$m^2/V\text{-}s$
ρ*	Effective resistivity	Ω-m
E	Electrical potential	V
J_i^{em}	Electromigration mass flux of solute, i	$mg/m^2\text{-}s$
v_i^{em}	Electromigration velocity of solute, i	m/s
J_i^{eo}	Electroosmosis mass flux of solute, i	$mg/m^2\text{-}s$
v_c^{eo}	Electroosmotic contaminant velocity	m/s
q^{eo}	Electroosmotic flow rate	m^3/s
k_e	Electroosmotic permeability	$m^2/V\text{-}s$
v_w^{eo}	Electroosmotic pore fluid velocity	m/s
u_p^*	Electrophoretic mobility of particle, p	$m^2/V\text{-}s$
v_p	Electrophoretic velocity of particle, p	m/s
F	Faraday constant	C/mol
H	Fluid viscosity	Pa-s

f_{OC}	Fraction of organic carbon	-
K	Hydraulic conductivity	m/s
H	Hydraulic head	m
z	Ion valence of solute, i	-
L	Length of sediment chamber	m
ρ_s	Particle density	g/mL
K_d	Partition coefficient	mL/g
K_{OC}	Partition coefficient onto organic carbon	mL/g
n	Porosity	-
$R_{H+/OH-}$	Rate of H+ or OH- generation	mol/s
R_f	Retardation factor	-
A	Sediment cross-sectional area	m^2
t	Time	s
τ	Tortuosity	-
a	Tube cross-sectional area	m^2
R	Universal gas constant	J/K-mol
v_c	Velocity contaminant	m/s
v_w	Velocity of pore fluid	m/s
ζ	Zeta potential	V

Chapter 1 Thesis Introduction

1.1 Impacts and challenges presented by contaminated land

Contaminated soil and groundwater arising from anthropogenic activities is a global problem. For example, in England and Wales 300,000 hectares (approximately 2% land area) are estimated to have been impacted by industrial activities (Environment Agency, 2005), in the US this figure is estimated at 9.3 million hectares (approximately 1% land area) (US EPA, 2013). The UK regulatory regime considers contaminated land as land where contaminants are present in sufficient quantities to pose an unacceptable level of risk, as defined by Part 2A of the Environmental Protection Act 1990 (DEFRA, 2008). Exposure to contaminated land presents potential risks to a range of receptors including humans, ecosystems and water quality (Environment Agency, 2009). Thus, in order to mitigate or remove this risk, remediation actions are required. The risk-based approach under Part 2A considers source-pathway-receptor linkages that create significant risk on site. These linkages are demonstrated in Figure 1.1 with a BTEX (benzene, toluene, ethylbenzene and xylene) release into the subsurface. In this example there is a potential risk to the receptor because there are complete S-P-R linkages identified, which have the potential to give rise to significant exposure to the receptors. Removing or reducing the risk can be achieved by breaking these linkages. Typically, this involves eliminating the source of contaminants, but can also include intercepting the pathway or changing the behaviour, use or sensitivity of the receptor.

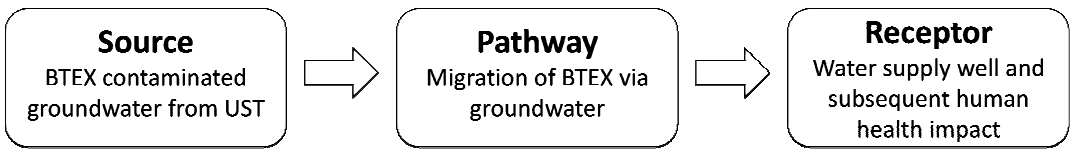

Figure 1.1 Diagram showing the relationship between contaminant sources, pathways and receptors. UST, Underground Storage Tank.

Contaminants can be defined on the basis of chemical structure. Organic contaminants are carbon-based molecules; common examples include: the BTEX group, chlorinated solvents and polyaromatic hydrocarbons. Inorganic contaminants are mineral-based and do not typically contain carbon atoms; common examples include: metals (e.g. lead, mercury or arsenic), nitrate and asbestos. Contaminated land can arise from a wide variety of different land uses that will define the contaminants present on site. For example, coal gasification plants can generate a mixture of both organic and inorganic contaminants (DoE, 1995a); whereas oil refineries will generate petroleum hydrocarbons and fuel additives (DoE, 1995b).

The mobility of contaminants in the subsurface is dependent on their physical and chemical characteristics and the subsurface hydrogeological and geological characteristics. Highly mobile contaminants such as low viscosity fluids and gaseous compounds (e.g. gasoline) will migrate furthest from a point source whereas high viscosity fluids (e.g. tars) will migrate slowly, if at all. Contaminant migration is retarded or attenuated by adsorption onto the surface of clays and organic matter; therefore, migration is highest in high permeability strata, such as sands and gravels with low organic matter content (Andrews et al., 2005). If contaminant migration is limited at or close to the soil surface wind-blown transport will be the dominant transport mechanism. This is typical for metal contaminants that are relatively immobile in soil due poor solubility at neutral pH (Andrews et al., 2005). Gaseous compounds will evaporate unless trapped by an impermeable layer; this characteristic can lead to accumulation within or under building presenting a ventilation or explosion risk. Contaminants that are miscible in water will be subject to groundwater flow and subsequent advection-dispersion transport mechanisms. At high concentrations they will form mobile contaminant plumes primarily in the high hydraulic conductivity zones of the aquifer (Hiscock, 2005).

In scenarios where contamination poses a risk to a receptor, remediation actions are required. Remediation technologies can be broadly defined based on their primary

mechanism whether it be physical, chemical or biological (or a combination) and their application, either *in situ* or *ex situ.* A list of commonly used remediation technologies for a range of different contaminants is shown in Table 1.1. There are several different methods of applying bioremediation, only biopiles and bioattenuation are considered in Table 1.1; additional methods include biostimulation and bioaugmentation (Boopathy, 2000). A common issue for all remediation technologies is mass transfer limitations between the contaminant in the soil or aquifer matrix and the aqueous or vapour phase. For example, pump and treat is a widely used treatment technology, however, it is commonly considered ineffective at completely removing contamination (Khan et al.,

Table 1.1 List of remediation technologies applicable to organic and inorganic contamination in soil and groundwater. Based on Khan et al. (2004).

Treatment	Description	Application
Soil vapour extraction	Involves inserting vertical or horizontal wells and applying a vacuum to volatilise contaminants. Extracted vapours are then treated before release into the atmosphere. Is often coupled with air sparging for contaminated groundwater treatment; it involves pumping air below the water table to enhance volatilisation.	Applied in situ to volatile contaminants such gasoline. Heavier fuels are not easily volatilised. The technology is most effective in high permeability soils that allow sufficient air flow.
Bioremediation (Biopiles)	Involves piling contaminated soil and stimulating microbial activity by aeration, adding nutrients and maintaining moisture content.	Applied ex situ to a range of biodegradable contaminants such as petroleum hydrocarbons, halogenated VOCs and pesticides. Soil type can influence treatment; for example, low permeability soils prevent aeration but retain moisture.
Soil Stabilisation	Involves encapsulating the material in a monolithic solid of high structural integrity. Requires mixing of the contaminated soil with a reagent (e.g. cement)	Applied in situ or ex situ to primarily inorganic contaminants; not as effective for volatile organic contaminants. Requires long-term monitoring to prevent contaminants leaching. Can increase the volume of contaminated soil.
Groundwater pump and treat	Involves inserting extraction wells within the contaminant groundwater plume. Once extracted the contaminants are treated and discharged back to either the aquifer, surface water or treatment plant.	Treatment is conducted ex situ and can be applied to a wide range of dissolved organic and inorganic contaminants, although operates over long timescales. Requires detailed consideration of site hydrogeological characteristics. Ineffective in low permeability sediments.
Bioremediation (bioattenuation)	Also known as natural attenuation, involves using natural biodegradation processes to contain and reduce contaminant concentrations.	In situ treatment can be applied to range of organic contaminants. Requires that the contamination poses no immediate risk to a receptor and that evidence of on-going attenuation from soil and groundwater samples is acquired for the site.
Reactive barriers	Involves inserting a treatment wall into the path of the groundwater flow. Contaminants pass through the barrier and are either trapped or degraded.	In situ treatment applicable to volatile and semi-volatile organics as well as inorganics. Reactive barriers can lose their reactive capacity with time and require replacement. This technique is applicable to shallow contaminant plumes.

2004). This is due to adsorption or permeability issues that limit the mass transfer of the sorbed contaminant into the grounwater (Mackay and Cherry, 1989).

At present the contaminated land sector has to balance and prioritise action on a high number sites versus the significant technical and financial cost of remediating them, hence there is a current debate on the application of sustainable practices for contaminated land remediation (Bardos, 2014). Sustainable remediation is defined by the Sustainable Remediation Forum, UK (SuRF-UK) as "the practice of demonstrating, in terms of environmental, economic and social indicators, that the benefit of undertaking remediation is greater than its impact" (CL:AIRE, 2010). There are two ways that sustainable remediation can be applied at contaminated sites (NICOLE, 2010): 1) at the management level, integrating sustainability assessments into the wider decision making process; and 2) at the site-specific level, by an assessment to compare options against certain sustainability indicators. SuRF-UK has produced a framework which provides a structure for implementing these two approaches within a contaminated site project. This includes both the plan and project design stage and the remediation option appraisal stage.

1.2 Coupling electrokinetics and bioremediation

This thesis focuses on the coupling of two remediation technologies, namely electrokinetics and bioremediation. The latter is a well-established technology used to treat biodegradable contaminants, according to concepts based in general on *ex situ* treatment of excavated material (mainly used in pollutant source removal, e.g. biopiles), and *in situ* treatment of sites with restricted access (where less disturbance is desirable and extended remediation timescales are acceptable, e.g. bioattenuation) (CIRIA, 2002). Bioremediation requires environmental conditions which are favourable for the particular biochemical process and interaction between microorganisms, contaminants, nutrients and electron acceptors/donors (Sturman et al., 1995). The mass transfer issues limiting *in situ* biodegradation are bioavailability: the immediate contact between microorganisms and

substances required for contaminant biodegradation; and, bioaccessibility: the fraction of these components accessible to microorganisms in the environment (Semple et al., 2004). Consequently, biodegradation processes may occur in the subsurface environment, but not at a rate sufficient to mitigate risks at a particular site.

These mass transfer limitations can be overcome by coupling bioremediation with electrokinetics (EK). EK remediation involves passing a direct current (DC) between two electrodes embedded within a porous medium. The electric current passes through pore fluid that acts as an electrolyte, and the interface between the pore fluid and soil substrate (Mitchell, 1993). This induces certain physical transport phenomena that can migrate bacteria, electron acceptors or contaminants (Figure 1.2). These include: (1) electroosmosis - the bulk movement of fluid through pores; (2) electromigration - the movement of ions in solution; and (3) electrophoresis - the movement of charged, suspended particles in pore fluid. Furthermore, electromigration and electroosmosis are

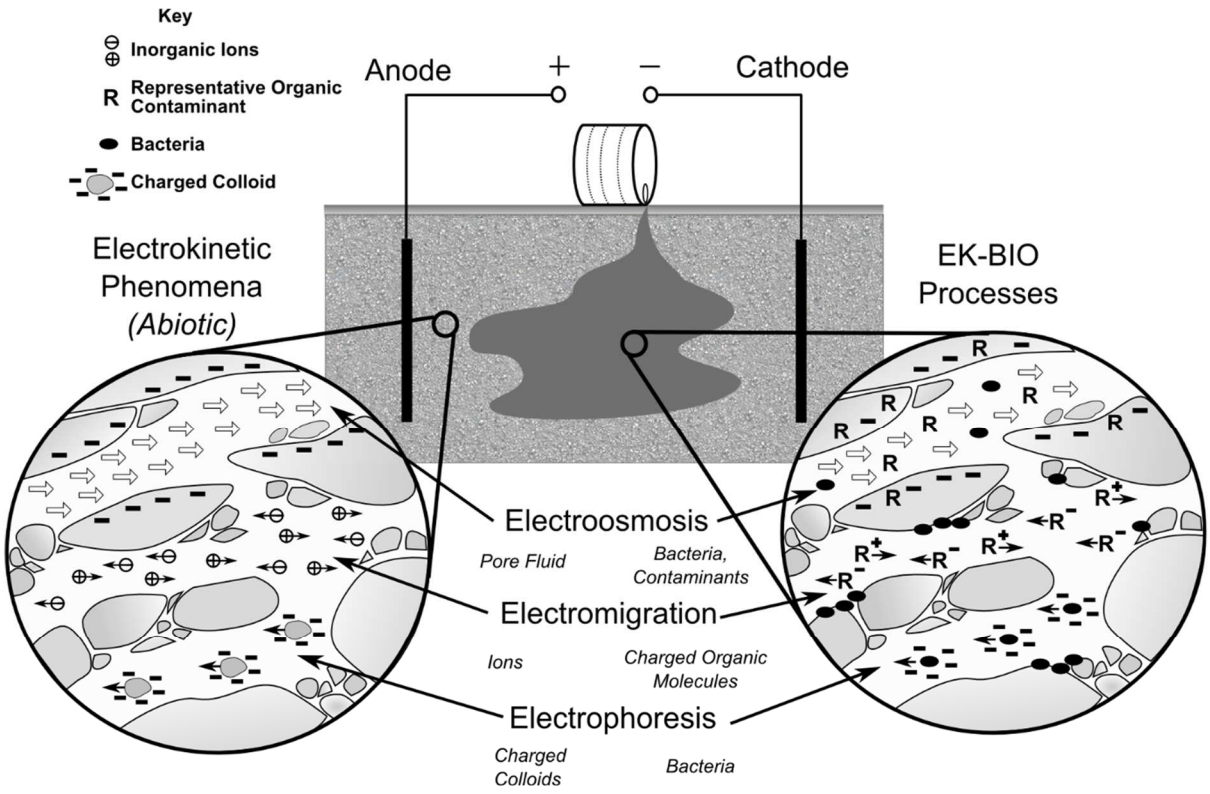

Figure 1.2 Conceptual model of electrokinetic processes which can enhance the biodegradation of dissolved-phase organic substances in the saturated zone under an applied direct current, known as EK-BIO.

independent of hydraulic conductivity and EK can be used to generate mass flux in zones impervious to advective transport (Jones, Lamont-Black et al., 2011). EK transport phenomena have also been coupled with *in situ* chemical oxidation / reduction and permeable reactive barriers; these are discussed in Chapter 2.

1.2.1 Principles of EK remediation

1.2.1.1 Electroosmosis

This phenomenon relates to the movement of pore fluid through a saturated or partially saturated porous media under the application of a direct electric current. It is a function of the interactions between a soil particle with an associated surface charge and ions in the electrolyte. The charge on soil particle surfaces is typically negative due to imperfections in the mineral lattice during formation (Acar et al., 1995), thus there will be an excess of positive ions (cations) in solution to counter the negative charge associated with the soil

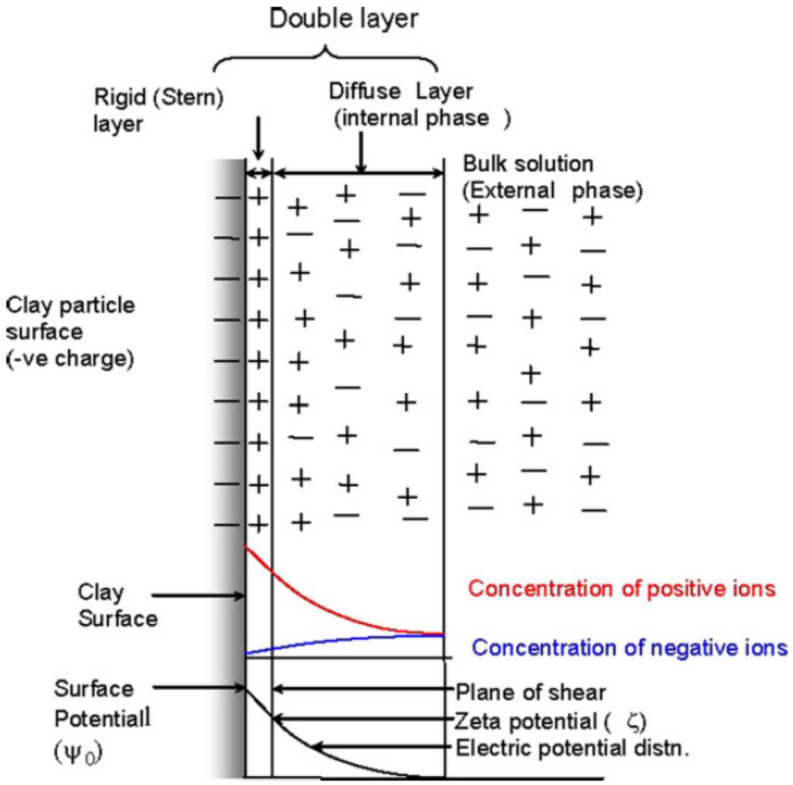

Figure 1.3 Conceptual diagram of the electric double layer at the surface of a negatively charged particle (Jones, Lamont-Black, et al., 2011).

particles. Ions in solution form a boundary between the particle surface and the bulk fluid comprising of an immobile layer of cations (Stern layer) and a mobile diffuse layer where cations are in abundance, this is known as the electric double layer (Figure 1.3). The potential of ions at the shear point between these two layers is known as the zeta potential. Typical values for the zeta potential range from -50 mV to 0 mV (Mitchell, 1993). The magnitude of the sign is highly dependent on the pore fluid chemistry, for example, at low pH the zeta potential can become positive due to the excess of hydrogen ions in the system (Pamukcu, 2009).

The most common description of electroosmotic flow is based on the Helmholtz – Smoluchowski theory, although others have been proposed (Mitchell, 1993; Pamukcu, 2009). It predicts that a liquid filled capillary is analogous to an electrical capacitor where the surface of the capillary is charged and a double layer of counter-charged ions form at the surface/ fluid interface (Figure 1.3). When an electric current is applied, the counter-charged ions in the diffuse layer will migrate towards their oppositely charged electrode along with their mobile shell of water molecules. Movement at the boundary is assumed to drag fluid in the central pore throat by plug flow. This is shown conceptually in Figure 1.4 where a negative charge (and negative zeta potential) on the particle surface indicates that there will be an excess of cations in the diffuse layer and therefore electroosmotic flow

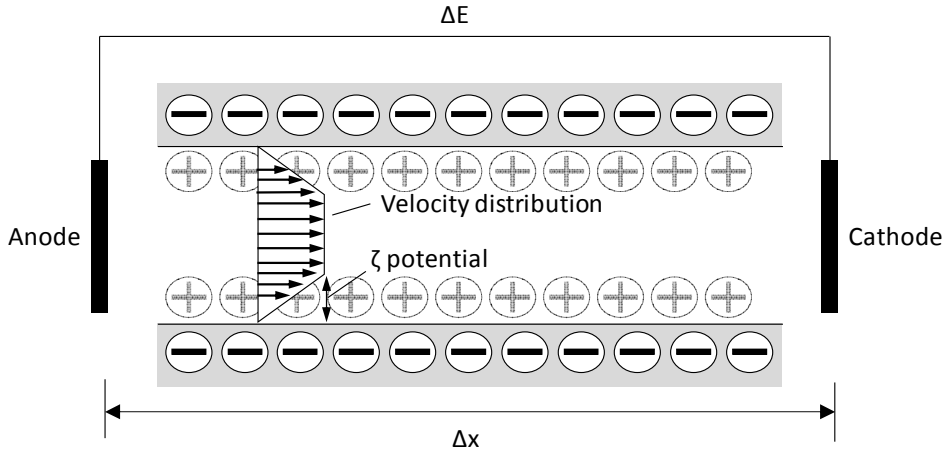

Figure 1.4 Helmholtz-Smoluchowski model for electroosmotic flow in a single capillary (based on Mitchell, 1993).

will be towards the cathode. Moreover, the velocity gradient between the surface of the capillary and the central pore throat is due to friction and the viscosity of the fluid (Mitchell, 1993). Thus, electroosmotic flow rate is a function of the electrical forces generating the movement and the retarding effects of frictional forces at the particle surface. The electroosmotic pore fluid velocity, v_w^{eo} (m/s) is described numerically as (Pamukcu, 2009):

$$v_w^{eo} = -\frac{\varepsilon\,\zeta}{\eta}\,\frac{\Delta E}{\Delta x} = -k_e\frac{\Delta E}{\Delta x}$$

Equation 1.1

where ε dielectric constant (-); ζ, zeta potential (V); η, fluid viscosity (Pa-s); E, electrical potential (V); x, distance (m); k_e, coefficient of electroosmotic permeability (m^2/V-s). The dielectric constant is the ease with which molecules can be polarised and orientated in an electric field (Mitchell, 1993). In systems where the zeta potential is positive, the direction of flow can be reversed from the cathode to the anode due to the abundance of anions in the diffuse layer (Yeung, 2006). The theory also states that k_e is independent of pore size, which is in contrast with hydraulic conductivity, K (m/s) (Page and Page, 2002). Reported values for k_e and K from Mitchell (1993) are presented in Figure 1.5. Values of k_e exist

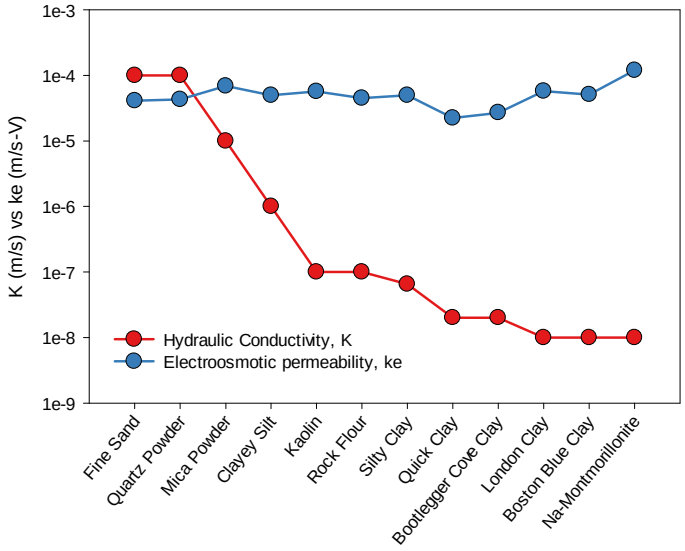

Figure 1.5 Comparison of electroosmotic permeability, k_e and hydraulic conductivity, K (based on Hodges, 2010)

within a narrow range compared with K values that decrease over orders of magnitude in clays and silts. Therefore, an electrical gradient is more effective at initiating fluid flow in fine grained materials compared with a hydraulic gradient.

1.2.1.2 Electromigration

Electromigration is the transport of ions through porous media. Under an electric field, ions move within the electrolyte towards their oppositely charged electrode. The mass flux of an ion, i by electromigration is expressed as (Acar and Alshawabkeh, 1993):

$$J_i^{em} = -u_i^* \, C_i \, \frac{\Delta E}{\Delta x}$$

Equation 1.2

where J_i^{em}, is the electromigration mass flux (mg/m^2-s); u_i^*, effective ionic mobility (m^2/V-s); and C_i, solute concentration (g/m^3). The effective ionic mobility is a function of the material type as expressed by (Acar and Alshawabkeh, 1993):

$$u_i^* = u_i \, n \, \tau$$

Equation 1.3

where n, porosity (-); τ, tortuosity (-); and u_i, ionic mobility (m^2/V-s). Thus, electromigration is a function of the electric field strength, ion properties, porous media properties and concentration of the ion in the electrolyte. It is also influenced by the total concentration ions in the electrolyte that subsequently influences the effective electrical conductivity of the system. This is described by the following relationship where N is the number of ionic species, i in solution (Alshawabkeh and Acar, 1996):

$$\sigma^* = \sum_{i=1}^{N} z_i F u_i^* \, c_i$$

Equation 1.4

where σ*, is effective electrical conductivity (S/m); z_i, ion valence (-); and F, Faraday constant (C/mol). There are numerous examples in the literature where a localised zone

of high electrical conductivity results in a decrease in the electric field and thus decrease in the electromigration mass flux, typically when high concentrations of inorganic amendments are added at the electrodes (Thevanayagam and Rishindran, 1998; Wu et al., 2012a).

1.2.1.3 Electrophoresis

Electrophoresis is the movement of charged suspended colloids in porous media under the application of an electric field. A charged colloid is surrounded by a double layer of charged ions that migrates towards its oppositely charged electrode. Hence, electrophoresis is the counterpart to electroosmosis (Lyklema, 2003). The migration velocity of a particle, p by electrophoresis is defined as (Delgado et al., 2007):

$$v_p = u_p^* \frac{\Delta E}{\Delta x}$$

Equation 1.5

where v_p, electrophoretic velocity (m/s); and u_p*, electrophoretic mobility (m^2/V-s). If the sign of the charge at the particle surface is negative, the electroosmotic pore fluid flux can then be counter to the electrophoretic transport and potentially override and reverse the process. Furthermore, the particle size creates a restriction when applying electrophoresis as the principle electrokinetic transport phenomena to fine grained soils as a narrow pore throat size will occlude the migrating particle. In suitable soils electrophoresis could enhance surfactant application by migration of micelles (Acar and Alshawabkeh, 1993) or migration of charged particle into a soil mass to facilitate remediation such as nano-zero valent iron (Jones, Reynolds et al., 2011).

1.2.1.4 Water electrolysis

A direct current applied to an electrochemical system initiates electrolysis reactions at the electrodes. In electrokinetic systems where water is the principal component of the electrolyte, water electrolysis is the dominant reaction. This is defined as (Kim and Han, 2003):

Anode (oxidising): $2H_2O - 4e^- \rightarrow O_2 + 4H^+$

Equation 1.6

Cathode (reducing): $2H_2O + 2e^- \rightarrow H_2 + 2OH^-$

Equation 1.7

The generation of hydrogen and hydroxyl ions at the electrodes will alter the pH of the system if un-controlled. At the electrodes the pH will reach pH 2 at the anode and pH 12 at the cathode after 12 hours depending on the electrode chamber volume (Lohner et al., 2008a). Within the sediment the hydrogen and hydroxyl ions will migrate towards their oppositely charged electrodes (Paillat et al., 2000) and create a pH front within the sediment (Xu et al., 2010; Harbottle et al., 2009). Furthermore, this gradient will impact the voltage gradient across the sediment. Where the hydrogen and hydroxyl fronts meet, an electrically insulating band of water with a low associated electrical conductivity is formed (Dzenitis, 1997). This corresponds to a localised high voltage gradient (Wada and Umegaki, 2001) that will have implications for the electromigration of solutes.

1.3 Technical problem

The technical problem addressed in this thesis is how to enhance the availability of substances that promote *in situ* biodegradation of contaminants where traditional hydraulic delivery methods fail. The specific scenario is biodegradation of organic contaminants within physically heterogeneous settings where hydraulic conductivity (K) varies. The main limitation on biodegradation in these settings is the mass transfer of substances across high-K/ low-K boundaries; there are two main examples of this: (1) contaminant mass is sequestered within low-K zones, therefore biodegradation is limited in the high-K host matrix based on the rate of back-diffusion; and (2) biodegradation of contaminants within the low-K zone is limited the by mass flux of substances such as electron acceptors across the K boundary. EK coupled with bioremediation is proposed as a solution to overcome these limitations by two concurrent mechanisms. Firstly, by enhancing the flux of

contaminants out the low-K zone by electroosmosis; and secondly by generating a flux of limiting substances such as electron acceptors added as an amendment into the low-K zone by electromigration. The following sections will detail the mass transfer limitations within physically heterogeneous settings and the suitability of EK-BIO for treating them.

1.3.1 Contaminant back-diffusion

The bioavailability of a contaminant in the high-K host matrix of a physically heterogeneous aquifer is controlled by the rate of back-diffusion from the sequestered contaminant mass

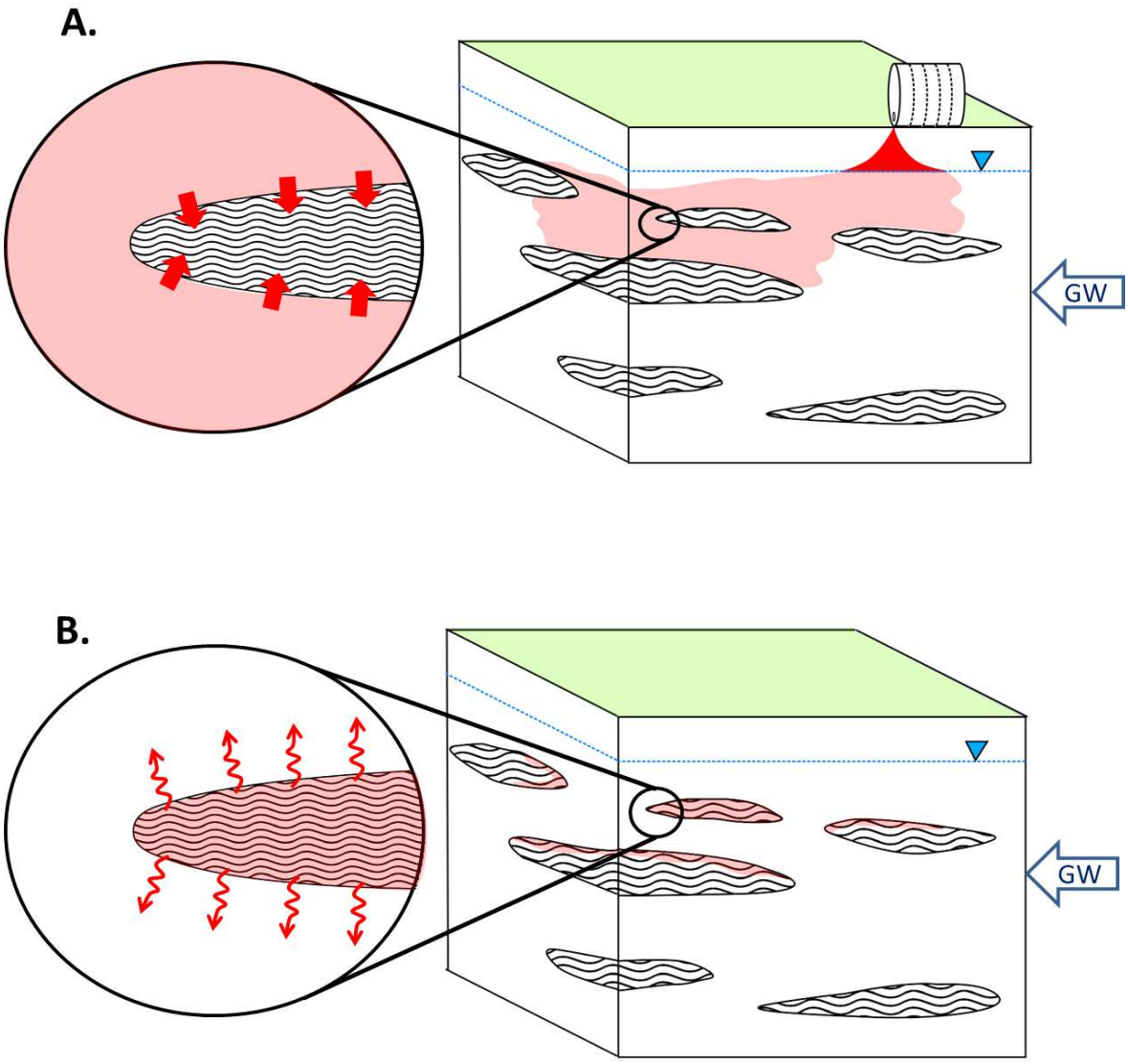

Figure 1.6 Conceptual diagram showing back diffusion from low hydraulic conductivity lenses within a high hydraulic conductivity host material.

in the low-K zone. Back-diffusion is a function of physical heterogeneity. It occurs following contaminant release when a steep concentration gradient exists across the interface between a low-K zone and high-K host matrix. This drives diffusion of contaminants into the low-K zone (Figure 1.6A) (US EPA, 1996). Following the advective transport (removal) of contaminants out of the high-K host matrix the contaminant concentration gradient is then reversed. Contaminants sequestered in the low-K zone will then back-diffuse into the host matrix over long time-scales under a lower concentration gradient (Figure 1.6B). Factors controlling contaminant mass release from low-K zones include the geometry and subsequent surface area of the low-K zone (Chapman et al., 2012) and the concentration profile associated with the initial diffusion into the low-K zone (Yang et al., 2015).

Back-diffusion can cause contaminant rebound which a common management issue at contaminated sites. This relates to the relatively rapid increase in contaminant concentrations following the cessation of remediation activities such as pump and treat

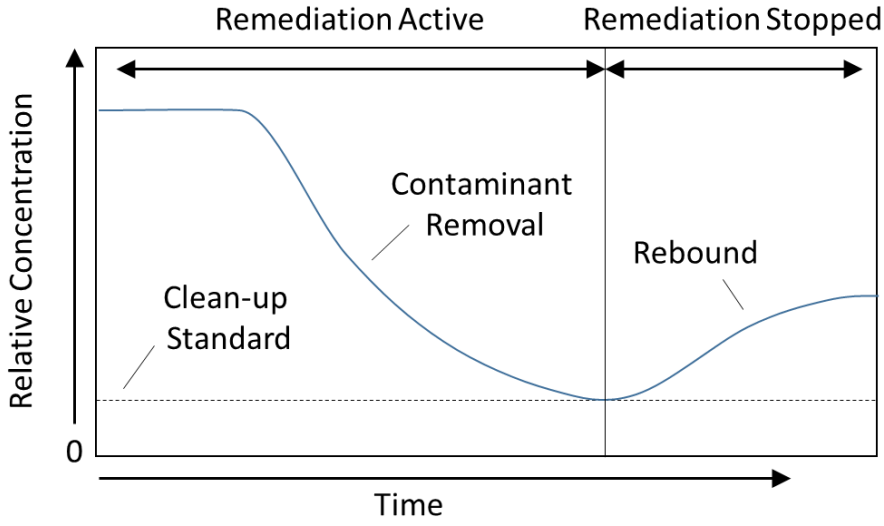

Figure 1.7 Diagram of rebound effect on contaminant concentrations over time in a contaminated aquifer (after Cohen et al., 1994)

(Mackay and Cherry, 1989) or air sparge (Bass et al., 2000). Thus, a rebound event that exceeds the remedial target will prolong remediation efforts (Figure 1.7).

1.3.2 Biodegradation limited by electron acceptor availability

Heterotrophic microorganisms are responsible for the degradation of a wide range of organic contaminants in the subsurface. They generate energy by the oxidation of organic compounds to carbon dioxide. These redox reactions are characterised by the transfer of an electron between an electron donor and electron acceptor. Organic contaminants act as the electron donors and degrade in the process. Electron acceptors are present in the surrounding groundwater and pore fluid and utilised in order of preference depending on the energy yield from the reaction (Carey et al., 2000). The order of preferred electron acceptors is oxygen, nitrate, manganese (IV), iron (III), sulphate and carbon dioxide.

A contaminant mass in soil or groundwater represents an excess of electron donors. Therefore, biodegradation is limited by the availability of electron acceptors. Electron acceptor supply can be limited, especially in oligotrophic aquifer settings and thus leads to contaminant plumes persisting in the environment (Meckenstock et al., 2015). The peripheries of the contaminated zone where a flux of electron acceptors into the contaminant mass exists generates biodegradation. For example, in contaminant plume scenarios the transverse dispersion of electron acceptors into the plume creates a reactive fringe (Thornton et al., 2001; Bauer et al., 2008). In heterogeneous settings where contamination is sequestered within low-K zones mixing is limited due to transport limitation across a high-K / low-K boundary. Where the K contrast is minimal, dispersion is still the dominant mixing process (Song and Seagren, 2008), whereas where there is a significant K contrast (e.g. sand vs clay) diffusion is often the dominant mechanism (Hønning et al., 2007). The naturally occurring mass transfer limitations of electron acceptors into a contaminant mass justifies enhancing the flux using electrokinetics, in certain situations. The selected electron acceptor to act as an amendment in this thesis is nitrate. Electron acceptors are theoretically utilised based on the free energy yielded by the degradation process; the order in which they are used is: oxygen, nitrate, manganese (IV), iron (III) and sulphate (Killham, 1994). Hence, nitrate is the most thermodynamically

favourable, ionic electron acceptor and has been used widely in the EK literature (Thevanayagam and Rishindran, 1998; Lohner et al., 2008a; Tiehm et al., 2010; Xu et al., 2010).

1.3.3 Electrokinetic treatment of physically heterogeneous settings

Back diffusion is likely to extend remediation efforts due to the long timescales associated with diffusive mass transport (Reynolds and Kueper, 2002). Conventional advection based remediation technologies, such as pump and treat, are ineffective in these scenarios because there is minimal flow across high- to low-K boundaries (Song and Seagren, 2008). Thus, remediation technologies applied in these aquifer settings should target the sequestered contaminants in low-K zones. Electrokinetic enhanced bioremediation (EK-BIO) is a good candidate for the following reasons:

- EK transport phenomena have been applied to heterogeneous settings in two capacities: (1) introducing amendments into low-K zones within a high-K host material by electromigration (Reynolds et al., 2008); (2) removing contaminant such as lead and phenanthrene from low-K zones by electroosmotic pore fluid movement (Alshawabkeh et al., 2005; Saichek and Reddy, 2005).

- Bioremediation has been successfully coupled with EK to enhance the degradation of contaminants specifically in low-K soils and sediments (e.g. Luo et al., 2005a; Wick et al., 2004; Xu et al., 2010). This is achieved by several methods, EK-biostimulation, EK-bioaugmentation and EK-attenuation (summarised in Chapter 2). The focus of this thesis is EK-biostimulation, the migration of an amendment to stimulate biodegradation in the contaminated zone. The use of amendments and target contaminants have varied in the literature. For example, lactate (Mao et al., 2012; Wu et al., 2012), nitrate (Tiehm et al., 2010); and nutrient mixes (Xu et al., 2010) have been applied to treat chlorinated solvents, toluene and poly-aromatic hydrocarbons respectively.

1.3.3.1 Electrokinetic theory related to physical heterogeneity

The influence of heterogeneity represented by a spatial change in K on EK phenomena is not covered specifically in the literature. However, the potential effects can be inferred from existing relationships. EK-biostimulation applies electromigration to deliver amendments for enhanced bioremediation. Electromigration is the most effective transport mechanism in an EK-dominated system (Acar and Alshawabkeh, 1993). Theoretically electromigration can be influenced by the type of host material, insofar as this affects the spatial variation in properties of the porous media which control the applied EK phenomena (Equation 1.3). The 1-D electromigration solute mass flux in homogeneous media is given by Equation 1.2 that includes the effective ionic mobility which is analogous to the effective diffusion coefficient:

$$u_i^* = \frac{D_i^* \, z_i \, F}{R \, T}$$

Equation 1.8

where D_i^* is the effective diffusion coefficient (m^2/s); R is the universal gas constant (J/K-mol); and T is absolute temperature (K). The effective solute diffusion coefficient has been shown to decrease with decreasing K due to a decrease in the tortuosity factor associated with the migration path length (Rowe and Badv, 1996). From this relationship effective ionic mobility should also vary between sand, silts and clays, i.e. decreasing with decreasing K. It is also likely that the counter pore fluid flux created by electroosmosis will increase with decreasing K, due to the presence of more fine grained particles with an associated larger surface charge, represented by the zeta potential (ζ). This is based on the relationship between k_e and ζ in Equation 1.1 that can be summarised as (Acar and Alshawabkeh, 1993):

$$k_e = -\frac{\varepsilon \zeta}{\eta} \, n$$

Equation 1.9

For example, electroosmosis is about five times higher in clays than fine-grained sands with hydraulic conductivities of 1 to $2x10^{-8}$ m/s and $3.5x10^{-5}$ m/s respectively (Wu et al., 2007). The electroosmotic flux is generally an order of magnitude lower than electromigration, and therefore electromigration is typically the dominant transport mechanism (Acar and Alshawabkeh, 1993).

Under 1-D physically heterogeneous conditions where the porosity and tortuosity of the material vary and therefore the effective ionic mobility varies, there will be step changes in the electromigration velocity. Moreover, there should also be an associated variation in the voltage gradient. This is based on the relationship between the effective electrical conductivity (Equation 1.4) and the electric current density (Alshawabkeh and Acar, 1996):

$$I = -F \sum_{i=1}^{N} z_i \, D_i^* \, \frac{\Delta C_i}{\Delta x} - \sigma^* \frac{\Delta E}{\Delta x}$$

Equation 1.10

where I is current density (C/s-m^2) and N is the number of ionic species, i in solution. Equation 1.10 can be rearranged to show that the effective electrical conductivity is inversely proportional to the voltage gradient:

$$\frac{\Delta E}{\Delta x} = \frac{F \, \sum_{i=1}^{N} z_i \, D_i^* \, \frac{\Delta C_i}{\Delta x} + \, I}{\sigma^*}$$

Equation 1.11

Hence material type (represented by the spatial change in effective ionic mobility) will have a control on the voltage gradient. Thus, in a physically heterogeneous setting where the concentration of chemical species is uniform, the voltage gradient should increase in material with a low effective ionic mobility relative to material with a high effective ionic mobility. This is in contrast to homogeneous systems where, if the effective ionic mobility and chemical species concentration are uniform, the voltage gradient is also uniform.

1.3.3.2 Electrokinetics as a sustainable remediation technology

EK-BIO has the potential to perform well against sustainable remediation indicators. Although the energy use for EK-BIO is comparable with other techniques, for example 7 – 16 kWh/t for EK-BIO (Fan et al., 2007; Luo et al., 2005b; Suni et al., 2007) compared to 12, 15.5 and 23.5 kWh/t for a cover system, soil washing and landfill option (Harbottle et al., 2008). The benefit is that the principal energy input is electricity (Alshawabkeh et al., 1999; Kim et al., 2014) which has the potential to be generated from low-CO_2 or renewable sources (Jeon et al., 2015; Yuan et al., 2009). In addition, *in situ* bioremediation is often considered a sustainable option, however without enhanced electron acceptor supply (e.g. from EK) it can require operation over long timescales, making it less favourable (Cadotte et al., 2007).

1.4 Research aim and objectives

The research aim is to investigate the influence of physical heterogeneity on the electromigration of amendments for the enhancement of bioremediation of petroleum hydrocarbons in granular porous media. The thesis consists of five research objectives with associated research questions (Figure 1.8). These are stated below. Research Objective 2 does not have an associated research question because it represents the development of laboratory apparatus. Research Objective 3 is addressed with two research questions. A chapter is defined by a research question and the specific

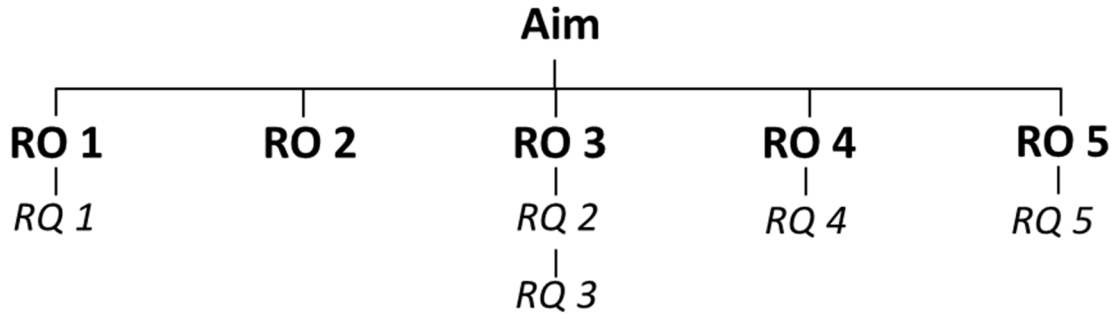

Figure 1.8 Diagram showing thesis structure. RO, research objective; and RQ, research question.

hypotheses evaluated by the work completed therein (with the exception of Research Objective 2).

Research Objective 1: Summarise the practical aspects of EK-BIO applications.

There are a number of literature reviews on the subject of EK and EK-BIO (e.g. (Acar and Alshawabkeh, 1993; Page and Page, 2002; Wick et al., 2007)), however very few focus on the practical applications of the technology. For example, there are currently no reviews that consider both the micro-scale influence of EK on bioavailability and the macro-scale applications such as EK-biostimulation. Furthermore, there has not been a review of the technical aspects of EK-BIO field application, such as the influence of subsurface properties and electrode configurations.

Research Question 1: Based on literature sources what are the main environmental processes that influence EK-BIO application, and what are the methods for optimisation at the field-scale?

Research Objective 2: Develop laboratory apparatus that conceptually represents the technical problem.

Bespoke laboratory apparatus is a key part of EK experiments in the literature. Different designs have been successfully employed that have accommodated amendment migration (Wu et al., 2007), heterogeneous configurations (Saichek and Reddy, 2005) and bioremediation of contaminants (Huang et al., 2013). The development for this objective considers existing designs and how best to represent the technical problem. Some key design criteria relating to the technical problem include: hosting saturated sediment, accommodating homogenous and heterogeneous sediment configuration, applying pH control and migrating nitrate as an amendment between electrodes. These aspects are tested in preliminary experiments.

Research Objective 3: Define the controlling mechanisms of physical heterogeneity on the electromigration of an inorganic amendment

EK phenomena have been observed in heterogeneous settings (Alshawabkeh et al., 2005; Reynolds et al., 2008), however they have not been quantified. It is known that in homogeneous settings material type will exert controls on certain properties of the EK system, namely: (1) the electromigration rates of dissolved ions; and (2) the effective electrical conductivity of the pore fluid. It is unknown how a spatial change in material type will influence these properties and what the subsequent effect on EK remediation effectiveness will be.

Research Question 2: What is the influence of a transition between high- and low-K on the electromigration of nitrate under ideal conditions?

Following on from Research Question 2; the following research findings were expanded upon: (1) it is known that material properties within a heterogeneous setting will exert a control on the voltage gradient; and (2) this gradient is expected to be higher in materials with a lower effective ionic mobility (i.e. low porosity or high tortuosity of migration path). In these experiments a low effective ionic mobility is associated with low-K material, hence there will be a higher voltage gradient across these zones. In a layered heterogeneous system spatial changes in the effective electrical conductivity of the pore fluid could generate a non-uniform electric field that will in turn result in non-uniform transport of ions. At present there is only limited evidence of ion migration transverse to the primary migration pathway between electrodes (Reynolds et al., 2008). Identifying and quantifying this flux will have timescale implications for EK applications at the field scale.

Research Question 3: What is the influence of layered heterogeneity on the electromigration of nitrate under ideal conditions?

Research Objective 4: Enhance the removal of an organic contaminant sequestered in a low-K zone by the electromigration of an inorganic amendment into that zone.

At present there is no investigation of EK-BIO within a heterogeneous setting in the literature. Most EK-BIO studies that enhance bioremediation by introducing an amendment are conducted within homogeneous setting (Mao et al., 2012; Pazos et al., 2012). Furthermore there are no published studies that combine both heterogeneity and a transformation process such as bioremediation or in situ chemical oxidation. By combining all the elements of the technical problem within a laboratory scale setup the processes and controlling mechanisms can be identified. These elements include: (1) heterogeneity represented by a K contrast as investigated in Objective 3; (2) a microbial variable represented by a single population as an inoculum; (3) a representative contaminant; and (4) an amendment that has been proved to enhance the biodegradation of the identified contaminant.

Research Question 4: Can electrokinetics increase the migration of nitrate through physically heterogeneous material, relative to advection, to enhance removal of toluene from a low-K zone containing denitrifying bacteria?

Research Objective 5: Compare the sustainability of EK-BIO to other remediation technologies using the SuRF-UK framework.

There are numerous examples of remediation technology comparisons in the literature (e.g. Blanc et al., 2004; Cadotte et al., 2007; Reddy and Chirakkara, 2013), but currently no studies that include EK-BIO as an option in a sustainable remediation assessment. The environmental impact of EK remediation operation has been shown to be low (Kim et al., 2014), it could therefore be a good candidate in a sustainable remediation appraisal of a site that is suitable for the technology. Evidence from this investigation can be used by practitioners in future remediation option appraisals to justify the inclusion of EK-BIO in similar comparisons. For this purpose, a real contaminated site is used as a case study.

Research Question 5: How does EK-BIO compare with other remediation technologies against a Tier 1 and 2 sustainability assessment for an MtBE contaminated site?

1.5 Thesis structure and author contributions

The thesis is structured around the stated research objectives. Material in some chapters has been submitted for publication in an abridged form (Chapters 2, 4, 5 and 7). Author contributions are from the primary author, R.T. Gill (University of Sheffield) and the supervisory team: S.F. Thornton (University of Sheffield); M.J. Harbottle (Cardiff University); and J.W.N. Smith (Shell Global Solutions).

Chapter 1: Thesis introduction.

This chapter presents the technical problem to be addressed in this thesis. That is the contaminant concentration rebound resulting from physically heterogeneous aquifer settings. It positions the application of coupled technology including, electrokinetics and bioremediation as a potential solution to this field scale problem based on its fundamental processes. It also outlines the principles of EK and the theory related to applications in heterogeneous porous media. This chapter is entirely the authors own work with corrections provided by the supervisory team. The section of EK theory in heterogeneous porous media is published in the reference associated with Chapter 4

Chapter 2: Summary of practical aspects of EK-BIO application from literature

This chapter presents a review of the current technical literature on the subject of EK-BIO as part of Research Objective 1. Literature is summarised on three broad themes: (1) principles of EK remediation; (2) EK-BIO processes in the subsurface environment; and (3) practical aspects of EK-BIO application. The literature review was compiled by the author with advice and corrections from the supervisory team. This work has been published in an abridged form in the journal *Chemosphere* as Gill et al. (2014), the formatted journal article is included in Appendix A.

Chapter 3: Laboratory apparatus development

In this chapter the development of laboratory apparatus to address Research Objective 2 is presented as well as the results and outcomes of preliminary experiments. In order to

achieve Research Objectives 3 and 4 a bespoke apparatus was required to conduct experiments. This chapter explains the design process and initial experiments that informed the experimental conditions for Chapter 4. This work was conducted by the author with corrections and advice from the supervisory team. It also includes contributions on the design of laboratory apparatus from J. Wang and D. Reynolds (both Geosyntec Consultants). The laboratory apparatus was constructed in the Dept. of Civil Engineering workshops, University of Sheffield by P. Blackbourn and D. Jenkins. Aspects of the preliminary experimental work were published within a conference proceeding from AquaConSoil 2013 as Gill et al. (2013) (Appendix B). Additional contribution for this paper is from S. Rolfe who provided advice on microbiological aspects of the experiments in the early stages.

Chapter 4: Electromigration of nitrate through hydraulic conductivity contrasts in porous media

This chapter represents the results and interpretation of experiments which address Research Objective 3. It investigates the influence of K contrasts arranged in series on the electromigration of nitrate in physically heterogeneous porous media. The experiments were conducted by the primary author with technical assistance from A. Fairburn and the results analysed under the guidance of the supervisory team. The chapter was written by the primary author with advice and corrections from the supervisory team. An abridged version has been published in *Groundwater Monitoring and Remediation* as Gill et al. (2015) and is included as Appendix C.

Chapter 5: Electromigration of nitrate through layered heterogeneous porous media

This chapter represents the results and interpretation of experiments which address Research Objective 3. The experiments incorporate a layered K contrast with the aim to observe the resulting non-uniform electromigration pathways. All experiments were conducted by the primary author with assistance on pore fluid sample analysis from A. Fairburn. The chapter was written by the primary author with advice and correction from

the supervisory team. An abridged version has been accepted for publication (subject to minor revisions) to *Electrochimca Acta* as Gill et al. (2016a); the submitted manuscript is included as Appendix D.

Chapter 6: Electrokinetic enhanced removal of toluene from physically heterogeneous porous media

This chapter addresses Research Objective 4. The experiments incorporate numerous variables: microbial activity, contaminant degradation, physical heterogeneity and electrokinetics. All experiments were conducted by the primary author with laboratory assistance from S. Broadhead and advice on microbiology from S. Rolfe. The chapter was written by the primary author with guidance from the supervisory team.

Chapter 7: Sustainability assessment of electrokinetic bioremediation compared with alternative remediation options for a petroleum release site

This chapter represents the work associated with Research Objective 5. It consists of a comparison of remediation technologies applied to a site contaminated with petroleum hydrocarbons and the fuel additive MtBE. Assistance developing the conceptual site model and remediation technology selection was provided by J.W.N. Smith, G. Spinnler and A. Mianzan (all Shell Global Solutions). The chapter was written by the primary author with guidance from the supervisory team. An abridged version has been accepted for publication in the *Journal of Environmental Management* as Gill et al. (2016b); the accepted manuscript is included in Appendix E.

Chapter 8: Thesis conclusion

This chapter is a synthesis which integrates the results from all chapters to develop a broader analysis and overall conclusions of the thesis. It was written by the primary author with guidance from the supervisory team.

Chapter 2 Electrokinetic enhanced bioremediation of organic contaminants: a review of processes and environmental applications

2.1 Introduction

Bioremediation is the process by which microorganisms transform contaminants into less harmful substances. When applied to contaminated soils and groundwater two broad methods can be identified, *in situ* and *ex situ*. This review will primarily focus on *in situ* bioremediation applications. Bioremediation requires environmental conditions which are favourable for the particular biochemical process (Sturman et al., 1995). Factors that limit the performance of *in situ* bioremediation are often highly site-specific (Boopathy, 2000) and commonly include: (1) mass transfer of electron acceptors and nutrients to microorganisms responsible for biodegradation (Simoni et al., 2001), (2) limited bioaccessibility of contaminants (e.g. partitioning to aquifer material) for biodegradation (Lohner et al., 2009); and (3) adaptation of the indigenous microorganisms for biodegradation of a particular contaminant (Mrozik and Piotrowska-Seget, 2010). The aim of coupling EK to bioremediation is to overcome these limitations by initiating electrokinetic transport phenomena.

2.1.1 Research question and hypotheses

The research question addressed in this chapter is: What are the main environmental processes that influence EK-BIO application, and what are the methods for optimisation at the field-scale? The hypotheses are: (1) that the environmental processes that control EK-BIO will vary depending on the material in which it is applied; and (2) aspects of the environmental setting will influence how EK-BIO is applied.

The objectives of this review are:

- To investigate EK-BIO processes at the micro and macro scale (e.g. Wick et al., 2007; Wick, 2009; Lohner et al., 2009a), but with greater focus on the interactions between EK-BIO processes and the subsurface environment;
- Identify the mechanisms supporting field application, considering the practical aspects of using EK-BIO in specific cases such as the direct influence of environmental factors on EK (e.g. Page and Page, 2002) with a critical focus on bioremediation;
- Consider aspects of upscaling EK-BIO to the field-scale including electrode configuration; and
- Demonstrate the viability of plume scale EK-BIO applications using a simple electron balance model.

2.2 EK-BIO processes in the subsurface environment

The processes and mechanisms that constitute EK-BIO operate at the micro and the macro scale (Sturman et al., 1995). Micro-scale (<10 mm) processes occur at pore-level and include interactions between contaminants, microorganisms and their surrounding subsurface environment. At the macro-scale (>10 mm) these processes are manipulated for application to plume-scale management and remediation.

2.2.1 Micro-scale

2.2.1.1 Substance transport by EK

EK enhances bioremediation by making bioaccessible contaminants, nutrients, electron acceptors (EAs) and electron donors (EDs) more bioavailable to catabolically active microorganisms (Wick, 2009). This is achieved by EK phenomena reducing spatial barriers to encourage greater contact between substances and releasing bound contaminants from the porous matrix (Wick et al., 2007). The relative influence of these phenomena depends on the nature of the substances present and their specific properties (Figure 1.2), broadly: microorganisms - electroosmosis and electrophoresis dominate (Wick et al., 2004); contaminants - electromigration and electroosmosis dominate (Luo et al., 2005a; Niqui-Arroyo

et al., 2006); and ionic nutrients and EAs/EDs - electromigration dominates (Thevanayagam and Rishindran, 1998).

Biodegradation in the subsurface can be controlled by the supply of limiting substances via advection, dispersion and infiltration (Aksu and Bülbül, 1998). Solute advection in low permeability porous media is limited by hydraulic mechanisms but transport velocities can be increased for various substances under an applied EK field (Table 2.1). In general the electromigration of microorganisms and nutrients/EAs/EDs is fastest in high permeability media, where the pore spaces are larger with less occlusion and reduced tortuosity (Rowe and Badv, 1996). Desorbed hydrophobic contaminants are more mobile in lower permeability clays, where electroosmosis is the primary transport mechanism. In contrast, the electromigration of hydrophilic compounds such as phenols is much less than for inorganic single ions due to their high mass to charge ratio (Table 2.1). The large variation in velocities for microbes in different materials (e.g. clay 0.05 - 0.15 cm^2/V-hr) and hydrophobic contaminants (0.001 – 0.26 cm^2/V-hr) is due to substance-specific properties. For example, microbe distribution is influenced by cell surface charge and tendency for attachment to sediments (Da Rocha et al., 2009; Wick et al., 2004), whereas increased contaminant transport relates to the water partition coefficient of the specific compound; more soluble compounds have greater mobility under an electric field (Bruell et al., 1992). Differences between the transport rates of single inoculum and mixed consortia can be explained by variation in the velocity of individual populations in consortia. Genetic profiling can be used to distinguish microbes that travel faster from those that adhere preferentially to sediment.

Table 2.1. Migration velocities of substances under an electric field determined in laboratory experiments.

Substance Subjected to Transport		EK Transport Velocity (cm/hr)/(V/cm)			References
		Sand	Silt	Clay	
Microorganisms	Single inoculum	0.1 [1], 0.5 [2]	-	0.05 [2], 0.08 [1], 0.15 [1]	[1] Wick et al., 2004; [2] Suni and Romantschuk, 2004
	Mixed consortia	0.24 [3]	0.99 [4]	0.84 [4]	[3] Maillacheruvu and Chinchoud, 2011; [4] Mena et al., 2012
Organic contaminants	BTX	-	-	0.16 [5], 0.26 [5], 0.22 [5]	[5] Bruell et al., 1992
	TCE	-	-	0.15 [5]	[5] Bruell et al., 1992
	Hexane	-	-	0.1 [5]	[5] Bruell et al., 1992
	Isooctane	-	-	0.001 [5]	[5] Bruell et al., 1992
	Phenols	0.02 [6], 0.04 [6]	-	0.06 [6]	[6] Luo et al., 2005a
Nutrients, EAs and EDs	Nitrate	0.57 [7], 0.67 [8]	-	0.94 [9]	[7] Lohner et al., 2008a; [8] Lohner et al., 2008b; [9] Thevanayagam and Rishindran, 1998
	Sulphate	0.67 [9], 0.96 [7]	-	0.42 [9]	[9] Acar et al., 1997; [7] Lohner et al., 2008a,
	Ammonium	0.2 [7], 0.36 [9]	-	0.38 [9]	[9] Acar et al., 1997; [7] Lohner et al., 2008a
	Lactate	0.21 [10]	-	0.13 [10], 0.15 [11], 0.17 [12]	[10] Wu et al., 2007; [11] Wu et al., 2012; [12] Mao et al., 2012

There are two mechanisms developed by EK which enhance contact between substrates when the combined transport rate of microbes, contaminants, nutrients, EAs and EDs are considered. These are: (1) substances travelling in opposite directions, for example, negatively charged electron acceptors will migrate towards the anode (Equation 1.2) against a counter pore fluid flux by electroosmosis (Equation 1.1) towards the cathode that can migrate dissolved non-ionic contaminants such as BTEX or microorganisms; and (2) migration velocities for substances travelling in the same direction differ, creating longitudinal mixing for example, the electrophoretic migration of a microbe (with a negative surface charge) (Equation 1.5) and electromigration of a negatively charged electron acceptor towards the anode (Equation 1.2) will occur at different rates due to different mass to charge ratios influencing the mobility. The relative importance of different EK processes, and therefore enhancement of solute/microbe migration is determined by the physical properties of the porous media and

the dominant transport mechanism. For example, in clays there is an increased likelihood of contact between substances as microbes and contaminants mobilised by electroosmosis migrate in the opposite direction to negatively charged ions moving by electromigration. However, the absence of a significant electroosmotic flux in sands means that contact between substances moving in opposite directions is controlled more by electromigration of negative and positive ions; thus contact in sands occurs primarily by overlapping migration paths.

2.3.1.2 Contaminant desorption by EK

Electrokinetics can aid the release of organic contaminants bound to clay particles and organic matter in soils and sediments (Maini et al., 2000 and Luo et al., 2005a). Shi et al. (2008a) proposed that this is due to disruption of the surface charge that binds molecules to soil particle surfaces by the advective flux resulting from electroosmosis. While studies show that this mechanism does not achieve complete contaminant extraction without facilitating agents (e.g. surfactants) (Saichek and Reddy, 2005), bioavailability and subsequently biodegradation can be enhanced (Niqui-Arroyo et al., 2006). However, it is unclear if electroosmosis-assisted desorption without facilitating agents can effectively enhance biotransformation of contaminants at large scales, due to the heterogeneity that occurs naturally in electroosmotic flow from spatial changes in pH, voltage gradient and electrical conductivity (Alshawabkeh et al., 2005; Eykholt, 1997).

2.3.1.3 Influence of EK on microbial community viability

Maintaining the viability of an active degrader species (e.g., bacteria, archaea) is important for bioremediation in the natural environment, where microbial populations exist as diverse communities (Megharaj et al., 2011) and utilise a network of compound and metabolite exchanges between members to biodegrade contaminants (Abraham et al., 2002). Understanding how they respond to contaminants is necessary to evaluate the suitability of bioremediation for a particular site (Paliwal et al., 2012; Kleinsteuber et al., 2012).

The application of a low intensity direct current (0.3 - 1 mA/cm^2) has no overall effect on the microbial community; localised negative effects result from pH changes close to the electrodes which can cause stress responses such as selection and catabolic pressures (Lear et al., 2004; Wick et al., 2010). These pH changes can alter the properties of some contaminants, for example pentachlorophenol is more lipophilic at pH 2 and may increase the system toxicity close to the anode (Lear et al., 2007). In addition, secondary electrode reactions can generate chlorine (Cl_2) and hydrogen peroxide (H_2O_2) which may inhibit the microbial community adjacent to the electrodes (Thrash and Coates, 2008). Positive effects associated with EK include the generation of oxidising and reducing zones favourable for biodegradation of contaminants close to the electrodes (Kim et al., 2010; Lohner et al., 2011). At the single cell level, low intensity electric field can stimulate adenosine triphosphate (ATP) production (Shi et al, 2008b; Velasco-Alvarez et al., 2011) and have minimal effect on the cell surface charge (Shi et al., 2008b). At high intensities (>40 mA) the cell surface becomes more hydrophobic and can cause the cell to change shape (Luo et al., 2005c). Hence, for successful bioremediation direct current should be applied at low intensities to maintain the viability of active microorganisms.

A mechanism that may initiate a stress response, which is overlooked in current studies, is the pressure exerted by electromigration where the distributions of trace ions required for growth are disrupted (Pazos et al., 2012). This is particularly relevant in oligotrophic environments, such as groundwater, where the ability to replenish nutrients from the geological matrix is limited over long time periods (Goldscheider et al., 2006). The implication is that measures (such as pH control) may limit the negative effects of EK but stresses on microbes will still occur. Microbes which are more tolerant to these stresses may be more useful in EK-BIO applications (Kim et al., 2010). The impact of various EK-BIO treatments on the viability of the microbial community requires further research to minimise the negative effects of EK and enhance the biodegradation capacity.

2.2.2 Macro-scale

At the field-scale bioremediation can be applied within a range of techniques (Table 2.2) (Coulon et al., 2012). Each may be limited by contaminant – microbe – EA/ED contact and mixing, or hydraulic transport issues. EK can be used to develop alternative flow fields to increase contact between microorganisms and contaminants or deliver a required amendment to a specific zone that is limited under ambient conditions. Table 2.2 summarises the mechanisms by which EK can enhance bioremediation techniques and frames these in the context of field-scale scenarios.

Table 2.2. Potential influence of electrokinetic processes on *in situ* bioremediation (adapted from Boopathy (2000)).

Bioremediation Process and Limitations	Electrokinetic Influence
Bioattenuation - transformation of pollutants by natural means (aka natural attenuation), mixing limited by hydrodynamic dispersion *in situ.*	*EK-Bioattenuation* - EK transport processes increase bioavailability of contaminants and naturally occurring nutrients and electron acceptors.
Biostimulation - Increased biodegradation by the addition of nutrients and/or oxygen or other electron acceptors to optimise the phosphorous: potassium: nitrogen ratio, improve redox conditions and increase bioavailability. Limited by hydraulic delivery and access to low permeability zones.	*EK-Biostimulation* - EK transport processes allow addition and delivery of nutrients, electron acceptors and surfactants into contaminated zones regardless of permeability to increase bioavailability of limiting substances.
Bioaugmentation - Introduction of allochthonous or cultured microbial species adapted to the biodegradation of a particular contaminant. Limited by hydraulic delivery and access to low permeability zones.	*EK-Bioaugmentation* - EK transport of bacterial population to specific zones regardless of permeability where indigenous community is not adapted.
Phytoremediation - Use of plants and or microbes in root zones to effect remediation. Limited by access to contaminants.	*EK-Phytoremediation* - EK transport processes increase the bioavailability of contaminants.

2.3.2.1 EK-Bioattenuation

Bioattenuation is a low impact and cost effective remediation technique, but is limited to sites where the contaminant is biodegradable and there is adequate mixing of contaminants, electron acceptors and microorganisms for biodegradation to occur at a suitable rate (Thornton and Rivett, 2008). Natural mixing can be enhanced with EK and optimised by increasing the number of electrodes, reversing the electrode polarity, placing electrodes in a radial configuration and rotating the polarity (Harbottle et al*.,* 2009; Luo et al*.,* 2006; Luo et al*.,* 2005b; Yuan et al*.*, 2013). This is in order to (1) increase the diversity and connectivity of flow-

paths for potential contact and mixing between microorganisms and contaminants (Luo et al., 2006), (2) maintain more uniform pH and moisture conditions (Fan et al., 2007) as well as microorganism distribution (Huang et al., 2013); and (3) increase the area over which the electric field and enhanced biodegradation is effective.

An important control on biodegradation under EK is the voltage gradient that limits the migration rate of substances *in situ*. This gradient can vary spatially and temporally and when highest maximises contact between substances, and therefore enhances biodegradation (Li et al., 2010). However this spatial and temporal variability can lead to uneven biodegradation of contaminants within the matrix (Luo et al., 2006).

Demonstrated and potential applications of EK-bioattenuation include:

- *Ex-situ* bioremediation treatment where electrodes are inserted into an excavated soil pile. Studies show EK-bioattenuation is an effective polishing treatment for oil-contaminated soil that had previously been land-farmed; the benefit of the EK treatment included increased biodegradation of more recalcitrant polyaromatic hydrocarbons (PAHs) (Acuňa et al., 2010).
- Groundwater contaminant plumes can persist due to inadequate mixing between contaminants and EA at the plume fringe for effective biodegradation (Thornton et al., 2001a) and a depletion of favourable electron acceptors in the plume core (Huang et al., 2003). EK could be used to increase mixing at the plume fringe with electrodes located transverse to the plume flow path and applying an electric field to drive electromigration of background EAs normal to (and into) a contaminant plume.

2.3.2.2 EK-Biostimulation

EK can enhance the delivery of nutrients (e.g. phosphate (Lee et al., 2007)), electron acceptors (e.g. nitrate and sulphate (Lohner et al., 2008a) and electron donors (e.g. lactate (Wu et al., 2007)) through different materials at rates greater than diffusion. EK-biostimulation in soils has been demonstrated for PCE (Mao et al., 2012; Wu et al., 2012), toluene (Tiehm et

al., 2010), diesel (Pazos et al., 2012) and PAHs (Xu et al., 2010). In addition to chemical amendments the gaseous products of water electrolysis (H_2 and O_2) can be used to stimulate reductive dechlorination of PCE and oxidation of VC, respectively (Lohner and Tiehm, 2009). This process has been demonstrated in a sequential column experiment where contaminated groundwater was first reduced as it passed through the cathode then oxidised in the anode column (Lohner et al., 2011).

Biostimulation can also be achieved through the addition of solubilising agents, to increase the dissolution and bioavailability of hydrophobic contaminants into the aqueous phase (Mulligan, 2005). EK phenomena enhance contact between surfactants and bound contaminants at the micro-scale and can deliver surfactants to polluted zones at the plume-scale (Saichek and Reddy, 2005). These modifications have been demonstrated with synthetic surfactants (Saichek and Reddy, 2003), biosurfactants (Gonzini et al., 2010), co-solvents (Gómez et al., 2009) and cyclodextrin (Ko et al., 2000). Experiments that combine EK-BIO with solubilising agents use surfactants or biosurfactants that are biodegradable (Mulligan, 2005). After addition of solubilising agents an increase in the bioaccessible fraction of the contaminant was reported (Niqui-Arroyo and Ortego-Calvo, 2010), leading to enhanced biodegradation (Gonzini et al., 2010). These studies also showed that variation in EK properties such as field strength and polarity reversals had limited effect on biodegradation over the presence of a surfactant (Gonzini et al., 2010; Niqui-Arroyo and Ortego-Calvo, 2010). However the soil samples contained a uniform distribution of surfactants at the start of the experiment; the implication is that macro-scale delivery of surfactants, either by EK or other means, is required to enhance biodegradation. Karagunduz et al. (2007) achieved the best macro-scale distribution in a soil with low electroosmotic conductivity using anionic surfactants transported by electromigration, alternative surfactants may be more suitable in soils with a higher electroosmotic conductivity.

Demonstrated and potential applications of EK-biostimulation include:

- In a contaminated groundwater plume the concentrations of the contaminant and substance limiting biodegradation are inversely proportional to each other (Bauer et al., 2008). EK could be used to migrate the limiting substance into the plume regardless of the subsurface permeability. The concept has been demonstrated at the laboratory scale by Tiehm et al. (2010), where nitrate was migrated laterally into a toluene plume to stimulate biodegradation.
- In the introduction chapter EK-biostimulation is proposed as a solution to enhancing bioremediation of contaminants sequestered within low-K zones. This could be achieved through either moving the contaminants out of the low-K zone with the aim of initiating degradation within the host material, or introducing electron acceptors into the low-K zone.

2.3.2.3 EK-Bioaugmentation

EK can enhance the migration of microorganisms through low permeability soils (Mao et al., 2012; Mena et al., 2012; Wick et al., 2004), despite potential occlusion of cells due to small pore throat size in fine grained materials (DeFlaun and Condee, 1997). This enhancement has been attributed to movement of microorganisms preferentially along a flow path through macro-pores within the soil by electroosmotic flow (Wick et al., 2004). EK-bioaugmentation has been used within sequential treatment of contaminated soil conditioned with an active degrader species. Mao et al. (2012) used EK to firstly distribute lactate, then the dechlorinating strain *Dehalococcoides* for treatment of PCE-contaminated soil. EK-Bioaugmentation can also be effective at redistributing bacteria as a pre-treatment step for soils contaminated with heavy metals (Lee and Kim, 2010).

Microbes maintain their membrane integrity (Shi et al., 2008c) and functionality during transport by EK, and effective biodegradation during migration has been observed for both dextrose (Maillacheruvu and Chinchoud, 2011) and diesel (Lee and Lee, 2001). Microbes have a strong tendency to attach to sediment and organic matter particles disrupting transport (Mrozik and Piotrowska-Seget, 2010), but this can be reduced when using EK by adding

surfactants (Wick et al., 2004). It is often difficult to maintain the survival of exogenous microbes introduced to a foreign environment (Megharaj et al., 2011). A possible alternative could be the addition of endospores instead of active bacteria. Endospores are more robust and migrate faster under EK than bacteria due to a high associated surface charge (Da Rocha et al., 2009).

2.3.2.4 EK-Phytoremediation

Phytoremediation of recalcitrant organic contaminants in the shallow subsurface (soil and root zone) requires a symbiotic relationship between the plant and the soil microbial community (Teng et al., 2011). Most EK-phytoremediation studies focus on treatment of heavy metal-polluted soils (Cameselle et al., 2013) where the electric field accumulates contaminants around the plant roots increasing bioavailability (Cang et al., 2011). EK processes have not been shown to significantly hinder the mechanisms by which plants enhance their degradation. For example: (1) under EK the biomass of certain plant species (lettuce and ryegrass) has been increased under AC electric fields demonstrating plant health can be maintained (Bi et al., 2010, 2011); and (2) the respiration and biomass of the microbial community can be enhanced under EK-phytoremediation (Cang et al., 2012). Chirakkara et al. (2015) conducted experiments on soil with mixed inorganic and organic contaminants (heavy metals and PAHs). They showed no uptake of PAHs by the plants and identified both volatilisation and microbial degradation as the main removal mechanisms.

2.3 Practical aspects of applying EK-BIO

2.3.1 Influence of subsurface environmental processes on EK-BIO

EK phenomena and success of EK-BIO treatment depend on environmental variables; therefore tailoring the treatment to the environment in which it is applied is important for managing electrode effects and predicting and sustaining EK phenomena. The principal environmental properties that influence EK-BIO are: the electrolyte (i.e. groundwater or soil moisture) through which the current travels, the geological strata that influence EK

phenomena, hydrodynamics that introduce advection as an additional transport vector, physical heterogeneity that can alter transport rates and the mixed nature of contaminants found at many sites.

2.3.1.1 EK and electrolyte properties

When an electric current is applied to a porous medium (e.g. soil or aquifer) the pore water acts as an electrolyte. The capacity of a system to accommodate an electric current is proportional to the concentration of ions in solution (Alshawabkeh and Acar, 1996). These ions are primarily derived from dissolution of minerals originating in the surrounding geological matrix (Paillat et al., 2001) but also anthropogenic sources. Thus, the soil or rock type imparts ionic characteristics that affect the electrochemical properties of the system (Reddy and Saichek, 2003). Similarly, soil and rock type heterogeneities can be reflected by electrolyte conductance heterogeneities and can lead to zones exhibiting a low voltage gradient that can slow electromigration (Li et al., 2013). At constant voltage, high concentrations of dissolved ions will allow more electric current to be transferred through the system, which in turn increases the rate of electrolysis reactions at the electrodes (Kim and Han, 2003) and increases power consumption (Wu et al., 2012b).

In unsaturated soils the electric current follows a more tortuous path than in saturated soils due to gas-filled pore spaces, and will travel preferentially through more saturated zones (Mattson et al., 2002). Electroosmosis can induce pore fluid flux and alter the moisture content, shifting the distribution towards the cathode (Elektrowicz and Boeva, 1996; Luo et al., 2005b, Harbottle et al., 2009; Fan et al., 2007; Ouhadi et al., 2010). This has the effect of increasing the electrical resistance and/or impeding the migration of an amendment by increasing the volume of pore space occupied by pore gas (Kim et al., 2012; Mattson et al., 2002). Moreover, for EK-BIO applications, electro-dewatering by electroosmosis can initiate water stress and impede the growth and survival of microorganisms (Li et al., 2012). These effects can be mediated by applying EK in rotational or bidirectional modes to better distribute moisture (Luo et al., 2005b; Li et al., 2012).

2.3.1.2 EK interactions with geological strata

The proportion of fine-grained sediments with net surface charge in a geological matrix determines the extent of electroosmotic flow. Electroosmosis requires a net charge on the surface of sediment and soil grains, hence clays and silts have the highest electroosmotic permeability due to a high surface charge density (Acar et al., 1995). The zeta potential, a measure of that charge, is susceptible to changes in pH and electrolyte conductivity (Vane and Zang, 1997). At neutral pH the zeta potential is often negative and indicates flow towards the cathode, if the pH drops (e.g. below pH 2 for kaolinite (Vane and Zang, 1997)) the zeta potential becomes positive and flow changes towards the anode (Yeung, 2006). Similarly, as electrical conductivity increases the zeta potential is closer to zero and is sensitive to the valence state of ions in solution (Yukselen-Aksoy and Kaya, 2010). The implication for EK-BIO is that electroosmosis presents a counter flux that hinders the migration of negatively charged amendments. Suppressing electroosmotic flow by acidification can have a negative impact on the microbial community, therefore increasing the electrical conductivity of the pore fluid is more effective for EK-BIO applications (Wu et al., 2007).

The pH buffering capacity of a soil is primarily controlled by the carbonate mineral content. Implications for EK-BIO include mediation of the acid front from the anode, which has been shown in soils with 15% carbonate content (Ouhadi et al., 2010). Minimising pH changes at the electrodes can reduce stress responses in microorganisms (Lear et al., 2004). It also ensures a more sustained and uniform electroosmotic permeability by maintaining neutral pH conditions favourable for a negative zeta potential (Eykholt, 1997; Reddy and Saichek, 2003). However, heterogeneous distribution of carbonate minerals in the subsurface could lead to spatial variability in the soil buffering capacity and therefore should not be relied upon to moderate pH changes at electrodes. To a lesser extent cation exchange in a soil can affect pH buffering and is a function of the clay type and organic matter content (Andrews et al., 2005). The presence of more exchange sites in a soil can result in greater sequestration of

contaminants (Reddy and Saichek, 2003), potentially reducing the fraction that is bioavailable or bioaccessible.

2.3.1.3 EK and hydrodynamics

In scenarios where EK is applied in saturated medium to high permeability zones, groundwater flow can significantly affect EK processes by introducing another transport vector. Complimentary applications of EK and hydraulic flow include using a perpendicular electric field to disperse nutrients upstream of contaminated groundwater (Godschalk and Lageman, 2005) or to deliver electron acceptors directly into a mobile contaminant phase (Tiehm et al., 2010). Electromigration against hydraulic gradients is effective at retaining substances close to the electrodes, but this decreases as hydraulic flow rate increases (Eid et al., 1999). An electromigration rate for nitrate of 2.4 cm^2/V-h has been achieved under perpendicular hydraulic flow (30 cm/h) (Tiehm et al., 2010). This is higher than in previous studies (0.57-0.67 cm^2/V-hr) of nitrate migration in a static system with deionised water and groundwater at (Lohner et al., 2008a, 2008b). The difference is proposed to result from dilution of the pH changes at the electrodes by the hydraulic flow (Tiehm et al., 2010). In either case the electromigration of nitrate transverse to advective flow is rapid relative to hydrodynamic dispersion and diffusion.

2.3.1.4 EK and physical heterogeneity

To date the majority of EK literature has focused on treatment of homogeneous material such as uniform clays and sands. Studies where EK is applied to physically heterogeneous systems include movement of charged substances into low permeability zones by electromigration (Reynolds et al., 2008) and where electroosmosis is used to remove organic contaminants (e.g. phenanthrene) from clay (Saichek and Reddy, 2005). In layered systems the migration of substances can be disrupted by electroosmotic flow through low permeability clay layers. This can cause a pressure difference between layers and introduces an alternative transport vector, which may disrupt the flow path of the target substance (Alshawabkeh et al., 2005).

Knowledge of how EK processes develop within physically heterogeneous systems is crucial to field-scale application of the technology. EK-enhanced migration of substances across permeability boundaries is greater than advective-dispersion and diffusion (Reynolds et al., 2008) because they are controlled by different mechanisms. For example, advection across permeability contrasts is controlled by the ambient flow field and diffusion is limited by the solute concentration gradient and diffusion coefficient, whereas electrokinetic migration is determined by the positioning of the electric field which can be orientated independent of the permeability field. However additional factors also apply. Wu et al., (2012b) discuss EK theory and suggest that the electromigration velocity of a substance moving from high- to low-K falls due to: (1) spatial changes in porosity and tortuosity (and subsequent change in effective ionic mobility) (Equation 1.2); and (2) a higher opposing electroosmotic flux in the low-K section, assuming that the low-K section has a negative charge at the soil particle surface. A more in depth discussion of EK applied to physically heterogeneous settings is presented in the Introduction and in Chapters 4 and 5.

2.3.1.5 EK and mixed contaminants

Contamination in the natural environment often occurs as mixtures of organic and inorganic contaminants that may require treatment by different remediation technologies. EK has been applied to remove both simultaneously. However, the removal of organics and heavy metals without facilitating agents can be problematic as both require different conditions for mobilisation, i.e. electromigration of metal ions under acidic conditions and electroosmotic flow of hydrophobic organics under neutral conditions (Maini et al., 2000). Successful removal of mixed contaminants from soils has required the use of cyclodextrin (Maturi and Reddy, 2006) or non-ionic surfactants and EDTA (Alcántara, 2012; Colacicco et al., 2010).

Remediating mixed contaminants with EK-BIO is poorly studied but could involve sequential processes in which inorganic contaminants are first removed by EK followed by EK-BIO treatment for the organic contaminants. Heavy metals can inhibit microbial growth, especially as their extraction using EK requires mobilisation into solution thereby increasing their

bioavailability (Cang et al., 2007). Studies show that microbial communities remain functional following heavy metal removal by EK (Wang et al*.,* 2009), although the use of facilitating agents such as EDTA can decrease microbial cell number and activity (Kim et al., 2010). It may be possible to enhance community viability by the pH control used to remove heavy metals, for example using lactic acid as an electrode conditioning solution that reduces pH at the cathode to favour acid conditions for metal extraction, while simultaneously providing microbes with a carbon source (Zhou et al., 2006).

2.3.2 Design of field-scale EK-BIO

2.3.2.1 Electrochemical optimisation of amendment addition

EK related electrochemical factors can be modified to enhance the migration and mass flux of an amendment. A linear relationship between the voltage gradient applied and electromigration rate has been demonstrated in homogenous sandy soils (Lohner et al., 2008a; Tiehm et al., 2010). In clay a minimum voltage gradient is required to ensure penetration of a negatively charged amendment (>80 V/m for lactate) (Wu et al., 2007). This is due to the counter flux from electroosmosis (Wu et al., 2007) and the higher tortuosity factor of fine grained sediment (Jones, Reynolds et al*.*, 2011). pH control at the electrodes can enhance amendment migration and distribution because it prevents the combination of acid and base fronts creates a band of water with a low associated electrical conductivity (Acar et al., 1993). This produces a zone where the amendment migration is increased significantly, resulting in non-uniform distribution of an amendment. It also stops the precipitation of the amendment out of solution, for example permanganate used for chemical oxidation precipitates below pH 3.5 preventing it from reaching the target location (Hodges et al*.*, 2013)

Ions are often added in mixtures when applied as nutrients (Gonzini et al., 2010; Pazos et al., 2012; Xu et al., 2010). This can reduce the effective ionic mobility and mass flux of an ion relative to a system where it is the only or dominant ion (Alshawabkeh and Acar, 1996). In mixtures, ions are subject to competitive transport due to the need to maintain electrical

neutrality in the system (Lohner et al., 2008a). In addition, the chemical form in which the amendment is transported can affect its migration; Lee et al. (2006) compared inorganic phosphate (K_2PO_4) to organic phosphate (triethyl phosphate) and found greater losses of the inorganic form due to reactions with available metal ions.

Mass transport of an amendment can be enhanced by increasing the inlet concentration (Lohner et al., 2008a), but this may result in a disproportionate amount of the amendment being retained within the soil between the inlet and target location (Thevanayagam and Rishindran, 1998). This is due to the increased electrical conductivity of the pore fluid caused by the amendment, which drops the voltage gradient, subsequently reducing the rate of electromigration. Thus the concentration of an amendment at a target location is reduced relative to an increase in the inlet concentration (Wu et al., 2012a). For EK-BIO applications the amendment must be added into the system at a rate which exceeds the microbial capacity in the contaminated zone to ensure an even distribution (Rabbi et al., 2000). Therefore if a biological amendment is to be applied it should be at a concentration that accounts for microbial consumption and the amount retained in the soil mass. Enhancing the concentration at the target locations can be achieved by moving the electrode or the inlet location closer to the target to reduce the distance the amendment needs to travel (Wu et al., 2012b).

2.3.2.2 Electrode optimisation

The application of EK-BIO determines the electrode material that should be used. For systems where an amendment is added under constant voltage, a material that reduces the voltage drop at the soil-electrode interface is preferable to retain a higher average voltage gradient in the rest of the soil. Mohamedelhassan and Shang (2001) noted the electrode material related to a significant drop in the voltage profile at the soil-electrode interface adjacent to the anode and was highest for materials with a high surface potential (e.g. carbon) relative to steel. Durability is also a factor; metal electrodes corrode more easily especially at low pH (Suni et al., 2007) and should therefore be used with pH control or with an appropriate surface coating to reduce corrosion. However, electrode coatings that raise the surface potential of the

electrode will generate more secondary products from electrochemical reactions, such as: chlorine (Cl_2), hydrogen peroxide (H_2O_2) or high energy free radicals (e.g. O_2^-• or •OH), which inhibit microorganisms adjacent to the electrode (Li et al., 2002; Tiehm et al., 2009). This is important in EK-BIO applications where the electrodes are in close proximity to the degrading microorganisms. Hence, metal electrodes may be most suitable for small-scale application whereas metal electrodes engineered to resist corrosion are more suitable for large-scale applications where long distances are involved. Titanium and stainless steel are noted as effective electrode materials at the field-scale because they are reliable with a low associated economic cost (Virkutyte et al., 2002).

2.3.2.3 Electrode configuration

Electrodes can be installed in different configurations, for example: unidirectional, bidirectional, radial - pairs or radial - bidirectional (Figure 2.1). These can be applied to achieve different outcomes. For example, a bidirectional or radial - bidirectional setup is suitable for the migration of amendment evenly and at high concentration (Wu et al., 2013), whereas a radial - pairs configuration is suitable for mixing substances *in situ* (Luo et al., 2006). Additional factors to enhance electrode configuration include:

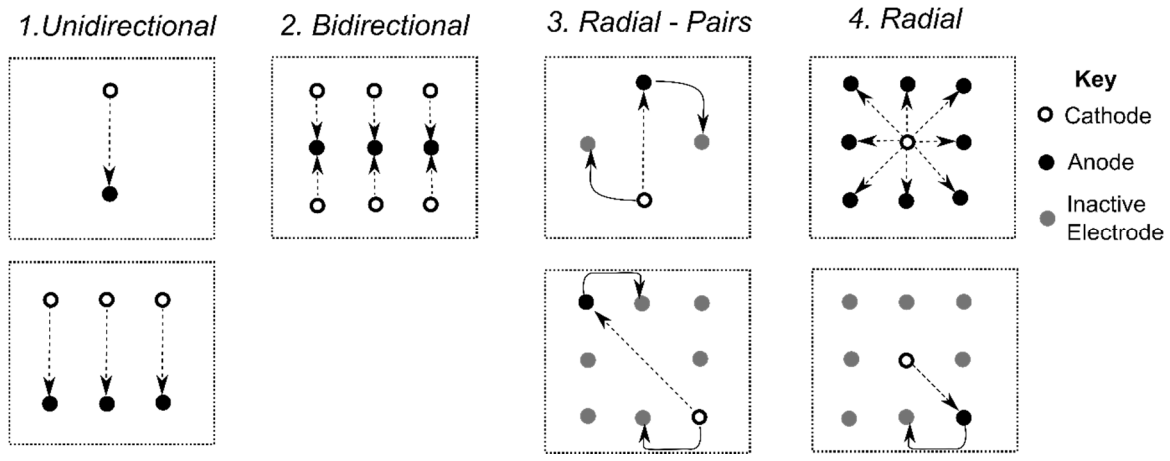

Figure 2.1. Illustration of different electrode configurations in the literature (polarity of electrodes is assumed to be reversible); e.g. 1. Unidirectional: Harbottle *et al*. (2009); Xu *et al*. (2010), 2. Bidirectional: Alshawabkeh *et al*. (2005); T. Li *et al*. (2010), 3. Radial pairs: Luo *et al*. (2006), and 4. Radial: Fan *et al*. (2007); Suni and Romantschuk (2004).

- Polarity reversals - effective at maintaining uniform pH conditions (Harbottle et al., 2009) and enhancing mixing of substances *in situ* by alternating the migration path (Luo et al., 2006). It is also effective to achieve a more even distribution of amendment in a unidirectional setup (Kim and Han, 2003; Xu et al., 2010). This technique may also be effective at removing the products of electrochemical reactions deposited on the electrode surface, which can reduce the active surface area of the electrode and therefore its efficiency over time;
- Electrode spacing - reducing the distance between electrodes increases the intensity of the electric field over an smaller area and in modelling simulations reduced remediation timeframes by enhancing oxidant distribution (Wu et al., 2013). However, it can lead to increased power consumption and cost through heating (Kim et al., 2012);
- Injection wells - adding an amendment into a well placed within or adjacent to a contaminated zone reduces the migration distance of the amendment compared with adding this via the electrode chamber (Wu et al., 2012b; Wu et al., 2013);
- Absence of metal debris – ensuring the subsurface is free of electrically conductive objects such as metal pipe networks or storage tanks prevents short-circuiting (Mattson et al., 2002a).

A by-product of an EK setup in the field is ohmic heating caused by the soil acting as an electrical resistor when an electric current is passed through it. Increasing soil temperature to ca. 30ºC is beneficial for microbial growth (Killham, 1994). For EK-BIO treatments it is an additional mechanism to enhance bioremediation, and in a field trial Suni et al. (2007) observed a temperature increase from ambient 6ºC to 16 - 50ºC with 1 - 1.5 A. However, for EK applications close to the surface, ohmic heating may increase evaporation leading to reduced moisture content and increased electrical resistance (Page and Page, 2002).

2.3.3 Additional techniques to develop the application of EK-BIO

2.3.3.1 Permeable reactive barriers

Permeable reactive barriers (PRBs) are an established technology typically used for the *in situ* treatment of groundwater contaminated with organic chemicals and metals, among others. PRBs are placed in the flow path of contaminated groundwater and operate by preventing or reducing the contaminant flux whilst permitting the groundwater to flow through (Smith et al., 2003; Obiri-Nyarko et al., 2014). They are typically made up of reactive materials that either immobilise the contaminant or transform it through either biotic or abiotic processes into less harmful substances. Examples of PRBs that enhance contaminant transformation by biological processes include Teerakun et al. (2011) where a zero valent iron PRB was coupled with an anaerobic and aerobic biobarrier to treat TCE, and Yeh et al. (2010), where the bioavailability of electron acceptors was increased by constructing a barrier of oxygen release compounds to enhance the aerobic biodegradation of BTEX compounds.

The role of EK to enhance PRB processes includes one or more of the following: (1) to migrate the contaminants into the PRB (Li et al., 2011); (2) to generate oxidising and reducing conditions at the anode and cathode, respectively, by electrolysis of water at the electrodes, to enhance the efficiency of zero valent iron PRBs (Moon et al., 2005); or (3) to electrochemically construct a PRB *in situ* using a sacrificial anode that will precipitate out of solution upon reaching the base front from the cathode (Faulkner et al., 2005). To date there have been few EK-BIO combinations with PRBs. Fonseca et al. (2012) compared two bio-barriers to treat hexavalent chromium (Cr^{6+}) made from zeolite and activated carbon placed before the anode in the path of the contaminant moving by electromigration and achieved removal rates of 60% and 79%, respectively. Ramírez et al., (2015) compared EK-BIO treatment of a diesel polluted soil and found that a nutrient-rich PRB (containing buffer solution) reduced the negative effects of EK application (such as the generation of pH fronts) leading to enhanced bioremediation over the no-PRB control. Areas for further research

include enhancing bio-barriers with EK by the addition of electrodes that could generate a limitless source of electron donors and acceptors (shown in Lohner et al. (2011)).

2.4.3.2 *In-situ* chemical oxidation and reduction

Coupling EK transport mechanisms with the delivery of substances into soils and sediments to oxidise or reduce contaminants has been demonstrated in the literature and includes the use of: permanganate ion to oxidise DNAPLs (Thepsithar and Roberts, 2006; Wu et al., 2012b); Fenton's reagent where H_2O_2 migrates with electroosmosis and is catalysed by either introduced or native Fe to oxidise PAHs (Kim et al., 2005; Reddy and Chandhuri, 2009); and nano zero valent iron migrated by electrophoresis to reduce chlorinated solvent DNAPLs (Jones, Reynolds et al., 2011). The sequential treatment of contaminants with chemical oxidants followed by bioremediation is well documented for less biodegradable compounds, as the chemical oxidation step enhances the bioaccessibility of the contaminants to the microbes (Goi et al., 2006; Palmroth et al., 2006a). However, chemical oxidants are typically aggressive and negatively impede microbial activity and growth (Palmroth et al., 2006b). As a combination, EK-ISCO-BIO could have significant potential to remediate less biodegradable compounds sequestered in low permeability zones, by first adding oxidants then following with EK-BIO methods to replenish and/or rejuvenate the native microbial population and complete the remediation process.

2.4 Simulating the performance of EK-BIO at field-scale

To explore the potential of EK-BIO applications at the field-scale a spreadsheet model was developed to simulate the effect of EK on the supply of dissolved EA for biodegradation of BTEX in groundwater. This analysis was based on outputs from the electron balance model in CORONAScreen, developed by Thornton et al. (2001b). CORONAScreen predicts the steady-state length of a contaminant plume in groundwater according to the balance of EA and ED flux into the plume from all sources. The EK element introduces an additional flux of dissolved EA, migrating normal to groundwater flow, into the plume. The model simulated

electromigration of nitrate and sulphate in the background uncontaminated groundwater into the plume and, separately, migration of nitrate and sulphate amendments added at the electrodes. The EK aspects of this model were applied using the 1-D electromigration mass flux equation, Equation 1.2.

The conceptual scenario developed evaluated the potential contribution of EK-BIO to reduce the remediation timescale of a plume in which monitored natural attenuation (MNA) is the management option, but where biodegradation is limited by transverse dispersion of dissolved EA. This is a very common limitation on biodegradation of organic contaminants in plumes (Thornton et al., 2001a, 2001b). The contribution from EK was the enhancement of the dissolved EA flux into the plume by electromigration, for biodegradation. The reference condition is a BTEX plume at steady-state, where the contaminant and EA flux into the plume are balanced. The model assumes the contaminant source has been removed and predicts the time taken until number of EDs in the plume is equalled by the flux of EAs in the absence of EK and by EK mechanisms. This is a suitable descriptor of remediation performance because management costs increase with remediation timescales.

The scenario was created using relevant information for the contaminant source, aquifer properties, groundwater and plume chemistry taken from a BTEX-contaminated aquifer (see Appendix F). The electrokinetic variables used include: voltage gradient (100 V/m), area of the electrode array (equivalent to 10% of the plume section along the flow path (9.4 m^2) and a bidirectional electrode configuration where the anode is located in the centre of the plume, with cathodes placed outside the plume (Figure 2.1). A bidirectional configuration allows electron acceptors to be introduced into the plume transverse to the flow path. Several set-up parameters were varied to assess the effectiveness of the EK treatment, these were the distance between the cathode and plume and the concentrations of nitrate and sulphate in the amendment solutions.

The results show that the time required to balance the ED and EA budgets within the plume and reach the steady state length is considerably reduced when using EK (Table 2.3). It implies that the treatment may also be effective in scenarios where MNA is not able to mitigate risk as the only management option, either to increase the natural flux of EAs into a plume for biodegradation or to supplement this with amendments. The benefits for introducing EAs by EK over hydraulic mechanisms in this scenario is EK-enhanced mixing of substances at the micro-scale and independence of EK phenomena to hydraulic conductivity controls.

Treatments where EAs from the background groundwater are migrated into the plume by EK require large distances between the electrode array and the plume to increase the catchment volume for EAs. This supports a higher mass flux of EAs for a longer period, but the treatment is no longer effective once the background EAs are depleted. A considerable reduction in treatment time compared to the base case could be achieved when adding amendment solutions at the electrodes. There is a small difference between the addition of nitrate and sulphate as single ions. This is due to the differences in the ionic mobility of the individual ions (nitrate: 7.4×10^{-8} $m^2/V\text{-}s$ and sulphate 8.3×10^{-8} $m^2/V\text{-}s$) (Thevanayagam and Rishindran, 1998).

Table 2.3. Results from the CORONAScreen and EK-BIO treatment model to predict the time to reach steady-state plume length for a BTEX-contaminated groundwater scenario (n/a = not applicable).

Scenario	Cathode - Plume Distance (m)	Amendment Solution (g/L)		Time Until Plume ED = EA (days)
		Nitrate	Sulphate	
Base Case[1]	n/a	n/a	n/a	241
EK migration of background EAs[2]	1	n/a	n/a	191
	5	n/a	n/a	166
	10	n/a	n/a	140
EK migration of background and amendment EAs[3]	1	1	0	37
	1	0	1	32
	1	1	1	19

[1] base case for development of plume with no EK treatment

[2] enhanced migration of dissolved EA into plume from background groundwater

[3] enhancement as per [2] with additional input of EAs via amendment at electrodes

The array area is expressed as a percentage of the plume area. As such, the treatment can only reach the section of the plume within that area. Therefore, it is important to know the best way to apply the technology in a certain situation. Several options include: (1) a fence of electrodes perpendicular to groundwater flow that supply EAs at a rate equivalent to the plume velocity (Godschalk and Lageman, 2005); (2) treatment of the plume in sections with movement of the electrodes accordingly; and (3) a static electrode array that the plume moves though and treatment is initiated at regular time intervals.

2.5 Conclusions

EK-BIO is a promising technology for the *in situ* treatment and remediation of many organic and inorganic contaminants in soil and groundwater. It has the potential to effectively enhance bioremediation in physically heterogeneous or low permeability matrices where alternative technologies may be ineffective. This review has focused on the factors associated with upscaling EK-BIO from the bench-scale to the field-scale. Conclusions drawn from the literature reviewed herein include:

- The mechanisms for EK-induced mixing to enhance bioremediation will vary depending on the host geological matrix;
- Novel field-scale applications of EK-BIO exist including the remediation of plume-scale contaminant scenarios and contaminants sequestered within zones of low permeability;
- Simple modelling of a relevant contaminated groundwater conceptual scenario to illustrate the performance of EK-BIO at the field-scale indicates that a considerable reduction in the time for a plume to reach steady-state length can be achieved. Relative to timescales which may typically occur for sites managed using MNA, EK-BIO could reduce overall remediation costs significantly;
- When EK is applied in the natural environment, complex physicochemical processes generate non-uniform pH, voltage and moisture gradients that can affect

bioremediation performance and need to be considered on a site-specific basis, for example, groundwater flow will influence amendment transport and pH changes at the electrodes;

- Numerous electrode material and configuration options exist to optimise the EK-BIO treatment demonstrating that there is flexibility to suit environmental setting or remediation objectives.

Overall this review demonstrates that, similar to other remediation technologies, the greatest challenges to EK-BIO applications at the field scale is understanding how it performs in different environmental settings. This is further justification for the aim of this thesis that seeks to apply EK-BIO to back-diffusion issues in physically heterogeneous settings.

Chapter 3 Development of laboratory apparatus and preliminary experiments

3.1 Introduction

This chapter describes the development of laboratory apparatus designed to conceptually replicate the technical problem presented in Chapter 1. This includes developing a list of requirements the design will need to accommodate as well as investigating existing designs. The apparatus constructed was tested in order to develop methods and ensure that EK phenomenon can be repeated within the test setup. The outcomes of these preliminary experiments were carried over to following experiments in Chapter 4 to inform the experimental design and operation.

3.2 Development of laboratory apparatus

In order to meet the research objectives outlined in Chapter 1, a novel laboratory apparatus design for EK experiments was required. To inform this design, a conceptual model was developed to show the progression from a field scale scenario to representation within a bench-scale rig. It presents a scenario where residual NAPL is sequestered within a low-K zone and is back-diffusing into the host matrix creating a rebound effect (Figure 3.1). A groundwater flow field is excluded from the scenario; this is to simplify the experiments and to focus in more detail on the processes of EK in saturated media.

The bench-scale rig needed to incorporate the following design criteria to represent the conceptual model:

- Maintain anaerobic conditions to provide realistic biodegradation conditions;

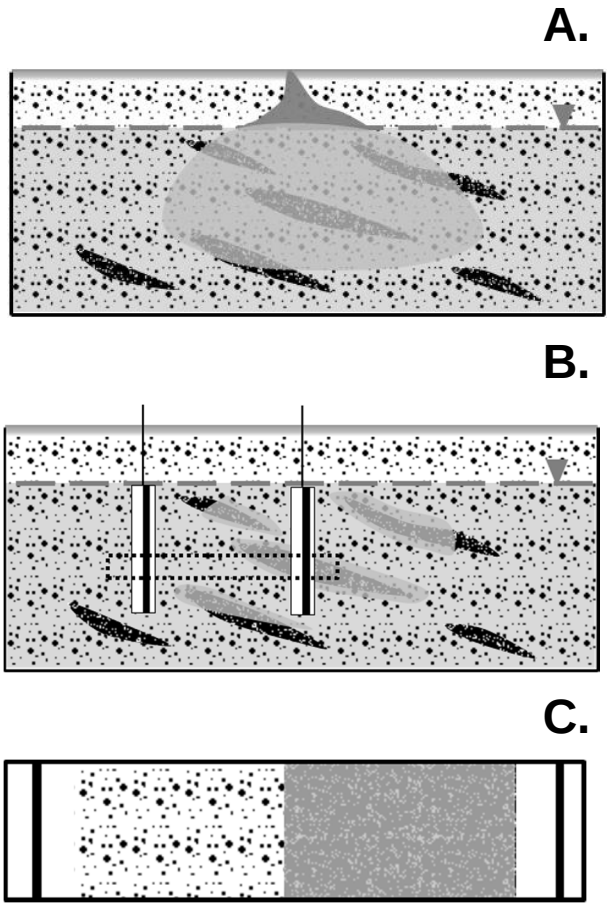

- Full access site;
- No groundwater flow field; and
- Low-K sections in sub strata - illustrated by dark lenses.

- Assume removal of source and dissolved phase in high permeability sections;
- Residual dissolved phase remains sequestered in low-K zones; and
- Dashed-box section represents area conceptualised within reactor design.

- Side view of a 1D reactor setup; and
- Two electrodes within electrode chambers either side of aquifer material containing a low-K zone with a dissolved phase contaminant sequestered within it.

Figure 3.1 Residual NAPL contaminated groundwater scenario in low permeability zones. Three different stages (A-C) show development of theory from field scale to reactor. Assumptions for each stage are included in bullet points.

- Accommodate consolidated physically homogeneous and heterogeneous granular porous material;
- Allow the compacted granular porous material to be fully saturated;
- Allow the injection of dissolved ionic amendments by electromigration;
- Provide high resolution *in situ* sampling of the pore fluid;
- Provide high resolution spatial data relating to the voltage gradient;
- Accommodate a dissolved phase contaminant within the system; and
- Accommodate different pH control methods such as recirculation of electrode chamber fluid.

Different designs were considered as the basis for the laboratory-scale rig (Figure 3.2). Figure 3.2A from Reynolds et al. (2008) represents a very good design that is capable of

reproducing a high level of physical heterogeneity; dimensions are: 499 (length) x 240 (height) x 50 (thickness) mm. A flow field was created through the sediment by head differences in the electrode chambers. This design was not selected for further development because the 2D aspect would make it difficult to quantify transport processes without modelling techniques. Also, pH control would be difficult to isolate from the sediment based on the flow field through high-K material.

Both designs in Figure 3.2B and Figure 3.2C from Reddy and Saichek (2003) and Harbottle et al. (2009) exhibit similar characteristics, i.e. a homogeneous soil between two

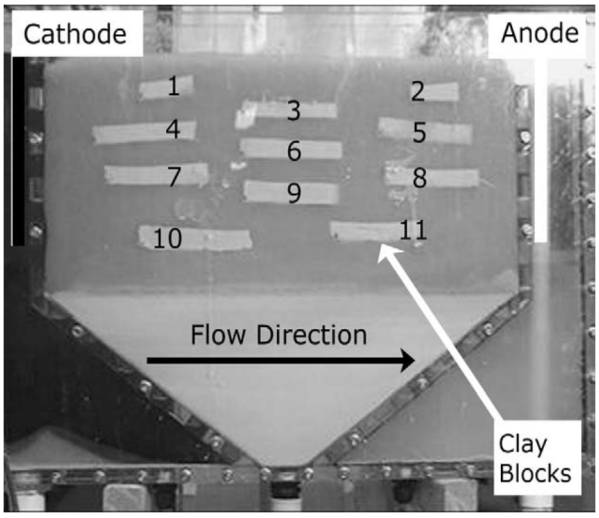

A.

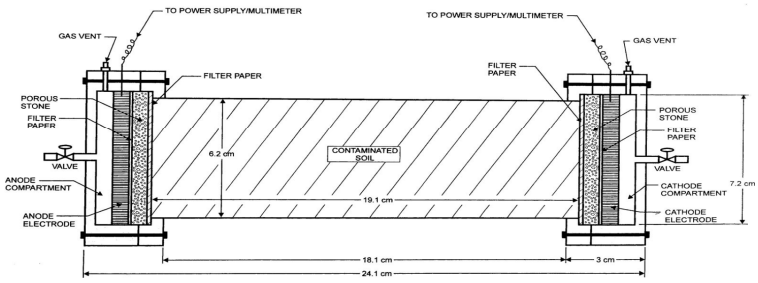

B.

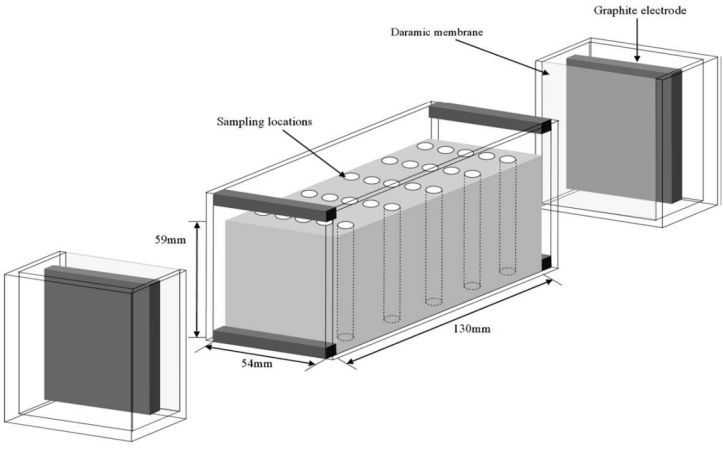

C.

D.

Figure 3.2. Different reactor designs from the EK literature: A. V-shaped 2D reactor (Reynolds et al., 2008); B, Cylindrical 1D reactor (Reddy and Saichek, 2003); C, Cartridge reactor (Harbottle et al. 2009); D, Cartridge reactor (Mao et al., 2012)

relatively small electrode chambers. Each design has a different shape; Reddy and Saichek (2003) is cylindrical (191 x 62 (dia) mm) and Harbottle et al. (2009) is rectangular (130 (length) x 59 (height) x 54 (thickness) mm). These designs would require significant modification to meet the specified design criteria. For example, ports along the side of the sediment chamber would need to be installed for *in situ* sampling and voltage readings; this is more achievable with the rectangular design because a flat surface would allow easier installation. These rigs have primarily been tested on homogeneous clayey, unsaturated soils. Design alterations would be required to ensure sediments with a range of K values could be saturated effectively because there is a potential for fluid level variation in the electrode chambers due to electroosmosis or evaporation. This could be achieved by extending the hydraulic head of the electrode chamber fluid above the sediment chamber. These design alterations are represented to some extent in Figure 3.2D from Mao et al. (2012). This design includes two extended electrode chambers that help maintain full sediment saturation and an enclosed section for the material to be packed into, also *in situ* sampling via horizontal ports at the side. This type of design is most suitable for modification to meet the research objectives of this thesis.

These designs were refined and developed (Figure 3.3) with the following features:

Electrode chambers – The electrode chamber is separated from the sediment chamber by a perforated acrylic divider fixed into the reactor with silicone sealant. They are extended in height by header tanks that elevate the water level above the sediment to maintain sediment saturation. The permeable acrylic barrier consists of an acrylic plate (125 x 125 x 6 mm) perforated holes 7 mm in diameter and arranged in 11 rows of 10 (110 holes in total). Before an experiment these plates are covered with filter paper (Whatman No 5) on either side to prevent contamination of the electrode chambers. There are fluid overflow ports in the header tank that allow the water level to be set during the experiment setup.

Sediment chamber – The sediment chamber accommodates the consolidated sediment, sample tubes and voltage probes. Two pairs of acrylic struts (6 x 6 x 125 mm) were fixed using silicone sealant to the side of the sediment chamber. This allowed a thin (0.5 mm) stainless steel plate to be inserted into sediment chamber. This plate acts as a temporary partition so different materials could be consolidated either side of the divide. In Figure 3.3 the interface where the tops of the struts meet the edge of the sediment chamber are shown in a highlighted bubble. Once the sediment chamber is filled a lid and gasket are screwed on to prevent fluid leakage.

Dimensions – The length of the rig is designed to allow a maximum average voltage gradient between electrodes of 100 V/m, assuming a power pack output voltage of 60 V. The height and width of the chamber was determined by the total volume of fluid extracted per sampling round being less than 1% of the total pore fluid in the rig. The aim of this was to minimise any perturbations caused by sampling. The dimensions were based on a minimum sediment porosity (0.25) and a maximum of 9 sediment sampling ports extracting a maximum of 2 mL each.

Nitrogen Sparge – From the top of the electrode header tank a pipe is inserted to deliver nitrogen into the electrode chambers. This will help maintain anaerobic conditions in experiments where the sediment chamber is inoculated with anaerobic bacteria. There is also a gas vent to prevent any pressure build up in the header tanks.

Electrodes – Graphite electrodes (125 x 125 x 10 mm) supplied by Olmec Advanced Materials were used in all experiments. It is a common electrode material for EK-BIO studies (e.g. Mao et al., 2012; Wu et al., 2012). Similar to the acrylic dividers, numerous holes were drilled into the electrodes to facilitate mixing within the electrode chamber (Harbottle et al., 2009). The connection between the graphite electrodes and copper wires to the DC power source was housed inside the electrodes and secured in place with a

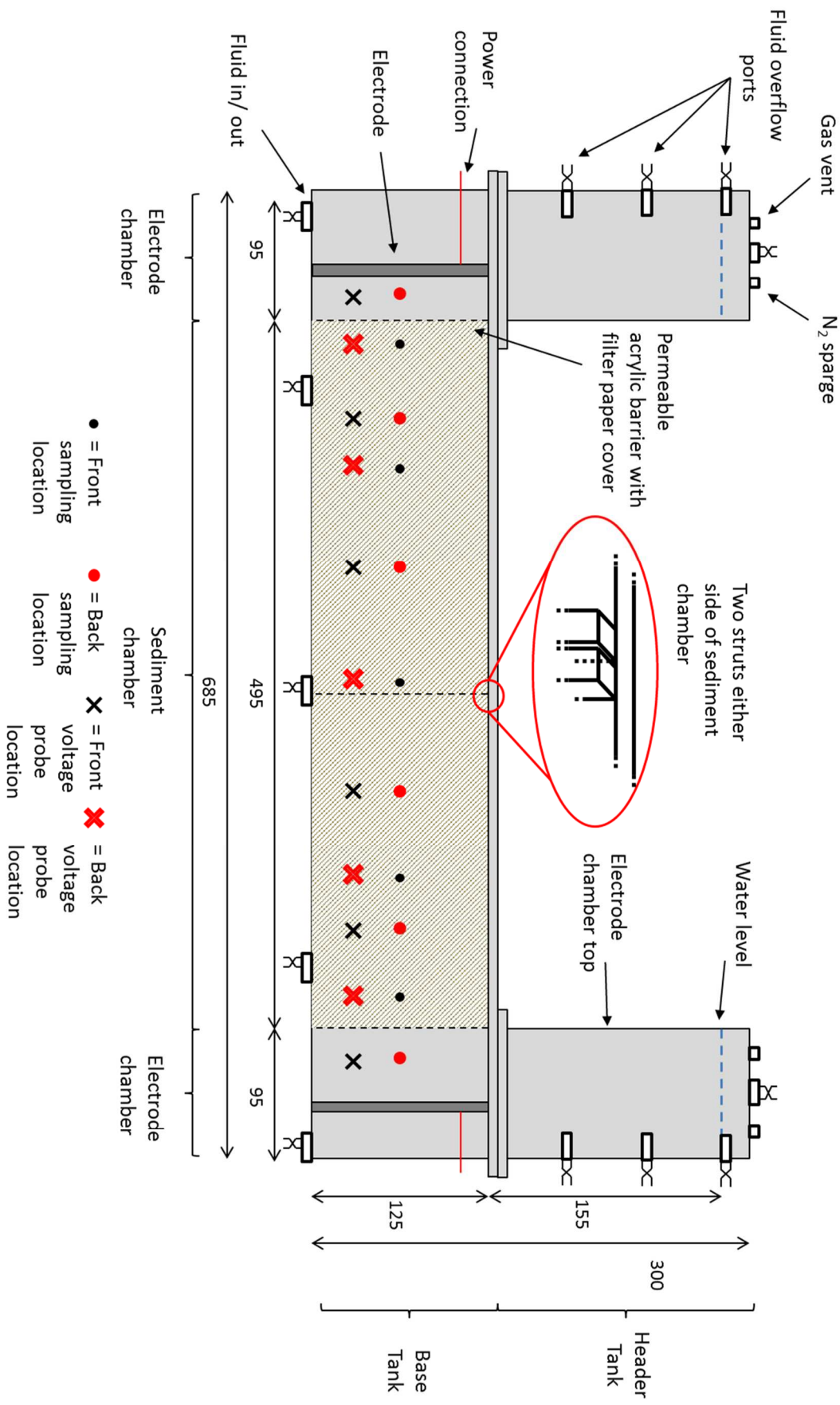

Figure 3.3. A labelled schematic of the reactor design with sizes given in mm.

threaded seal and silicone sealant to give a water-tight seal. This also reduced the risk of contaminating the electrode chambers by metal corrosion.

3.2.1 Apparatus construction

Four laboratory scale rigs based on the design in Figure 3.3 were constructed in March 2012 and April 2013. Each pair took ca. 2 months to construct. Both sets of pairs were constructed to the same design, the only difference was the thickness of the acrylic used in construction that changed from 10 mm to 12 mm (internal dimensions were kept the same). An example of a finished rig is given in Figure 3.4. There are several discrepancies between this image and the design in Figure 3.3 such as the acrylic plates to separate sediment and electrode chambers, these features were added at a later date.

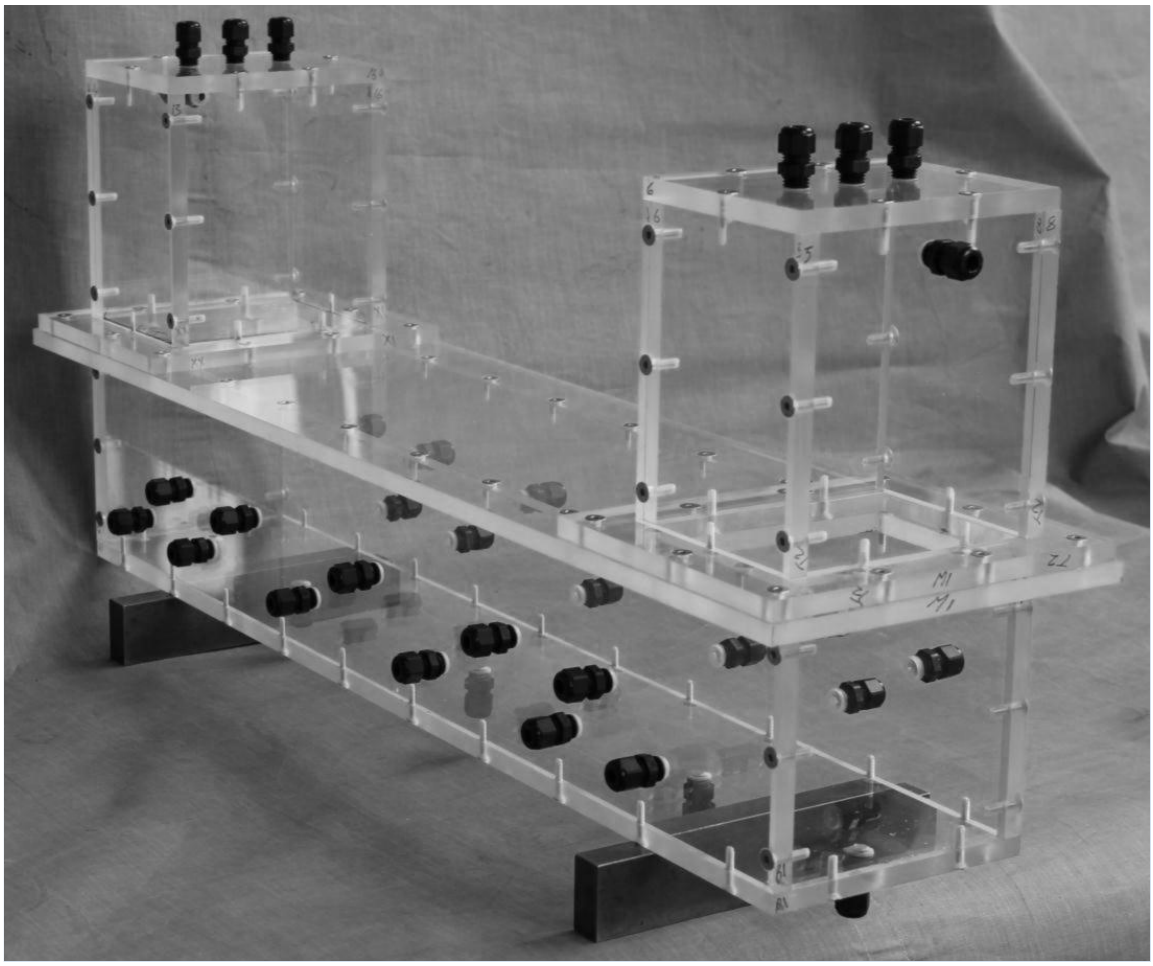

Figure 3.4. Digital image of a completed laboratory scale rig, March 2012.

3.3 Experimental method development

Preliminary experiments are used to develop the experimental setup and are the basis for the methods used in Chapters 4-6. The material and methods sections for these chapters will specify where the methods deviated from those presented here.

The purpose of conducting preliminary experiment is to produce a series of procedures that ensure an optimised and reproducible experimental setup prior to addressing the research questions. The individual preliminary experiment aims include:

1. Defining the rig construction protocol to ensure that each experiment is setup in the same way to ensure reproducibility;
2. Developing the pore fluid and voltage reading protocol to minimise sample tube blockages and ensure voltage readings are taken in the same way;
3. Defining the methods for pore fluid analysis for major ions, pH and electrical conductivity;
4. Developing the sediment consolidation protocol to ensure that the porosity of the material used in these experiments can be reproduced;
5. Defining a method to test the hydraulic conductivity of the sediments used in the experiments;
6. Defining the need for pH control to be applied in experiments and developing the rig design to identify the most suitable method; and
7. Determining how the amendment is added to the experimental setup to optimise the sampling/ procedure.

Preliminary experiments for points 6 and 7 required several iterations of the experimental setup, these are shown in Table 3.1. They included variations in whether pH control was applied, the configuration of how fluid was circulated around the rig and whether nitrate was added as a single or constant concentration. Four different fluid circulation

Table 3.1 Details of all preliminary experiments. EKP, electrokinetic preliminary experiment; HOM, homogeneous sediment; and HET, heterogeneous sediment.

Experiment Name	Rig Designation	pH control	Fluid circulation configuration	K-HOM (m/s)	K-HET		Nitrate conc (g/L)	Nitrate addition method	Duration (hours)
					High-K (m/s)	Low-K (m/s)			
EKP-HOM_1	Active	No	Rig-1	$2x10^{-5}$	n/a	n/a	0.1	Single	69
	Control								
EKP-HOM_2	Active	Yes	Rig-2	$2x10^{-5}$	n/a	n/a	0.1	Single	161
	Control								
EKP-HET_1	Active	No	Rig-3	n/a	$2x10^{-4}$	$2x10^{-5}$	0.1	Single	134
	Control								
EKP-HOM_3	Active	No	Rig-1	$2x10^{-4}$	n/a	n/a	0.1	Single	140
	Control								
EKP-HET_2	Rep 1	No	Rig-4	n/a	$2x10^{-4}$	$2x10^{-5}$	0.1	Constant	192
	Rep 2								
EKP-HOM_4	Rep 1			$2x10^{-5}$	n/a	n/a	0.1	Constant	192
	Rep 2								
EKP-HET_3	Rep 1	Yes	Rig-4	n/a	$2x10^{-4}$	$2x10^{-5}$	n/a	n/a	144
	Rep 2								
EKP-HOM_5	Rep 1			$2x10^{-5}$	n/a	n/a	n/a	n/a	144
	Rep 2								

configurations were tested and are shown in Figure 3.5A-D, they are labelled Rig-1 to Rig-4.

The material used for all experiments in Table 3.1 was glass beads (Potters Ballotini Ltd). Two diameters were used, 1.4 mm and a mix of 0.25 and 0.3 mm that corresponded to a K value of $2x10^{-4}$ and $2x10^{-5}$ m/s respectively. Homogeneous experiments consisted of the sediment chamber filled with either diameter of glass bead. Heterogeneous experiments consisted of splitting the sediment chamber between the different diameter glass beads to create a K contrast.

The electrolyte used in these experiments for FT, EKP-HOM_1 and EKP-HOM_2 was tap water. For all other preliminary experiments a synthetic groundwater was used with an equivalent electrical conductivity of 700 µS/m similar to natural groundwater sampled in a UK aquifer (Thornton et al. 1995). This solution was achieved by adding 0.3 g-NaCl/L to deionised water. Nitrate was used as the amendment in these experiments.

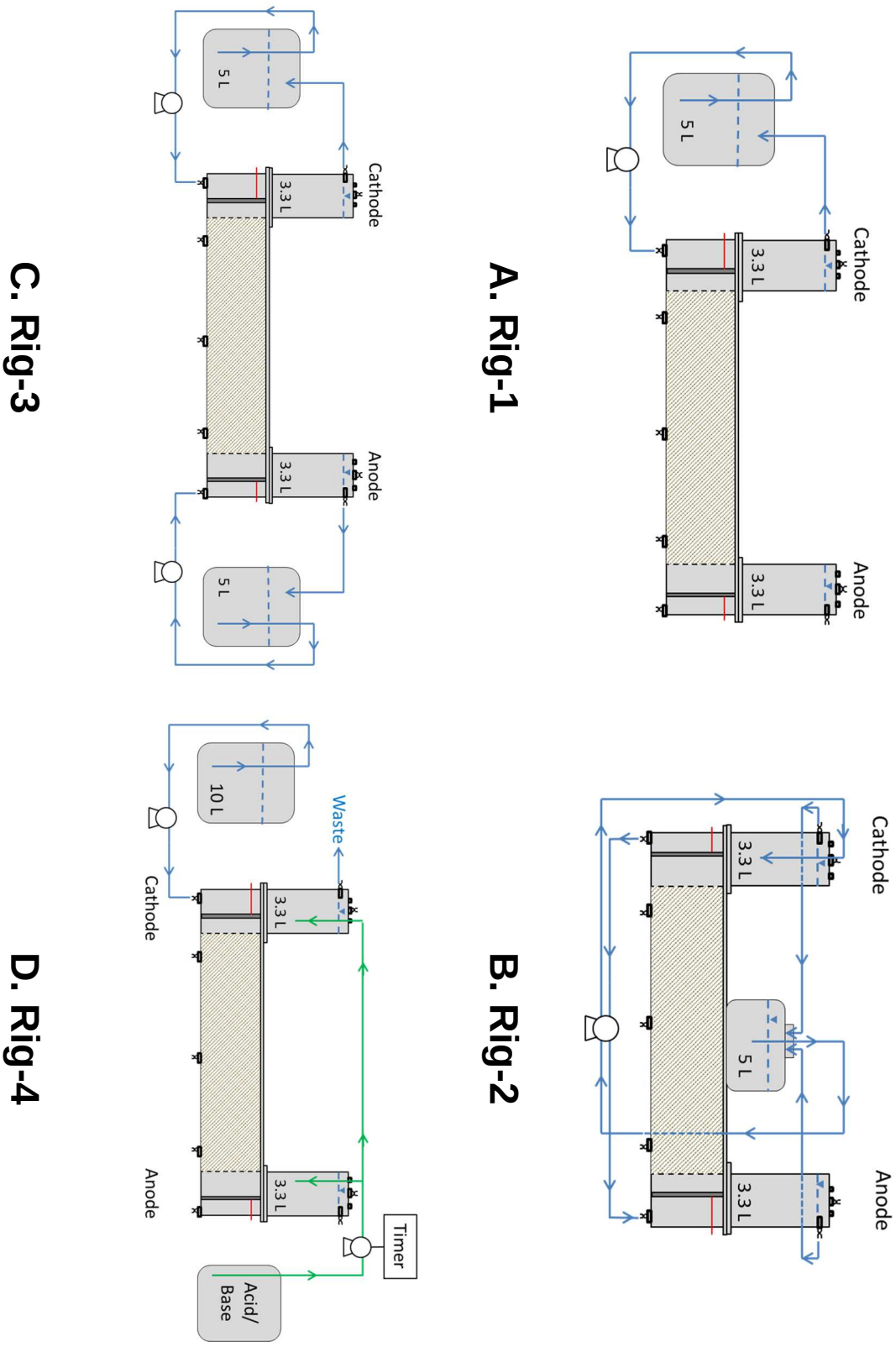

Figure 3.5 Different fluid circulation configurations used in preliminary experiments. A. method Rig-1; B. method Rig-2; C. method Rig-3; and D, method Rig-4

All preliminary experiments were conducted between May 2012 and September 2013. The results from EKP-HOM_1 are reported as part of a conference paper (Gill et al., 2013) included in Appendix B. An additional set of experiments conducted within a modified fish tank prior to the construction of bench-scale apparatus are in Appendix G. They are not included in this section because they do not relate to the development of methods in the rig experiments. Raw data for the experiments listed in Table 3.1 is given in Appendix H.

3.3.1 Rig construction protocol

The rig construction protocol prior to the beginning of an experiment was considered during the design process. For a homogeneous experiment it consists of seven steps shown in Figure 3.6:

1. Placing the perforated acrylic dividers to create a partition between the electrode and sediment chambers and securing them in place using silicone sealant within the base tank. Once the dividers were in place, filter paper (Whatman grade No5) was cut to size and fitted onto both faces of the dividers (the electrode and sediment face). At this point the electrodes were also placed into the electrode chambers. The wire that supplied the electric current to the electrode was fed through a hole in the side of the electrode chamber. It was made water tight using a silicone septum and threaded fitting.
2. The sampling and voltage probe apparatus was then inserted into the sediment and electrode chambers. The sampling and voltage probe protocol is developed in section 3.3.2. The sediment material was then added to the sediment chamber, the method of sediment consolidation is described in section 3.3.3.
3. The sediment was saturated from the base up to remove air trapped in pore spaces. However, this created problems observed in experiments EKP-HOM_1 and 2, where the sediment chamber lid could not be secured without air being trapped or excessive pore fluid loss. At experiment EKP-HET_1 evenly spaced threaded holes (12 holes, 0.7 mm diameter) were drilled in the sediment chamber

lid, allowing this to be secured after the material has been consolidated and for air to escape more easily while the lid was in place. Once fluid was observed emerging from the holes in the lid they were sealed with threaded fittings.

4. The electrode chamber header sections were added as the sediment was being saturated. This required a rubber gasket to be fitted prior to the header tanks being secured to the sediment lid.
5. Once the header tanks were in place and the sediment saturated they could be filled to the required level. The level at which the header tanks were filled to in EKP-HOM_1 and 2 was 280 mm from the base of the rig. This created some leaks and it was decided to drop the head to 170 mm from the base of the rig. At this point the tanks were left overnight to allow the system to settle.
6. Once the rig was fully saturated the relevant pH control and amendment delivery method for the specific experiment could be connected. Methods for both changed over the preliminary experiment program. An analysis of the pH control and the amendment delivery methods is provided in section 3.3.6 and 3.3.7 respectively.
7. The electrodes are connected to the power packs and a direct current is applied. In these preliminary experiments, a constant voltage is applied in all experiments equivalent to a voltage gradient of 100 V/m.

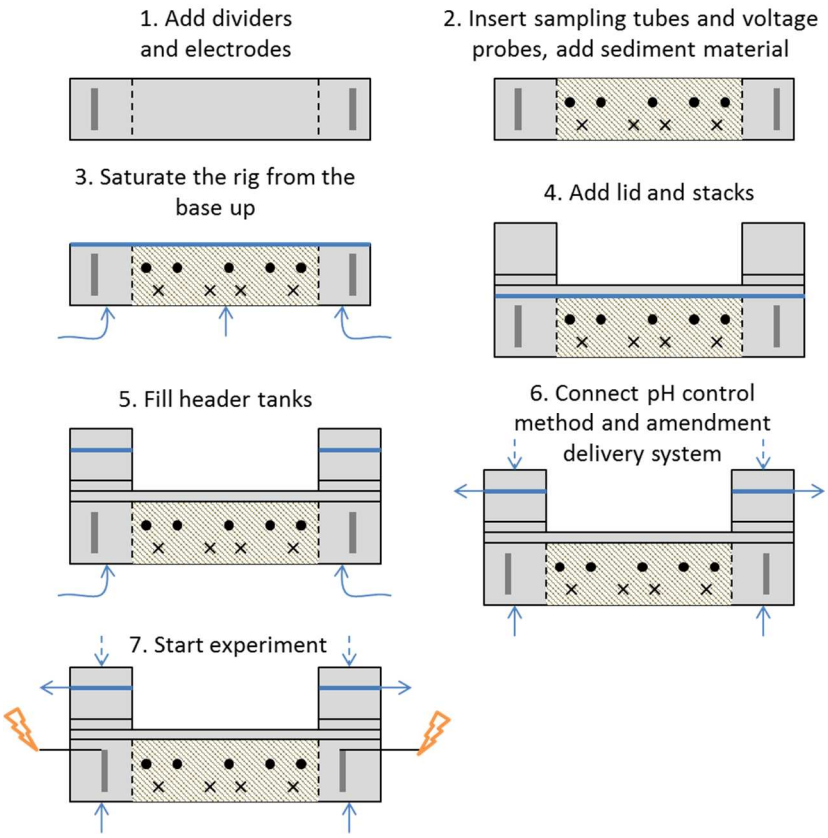

Figure 3.6 Rig construction protocol.

3.3.2 Pore fluid sampling and voltage reading protocol

Two types of sampling apparatus were used in the preliminary experiments, firstly long needles that were replaced in experiment EKP-HET_1 with PEEK sampling tubes. The sampling needles were 115 mm long with an outer diameter of 0.63 mm. They blocked easily in glass bead experiments where the bead diameter was < 1.4 mm. The PEEK sampling tubes (120 mm long with outer and inner diameters of 1 and 0.5 mm respectively) were more effective because a sintered glass block (10 x 5 x 15 mm) could be fitted over the end of the tube. This successfully prevented sampling blockages.

The pore fluid sampling protocol included the following:

1. Preparation of the sampling apparatus. This included rinsing with distilled water and autoclaving to reduce the risk of biological contamination prior to the experiment starting.

2. Assembly of the apparatus components and fitting them within the rig. Fluid leaks were minimised by pushing the sampling tube through a silicone septum.
3. At a designated sampling point the plug at the end of the sampling tube was removed and a syringe attached, 1 mL of fluid was then extracted and discarded. This accounted for the fluid present in the tube since the last sampling point.
4. A sample of the pore fluid (1 mL) was then taken for analysis. The sampling tube plug was placed back on the end of the sampling tube.

Voltage and electric current readings were taken using a multimeter (Digitek, DT-4000ZC) and recorded in a lab-book. Voltage was measured via a 316 stainless steel rod inserted into the sediment from ports in the side of the rig. These rods were encased in a HDPE piping with the end of the rod exposed to the sediment and sealed using silicone sealant. This prevented corrosion of the rods over time. Electric current readings were taken by connecting the multimeter in series with the experiment.

3.3.3 Water sample analysis

Water samples taken from the sediment, electrode and reservoir tanks at specific time points were analysed in the EKP experiments for major ions (nitrate, bromide, chloride, sulphate, sodium and potassium) and pH.

Major ions were analysed using a Dionex DX-120 ion chromatograph. This allowed the quantification of the main components in the electrolyte. The anion column was an AS14A with a mobile eluent consisting of 8 mM sodium carbonate and 1 mM sodium bicarbonate at a flow rate of 1.34 mL/min. The cation column was an CS12A with a mobile eluent of 20 mM methane sulphonic acid at a flow rate of 1.05 mL/min. Calibration standards were run at the beginning of each batch and quality control standards were included every 15 samples. The maximum and minimum detection limits for the ions analysed were: 0.8 mg/L (sulphate) and 0.1 mg/L (sodium); and analytical precision: ±5.9% (potassium) and ±2.0% (bromide).

Measurements of pH were made using a specialised micro pH probe to accommodate the small sample volume. After calibration the probe was simply inserted into the sample tube.

3.3.4 Sediment consolidation protocol

A sediment consolidation test for loose granular material within the rigs was conducted to determine the most repeatable method (not shown in Table 3.1). The material used was a well graded natural sand with a particle density of 1.8 g/mL. The two methods identified: (1) consolidation by tamping using a single weight (i.e. 1.1 kg hammer) with a metal plate (125 mm x 125 mm) to spread the load; and (2) consolidation by vibrations (31 Hz) on a shaker table for intervals of 20 seconds. In both methods the following steps were followed:

1. Weigh the empty rig;
2. Add sediment up to 3 cm from the base and consolidate with either the hammer or shaker table depending on method;
3. Repeat step 1 for layers of material 6, 9 and 12 cm up from the base;
4. Once the rig was filled, flatten the surface with a metal spatula;
5. Weigh the rig (with sediment) and calculate the bulk density from the weight of the sediment added to the rig divided by the sediment chamber volume; and
6. Calculate the porosity based on the following relationship (Hiscock, 2005):

$$n = 1 - \frac{\rho_b}{\rho_s}$$

(Equation 3.1)

Where n is porosity; ρ_b, is the bulk mass density (g/mL); and ρ_s is the particle density (g/mL).

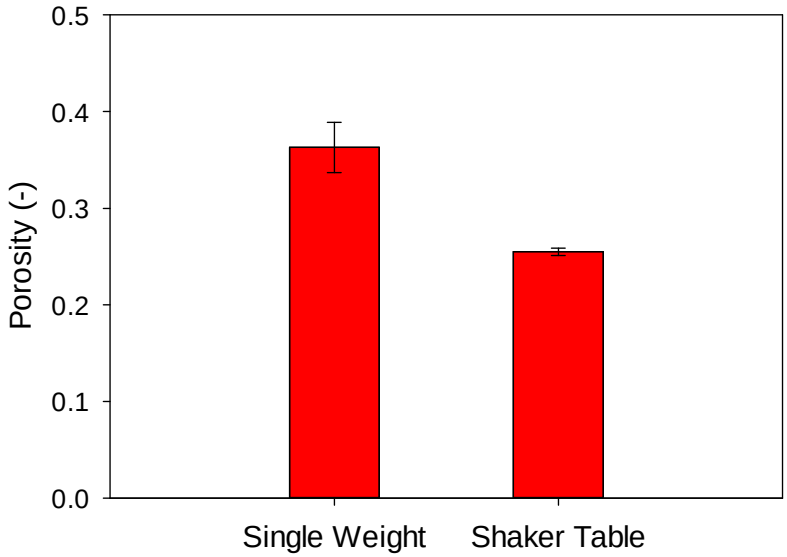

Figure 3.7 Comparison of consolidation methods. Error bars represent standard deviation from the mean of repeated tests.

The average porosity of the material created by each consolidation method is shown in Figure 3.7. These values are based on three repeated tests of each method. The shaker table method provides more reproducible results with less-variation. The shaker table method also produces a lower porosity, suggesting it is more effective at consolidating the material.

The influence of vibration frequency was also investigated. The consolidation tests using the shaker table were repeated on a high and low vibration setting (accurate vibration frequency values could not be obtained at the time of the experiment). Porosity values varied from 0.22 in high frequency experiments to 0.27. This demonstrates that the frequency influences the porosity value but over a narrow range, compared to results from the single weight consolidation method. This shaker method applies to all experiments from EKP-HET_1. The heterogeneous sediment configuration applied in the EKP experiments was achieved by dividing the sediment chamber with a stainless steel plate (Figure 3.3). The different materials were then consolidated using the shaker method

within their respective compartment. There was some difference between the porosities of materials consolidated within a homogeneous and heterogeneous setting. For example, the porosity of the fine-grained material in homogeneous experiment, EKP-HOM_5 was 0.37 and 0.38 between replicates whereas under heterogeneous conditions for EKP-HET_3 it was 0.36 and 0.34 between replicates.

3.3.5 Hydraulic conductivity

To test the hydraulic conductivity (K) of the sediment in these experiments a falling head permeameter was developed based on the design in Freeze and Cherry (1979) (Figure 3.8). A falling head permeameter setup is more applicable to materials with a low-K value (such as those described in Chapter 4) compared to a constant head permeameter. This is due to the low volumes of water that are required to move through the sample before a measurement can be taken (Fetter, 2001). Values of K for different materials were calculated from the following:

$$K = \frac{aL}{At} ln\left(\frac{H_0}{H_1}\right)$$

Equation 3.2

Where a, is tube cross-sectional area; A is sediment cross-sectional area; L is length of sediment chamber; t is time; H_0 and H_1 are the head drop. Consolidation of the sediment was conducted using a shaker table. Tests were repeated 3 times to determine the consistency of the results. Porosity values for sediment consolidated within the falling head permeameter are comparable to the rig experiments. For example the fine grained glass beads had a porosity of 0.33 and 0.36 for the permeameter and rig experiments (rig experiment porosity based on average of values from EKP-HOM_5 and EKP-HET_3).

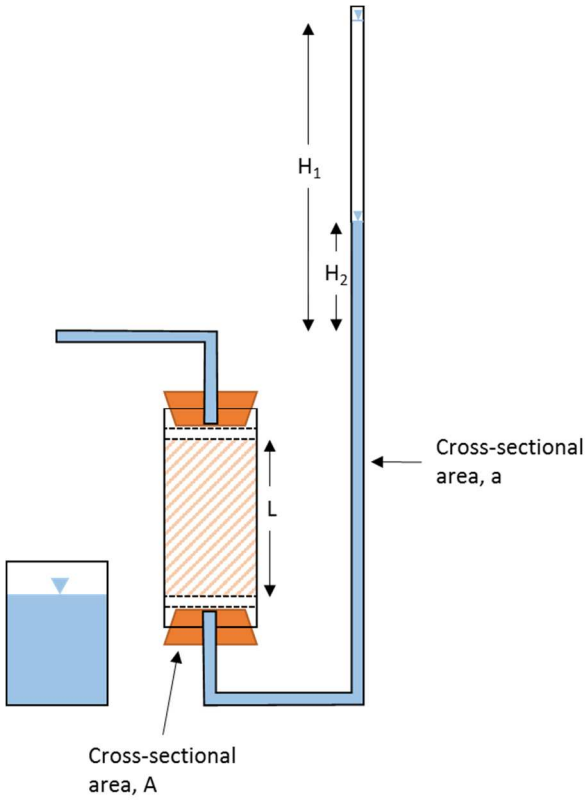

Figure 3.8 Falling head permeameter setup.

3.3.6 pH control method

Controlling the pH changes at the electrodes is an important consideration for EK-BIO applications. Maintaining pH within a specific range (pH 6-8) ensures microbial cell survival, reduce stress on microorganisms and supports biodegradation of contaminants (Lear et al., 2004). There are several pH control methods applied in EK-BIO studies. These include electrode polarity reversals (Harbottle et al., 2009), electrode chamber fluid recirculation (Wu et al., 2012) and electrode conditioning (Pazos et al., 2012). Polarity reversals are not considered in these experiments because the research objectives focus on the migration of an amendment between electrodes. Reversing electrode polarities would complicate nitrate transport pathways, therefore recirculation and electrode conditioning were considered.

3.3.6.1 Method 1 – recirculation

A recirculation system to neutralise pH changes was applied in experiment EKP-HOM_2 (Figure 3.5B). The design is based on similar recirculation systems in Mao et al. (2012) and Wu et al. (2012). Fluid was initially pumped round the system at 20 mL/min using a Watson Marlow 505Du peristaltic pump. This was based on circulating the electrode and reservoir tank fluid at least once before pH changes were observed in the electrode chambers. This occurred within 21 hours in EKP-HOM_1, hence a conservative estimate of 10 hours was used. In EKP-HOM_1 no pH control was applied; fluid was only circulated between the cathode chamber and the reservoir tank to allow addition of nitrate.

The effectiveness of the recirculation system at neutralising pH is shown in Figure 3.9 by comparing pH values for experiments EKP-HOM_1 and EKP-HOM_2. In EKP-HOM_1, the pH in the electrode chambers changes dramatically within 21 hours and within 70 hours a clear pH front has formed within the sediment chamber. In EKP-HOM_2 these pH changes appear to be mitigated based on the effect from the recirculation system. Up to 71 hours, there is still a pH gradient across the sediment, this was further improved by increasing the rate at which fluid was circulated from 20 to 37 mL/min after 90 hours. The pH profile at 161 hours shows a decreased pH gradient across the sediment.

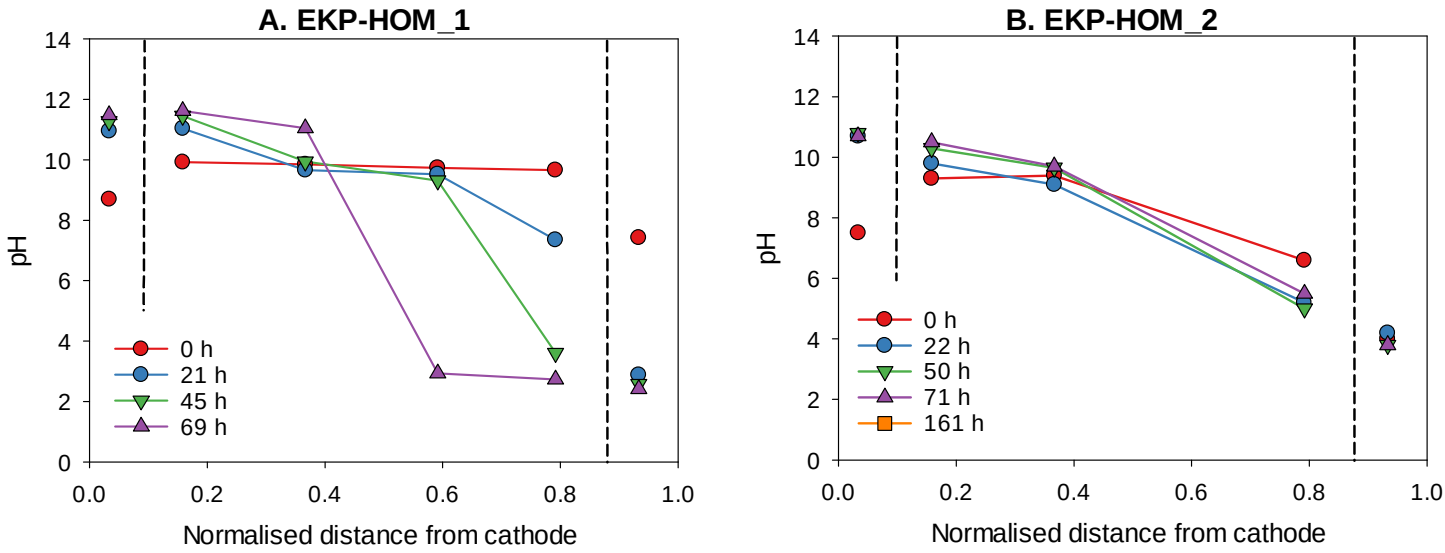

Figure 3.9 pH profiles in the electrode chambers and across the sediment sections for EKP-HOM_1 and EKP-HOM_2. Dashed lines represent the sediment – electrode chamber boundary.

The nitrate concentrations for EKP-HOM_2 shows that the recirculation system influences this species (Figure 3.10). In the rig where EK is applied, nitrate appears to migrate from the anode to the cathode as expected (Figure 3.10A). However, in the control system nitrate concentration is elevated after 71 hours in the zone adjacent to the anode (Figure 3.10B). This probably results from the pulsing effect from the high rate of pumping into the base of the anode chamber. After 71 hours there is a uniform concentration of nitrate across the sediment chamber (161 hours) following the increase in recirculation flow rate. This is due to fluid being pumped in at the anode and out at the cathode effectively turning the sediment section into a flow cell. This was confirmed with an experiment under the same conditions (no EK) using fluorescein to visually monitor fluid advection. On this basis the recirculation system in Figure 3.9 was not continued as a viable pH control method in this experimental setup.

3.3.6.2 Method 2 - electrode conditioning

The pH control method was changed to electrode conditioning. This allowed the pH control method and the amendment delivery mechanism to be separated and provided nitrate

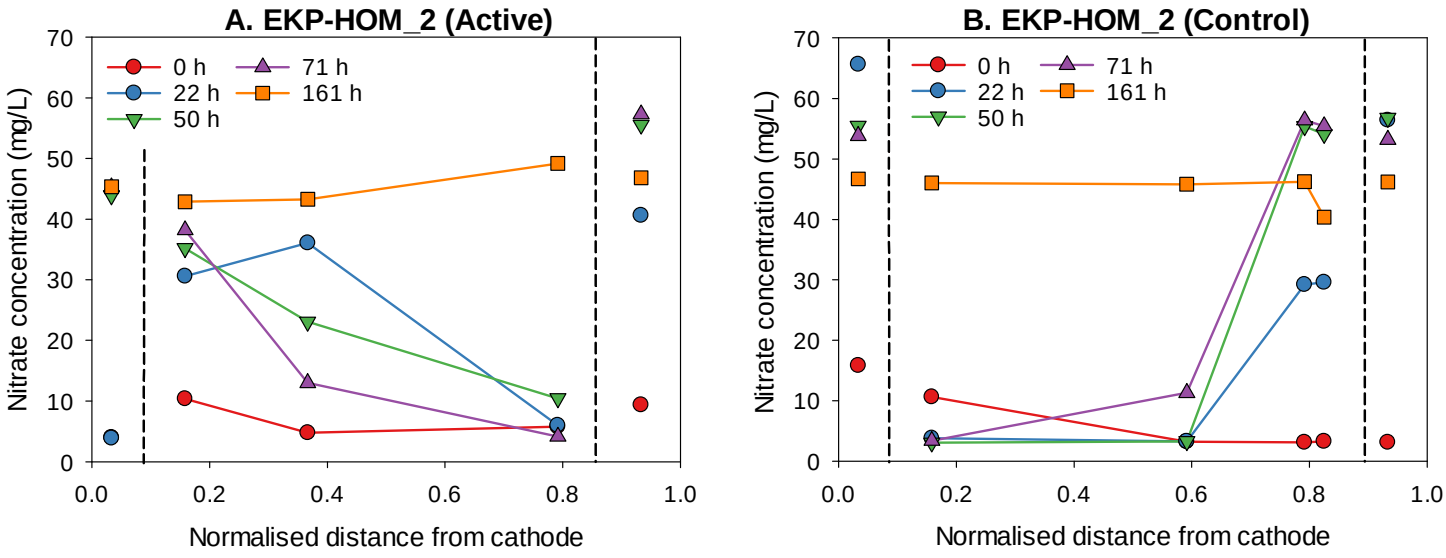

Figure 3.10 Nitrate concentrations for experiment EKP-HOM_2. A is the active rig with EK applied; and B. is the control rig with no EK applied. Dashed lines represent the sediment – electrode chamber boundary.

breakthrough profiles at the anode. Better characterisation of nitrate migration was required as part of the third research objective.

The electrode conditioning method presented in Wu et al. (2007) was developed for the experimental setup with several modifications. This configuration is referred to as Rig-4 (Figure 3.5D). Concentrated acid and base solutions (1 M HCl and NaOH) were added to neutralise electrolysis reactions in the cathode and anode respectively. Delivery was regulated using a timer that would activate and deactivate the pump (Ismatec, Ecoline VC-MS/CA 8-6) every 3 hours. The duration of pumping controlled how much acid and base was added to the electrodes which in turn was informed by the rate of hydrogen (H^+) and hydroxyl (OH^-) ion generation (Kim and Han, 2003):

$$R_{H^+/OH^-} = \frac{I}{F}$$

(Equation 3.3)

Where $R_{H+/OH-}$ is the rate of H^+ (or OH^-) generated (mol/s); I is the electric current; and F is Faraday constant. The calculation assumes 100% Faradaic efficiency at the electrode. The rate of H^+ and OH^- generation in experiment EKP-HET_3 and EKP-HOM_5 was informed by the maximum current observed in experiment EKP-HET_2 and EKP-HOM_4 as 50 mA. Based on this $5.6x10^{-3}$ mol of H^+ or OH^- are generated over a 3 hour period at the electrodes. This would require a flow rate of 0.41 mL/min to deliver 1 M solution over a 13.7 min period.

Experiments using Rig-4 (Figure 3.5D) included both heterogeneous and homogeneous sediment configurations. The pH of pore fluid samples for experiments EKP-HET_2, EKP-HOM_4, EKP-HET_3 and EKP-HOM_5 is shown in Figure 3.11A-D. No pH control is applied in EKP-HET_2 and EKP-HOM_4, whereas electrode conditioning was used in EKP-HET_3 and EKP-HOM_5. It is clear that the pH front is generated quickly (within 96 hours) where no pH control is applied (Figure 3.11A and B). These changes are avoided in experiments where electrode conditioning is used, but some variations in the pH across

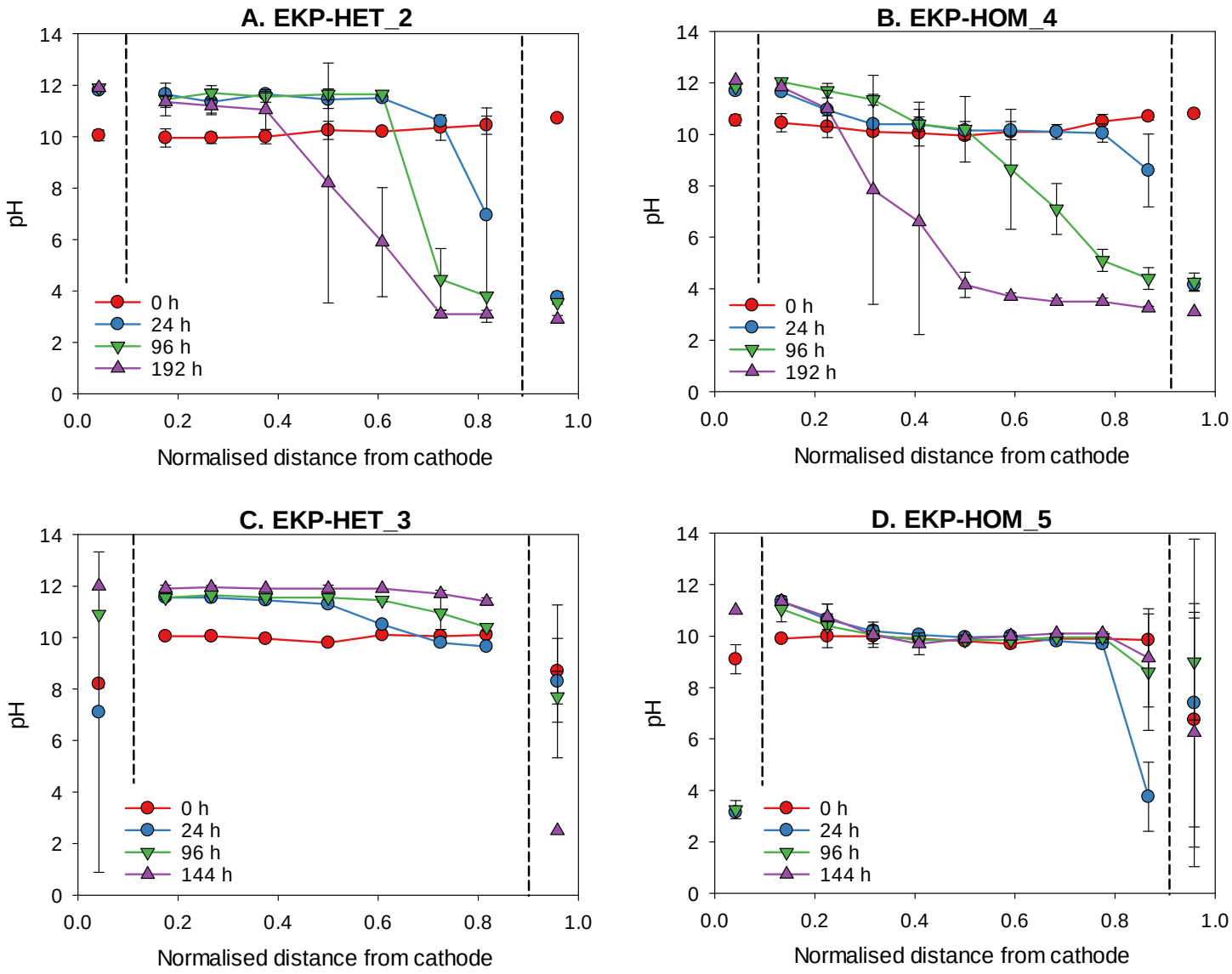

Figure 3.11 pH profiles in the electrode chambers and sediments sections for: A, EKP-HET_2; B, EKP-HOM_4; C, EKP-HET_3; and D, EKP-HOM_5. Error bars represent one standard deviation from the mean of two replicates. Dashed lines represent the sediment – electrode chamber boundary.

the sediment still remains (Figure 3.11C and D). In EKP-HET_3 and EKP-HOM_5 pH varies considerably within the electrode chambers as the acid and base are added, creating short term fluctuations. Within the sediment pH varies, for example in EKP-HOM_5 the pH decrease adjacent to the anode after 24 hours.

These results also highlight an interesting effect of heterogeneity. In EKP-HET_2 the pH fronts form further into the sediment chamber within a heterogeneous setting compared with the corresponding homogeneous setting, EKP-HOM_4 (Figure 3.11A and B). This is

the result of OH^- ions in the heterogeneous setting migrating faster into the sediment than OH^- ions in the homogeneous setting. It is related to the influence of the sediment setting on the voltage gradient. A higher voltage gradient is observed across the cathode-sediment interface in EKP-HET_2 compared with EKP-HOM_4, supporting a greater mass flux of OH^- ions into the sediment (Figure 3.12). This phenomenon is investigated in more detail with regards to nitrate migration in Chapter 4.

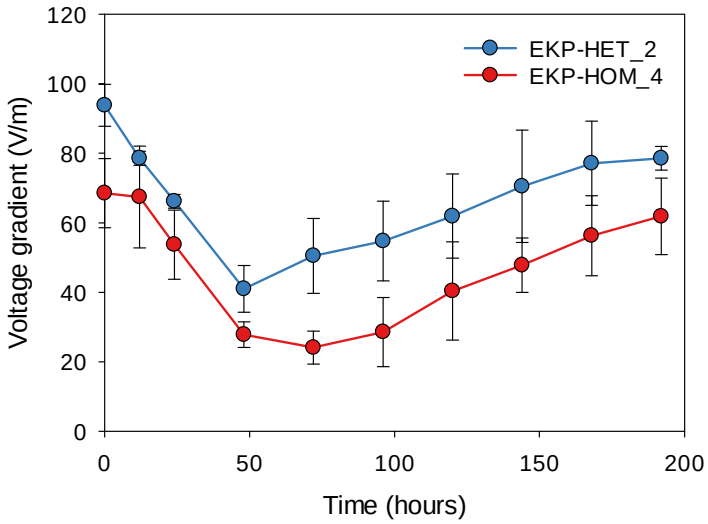

Figure 3.12 voltage gradient across the cathode – sediment interface for EKP-HET_2 and EK-HOM_4. Error bars represent one standard deviation from the mean of two replicates. Dashed lines represent the sediment – electrode chamber boundary.

Given the effectiveness of electrode conditioning at neutralising pH at electrodes, this method was used in all subsequent experiments. Constant current was applied in future tests to reduce pH fluctuations at the electrodes. Constant current provides a fixed value for the electric current passed through the system, making it easier to predict the amount of acid and base needed to neutralise pH changes. The effect of constant current is demonstrated with two profiles from experiments RQ2-HET_1 and RQ2-HOM in Chapter 4 (Figure 3.13). These experiments have the same setup configuration as EKP-HET_3 and EKP-HOM_5. The results show that pH variation within the electrode chambers is minimised, but with minor fluctuations in pH from the baseline value (pH 8, 0 hours) (Figure 3.13).

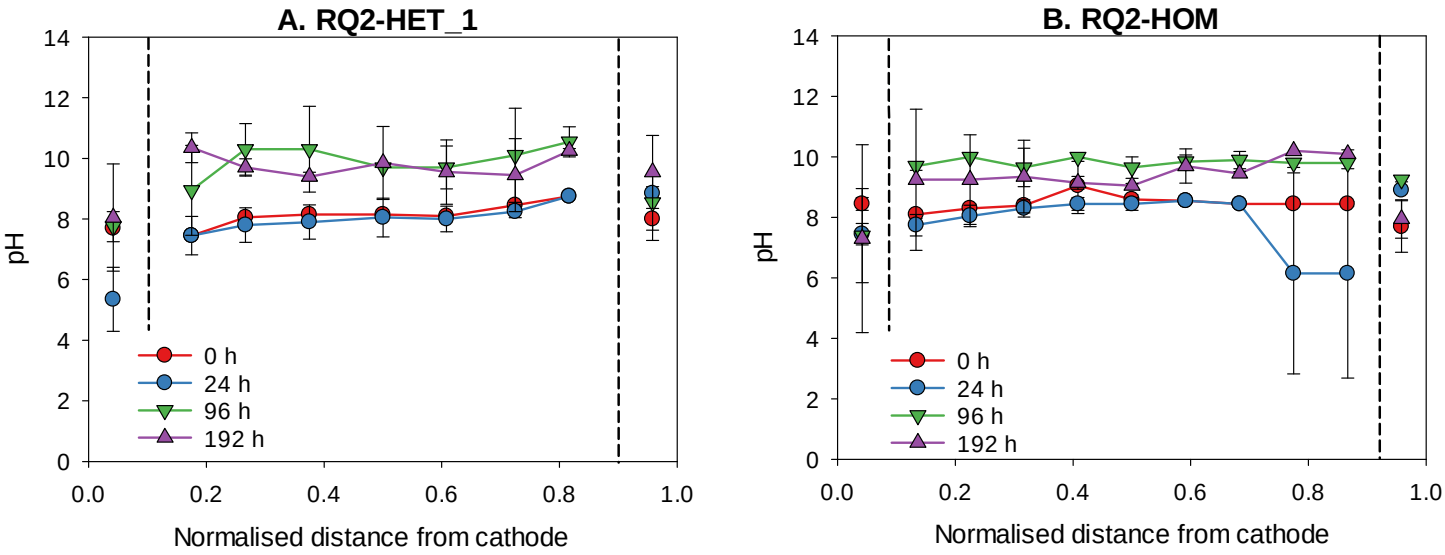

Figure 3.13 pH profiles in the electrode chambers and sediments sections for: A, RQ2-HET_1; and B, RQ2-HOM. Error bars represent one standard deviation from the mean of two replicates. Dashed lines represent the sediment – electrode chamber boundary.

In experiments where electrode conditioning is applied pH increases in the sediment over time, from pH 7-8 up to pH 10 (EKP-HET_3, Figure 3.11C; RQ2-HET_1, Figure 3.13A; RQ2-HOM, Figure 3.13). This is due to the fluid circulation setup, Rig-4 where pH changes at the anode are being neutralised more effectively than the cathode (Figure 3.5D). In the cathode chamber, fluid containing the amendment is pumped into the base and excess overflows to waste whereas in the anode fluid is stationary. The acid added at the cathode is less effective because neutralised electrode chamber fluid is lost to waste. This was not anticipated to affect the migration of nitrate because sharp pH gradients and subsequent spikes in the voltage gradient were avoided (see Section 3.3.6.3). However, this pH control technique would not be suitable for experiments that included a biological variable, where pH must be maintained around pH 7.

3.3.6.3 Influence on nitrate migration

Running an experiment with no pH control creates a front of OH- and H+ ions that meet in the sediment chamber and combine to create a band of low electrical conductivity fluid. This zone of low electrical conductivity creates a spike in the voltage gradient. Results from EKP-HOM_3 show this phenomenon by comparing pH and voltage gradient profiles

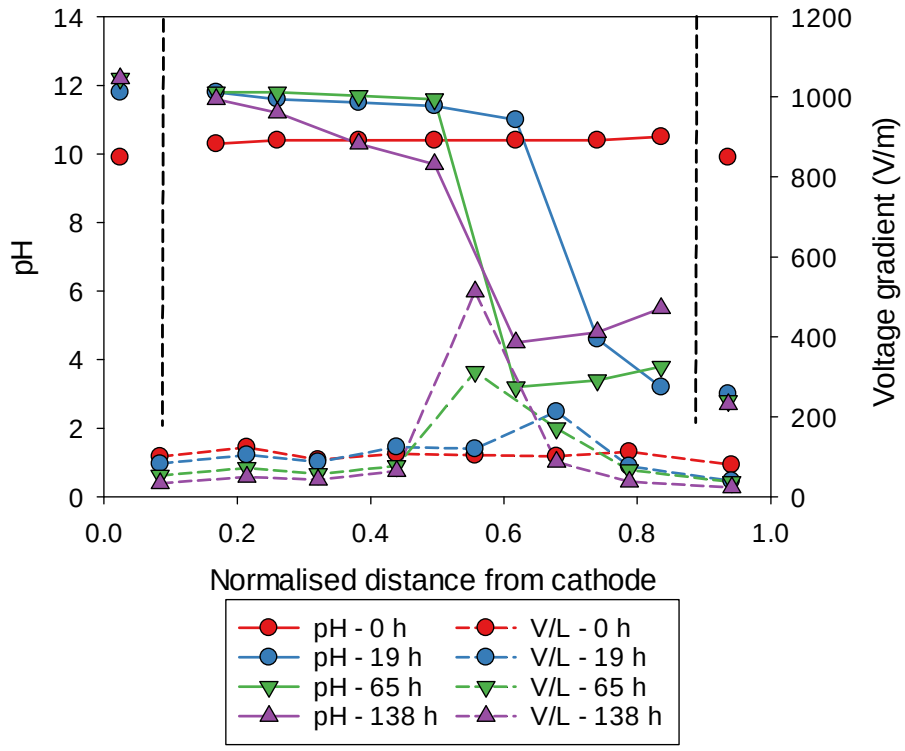

Figure 3.14 pH and voltage gradient profiles at different time points in the electrode chambers and sediments sections for experiment EKP-HOM_3. Dashed lines represent the sediment – electrode chamber boundary.

(Figure 3.14). The voltage gradient is calculated from the voltage difference between probe ports divided by the distance between them. There is a clear spatial correlation between the meeting of pH fronts and a spike in the voltage gradient.

A spike in the voltage gradient has an implication for nitrate electromigration. In Figure 3.15 a nitrate concentration profile is compared against spatial changes in the voltage gradient in an experiment with no pH control and a constant nitrate concentration at the cathode (EKP-HOM_4). At both time points (96 and 192 hours, Figure 3.15A and B respectively) there appears to be an inverse relationship between the spike in the voltage gradient and nitrate concentration. This is because the voltage gradient is proportional to the nitrate electromigration velocity. In zones where voltage gradient (and therefore nitrate transport velocity) is high there is a low nitrate concentration because ions will migrate out of that zone faster. Conversely, nitrate will accumulate in adjacent zones where the voltage

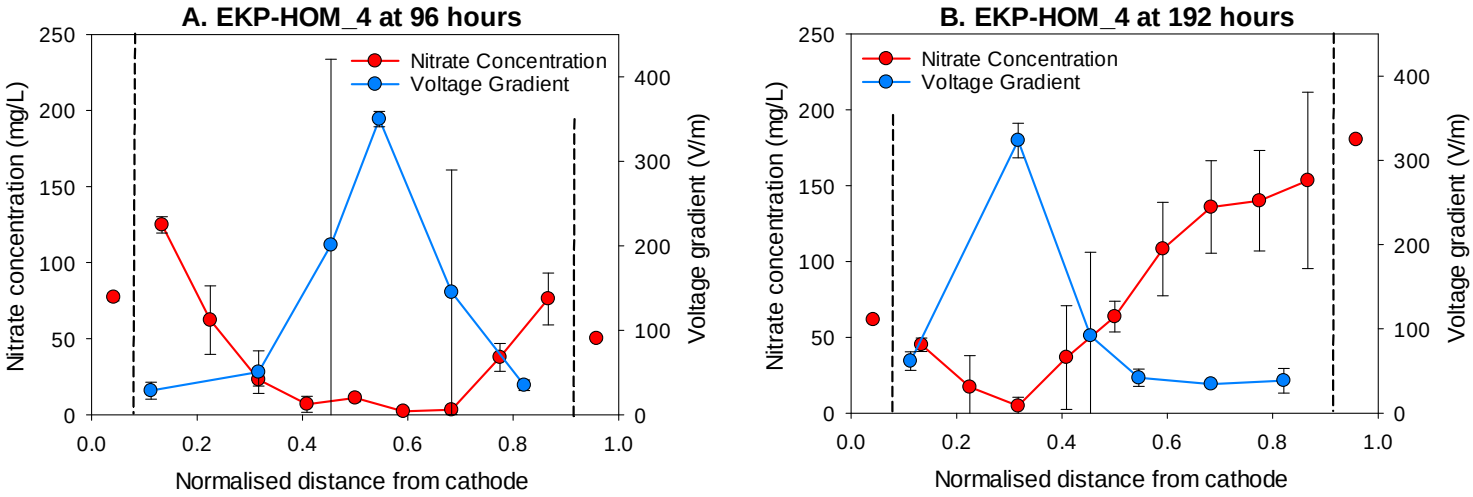

Figure 3.15 Nitrate concentration and voltage gradient profiles for EKP-HOM_4 at 96 and 192 hours. Error bars represent one standard deviation from the mean of two replicates. Dashed lines represent the sediment – electrode chamber boundary.

gradient has decreased. This phenomenon is known as amendment stalling. It was described by Hodges et al. (2013) who demonstrated permanganate stalling in clay cores in experiments where no pH control was applied.

Overall, this stalling phenomenon can effect nitrate migration through the sediment. In Figure 3.16 nitrate breakthrough at the anode is normalised to the voltage between the electrodes and compared between experiments where a constant concentration of 100 mg/L is migrated across the sediment section. EKP-HOM_4 and EKP-HET_2 do not have pH control, whereas the examples from Chapter 4, RQ2-HOM and RQ2-HET_1 have electrode conditioning applied. The results show that nitrate migration across the sediment is reduced in the absence of pH control compared with experiments with pH control. Furthermore, where pH control is applied there is greater differentiation between the homogeneous and heterogeneous system, which improves the interpretation of results. Hence all subsequent nitrate migration experiments were conducted with pH control.

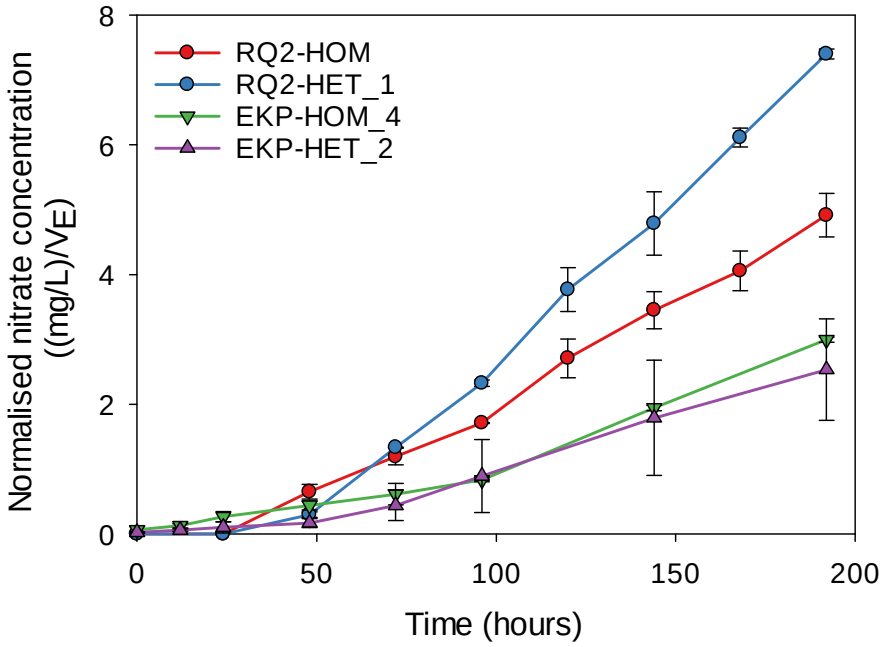

Figure 3.16 Nitrate breakthrough at the anode normalised to the voltage difference between electrodes for experiments without pH control, EKP-HET_2 and EKP-HOM_4, and with pH control, RQ2-HET_1 and RQ2-HOM. Error bars represent one standard deviation from two replicates.

3.3.7 Nitrate addition method

The method used to add the nitrate amendment to the cathode chamber changed during the preliminary experiment program. The order in which the methods were applied is shown in Table 3.1 and Figure 3.5 and range from Rig-1 to 4. Methods Rig 2 and 4 have already been discussed in relation to pH control; methods Rig 1 and 3 are shown in Figure 3.5A and C respectively. The decision to continue method Rig-4 in later experiments was based on: (1) the addition of a constant rather than single nitrate concentration; and (2) the influence of the method on the unintended advection of nitrate through the sediment.

Amendment addition methods Rig-1 to 3 were designed to add a single concentration of nitrate to the cathode chamber by circulating the nitrate concentration between the reservoir tank and the cathode chamber. A single nitrate concentration was used in other amendment electromigration studies (Lohner et al., 2008a, 2008b), but in the current experiments resulted in poor data resolution with regards to determining a relationship

between nitrate migration and pH values. For example, the nitrate concentrations in the reservoir tank and cathode chamber for EKP-HOM_3 are shown in Figure 3.17. The nitrate concentrations decrease rapidly within 60 hours around the time the pH front is beginning to form (Figure 3.14) making it difficult to determine the influence of pH fronts on nitrate migration.

A constant nitrate concentration addition method was achieved by slowly flushing the cathode chamber with a nitrate solution stored in the reservoir tank. The excess cathode chamber fluid then drained off to waste. The nitrate concentration in the reservoir tank was kept constant, while the concentration in the cathode chamber was allowed to fluctuate (Figure 3.17). Maintaining a constant cathode chamber nitrate concentration is difficult because it is subject to the mass flux of nitrate out of the chamber, which is subsequently affected by changes in voltage gradient. All future experiments used nitrate added at a constant concentration.

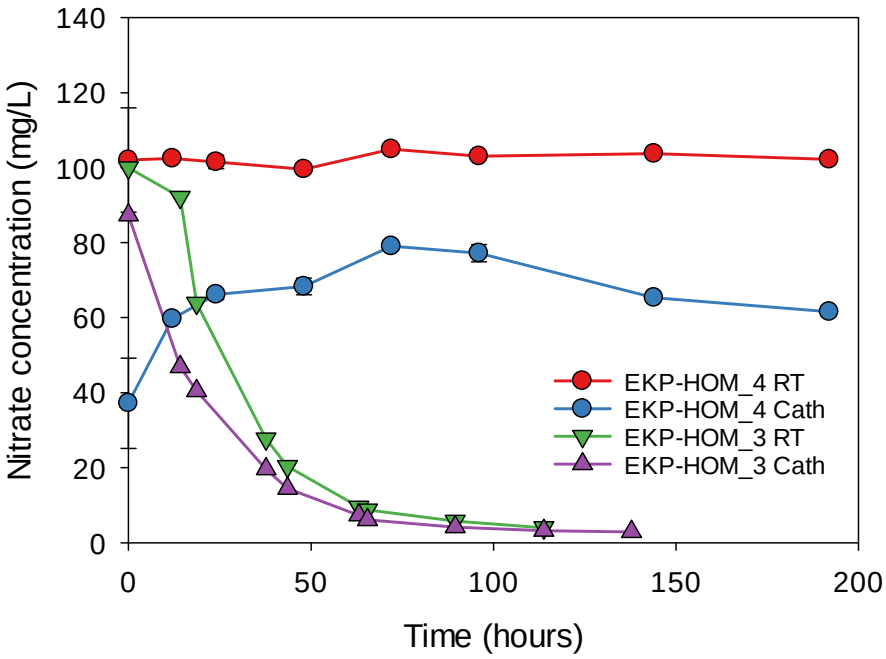

Figure 3.17 Nitrate concentrations in the reservoir tank (RT) and cathode (Cath) for experiments where nitrate is applied constantly (EKP-HOM_4) and at a single concentration (EKP-HOM_3). Error bars on EKP-HOM_4 represent one standard deviation from the mean of two replicates.

Some nitrate addition methods introduced nitrate via advection and/or dispersion. Ideally this effect is minimised because it is a competing transport mechanism to electromigration, and could therefore unintentionally affect the results. The influence of advection has been noted in Rig-2 (Figure 3.10) and Rig-3 (Figure 3.5C) fluid circulation methods (Figure 3.5). The Rig-3 setup was similar to that used in Lohner et al. (2008a); it was selected for these experiments because it allowed electrode chamber fluids to be isolated from the effect of the electrode, allowing the option for *in situ* pH monitoring and control. The Rig-3 setup was tested in EKP-HET_1 and fluid was pumped between the reservoir tank and electrode chamber at 10 mL/min (Ismatec, REGLO MS-4/8). Results show the nitrate concentration increased in both the active (EK applied) and control (no EK applied) anode reservoir tanks over time (Figure 3.18). This implies that the nitrate addition method was introducing an additional transport mechanism for nitrate because no nitrate accumulation should occur in the control experiment. The cause is not related to an imbalance in the hydraulic head because this was maintained at a constant level through the experiments. Instead, it is

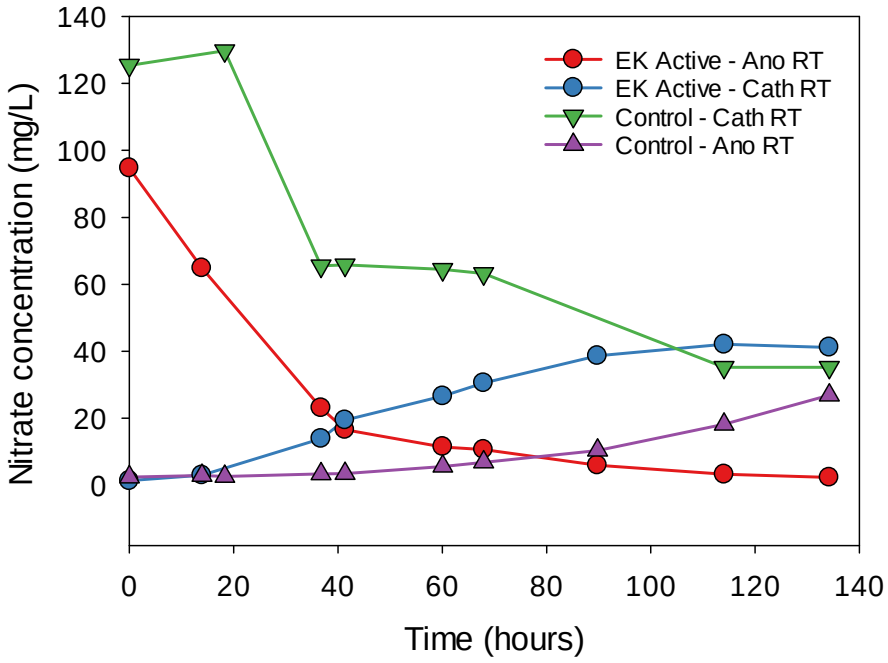

Figure 3.18 Nitrate concentrations in the cathode (Cath) and anode (Ano) reservoir tanks (RT) for the control and active experiments in EKP-HET_1.

likely that a discrepancy in the pumping rate into each electrode chamber created a pressure difference that initiated fluid advection. This amendment addition method was not used in later experiments.

The best methods for minimising non-EK related transport of nitrate into the sediment were Rig-1 and Rig-4 (Figure 3.5A and D respectively). There is no circulation around the anode chamber, therefore no viable flow paths are generated. Furthermore, there is a very low pumping rate (2 mL/min) from the reservoir tank into the cathode, which is based on the observed flux of nitrate into the sediment versus the rate it is replenished by the reservoir tank. Nitrate profiles for Rig-1 and Rig-4 control experiments with no-EK are shown in Figure 3.19. The control experiment for Rig-4 is taken from Chapter 4, RQ2-Control_2 (Figure 3.19B). Both profiles show a low level of nitrate intrusion into the sediment; any movement of nitrate into the sediment is likely to arise from pore fluid sampling. This effect will be exacerbated in EKP-HOM_3 (Figure 3.19A) due to the high K value of the material ($1x10^{-4}$ m/s) and could explain the relatively high nitrate concentrations after 138 hours. Further analysis of the pore fluid sampling versus electromigration flux is included in Chapters 4 and 5.

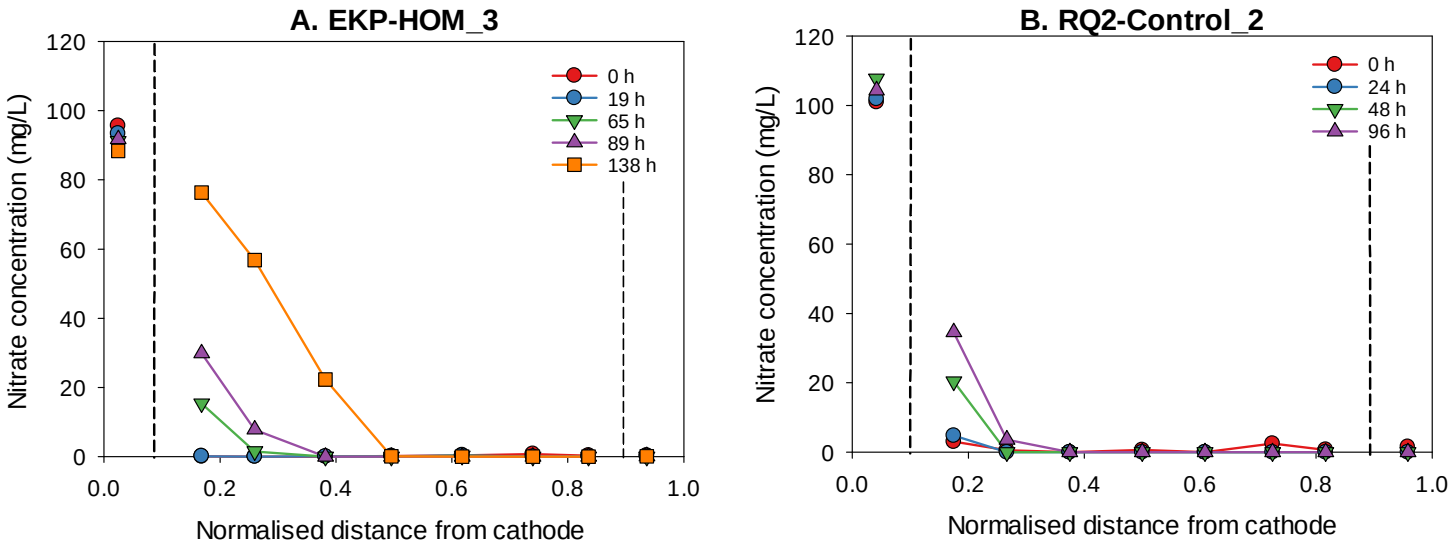

Figure 3.19 Nitrate concentration profiles across the sediment section at different time points for: A, EKP-HOM_3 and B, RQ2-Control_2. Dashed lines represent the sediment – electrode chamber boundary.

3.4 Conclusions

The experimental laboratory apparatus design to accommodate electrokinetic experiments is suitable for its intended use based on the results from these preliminary experiments. As well as accommodating a saturated and consolidated sediment chamber, the setup also identified key EK phenomena related to the research objectives. These included: (1) pH changes at the electrodes and the subsequent pH fronts that migrate into the sediment chamber; (2) voltage gradient spikes associated with the meeting of pH fronts; (3) the need to control electrolysis reactions to minimise pH changes; and (4) nitrate migration behaviour from the cathode to anode in both homogeneous and heterogeneous sediment configurations.

The results from these preliminary experiments informed the method development that was carried forward into later experiments. These include:

- Consolidating material within the rigs using a shaker table to achieve a more repeatable porosity value compared with repeated tamping using a single weight.
- Pore fluid sampling using narrow bore PEEK tubing with a sintered glass cube fitted to the end, to prevent blockages and improve resolution of results.
- Conducting all nitrate migration experiments with pH control by electrode conditioning. Allowing the pH front to propagate through the sediment can stall nitrate electromigration and influence results.
- Adding nitrate to the cathode as a constant concentration rather than a single concentration. The former extends the experiment duration and allows better capture of electromigration phenomena

Chapter 4 Electromigration of nitrate through hydraulic conductivity contrasts

4.1 Introduction

Most studies of EK applications have been conducted in homogeneous rather than heterogeneous materials, although the latter more appropriately represent the subsurface environment. In many cases physical heterogeneity, represented by spatial variability in the distribution and form of materials with different K, exerts a significant control on solute transport by advection-dispersion (Song et al., 2014), contaminant distribution (Rahman et al., 2005) and options for remediation strategies in soils and aquifers (McCray et al., 2011). EK-moderated transport of substances into, and out of, low K zones in a heterogeneous setting can be significantly more effective than advection (Reynolds et al*.,* 2008; Saichek and Reddy, 2005). However, to date there are no empirical studies of the influence of physical heterogeneity on EK transport. Nitrate is often used as an amendment to support the *in situ* bioremediation of organic chemicals in contaminated aquifers, because it is less affected by solubility limitations (unlike oxygen) and can support the anaerobic biodegradation of a wide range of organic compounds (Spence et al., 2001; Bauer et al., 2008; Xu et al., 2010). However, the performance of bioremediation can be significantly limited due to the effect that physical heterogeneity exerts on the distribution and mixing of microbes and solutes in the subsurface (Song and Seagren, 2008). Therefore, if the migration and bioavailability of an amendment across a K boundary where advection is significantly reduced can be increased using EK transport processes, biodegradation rates for bioremediation may be enhanced in these scenarios.

4.1.1 Research question and hypotheses

The research question addressed in this chapter (RQ2) is: What is the influence of a transition between high- and low-K on the electromigration of nitrate under ideal

conditions? In these experiments, nitrate is used as a representative amendment for EK-BIO applications (Thevanayagam and Rishindran, 1998; Tiehm et al., 2010). The hypotheses associated with this question are based on the electrokinetic theory in the introduction chapter, they include: (1) that mass transport of an amendment will decrease as K decreases based on a lower effective ionic mobility (resulting from an increase in the tortuosity factor, Equation 1.3) and increasing electroosmotic permeability value (due the presence of materials with a high surface charge and therefore zeta potential, Equation 1.1); and (2) voltage gradient will be higher across zones of low-K material due to the influence of material properties (namely the effective ionic mobility) on the effective electrical conductivity (as per Equation 1.4, 1.10 and 1.12).

The objectives of these experiments were to:

1. Compare the migration of nitrate under homogeneous and heterogeneous conditions. Heterogeneity is represented by a K contrast perpendicular to the direction of the electric current;
2. Determine the effect of physical heterogeneity described in (1) on an amendment applied at different concentrations, and;
3. Determine the effect of varying the K contrast described in (1) on the amendment mass flux and distribution of the voltage gradient.

4.2 Materials and methods

4.2.1 Material properties

The porous medium was created using soda-lime-silica glass beads (Potters Ballotini Ltd) (the same as the preliminary experiments) and Speswhite kaolin (Imerys Performance Materials Ltd) to represent a model system composed of two materials with consistent properties. The physical heterogeneity in these experiments is a contrast between high and low K, created by positioning layers of appropriate material in the test cell as shown in Figure 4.1A. High hydraulic conductivity (high-K) sections were consistently produced

using 1.4 mm diameter glass beads, whereas low hydraulic conductivity (low-K) sections were produced using a 90/10 mix of 0.25 and 0.5 mm glass beads. Between experiments

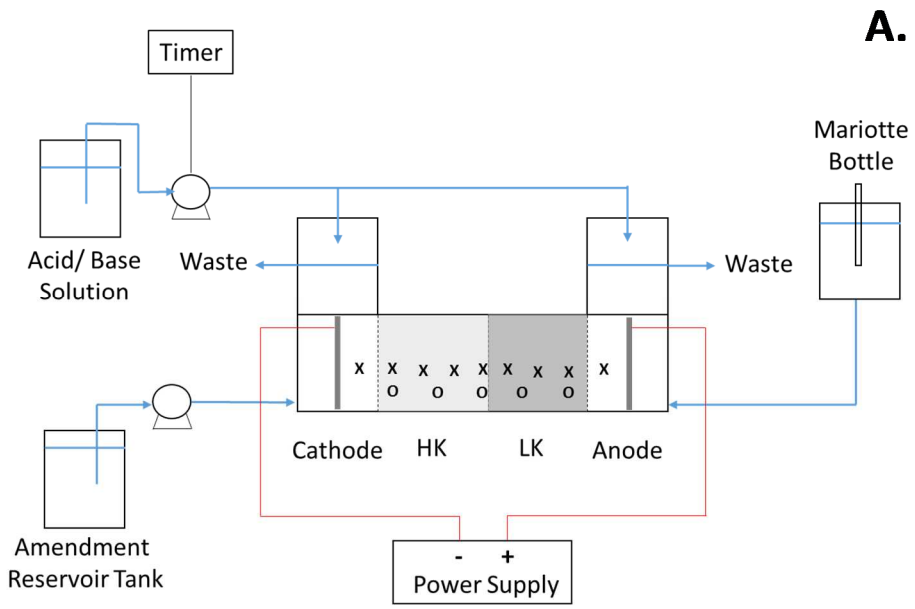

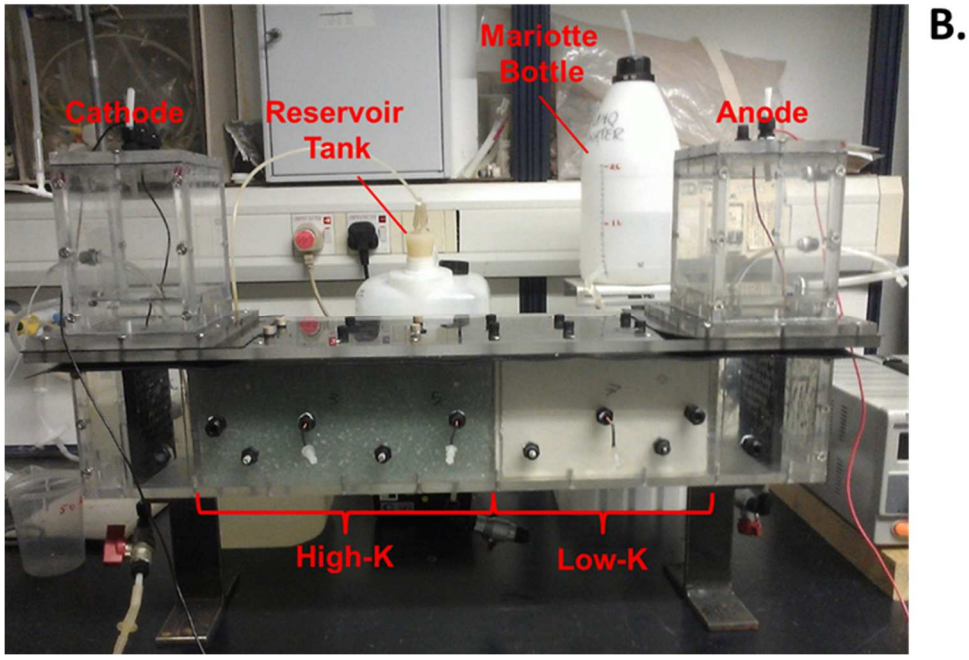

Figure 4.1A, Schematic of experimental set-up used in tests. Sediment chamber volume: 7.5 L; and electrode chamber 2 L. HK and LK represent the high- and low- K contrasts in the sediment, X and O represent sampling and voltage probe ports; B, annotated digital image of the experimental setup.

the glass beads were cleaned with deionised water and autoclaved to minimise biological activity in the tests. Additional K contrasts were achieved by blending the small glass bead mix with different proportions by weight of kaolinite. The clay grain size distribution is 76 - 83% ≤ 2 µm and introduced a small amount of surface-adherent dissolvable salts (approximately 0.2 % by mass of sodium and sulphate ions based on dissolution tests, see figure in Appendix I) into the test fluids.

Consolidation of glass beads in preparation for tests was achieved using the consolidation method applied in Section 3.3.4. The shaker table was calibrated to a frequency of 31 Hz using a hand-held accelerometer. The test cells were filled with material in layers up to 3 cm and placed on the shaker table for intervals of 20 s. This was repeated until the test cell was full, excess material removed and the lid secured. The glass bead mix and clay was added together and combined with sterilised synthetic groundwater to give a mass equivalent to the clay's plastic limit (approximately 30% by weight of the clay). This was to facilitate mixing and aid compaction. The mixture was then wet packed into the sediment chamber in the test cell (Figure 4.1B) and tamped down using a ceramic pestle, similar to the method used in Saichek and Reddy (2005).

The K contrast in these experiments was the same as the preliminary experiments. It was achieved by inserting a 0.5 mm thick stainless steel plate into vertical slots on the inside of the sediment chamber to separate the high- and low-K sections. The material was then packed in the respective compartment either side of the plate, and the plate removed. This left a small space (approx. 0.5 mm wide) that was then back-filled by further consolidation. Following consolidation, the rig was constructed as per the protocol in section 3.3.1. The dimensions of the high- and low-K sections were H:125 x W:125 x L:280 mm and H:125 x W:125 x L:210 mm respectively; the difference accommodates the distribution of sample and voltage probe ports (Figure 4.1B).

The electrolyte used in these experiments was the same used in the preliminary experiments. A synthetic groundwater with an electrical conductivity of 700 µS/cm, achieved using a NaCl-deionised water solution to give 0.3 g-NaCl/L. Prior to adding NaCl deionised water was run through a tangential flow filtration unit (aperture 1µm) to remove bacterial cells and minimise biological activity during tests. The test cells containing the consolidated material were saturated with synthetic groundwater from the base up to remove any trapped air. Saturation was considered complete when water was observed to emerge from 12 evenly spaced ports in the lid; these were then sealed.

4.2.2 Bench-scale setup

A 1-D experimental test cell was developed for the preparation of reproducible sections of packed materials with high- and low-K (Figure 4.1B). The design of the experimental rig is detailed in section 3.2. Leaks were prevented using rubber gaskets and silicone grease for the lid and header tanks. Once material was consolidated within the test cell and the lid and header tanks secured synthetic groundwater and the amendment solution was circulated using a peristaltic pump (Ismatec, REGLO MS-4/8) from the reservoir tank into the cathode chamber at 10 mL/min. This was done until the fluid in the cathode chamber had been displaced (approx. 3.5 hr); at this point a pore fluid baseline sample was taken. After this a direct current was applied to the system from a power pack (Digimess, PM6003-3). Constant current was established and checked with a multimeter (Digitek, DT-4000ZC).

Samples of the pore fluid for chemical analysis were taken every 2 – 4 days during the experiment via 9 narrow bore (ID = 0.5 mm) PEEK tubes located along the length of the test chamber. The sampling tubes extended from the edge of the sediment chamber into the centre of the sediment mass and were offset to each other on either side of the chamber. This ensured that any edge effects from the chamber panels on fluid sampling were avoided and that the centreline of the fluid flow path could be sampled in detail. At each time point 7 samples of the pore fluid in the sediment chamber and 1 sample from

each electrode chamber were taken. Five voltage probes consisting of 4 mm diameter grade 316 stainless steel rods housed in HDPE piping were fitted within the chamber. Voltages and current were logged every 24 hours or after sampling during the tests. The sample and voltage reading protocol was conducted as per section 3.3.2.

Nitrate was selected as it is a representative amendment used extensively in electrokinetic-bioremediation studies (Thevanayagam and Rishindran, 1998; Tiehm et al., 2010). Bromide was used as a tracer under an electric field because it is chemically conservative and has similar electromigration transport properties to nitrate. Amendments were added to the cathode at a rate 1.5 mL/min from a 10 L reservoir tank maintained at a constant concentration of either nitrate or bromide solutions. The reservoir tank was topped up at regular intervals.

4.2.3 Electrokinetic apparatus and test conditions

A direct current was applied at a constant current strength of 25 mA (1.6 A/m^2) to allow more effective control of pH changes at the electrodes. The benefits of applying a constant current over a constant voltage on the nitrate migration in these experiments are discussed further in Chapter 3, Section 3.3.6.2 and 3.3.6.3. Electrodes were made from a 125 x 125 x 10 mm graphite block (Chapter 3, section 3.2).

The electrode conditioning method presented in Chapter 3, Section 3.3.6.2 was used to neutralise electrolysis reactions (see Equation 1.6 and Equation 1.7 for anode and cathode reactions respectively). This is the addition of acid and base solutions (1 M HCl and NaOH) to the cathode and anode controlled by a timer that doses the electrode chambers every 3 hours. The application of constant current allowed a more accurate prediction of the rate of acid (H^+) and base (OH^-) generation compared to the preliminary experiments. Based on Equation 3.3, a current of 25 mA and a pumping rate of 0.41 mL/min the timer will need to initiate the pump for 6.8 min every 3 hours. In experiments where electroosmotic flow

was evident a Mariotte bottle was used to ensure that the anode compartment was not depleted of water and no hydraulic gradient developed.

4.2.4 Experimental design

Two types of experiment were undertaken to address the research question in this chapter: (1) bromide tracer tests to determine the effective ionic mobility of the materials used in the high-K and low-K sections; and (2) nitrate migration experiments under homogeneous and heterogeneous conditions. The experimental conditions for both types of experiment are given in Table 4.1 and Table 4.2 respectively.

The bromide tracer tests were all run under homogeneous conditions. The materials tested (properties shown in Table 4.1) are generated to the same specifications as the materials for the nitrate migration experiments and therefore represent the range of material types used including both high and low-K materials. Bromide was added to the system at 1 g-Br/L in the reservoir tanks and a constant current strength of 25 mA was applied in all experiments. The tracer experiments were run with no replicates. Fluid samples and voltage readings were taken every 24 hours.

Table 4.1 Experimental details for the bromide tracer experiments.

Experiment name	Material properties			Experiment duration (hours)
	n* (-)	Clay (%)	K† (m/s)	
RQ2-Tracer_1	0.29	-	$2.2x10^{-4}$ (± $2.1x10^{-5}$)	192
RQ2-Tracer_2	0.37	-	$1.5x10^{-5}$ (± $1.6x10^{-6}$)	192
RQ2-Tracer_3	0.29	5	$1.6x10^{-6}$ (± $2.7x10^{-7}$)	240
RQ2-Tracer_4	0.34	10	$1.2x10^{-7}$ (±$2.4x10^{-7}$)	240
RQ2-Tracer_5	0.41	20	$4.5x10^{-9}$ (±$1.1x10^{-9}$)	263

* Determined by method in Chapter 3, Section 3.3.4
† Determined by method in Chapter 3, Section 3.3.5

Nitrate migration experiments were run under both homogeneous and heterogeneous conditions. For heterogeneous experiments the properties of the high-K material section remained the same between experiments: K, 2.2 x 10^{-4} (± $2.1x10^{-5}$) m/s; and porosity, 0.29. Experiments included low and high nitrate inlet concentrations of 0.1 and 1 g-NO_3/L, respectively. At low concentration nitrate migration was compared under heterogeneous

Table 4.2 Experimental details for nitrate migration experiments under homogeneous (HOM) and heterogeneous (HET) conditions.

Name	Reservoir tank concentration (g/L)	Low-K properties/ HOM properties			Reps	Duration (hours)
		n* (-)	Clay (%)	K† (m/s)		
RQ2-HOM	0.1	0.37	-	$1.5x10^{-5}$ ($\pm$ $1.6x10^{-6}$)	2	192
RQ2-HET_1	0.1	0.37	-	$1.5x10^{-5}$ ($\pm$ $1.6x10^{-6}$)	3	192
RQ2-HET_2	1	0.37	-	$1.5x10^{-5}$ ($\pm$ $1.6x10^{-6}$)	2	192
RQ2-HET_3	1	0.29	5	$1.6x10^{-6}$ ($\pm$ $2.7x10^{-7}$)	1	288
RQ2-HET_4	1	0.34	10	$1.2x10^{-7}$ ($2.4x10^{-7}$)	1	288
RQ2-HET_5	1	0.41	20	$4.5x10^{-9}$ ($1.1x10^{-9}$)	1	288
RQ2-Control_1	-	0.37	-	$1.5x10^{-5}$ ($\pm$ $1.6x10^{-6}$)	1	192
RQ2-Control_2	0.1	0.37	-	$1.5x10^{-5}$ ($\pm$ $1.6x10^{-6}$)	1	192

* Determined by method in Chapter 3, Section 3.3.4
† Determined by method in Chapter 3, Section 3.3.5

and homogeneous conditions, whereas at high concentration nitrate migration was evaluated for increasing K contrasts (Table 4.2). RQ2-Control_1 was run without nitrate in the reservoir tank and is used isolate the effects of EK application on background ions. All experiments were run under a constant current strength of 25 mA, except for RQ2-Control_2 where no EK was applied. This experiment was used to determine the influence pore fluid extraction on nitrate migration into the sediment (Chapter 3, Section 3.3.7). Replicates were run for experiments with low nitrate inlet concentration, RQ2-HET_1, RQ2-HOM, and high inlet concentration, RQ2-HET_2. Experimental reproducibility is inferred from tests with one or more replicates.

The experimental results were interpreted according to theoretical predictions using numerical analysis of the nitrate accumulation at the anode over time from the point it is first detected (i.e. nitrate breakthrough). This is based on the predicted electromigration mass flux (Equation 1.2) into the anode chamber over a specified time period across the sediment/ anode chamber interface. It is determined by:

$$C_i^{Ano} = \frac{J_i^{em} t A}{V^{Ano}}$$

Equation 4.1

where C_i^{Ano}, is the concentration at the anode (mg/m^3); and V^{Ano} (m^3), is the volume of the anode chamber. The calculation assumes that nitrate mass in the anode is conserved. Calculations of the effective electrical conductivity (Equation 1.4) are based on ion concentrations determined by major ion analysis (Chapter 3, Section 3.3.3). All experiments were run with pH control to prevent the generation of a sharp pH gradient across the sediment and the subsequent effect on the voltage gradient as per the observations in Chapter 3, Section 3.3.6.2. Values for nitrate breakthrough at the anode, nitrate mass transport and velocity are all normalised against the voltage between electrodes (V_E). This accounts for the fluctuating voltage value due to the influence of applying DC as a constant current. Raw data for these experiments are presented in Appendix I.

4.2.5 Analytical methods

The same analytical methods applied in the preliminary experiments, outlined in Chapter 3, Section 3.3.3 were applied in these experiments.

4.3 Results and discussion

4.3.1 Bromide electromigration under homogeneous conditions

Tracer experiments were conducted using bromide to determine the effective ionic mobility of nitrate for the different materials evaluated in the nitrate migration experiments. This is justified as bromide has similar transport properties to nitrate under an electric field, for example both have similar ionic mobility at infinite dilution (bromide: 8.1x10^{-8} m^2/s-V; nitrate: 7.4x10^{-8} m^2/s-V (CRC, 2002)).

Results from the bromide tracer experiments are shown in Table 4.3. Average values for bromide mass transport are based on data from time points after 100 hours. At this point in the experiments the system is in equilibrium with respect to bromide (or nitrate) mass transport. This is when amendment mass transport is into the sediment from the cathode boundary and out of the sediment at the anode boundary. Mass transport is defined as the

mass of bromide that passed through the sediment over time and accumulated at the anode, normalised to the voltage between electrodes. The mass flux can be determined by dividing the mass transport by the sediment area cross-section, this can then be used to find the effective ionic mobility by re-arranging Equation 1.2:

$$u_i^* = \frac{J_i^{em}}{C_i^{Cath}\frac{\Delta E}{\Delta x}}$$

Equation 4.2

where C_i^{Cath} is the concentration at the cathode. The mass flux at the anode/ sediment boundary, voltage gradient between electrodes and the concentration of bromide at the cathode are all measured directly from the experiment. This equation assumes that the mass flux at the cathode/ sediment boundary is equal to the mass flux at the anode/ sediment boundary. This is a reasonable assumption given the relationship between the observed nitrate mass fluxes at the cathode/ sediment and sediment/ anode boundaries for RQ2-HOM (Figure 4.2). These values are calculated based on nitrate mass in the sediment from pore fluid samples and nitrate mass at the anode. Mass flux data for the bromide tracer experiments is not available because sediment pore fluid samples were not taken.

Table 4.3 Bromide transport properties estimated from tracer tests. Mass transport and migration velocity are normalised against the voltage difference between electrodes. The error represents one standard deviation from the mean of time points after 100 hours.

Experiment	Bromide Mass Transport [(mg/s)/V_E]	Bromide Effective Ionic Mobility* (m^2/s-V)	Tortuosity Factor† (-)	Migration Velocity [(m/s)/V_E]	Nitrate Effective Ionic Mobility‡ (m^2/s-V)
RQ2-Tracer_1	$1.4x10^{-4}$ (± $4.5x10^{-5}$)	$1.4x10^{-8}$ (± $1.1x10^{-9}$)	0.56 (± 0.04)	$5.1x10^{-8}$	$1.3x10^{-8}$ (± $1.0x10^{-9}$)
RQ2-Tracer_2	$1.7x10^{-4}$ (± $7.6x10^{-5}$)	$1.5x10^{-8}$ (± $1.6x10^{-9}$)	0.55 (± 0.06)	$4.1x10^{-8}$	$1.4x10^{-8}$ (± $1.5x10^{-9}$)
RQ2-Tracer_3	$1.1x10^{-4}$ (± $1.2x10^{-5}$)	$1.1x10^{-8}$ (± $1.5x10^{-9}$)	0.47 (± 0.06)	$3.5x10^{-8}$	$1.0x10^{-8}$ (± $1.3x10^{-9}$)
RQ2-Tracer_4	$9.0x10^{-5}$ (± $7.7x10^{-6}$)	$8.2x10^{-9}$ (± $7.5x10^{-10}$)	0.30 (± 0.03)	$3.5x10^{-8}$	$7.5x10^{-9}$ (± $6.9x10^{-10}$)
RQ2-Tracer_5	$4.3x10^{-5}$ (± $4.0x10^{-7}$)	$7.2x10^{-9}$ (± $5.4x10^{-11}$)	0.22 (± 0.002)	$1.1x10^{-8}$	$6.5x10^{-9}$ (± $4.9x10^{-11}$)

* Calculated using Equation 4.2
† Calculated using Equation 4.3
‡ Calculated using Equation 1.3

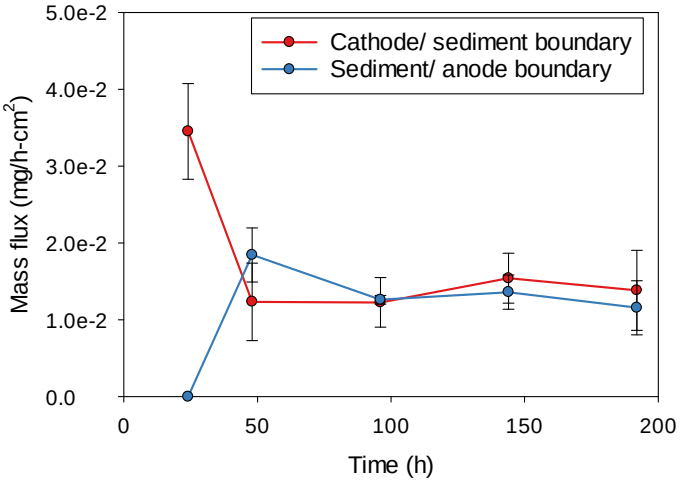

Figure 4.2 Relationship between nitrate mass transport at the cathode/ sediment and the sediment/ anode boundaries in RQ2-HOM experiments.

The tortuosity factor in Table 4.3 reflects the path length that ions must take through the sediment, in porous media it is always less than one and decreases as the tortuosity of the flow path increases (Fetter, 1993); it is calculated by re-arranging Equation 1.3:

$$\tau = \frac{u_i^*}{u_i n}$$

Equation 4.3

The calculated tortuosity value is used with the sediment porosity value to calculate the effective ionic mobility for nitrate using Equation 1.3. The migration velocity is the distance across the sediment chamber divided by the time bromide is first observed in the anode chamber and is normalised to the voltage between electrodes (Lohner et al., 2008a).

Values for mass transport, effective ionic mobility and migration velocity all decrease with decreasing K (Table 4.3), with the exception of values for RQ2-Tracer_1 which are slightly lower than RQ2-Tracer_2. K and the effective ionic mobility have no direct relationship, as both reflect the porous material used. Results from these experiments demonstrate that under certain conditions these two parameters can be indirectly related by the tortuosity factor, which decreases in fine grained sediments (Rowe and Badv, 1996). Thus, as K

decreases the effective ionic mobility also decreases. For example, as clay content increases between RQ2-Tracer_2 and RQ2-Tracer_5 there is greater occlusion of the pore spaces between the larger glass beads, which impedes solute migration. The effective ionic mobility estimated for nitrate in the different materials is similar in trend to, but slightly lower than, the bromide results due to the differences in ionic mobility value at infinite dilution. This range of values is lower than those reported for pure kaolin (1.55 – 1.65 x 10^{-8} m^2/s-V), which has high porosity and tortuosity values (0.6 and 0.35, respectively) (Acar and Alshawabkeh, 1993; Thevanayagam and Rishindran, 1998).

Electromigration of negative species such as bromide and nitrate towards the anode can be hindered by a counter electroosmotic flow in fine-grained material with a high surface charge (Acar and Alshawabkeh, 1993). Other authors have noted this phenomena, whereby a negatively charged ion migrates faster through sands than clays due to the presence of counter electroosmotic flow (Acar et al., 1997; Wu et al., 2007). In these experiments electroosmotic flow was only observed in RQ2-Tracer_5, with a 20% clay content (electroosmotic permeability: 2.7x10^{-9} (±3.6x10^{-10}) m^2/s-V). This value was calculated by rearranging the following equation (Acar and Alshawabkeh, 1993):

$$q^{eo} = k_e \frac{\Delta E}{\Delta x} A$$

Equation 4.4

where q_e is the electroosmotic flow rate (m^3/s); and A is cross sectional area (m^2). The flow rate was determined by a change in volume noted in the Mariotte bottle attached to the anode chamber (Figure 4.1A).

The data in Table 4.3 supports the first hypothesis in Section 4.1.1 that mass transport can decrease with K based on the influence of a decreasing effective ionic mobility and increased counter electroosmotic flow.

4.3.2 Nitrate electromigration under heterogeneous and homogeneous conditions

Observed and calculated values for nitrate breakthrough at the anode in experiments RQ2-HET_1, RQ2-HOM and RQ2-HET_2 are shown in Figure 4.3. RQ2-HET_1 and RQ2-HOM experiments were run at an inlet concentration of 0.1 g-NO_3/L under heterogeneous and homogeneous configurations, whereas RQ2-HET_2 is the same heterogeneous configuration to RQ2-HET_1 but with an inlet concentration of 1 g-NO_3/L. Results in Figure 4.3 are normalised to the starting inlet concentration and the voltage between electrodes. Calculated values for the RQ2-HOM experiment were obtained using Equation 1.2 for 1-D electromigration. Calculated values for heterogeneous experiments can be obtained by modifying Equation 1.2 and applying it to a conceptual understanding of nitrate migration in the experiments through a heterogeneous setting illustrated in Figure 4.4. Annotations A and B refer to the mass flux at the cathode/ high-K and high-K/ low-K boundaries respectively, these are:

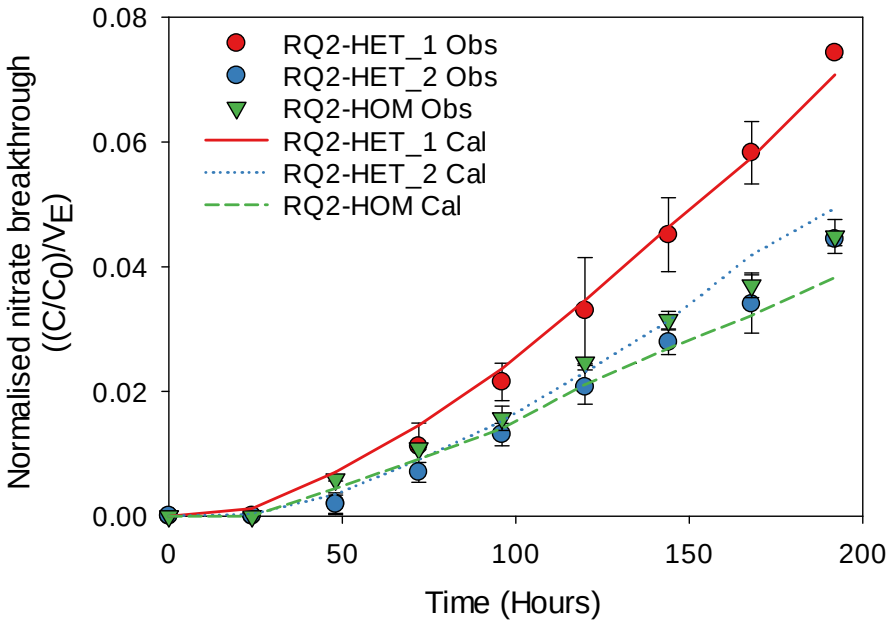

Figure 4.3 Nitrate breakthrough at the anode normalised to inlet concentration and voltage between electrodes for experiments RQ2-HET_1, RQ2-HOM and RQ2-HET_2. Dots and dashed lines represent observed and calculated values, respectively. Error bars represent one standard deviation from the mean; error associated with the calculated values is within the same range for observed values.

$$J_i^{Cath} = C_i^{Cath} u_i^{*HK} \frac{\Delta E^{HK}}{\Delta x^{HK}}$$

Equation 4.5

$$J_i^{LK} = C_i^{HK} u_i^{*LK} \frac{\Delta E^{LK}}{\Delta x^{LK}}$$

Equation 4.6

where J_i^{Cath} and J_i^{LK} are the mass flux of ionic species, i across the cathode/ high-K boundary and the high-K/ low-K boundary, C_i^{Cath} and C_i^{HK} are the concentrations in the cathode compartment and high-K section; x^{HK} and x^{LK} are the distances across the high-K and low-K sections; and E^{HK} and E^{LK} are the electrical potentials across the high-K and low-K sections. Calculated mass flux values are derived from the effective ionic mobility determined in the bromide tracer experiments, observed voltage gradient and inlet nitrate concentration values at the cathode (either 0.1 or 1 g-NO_3/L). Annotations C and D in Figure 4.4 refer to the equations used to calculate the solute concentrations resulting from the mass flux into that zone over a specified time period (based on Equation 4.1):

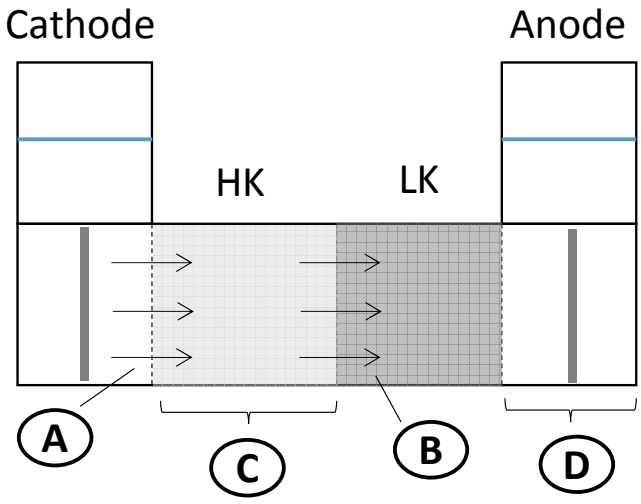

Figure 4.4 Conceptual diagram of nitrate migration in the experimental setup through a heterogeneous sediment configurations. The letters refer to different calculations: A, mass flux cathode/ high-K boundary (Equation 4.5); B, mass flux high-K/ low-K boundary (Equation 4.6); C, high-K nitrate concentration (Equation 4.7); and D, anode nitrate concentration (Equation 4.8).

$$C_i^{HK} = \frac{(J_i^{Cath} - J_i^{LK})t\ A}{V^{HK}}$$

Equation 4.7

$$C_i^{Ano} = \frac{J_i^{LK} t\ A}{V^{Ano}}$$

Equation 4.8

where C_i^{HK}, is the concentration in the high-K section; and V^{HK} is the volume of the high-K section. In these calculations the t value represented the time between voltage readings. The nitrate concentration determined in Equation 4.7 is used to inform the mass flux into the low-K zone in Equation 4.5, this is justified because it is more representative of the conditions that determine the flux at the high-K/ low-K interface. Furthermore, the concentration in the high-K section at a particular time point has to account for the nitrate mass flux into and out of that zone, the J_i^{LK} value in Equation 4.7 is calculated based on Equation 4.6 using concentration and voltage gradient values from the previous time point. This method was used to calculate the nitrate concentration at the anode over time. Good agreement between the observed and calculated values shows that the observed experimental values conform to applicable EK theory (Figure 4.3).

The observed nitrate breakthrough for RQ2-HET_1 is higher than RQ2-HOM and RQ2-HET_2 after 100 hours, relative to the inlet concentration and voltage difference between electrodes (Figure 4.3). This is due to a higher voltage gradient across the high-K section in RQ2-HET_1 (Figure 4.5A). This allows more nitrate to enter the sediment section from the cathode and increase the proportion passed through the low-K section, relative to RQ2-HOM and RQ2-HET_2.

The increased voltage gradient across the high-K section in RQ2-HET_1 can be attributed to several factors. Firstly, the voltage gradient is distributed in relation to the heterogeneous sediment configuration. This is shown theoretically in Chapter 1, Section 1.2.1.2. Material properties (porosity and tortuosity) control the effective ionic mobility of an ion (Equation 1.3), which is directly proportional to the effective electrical conductivity of the electrolyte (Equation 1.4). Moreover, Chapter 1, Section 1.3.3.1 show that the effective electrical conductivity is inversely proportional to the voltage gradient (Equation 1.11), thus spatial changes in material type (where porosity and tortuosity varies) will lead to changes in the voltage gradient. In these experiments the nitrate effective ionic mobility is slightly lower in the high-K section compared with the low-K section (Table 4.3, RQ2-Tracer_1 and RQ2-Tracer_2 respectively). Therefore, there should be an elevated voltage gradient across the high-K section, which is evident for both RQ2-HET_1 and RQ2-Control_1 in Figure 4.5A. This phenomenon is the likely cause for the divergence in effective electrical conductivity between the high- and low-K sections of RQ2-HET_1 and Control_1 in Figure 4.5B. Ions will move faster through the high-K section where the

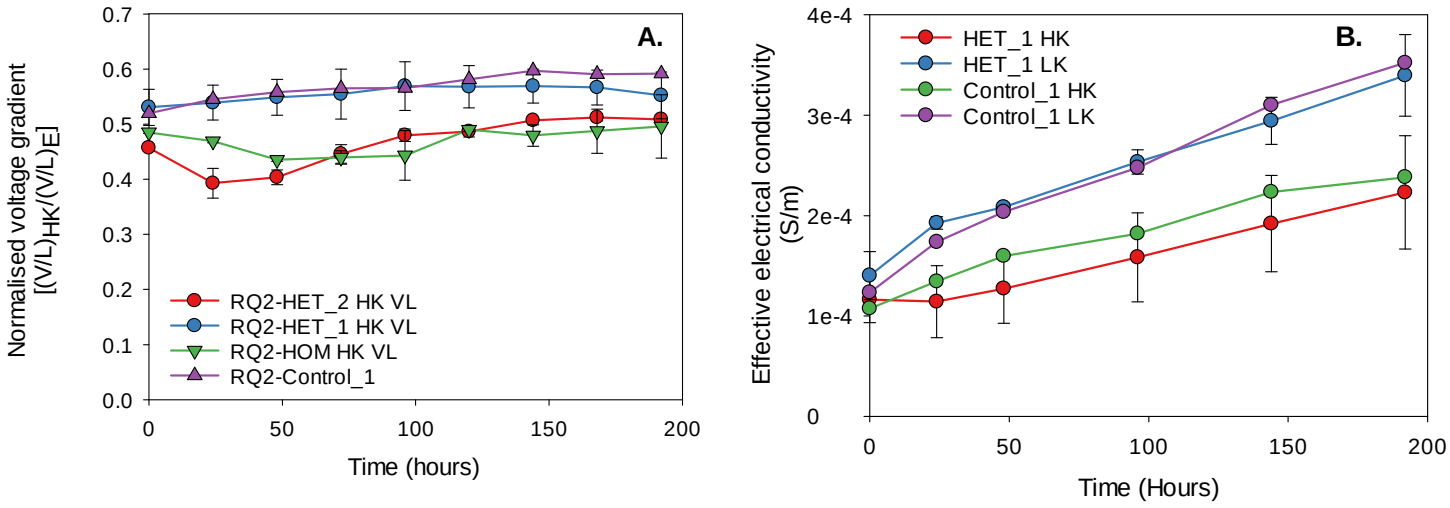

Figure 4.5.A. Proportion of voltage gradient across the high-K section for RQ2-HET_1, RQ2-Control_1 and RQ2-HET_2 and the equivalent section in the RQ2-HOM experiment. B. Effective electrical conductivity for the high- and low-K sections in RQ2-HET_1 and RQ2-Control_1 calculated using Eq. 6 and the ionic composition of the pore fluid from sample ports in the respective sections. Error bars for values from experiments RQ2-HET_1 and RQ2-HET_2 represent one standard deviation from the mean between replicates.

voltage gradient is highest but accumulate in the low-K section where it decreases and electromigration rate subsequently falls. Li et al. (2013) noted similar phenomena when investigating the influence of bands with a high associated electrical conductivity within a homogeneous soil. They found that the associated decrease in the voltage gradient caused the electromigration rate to fall. Over time these bands dissipated due to chemical diffusion, but in physically heterogeneous settings the contrast in migration rates could establish a permanent change in the voltage gradient.

Secondly, between RQ2-HET_1 and RQ2-HET_2 nitrate accounts for different proportions of the total electrolyte. Based on Equation 1.4 and accounting for the major ions in the electrolyte (nitrate, chloride, sulphate, sodium and potassium), nitrate in RQ2-HET_1 is 3.4% (± 0.4%) when added at 0.1 g-NO_3/L compared with RQ2-HET_2, where it accounts for 22.8% (± 2.3%) when added at 1 g-NO_3/L. Therefore, nitrate should have a greater effect on the voltage gradient in RQ2-HET_2 compared with RQ2-HET_1. This is observed in Figure 4.5A, where the voltage gradient across the high-K system dips for RQ2-HET_2 over the first 100 hours due to nitrate entering the system and increasing the electrical conductivity of the electrolyte in that zone. This phenomena is noted by Wu et al. (2012a), who found that increasing the concentration of the amendment in homogeneous settings increased the depression in the voltage gradient adjacent to the cathode and thus reduced the relative amount of amendment that migrated into the material.

4.3.3 Nitrate electromigration under an increasing hydraulic conductivity contrast

Experiments RQ2-HET_2 to RQ2-HET_5 quantify the effect of an increasing contrast in the K between two host materials on the electromigration of nitrate through them (Table 4.4). Similar to bromide results, these values are averages of time points after the system reaches equilibrium with respect to nitrate mass transport.

Table 4.4 Nitrate transport properties for experiments RQ2-HET_2 to RQ2-HET_5 quantifying the effect of increasing K contrasts on nitrate migration. The error represents one standard deviation from the mean of values obtained once the experiment had reached equilibrium with respect to nitrate mass transport. Both replicates for RQ2-HET_2 are shown.

Experiment	High-K Transport Properties		Low-K Transport Properties		
	Mass Transport [(mg/s)/V_E]	Migration Velocity [(m/s)/V_E]	Mass Transport [(mg/s)/V_E]	Migration Velocity [(mg/s)/V_E]	Electroosmotic Permeability (m^2/s-V)
RQ2-HET_2A	$1.3x10^{-4}$ (± $3.7x10^{-5}$)	$8.6x10^{-8}$	$1.3x10^{-4}$ (± $1.9x10^{-5}$)	$3.7x10^{-8}$	-
RQ2-HET_2B	$1.1x10^{-4}$ (± $5.0x10^{-5}$)	$1.1x10^{-8}$	$1.2x10^{-4}$ (± $2.6x10^{-5}$)	$3.7x10^{-8}$	-
RQ2-HET_3	$1.2x10^{-4}$ (± $6.2x10^{-5}$)	$8.7x10^{-8}$	$1.2x10^{-4}$ (± $2.1x10^{-5}$)	$3.4x10^{-8}$	-
RQ2-HET_4	$1.3x10^{-4}$ (± $6.7x10^{-5}$)	$8.5x10^{-8}$	$1.1x10^{-4}$ (± $2.2x10^{-5}$)	$3.7x10^{-8}$	-
RQ2-HET_5	$7.8x10^{-5}$ (± $2.3x10^{-5}$)	$8.7x10^{-8}$	$5.6x10^{-5}$ (± $6.2x10^{-6}$)	$1.4x10^{-8}$	$3.8x10^{-9}$ (± $6.4x10^{-10}$)

The transport properties of nitrate through high- and low-K sections of the sediment are in broad agreement with the bromide tracer results from homogeneous settings (Table 4.4). For example, the range in high-K mass transport and migration velocity values (except RQ2-HET_5) are equivalent to RQ2-Tracer_1 and the trend in decreasing mass transport and migration velocity between RQ2-Tracer_2 to RQ2-Tracer_5 is repeated in the low-K results. In addition, electroosmotic flow is observed in RQ2-HET_5 that originates in the low-K section and transfers through the high-K section, contributing to the relatively low mass transport value; migration velocity is not restricted because nitrate was detected in the low-K section after 24 hours. However, mass transport estimates are either equivalent to, or higher in, the low-K section compared with the relevant bromide tracer experiment. This results from the influence of the voltage gradient on the heterogeneous setting.

Furthermore, nitrate concentration in the high-K section increases as the effective ionic mobility ratio between high-K / low-K sections increases (Figure 4.6). This is due to a reduction in electromigration rates from the high- to low-K sections. The range calculated concentrations under homogenous conditions are shown as dotted lines and show the expected conditions without the associated influences of a heterogeneous system. These are determined using the method in Wu et al. (2012a), applying the bromide mass transport values from experiment RQ2-Tracer_1 (Table 4.3). Results for RQ2-HET_2 are

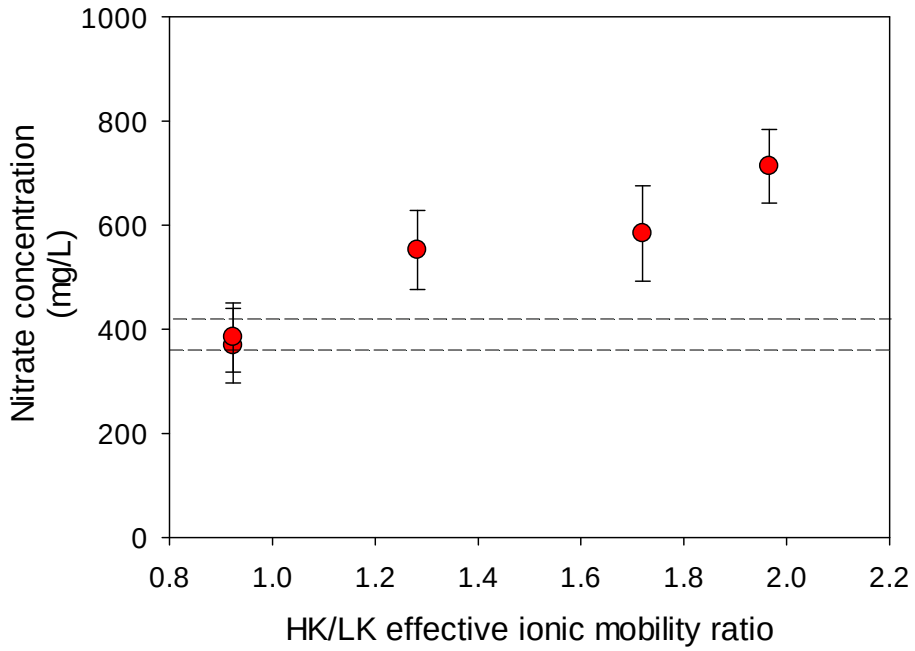

Figure 4.6. Nitrate concentration in the high-K material, calculated from the total mass of nitrate detected in the sample ports along the high-K section and divided by the domain volume. Lines plotted at nitrate concentrations of 412 and 373 mg-NO_3/L represent the maximum and minimum concentration calculated using values for equivalent material from the bromide tracer experiment. The error bars represents one standard deviation from the mean of values obtained once the experiment had reached equilibrium with respect to nitrate mass transport.

closest to the calculated nitrate concentration because the high- and low-K effective ionic mobility values are closest. Conversely, RQ2-HET_5 values are furthest from the calculated nitrate concentration due to the combined effect of a low associated effective ionic mobility in the low-K section and counter electroosmotic flow, which hinders nitrate migration.

4.3.4 Influence of increasing hydraulic conductivity contrasts on the voltage gradient

EK-driven mass transport increases in heterogeneous relative to homogeneous systems (Table 4.3 and Table 4.4), for example the mass transport for RQ2-HET_4 is 1.2×10^{-4} ($\pm$ 2.2×10^{-5}) compared with 8.3×10^{-5} ($\pm$ 7.7×10^{-6}) (mg/s) / (V_E) in equivalent material for RQ2-Tracer_4. This is because in heterogeneous settings the voltage gradient is higher across the zone with a low effective ionic mobility compared with a homogeneous setting where

Table 4.5. Percentage change in the voltage gradient across the high- and low-K sections relative to a fixed voltage gradient. The error represents one standard deviation from the mean of values obtained once the experiment had reached equilibrium with respect to nitrate mass transport. Both replicates for RQ2-HET_2 are shown.

Experiment	High-K / low-K Effective Ionic Mobility Ratio	High-K Section	Low-K Section
RQ2-HET_2A	0.92	-0.7% (± 3.9%)	0.7% (± 3.9%)
RQ2-HET_2B	0.92	0.3% (± 2.0%)	-0.3% (± 2.0%)
RQ2-HET_3	1.28	-19.6% (± 3.0%)	19.6% (± 3.0%)
RQ2-HET_4	1.72	-18.5% (± 2.0%)	18.5% (± 2.0%)
RQ2-HET_5	1.97	-30.1% (±1.6%)	30.1% (±1.6%)

the voltage gradient is more uniform. These experiments show that increasing the K and associated effective ionic mobility contrast increases the difference in voltage gradient between the high- and low-K sections (Table 4.5). In experiments with a low effective ionic mobility contrast (RQ2-HET_2) the observed voltage gradient is distributed evenly, i.e. there is little change in the voltage gradient across the high- and low-K zones relative to a uniform voltage gradient. At higher K contrasts there is a difference of up to 30% relative to a fixed voltage gradient (RQ2-HET_5). Conversely, the decrease in voltage gradient creates a reduced mass flux in high-K material within heterogeneous settings. Although the difference is not as prominent due to a higher associated error (e.g. RQ2-Tracer_1 $1.4x10^{-4}$ ($\pm$ $4.5x10^{-5}$) (mg/hr)/V_E compared to $1.3x10^{-4}$ ($\pm$ $6.7x10^{-5}$) (mg/hr)/V_E for RQ-HET_4). The factors controlling this difference can be identified from Equations 1.4 and 1.10 as the spatial change in effective ionic mobility and subsequent spatial change in the effective electrical conductivity and voltage gradient.

A comparison of the major ion concentrations in the electrolyte (nitrate, chloride, sulphate, sodium and potassium) across two different K contrasts highlights the complex interactions between the effective ionic mobility and the voltage gradient in heterogeneous settings (Figure 4.7). In experiment RQ2-HET_2 there is minimal difference between the total ion concentration and voltage gradient (Figure 4.7A). However, in RQ2-HET_4 there is a higher total ion concentration in the low-K zone compared with the high-K zone (Figure

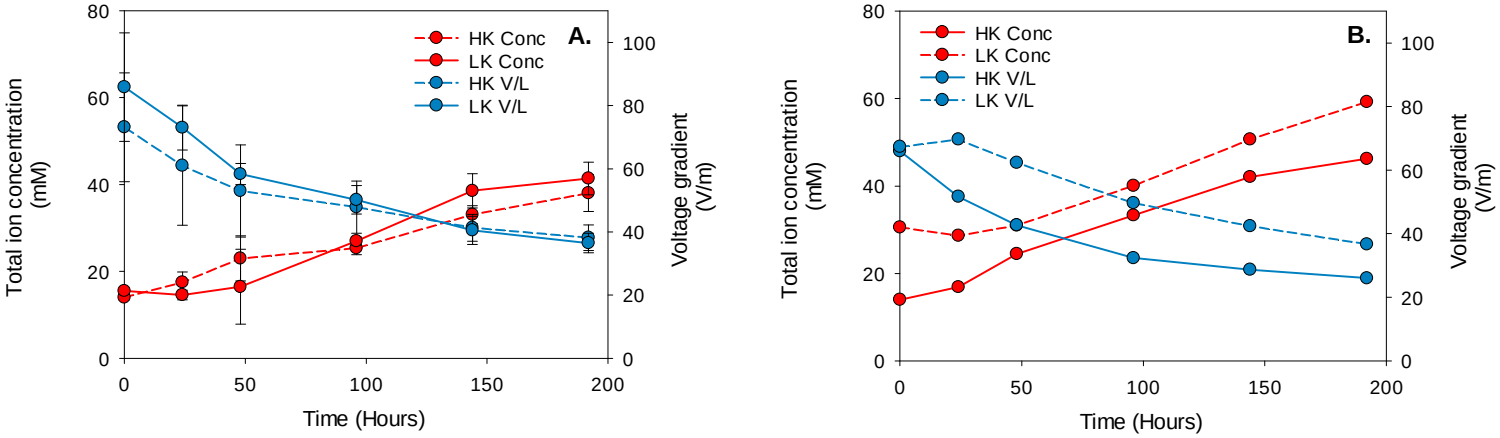

Figure 4.7. Total ion concentrations and voltage gradient (VG) for experiments (A) RQ2-HET_2 and (B) RQ2-HET_4. Values for the total ion concentration are calculated from the cumulative mass of each ion identified at sample ports along the high- and low-K sections divided by the volume of the domain. These values are in mM because five different ions are included in the analysis. Error bars on (A) represent one standard deviation from the mean between replicates.

4.7B). Assuming uniform effective ionic mobility (and according to Equation 1.10) this should be reflected by a higher voltage gradient across the high-K section relative to the low-K section because there is a lower concentration and therefore a lower electrical conductivity. However, the opposite is observed due to the difference in effective ionic mobility. This demonstrates that under heterogeneous conditions where ionic mobility varies spatially there will be associated changes in the voltage gradient.

The findings from this section support the second hypothesis that the voltage gradient will he higher in zones of low effective ionic mobility in a heterogeneous setting. The implications of this observation are discussed in a wider field scale context in Chapter 8.

4.3.5 Experiment mass balance

As a quality control check on the operation of the experiments a mass balance for nitrate was undertaken, by comparing the mass of nitrate recovered at the end of the experiment with the known input (Table 4.6). The amount of amendment recovered (80 - 90%) is similar to that found in other electrokinetic transport experiments (73 – 106%) (Lohner et al., 2008a; Wu et al., 2007). Every effort was made to minimise the loss of nitrate via biological processes (e.g. denitrification), by sterilising glass beads, synthetic groundwater

and test cell components to kill any microorganisms present. Abiotic losses of nitrate by electroreduction is expected to be minimal because a high electric current density is required. In these experiments it was 1.6 A/m^2, which is up to several orders of magnitude lower than studies that observe high levels of nitrate reduction (e.g. 11 – 4500 A/m^2 yield between 80 – 100% nitrate removal) (Pulkka et al., 2014). Furthermore, under acidic conditions nitrate will reduce to nitrogen gas. The presence of pH control and stabilised pH values in the electrodes prevents this occurring (Xu et al., 2010). Overall, the mass balance suggests any biotic or abiotic losses were limited to 10 - 20% in these experiments.

Table 4.6. Nitrate mass balance at the end of the experiment run for RQ2-HET_2 to RQ2-HET_5.

Experiment	Mass Balance		
	Mass added (mg)	Mass Recovered (mg)	Recovery (%)
RQ2-HET_2A	4984	4422	89
RQ2-HET_2B	4582	4119	90
RQ2-HET_3	5907	5271	89
RQ2-HET_4	6536	5215	80
RQ2-HET_5	4644	4067	88

4.4 Conclusions

Physical heterogeneity in granular porous media, represented by a K contrast, exerts an important influence on the electromigration of nitrate used as an amendment for bioremediation. These experiments demonstrate this influence by posing two hypotheses based on EK theory. The first hypothesis establishes an indirect link between K and the effective ionic mobility value through the porosity and tortuosity values. Thus, heterogeneous setting where K varies will represent a spatial change in the effective ionic mobility with subsequent controls on the amendment mass transport. An example of which was an accumulation of the amendment at the interface between high- and low- K zones, relative to the calculated nitrate concentration. The second hypothesis predicted that the spatial change in effective ionic mobility will be inversely proportional to a spatial change in the voltage gradient. This resulted in an elevated voltage gradient over the low-K zone

in heterogeneous settings. This phenomena is attributed to a higher mass transport of the amendment in the same material for heterogeneous compared to homogeneous settings. It was also observed that the voltage gradient was more pronounced in heterogeneous settings where the ratio between the effective ionic mobility of the high- and low-K zone is greater.

Furthermore, the influence of physical heterogeneity in the host material was observed to vary relative to the inlet concentration of the amendment. For a low K contrast and low inlet concentration the influence of heterogeneity was greater compared with a high concentration, where the effect of this heterogeneity was minimised due to the influence of nitrate on the voltage gradient.

Overall these results show that EK application in heterogeneous settings is controlled by the same mechanisms in homogeneous settings, but that the distribution in amendment migration rates and voltage gradient vary relative to the change in the effective ionic mobility. This forms the basis of a conceptual framework for understanding the influence of heterogeneity on EK and is expanded further in Chapters 5 and 6.

Chapter 5 Electromigration of nitrate through layered heterogeneous porous media

5.1 Introduction

In advection-dominated systems there is limited flow across high to low-K boundaries. Therefore, in physically heterogeneous settings bioremediation of low-K zones will be limited by the distribution and mixing of microbes and solutes (Song and Seagren, 2008). In EK dominated systems physical heterogeneity is less inhibiting because the electric field is not directly affected by K. EK can be used to directly remove contaminants, such as lead and phenanthrene, from heterogeneous settings by electromigration and electroosmosis (Alshawabkeh et al., 2005; Saichek and Reddy, 2005) and also introduce amendments within heterogeneous settings. For example, Reynolds et al. (2008) migrated potassium permanganate into clay blocks within a high permeability host material to show the effectiveness of coupling EK with *in situ* chemical oxidation. However spatial changes in material type will still exert a control on solute migration by EK. Chapter 4 showed that the transition from high- to low-K porous media corresponds to a decrease in nitrate mass flux and increase in the voltage gradient. Both factors depend on the effective ionic mobility, itself a function of the porosity and tortuosity of a porous medium (Alshawabkeh and Acar, 1996).

Electric fields in homogeneous 2-D settings can be non-uniform and create tortuous migration pathways for solute migration between electrodes (Segall and Bruell, 1992). Physical heterogeneity affects the arrangement of electric fields as seen in Chapter 4, and will therefore create non-uniform flow paths relative to the distribution of high- and low-K zones (Figure 5.1). These non-uniform flow paths are equivalent to fluxes and are important when trying to understand the efficacy of amendment delivery by EK in a remediation scenario.

5.5.1 Research question and hypotheses

The research question addressed in this chapter is: What is the influence of layered heterogeneity on the electromigration of nitrate under ideal conditions? This research question is referred to as Research Question 3 (RQ3). Heterogeneity in this study is represented by two layers of granular porous media with different K values. The following hypotheses were tested:

1. A small voltage difference will exist between layers of material with different effective ionic mobilities, due to the subsequent variation in ion mass flux into the sediment and effective electrical conductivity. Furthermore, this difference will increase with nitrate concentration;
2. This difference in voltage gradient will create an associated electromigration mass flux between layers and can be quantified by comparing nitrate transport in heterogeneous and homogeneous systems.

The objectives were to deduce the effect of EK transport on nitrate migration within homogeneous and heterogeneous settings, identify the controlling mechanisms for any

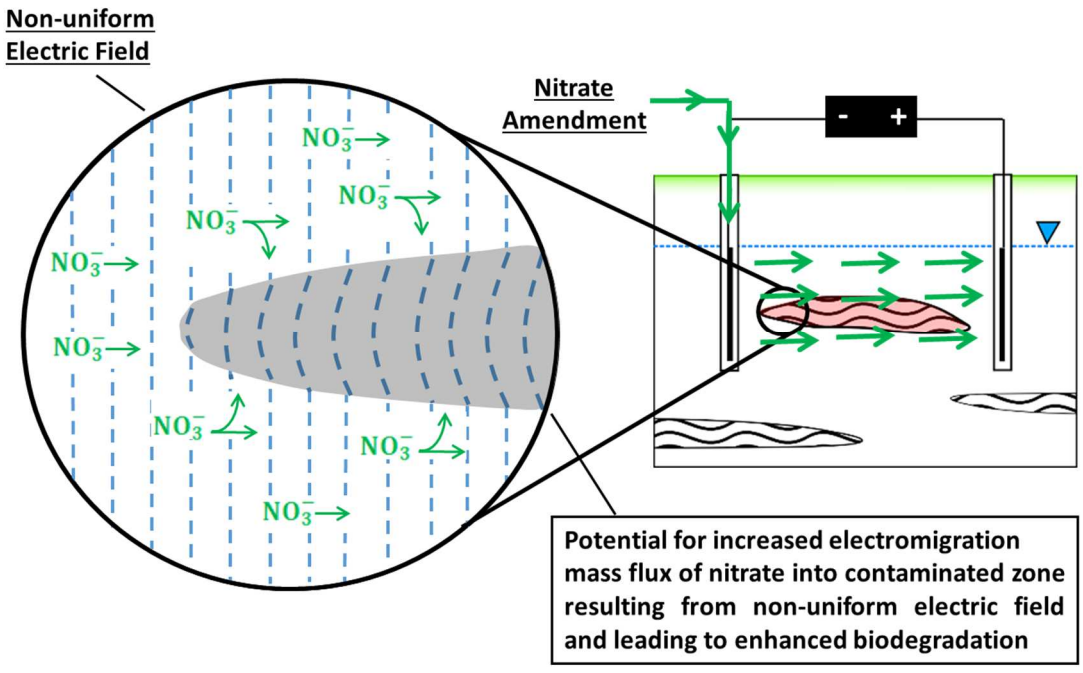

Figure 5.1 Conceptual diagram of the phenomena described in these experiments.

differences observed and determine the influence of variations in nitrate concentration on amendment flux.

5.2 Materials and methods

5.2.1 Material properties

The porous medium was created with two materials: soda-lime-silica glass beads (Potters Ballotini Ltd), to represent an ideal system, and silica sand (David Ball Group PLC and Marchington Stone Ltd), to represent natural sediment. Homogeneous and heterogeneous configurations of these materials were developed, the latter having a layered contrast between high- and low-K media. High-K and low-K material was produced for both glass beads and natural sediment (Table 5.1). High- and low-K material have respectively large and small grain sizes, with extra kaolin clay (Speswhite, Imerys Performance Materials Ltd) added to the low-K material to further reduce the K value. Glass beads were cleaned with deionised water between experiments, and both glass beads and sand were sterilised by autoclaving prior to consolidation in the test cell. Adding the kaolin fraction (grain size distribution of 76 - 83% ≤ 2µm) introduced a small amount of surface adhered soluble salts (0.2 % by mass of sodium and sulphate ions based on dissolution tests) into the pore fluid. The sediment chamber was filled completely with either the high-K or low-K material for

Table 5.1 Properties of material used in experiments

Material Property	**Glass Beads**		**Natural Sediment**	
	High-K	**Low-K**	**High-K**	**Low-K**
Grain Size (GB) (mm)	**Fraction (%)**	**Fraction (%)**	**Fraction (%)**	**Fraction (%)**
1.4	100	-	-	-
0.25	-	80	-	-
0.50	-	10	-	-
Grain Size (NS) (mm)				
<4-2	-	-	1.02	-
<2-1	-	-	98.75	-
<1-0.5	-	-	0.20	0.37
<0.5-0.1	-	-	0.02	84.88
<0.1-0.05	-	-	-	3.96
<0.05-0.01	-	-	-	2.12
<0.01-0.005	-	-	-	2.72
<0.005-0.001	-	-	-	1.86
<0.001-0.005	-	-	-	0.21
<0.005-0.0001	-	-	-	0.53
Porosity (-)	0.30	0.34	0.39	0.44
Hydraulic Conductivity (m/s)	9.2×10^{-4} ($\pm8.8\times10^{-5}$)	5.7×10^{-7} ($\pm2.4\times10^{-7}$)	7.0×10^{-4} ($\pm4.9\times10^{-5}$)	5.9×10^{-7} (2.8×10^{-8})

the homogeneous experiments (Figure 5.2). The loose high-K material was consolidated using a shaker table at a frequency of 31 Hz, calibrated with a hand-held accelerometer. The test cells were filled with material in layers up to 3 cm and placed on the shaker table for intervals of 20 s. This was repeated until the test cell was full, excess material removed and the lid secured. The low-K material was mixed before consolidation in the sediment chamber. The fine grained glass beads (or fine sand depending on the experiment) and kaolin were added together in a sterilised (60% isopropanol) metal mixing bowl and mixed thoroughly to ensure even distribution of the kaolin within the sand. Sterilised synthetic groundwater was added at a ratio equivalent to the clay's plastic limit (approximately 0.3:1 by volume water to clay) to enhance mixing. The mixture was then wet packed into the sediment chamber in the test cell (Figure 5.2) and tamped down using a ceramic pestle, following the method used in Saichek and Reddy (2005).

The layered K contrast was achieved by first wet packing the low-K material into the test cell until the compacted material filled half the chamber. The surface of the low-K material was smoothed with a metal spatula and the loose high-K material added above and consolidated using the shaker table method. No movement in the low-K layer was observed during or after the method was applied. After the addition of high- and low-K material the chamber lid was secured before saturation of the media with synthetic groundwater. The sediment chamber was separated from the electrode chambers by a perforated acrylic plate covered with filter paper (Whatman Grade No. 5) with pore size less than the sediment grain size used.

A synthetic groundwater was used to simulate an electrical conductivity of 700 µS/cm, based on natural groundwater sampled in a UK aquifer (Thornton et al., 1995). This is the same as applied in Chapters 3 and 4. The test cells containing the consolidated material

were saturated with synthetic groundwater from the base up at a low flow rate to remove entrapped air and then sealed.

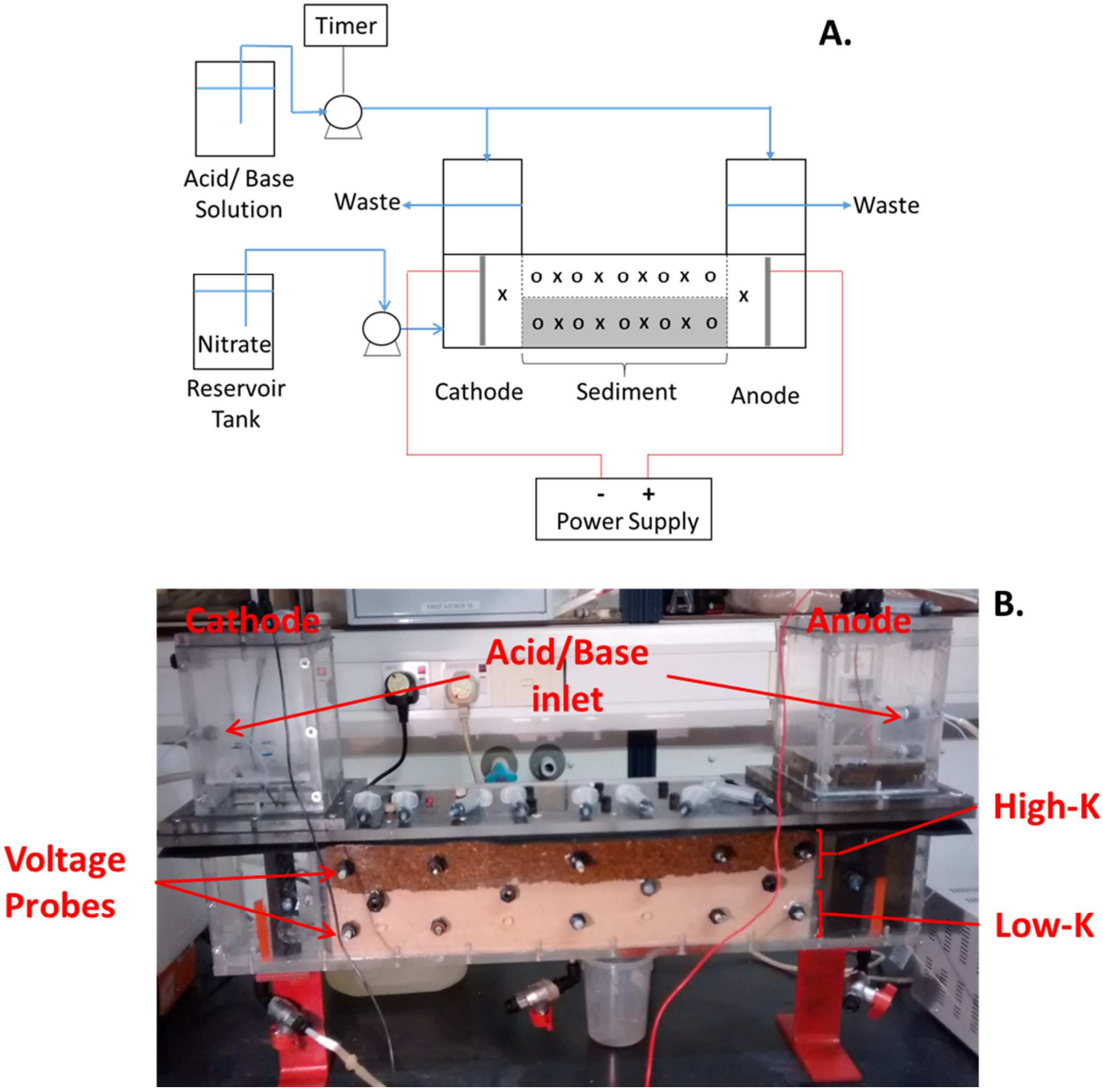

Figure 5.2 A, Schematic of test cell design (volume 7.5 L), showing sediment chamber containing high- and low-K zones (light and dark shades respectively), voltage probes (O) and sampling ports (X). Electrode chambers (each 2 L), power supply, pH control and amendment delivery mechanisms are included. B, Annotated digital image of the experimental setup.

5.2.2 Bench-scale setup

An experimental test cell was developed for the preparation of reproducible sections of packed materials with high- and low-K (Figure 5.2). This test cell was developed in Chapter 3 and applied in the experiments for Chapter 4. The dimensions of the high-K and low-K sections were equivalent to half the height of the sediment chamber (H: 62.5 x W: 125 x L: 480 mm). Leaks were prevented using rubber gaskets and silicone grease for the lid and header tanks. Similar to Chapter 4, after consolidation and enclosure of material in the test cell synthetic groundwater and the amendment solution was circulated at 10 mL/min from the reservoir tank into the cathode chamber using a peristaltic pump (Ismatec, REGLO MS-4/8). This was done until the fluid in the cathode chamber had been displaced to waste (approx. 3.5 hr). A baseline sample of the pore fluid (using ports along the cell side) was taken before direct current was applied to the system from a power pack (Digimess, PM6003-3).

Samples of pore fluid for chemical analysis were taken every 2 days during the experiment, with the exception of a 4-day break between the 5th and 6th sampling time points (at days 10 and 14). The sampling tubes and voltage probes are the same as those applied in Chapter 3 and 4. For these experiments the sample tubes were distributed in two rows of four, one for each of the high- and low-K layers, with an extra sampling tube in each electrode chamber. Ten voltage probes consisting of 4 mm diameter 316 stainless steel rods housed in HDPE piping and distributed in two rows of five, one for each of the high- and low-K layers. Voltage and electric current was logged every 24 hours during tests using a multimeter (Digitek, DT-4000ZC). All heterogeneous experiments included two layers of sampling ports, although the majority of the homogeneous media tests used a single layer of sampling ports in the centre of the test cell

Similar to Chapters 3 and 4, nitrate was used as the amendment and bromide was used as a conservative tracer based on similar properties. Amendments were added to the cathode at a rate of 1.5 mL/min from a 10 L reservoir tank maintained at a constant concentration of either nitrate or bromide solutions. The reservoir tank was topped up at regular intervals.

5.2.3 Electrokinetic apparatus and test conditions

A direct current was applied at a constant current strength of 25 mA (1.6 A/m^2) to allow more effective control of pH changes at the electrodes. Electrodes were made from a 125 x 125 x 10 mm graphite block (Chapter 3, section 3.2).

The electrode conditioning method presented in Chapter 3, Section 3.3.6.2 was used to neutralise electrolysis reactions (see Equation 1.6 and Equation 1.7 for anode and cathode reactions respectively). The addition of acid and base solutions was according to the method in Chapter 4, Section 4.2.3. The pH of the electrode chambers was checked every two days by removing a 1 mL aliquot and manually titrating it to pH 7 if required. In experiments where electroosmotic flow was evident a Mariotte bottle was used to ensure that the anode compartment was not depleted of water and no hydraulic gradient developed. This was only relevant in homogeneous systems because any transference of fluid by electroosmosis in heterogeneous systems could be countered by fluid flow through the high-K section.

5.2.4 Experimental design

The details of all experiments run are shown in Table 5.2. Heterogeneous experiments comprised two layers of high- and low-K glass bead/ kaolin mixes, one run without nitrate (RQ3-HET_1) and three with different starting concentrations (0.1, 1 and 5 g-NO_3/L, RQ3-HET_2-4, respectively). Homogeneous experiments consisted of the same low-K material used in heterogeneous experiments, with one containing no nitrate (RQ3-HOM_1) and three with different starting concentrations (0.1, 1 and 5 g-NO_3^-/L, RQ3-HOM_2-4, respectively). Furthermore, both homogeneous and heterogeneous scenarios were run using natural sediment with a nitrate concentration of 1 g-NO_3/L (RQ3-NS-HOM_5 and RQ3-NS-HET_5, respectively). Two types of control experiments using bromide were run, in which (1) no electric field was applied, to isolate the influence of nitrate migration into the sediment by non-EK transport processes, namely, diffusion and advective flow generated from extracting pore fluid (RQ3-C-HOM_3 and RQ3-C-HET_1), and (2) a homogeneous system with two layers of sampling and voltage ports, to confirm that any difference between layers is not an artificial variation caused by the bench-scale setup

(RQ3-C-HOM_1 and RQ3-C-HOM_2). Replicates of homogeneous and heterogeneous systems were run for experiments at 1 g-NO_3^-/L (Table 5.2). All experiments were run for 336 hrs, except the bromide tracer experiments (192 hrs), the first pore fluid sample was taken 24 hrs after the baseline and then every 48 hrs to ensure minimal disturbance of the system. Raw data for these experiments is given in Appendix J.

Table 5.2 Design of nitrate migration and control experiments.

Name	EK Properties		Reservoir Tank Properties		Sediment Properties		Reps
	Current applied	Current (mA)	Ion	Conc (g/L)	Type	Configuration	
RQ3-HOM_1	Yes	25	-	-	GB	HOM - Low-K	1
RQ3-HOM_2	Yes	25	NO_3^-	0.1	GB	HOM - Low-K	1
RQ3-HOM_3	Yes	25	NO_3^-	1	GB	HOM - Low-K	2
RQ3-HOM_4	Yes	25	NO_3^-	5	GB	HOM - Low-K	1
RQ3-NS-HOM_5	Yes	25	NO_3^-	1	NS	HOM - Low-K	1
RQ3-HET_1	Yes	25	-	-	GB	HET	1
RQ3-HET_2	Yes	25	NO_3^-	0.1	GB	HET	1
RQ3-HET_3	Yes	25	NO_3^-	1	GB	HET	2
RQ3-HET_4	Yes	25	NO_3^-	5	GB	HET	1
RQ3-NS-HET_5	Yes	25	NO_3^-	1	NS	HET	1
RQ3-C-HOM_1	Yes	25	Br^-	1	GB	HOM - High-K	1
RQ3-C-HOM_2	Yes	25	Br^-	1	GB	HOM - Low-K	1
RQ3-C-HOM_3	No	-	Br^-	1	GB	HOM - High-K	1
RQ3-C-HET_1	No	-	Br^-	1	GB	HET	1

5.2.5 Analytical methods

The same analytical methods applied in the preliminary experiments, outlined in Chapter 3, Section 3.3.3 were applied in these experiments.

5.3 Results and discussion

5.3.1 Influence of sediment configuration on voltage gradient

Sediment configuration has an effect on the voltage difference between layers. This phenomenon is described by analysing voltage readings taken from the experiments and linking this to the pore fluid properties using a conceptual model. These results relate to the first hypothesis presented in the introduction.

5.3.1.1 Observed voltage difference between layers in heterogeneous and homogeneous sediments

Voltage readings taken at the same point along the sediment chamber and different heights show a greater difference in heterogeneous experiments than homogeneous experiments. This is shown in Figure 5.3 where values are derived by subtracting the voltage reading of the high-K layer from the low-K layer and normalising the difference against the voltage between electrodes. Values are averages of the voltage differences observed over 10 time points after 100 hours until the end of the experiment (336 hours). Values are taken after 100 hours because at this point equilibrium is reached with respect to nitrate mass flux into and out of the sediment chamber. This minimises perturbations in the voltage gradient associated with the initial nitrate migration into the sediment. Values for both RQ3-HET_3 replicates are included in Figure 5.3A (RQ3-HET_3.1 and RQ3-HET_3.2).

Positive and negative values in Figure 5.3 indicate a higher voltage in the low- and high-K layers, respectively. Heterogeneous experiments have a predominantly positive voltage difference between layers, whereas the differences in homogeneous experiments are minimised, and either positive or negative. The heterogeneous experiment (Figure 5.3A) with the highest nitrate concentration added at the cathode, RQ3-HET_4, has a higher

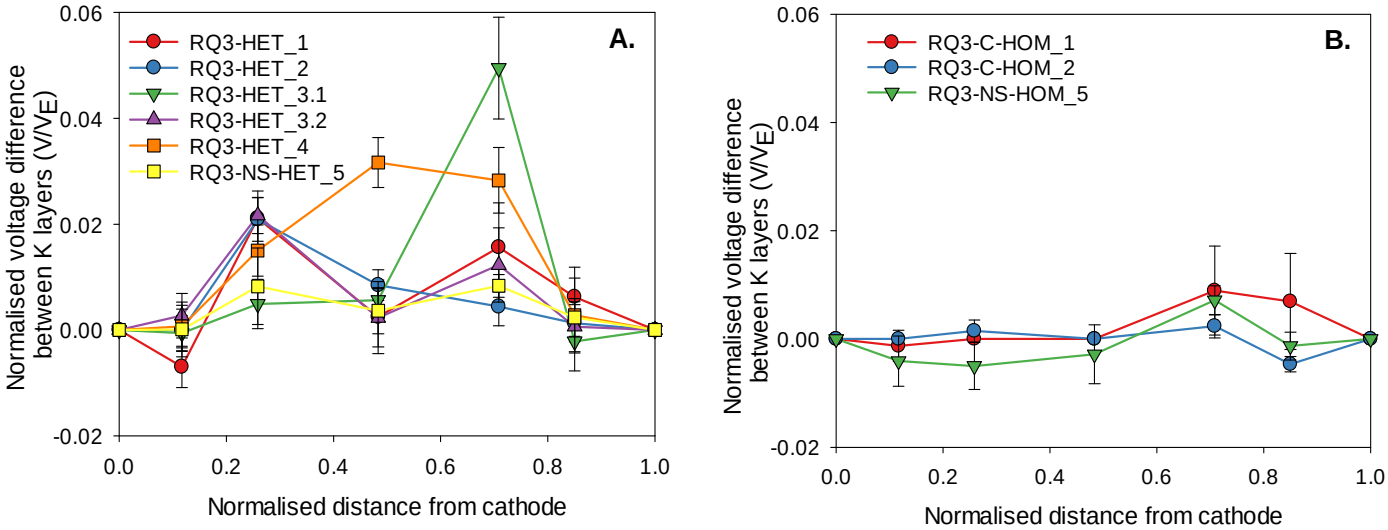

Figure 5.3. Voltage difference between upper and lower sediment layers, normalised to the voltage between electrodes (V_E), against normalised distance from cathode. Graphs A and B show values from heterogeneous and homogeneous experiments, respectively. Error bars are one standard deviation from the mean.

consistent voltage difference compared with other experiments. RQ3-HET_3.1 shows a high peak adjacent to the anode that is not sustained across the remaining sediment. This is in contrast to replicate RQ3-HET_3.2 where the voltage difference is comparable to the remaining experiments. Homogeneous experiments (Figure 5.3B) cover the range of material properties applied in this study (high-K, RQ3-C-HOM_1; low-K, RQ3-C-HOM_2; and low-K natural sediment, RQ3-NS-HOM_5) and there is minimal difference between experiments (Figure 5.3B). This implies that the properties of the heterogeneous system create this phenomenon.

A conceptual model for the processes in the heterogeneous experiments is presented in Figure 5.4 to develop these observations. The principal mechanism is the transfer of electrical current between layers that distorts the electric field accordingly. In order for the experimental system to replicate the conceptual model it must exhibit two specific properties: (1) the resistivity of the low-K layer must be greater than the high-K layer; and (2) a resistivity gradient must exist in the low-K layer, increasing in magnitude between the anode and cathode, that is greater than the resistivity gradient in the high-K layer. These two properties ensure that the preferential flow path for electric current is from the low- to high-K layer.

The conceptual model is based on observations made in Chapter 4, where a K contrast (equivalent to a spatial change in effective ionic mobility) is arranged in series. The findings indicate that zones of low effective ionic mobility (low-K zones) corresponded to areas of low mass transport and a high voltage gradient compared with adjacent material with a high effective ionic mobility (high-K zones). These observations apply to the conceptual model because the effective ionic mobility is proportional to the electric current density (Alshawabkeh and Acar, 1996), implying that current density will be higher in the high-K layer than the low-K layer (assuming a uniform distribution of ions). However, these are highly dynamic systems where the movement of electric current within a 2D setting is variable and subject to numerous factors, with implications for the voltage difference between layers. For example, the shift in electric current depicted in Figure 5.4 is fairly uniform and corresponds to a voltage difference between layers most similar to RQ3-HET_4 (Figure 5.3A). This contrasts with profiles from other heterogeneous experiments which indicate that current transfer is not uniform and can occur at different locations along the sediment chamber. This is represented by either a single or double peak in the voltage

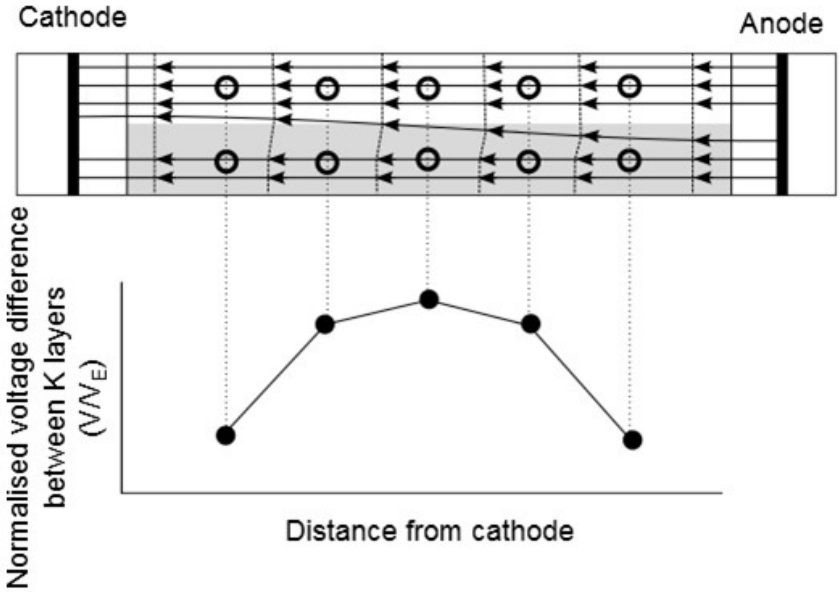

Figure 5.4. Conceptual diagram showing the direction and movement of electric current (solid lines with arrow heads) through a layered heterogeneous system and subsequent effect on electric field (dashed lines). Open circles represent the location of voltage probes; the difference between readings from high- and low-K layers is shown in closed circles below.

difference, e.g. RQ3-HET_2 and RQ3-HET_3.1 or RQ3-HET_1, respectively (Figure 5.3A).

The natural sediment experiment exhibits a small voltage difference between layers compared to the other glass bead experiments. The conceptual model suggests that this is due to minimal current transfer between layers, certain properties of the low-K layer could create this effect. Electroosmotic flow is observed in the homogenous natural sediment experiment (discussed in Section 5.3.2.1). This indicates that there is a sufficient surface charge within the low-K material to sustain electroosmotic flow. Hence, a greater proportion of the electric current could be transferred by this charge. The implication for the conceptual model is that the low-K layer of natural sediment will be more electrically conductive, minimising the movement of electric current from low to high-K layers. Furthermore, it is important to consider the implication of an increased effective ionic mobility value in the low-K sediment that would be more representative of clays with a high moisture content such as kaolin. This analysis is in Chapter 8, Section 8.3.3.1.

5.3.1.2 Relationship between voltage difference and pore fluid resistivity

The effective resistivity is a property of the major ion composition of the pore fluid and is used to demonstrate how experimental observations adhere to the conceptual model outlined above (Figure 5.5A-F, values for experiments RQ3-HET_1 to RQ3-NS-HET_5 and RQ3-C-HOM_2). The parameter is derived from the effective electrical conductivity, defined by Equation 1.4 (Alshawabkeh and Acar, 1996). For this calculation, the concentration, effective ionic mobility and valency of major ions (sodium, chloride, nitrate, sulphate and potassium) in the pore fluid are used. The effective ionic mobility is determined by Equation 1.3 (Acar and Alshawabkeh, 1993). Values for porosity are defined in Table 5.1, tortuosity values for glass beads / kaolin mix are 0.56 and 0.30 for high- and low-K material, respectively (see Chapter 4, Table 4.2). These tortuosity values are used to inform effective ionic mobility values for the natural sediment experiments. The

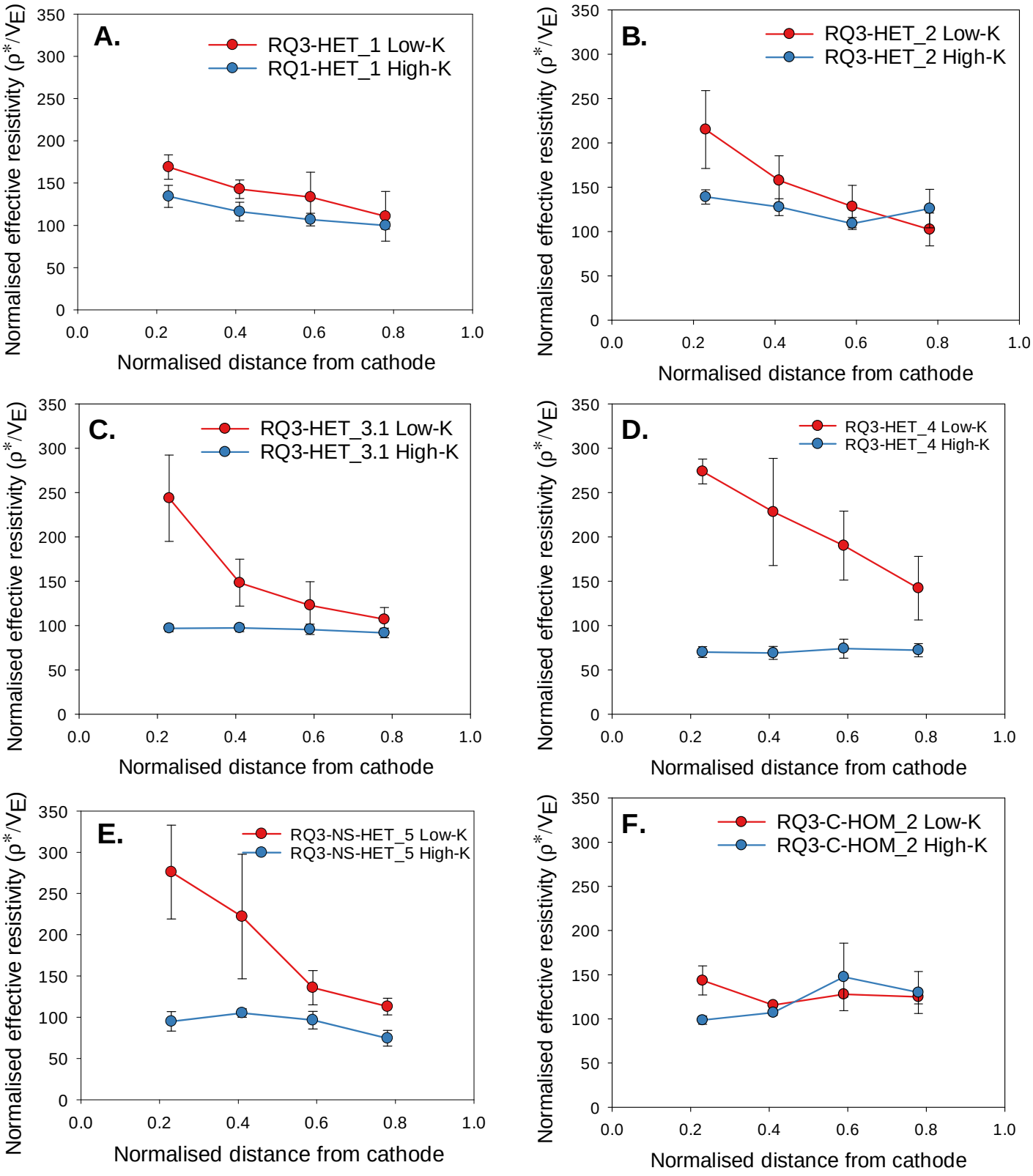

Figure 5.5 Profiles of effective resistivity (ρ*) normalised to the voltage between electrodes (VE). Graphs represent experiments: A, RQ3-HET_1; B, RQ3-HET_2; C, RQ3-HET_3.1; D, RQ3-HET_4; E, RQ3-NS-HET_5; F, RQ3-C-HOM_2. Orange series represents data from the low-K (Tier 2 sampling ports) and blue series represents high-K (Tier 1 sampling ports). Values are an average of 10 time points after 100 hours and error bars are one standard deviation from the mean.

effective ionic mobility values for the major ions are presented in the Appendix K (Table K.1). Effective resistivity is the reciprocal of effective electrical conductivity:

$$\rho^* = \frac{1}{\sigma^*}$$

Equation 5.1

where ρ* is the effective resistivity (Ω-m). The effective ionic mobility for the materials in this experiment have already been characterised in Chapter 4 and observed lower values for the low-K compared to the high-K material. Therefore, based on equations 4, 5 and 6 low-K material will have a higher effective resistivity compared to high-K material assuming uniform concentration.

In Figure 5.5, effective resistivity is normalised to the voltage difference between electrodes to account for the effect of constant current. In these experiments applying constant current results in a voltage decrease between the electrodes over time, which corresponds to a decreasing mass flux in and out of the sediment. Some experiments are not included in Figure 5.5 because blocked sample tubes limited sampling; these include RQ3-HET_3.2, C- RQ3-HOM_1 and RQ3-NS_HOM_5. An ion charge balance was conducted for all experiments to confirm the solute transport behaviour (see Appendix K, Figure K.1). Two experiments observed a difference between cations and anions of greater than 10%: RQ3-HOM_3.2, 13.1%; and RQ3-HET_2, 15.8%. These experiments include kaolin as part of the low-K layer mix and is comparable with Acar et al. (1997) that observed an imbalance of charge in a kaolin clay experiment between 8-24%.

The conceptual model in Figure 5.4 requires a higher resistivity in the low-K layer relative to the high-K layer. Evidence of this is observed in Figure 5.5A-E. The smallest difference in resistivity between layers is for experiments RQ3-HET_1, RQ3-HET_2 and RQ3-C-HOM_2 (Figure 5.5A, B and E respectively). Both RQ3-HET_1 and RQ3-HET_2 represent experiments where no nitrate or a small amount of nitrate (0.1 g-NO_3/L) is added at the cathode. Under these conditions there are less ions migrating into the sediment to

enhance the differences between layers. Conversely, in experiment RQ3-C-HOM_2 1 g-Br/L is added at the cathode, but there is minimal difference between layers across most of the sediment, except adjacent to the cathode. When compared against other heterogeneous experiments, RQ3-HET_3.1 and RQ3-NS-HET_5 (Figure 5.5C and E respectively) with a similar 1 g-NO_3/L nitrate addition, it is evident that the effect on resistivity is minimised in the homogeneous setting. Furthermore, Figure 5.5D (RQ3-HET_4) shows the greatest difference in resistivity between layers, which corresponds to the highest concentration of nitrate added at the cathode (5 g-NO_3/L).

There is evidence of a potential link between the scale of effective resistivity difference (Figure 5.5A-E) and the voltage difference between sediment layers (Figure 5.3A). Experiment RQ3-HET_4 has the highest difference in effective resistivity (Figure 5.5D), which corresponds to the highest consistent voltage difference (Figure 5.3A). In other experiments with an increase in resistivity between layers (e.g. RQ3-HET_1, RQ3-HET_2, RQ3-HET_3.1 and RQ3-NS-HET_5, Figure 5.5A-C and E respectively), there is no corresponding increase in the voltage difference (Figure 5.3A, experiments RQ3-HET_1, RQ3-HET_2, RQ3-HET_3.2 and RQ3-NS-HET_5). However, these experiments have a voltage difference within the same range (maximum and minimum values between 0.02 to 0.005 V/V_E, respectively, Figure 5.3A). This suggests that the voltage difference between layers increases as more nitrate is added at the cathode, but also that there is a threshold value at which greater differences are observed beyond the effect of background ions. This could be linked to the proportion of the total electrical conductivity of the system, contributed by the nitrate. For example, in these experiments nitrate in RQ3-HET_2, RQ3-HET_3.2 and RQ3-HET_4 contributed 3.4% (± 0.3%) 22.6% (± 1.0%) and 67.2% (± 5.5%), respectively, of the total electrolyte (based on Equation 4 using ions: nitrate, chloride, sulphate, sodium and potassium).

The presence of an electrical resistivity gradient increasing from anode to cathode is an important aspect of the conceptual model (Figure 5.4) and is observed in all

heterogeneous experiments for either the low-K or both high- and low-K layers (Figure 5.5). The presence of a resistivity gradient that is higher in the low-K layer than high-K layer ensures electric current travelling from the anode will shift between layers as it moves towards the cathode. If the gradient was equal or absent both the high- and low-K layers would act as resistors in parallel and no voltage gradient difference would be observed. It is difficult to elucidate a direct relationship between the observed voltage differences and resistivity gradients because additional factors could be influencing the electric field. For example, all experiments in Figure 5.3A show a divergence towards the centre of the sediment section and recombine towards the electrode chambers. There is no evidence for this in the resistivity profiles, therefore the electric current could be influenced by additional factors, such as edge effects exerted by the interface between the electrode and sediment chambers. However, resistivity gradients could help explain RQ3-HET_3.1 in Figure 5.3A, which shows a high peak adjacent to the anode that is not observed in the replicate, RQ3-HET_3.2, or equivalent natural sediment experiment, RQ3-NS-HET_5. The resistivity profile for RQ3-HET_3.1 in Figure 5.5C clearly shows a high gradient adjacent to the cathode that is not observed to the same extent in RQ3-NS-HET_5, Figure 5.5D or other heterogeneous experiments. The locations of voltage difference and resistivity peak do not match, although if they are linked it would imply that a shift in electric current between layers is highly sensitive to sharp peaks in resistivity. Future experiments should consider a higher resolution of sample ports to enable more effective comparisons between the voltage difference between layers and pore fluid properties.

The method of pH control is one of the main factors for the increase in effective resistivity towards the cathode. In these experiments sodium hydroxide and hydrochloric acid were added to the anode and cathode, respectively. Fluid in the cathode is regularly cycled to supply new amendment, whereas fluid in the anode is stationary, to observe nitrate accumulation over time. Sodium ions will accumulate in the anode because the rate of addition to neutralise electrode reactions is greater than the flux into the sediment. This will influence the rate of sodium mass flux into the sediment over time to the point that it is greater than or equivalent to the mass flux of nitrate from the cathode (Figure 5.6A). A comparison of nitrate and sodium mass transport into the sediment over time is shown in Figure 5.6A. Furthermore, an increased flux of sodium ions facilitates a decrease in voltage gradient adjacent to the anode over time (Figure 5.6B). The main effect of this is to reduce the migration of ions in that zone and therefore increase the concentration. Overall, these factors increase the effective electrical conductivity at the anode, which is inversely proportional to a decrease in resistivity.

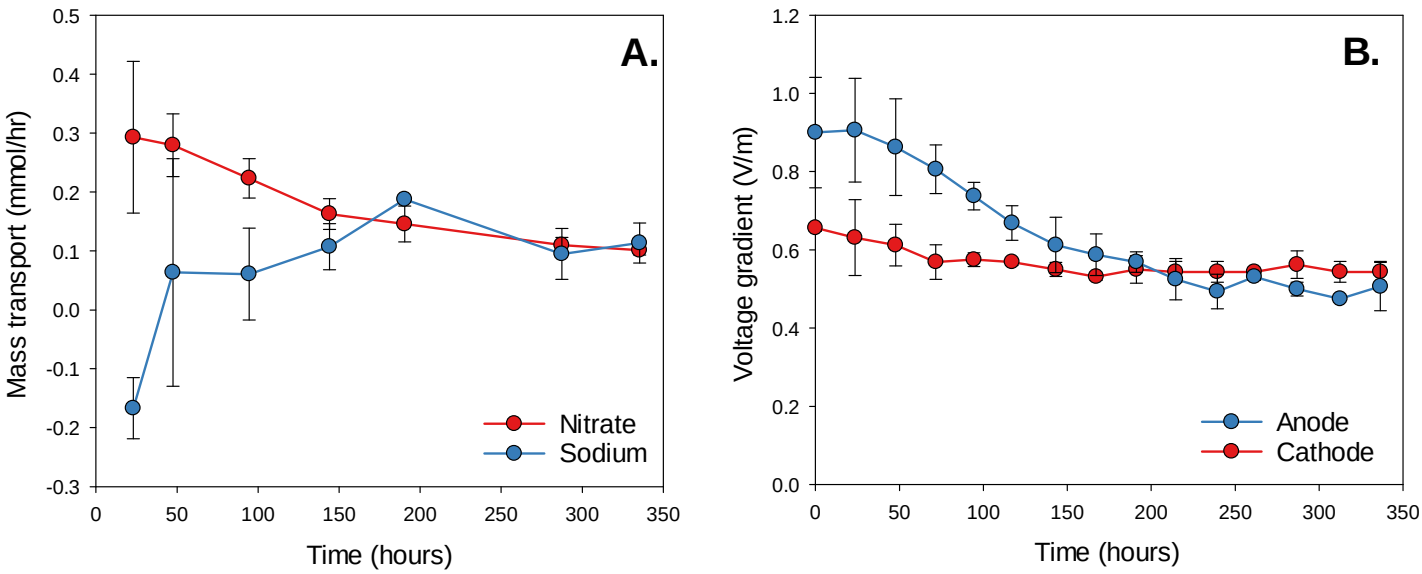

Figure 5.6. Factors related to decreasing resistivity gradient from cathode to anode in experiment RQ3-HOM_3. A, nitrate and sodium mass transport; and B, voltage gradient over the cathode and anode boundary. Error bars represent one standard deviation from the average of values between RQ3-HOM_3.1 and RQ3-HOM_3.2.

5.3.1.3 Influence of experimental parameters on voltage difference between layers

The voltage difference between layers of sediment may be sustained by the experimental setup, creating a constant rather than a transient effect. Under ideal conditions the phenomenon observed in these experiments could be assumed to dissipate once at steady-state. At this point, ion concentrations within layers would have equalised and therefore electric current would be carried proportionally through each layer and not be transferred between them to create the voltage difference. The experimental processes that could influence the voltage difference include those that increase ion concentrations within the sediment chamber over time and prevent it from reaching a steady-state, such as the method of pH control and application of constant current. The method of pH control in these experiments was electrode conditioning, which effectively maintained a uniform pH across the sediment (Figure 5.7). However, as previously mentioned, it introduced high concentrations of chloride and sodium ions, which could contribute to the voltage difference in experiments with low concentrations of nitrate (e.g. RQ3-HET_1 and RQ3-HET_2). Methods used in biodegradation experiments that also limit the mass flux of additional ions into the sediment include recirculation (Kim and Han, 2003; Mao et al., 2012) and polarity reversals (Harbottle et al., 2009; Luo et al., 2005b).

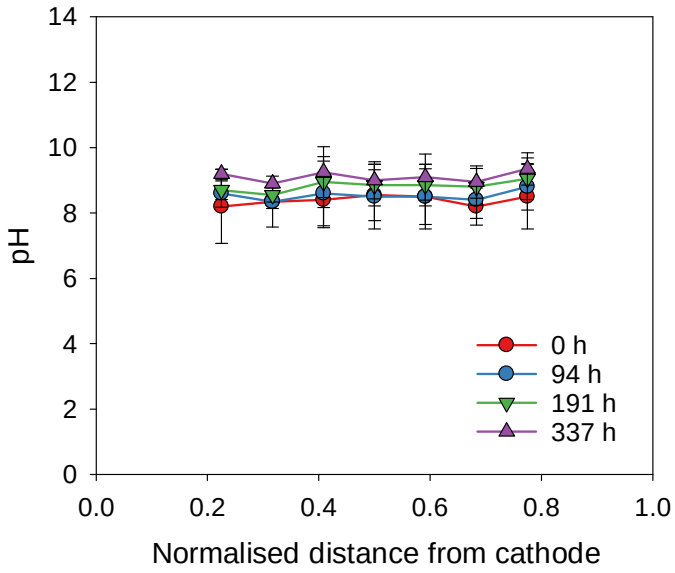

Figure 5.7 Pore fluid pH in samples from experiments RQ3-HOM_3. Values represent the average of RQ3-HOM_3.1 and RQ3-HOM_3.2. Error bars are one standard deviation from the mean.

A constant current, where current density is fixed and voltage varies, or constant voltage where the voltage is fixed and current varies are typically used in EK experiments (Acar et al., 1997). In both cases the electrical conductivity of the system drives the fluctuation of either voltage or current. This is shown in Figure 5.8 where the voltage between electrodes for heterogeneous experiments decreases over time due to the increase in pore fluid electrical conductivity. Experiment RQ3-HET_4 decreases quickest due to the high concentration of nitrate added at the cathode (5 g-NO_3/L). A constantly decreasing voltage equates to an increase in the residence time of ions within the sediment. This effect prevents the system reaching steady-state with respect to electrical conductivity because pore fluid concentrations increase over time. Future experiments could reduce this effect by applying a constant voltage and allowing the current to vary. The limitation to this method is that pH changes at the electrodes are less predictable.

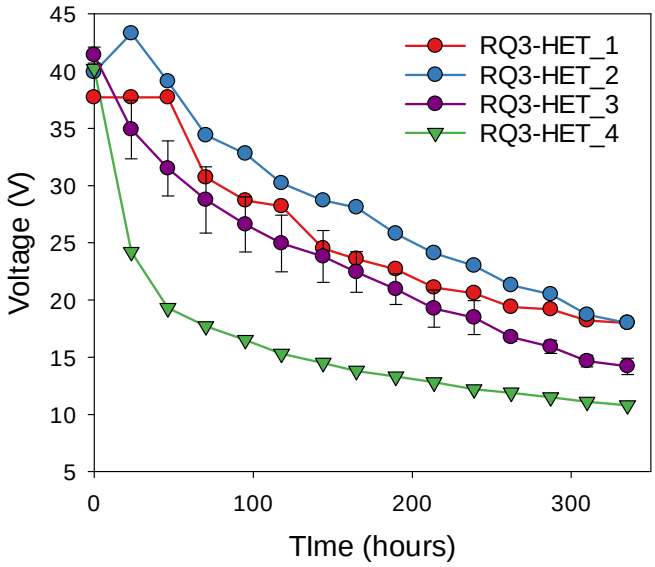

Figure 5.8 Voltage difference between electrodes for heterogeneous experiments. Values for RQ3-HET_3 represent the average of RQ3-HET_3.1 and RQ3-HET_3.2. Error bars are one standard deviation from the mean.

5.3.2 Transverse nitrate flux

The difference in voltage between layers is equivalent to a gradient, therefore creating a transverse electromigration mass flux. This is shown conceptually in Figure 5.9. Nitrate migrates into the layered sediment from the cathode boundary. Within the sediment, the voltage difference between layers will create a transverse flux across the K boundary. This phenomenon is demonstrated by characterising nitrate migration in homogeneous sediment and then predicting the nitrate concentration in the heterogeneous low-K layer by quantifying the flux between layers. These results relate to the second hypothesis presented in the introduction.

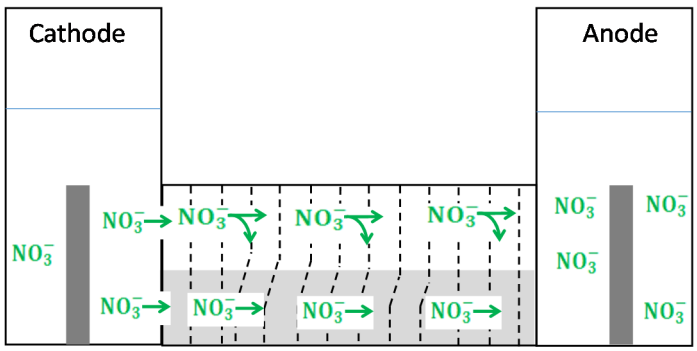

Figure 5.9 Conceptual diagram showing the transverse nitrate flux within the laboratory apparatus and the voltage profile for the high- and low-K layers between electrodes.

5.3.2.1 Nitrate migration through homogeneous sediment

Observed and calculated values of nitrate mass flux and velocity for homogeneous experiments are presented in Table 5.3. Values are measured from the point the experiment reaches equilibrium with respect to nitrate flux in and out of the sediment after 100 hours. Nitrate mass in the sediment is determined from the product of pore fluid nitrate concentration and pore volume. The mass flux values represent the difference in nitrate mass in the sediment and anode chambers over time. They are determined using the equation for 1-D electromigration mass flux (Equation 1.2). The observed nitrate electrokinetic transport velocity is the time taken for ions to move from the cathode to the anode normalised to the voltage gradient between electrodes. The electroosmotic permeability was calculated using the same method described in Chapter 4, Section 4.3.1.

In these experiments the observed and predicted nitrate flux are in good agreement, showing that nitrate migration in the experiments conforms to theory (Table 5.3). These results are also consistent with the findings of Lohner et al. (2008a) who observed an increase in mass flux with inlet concentration, whereas solute velocity did not change significantly. Velocity values for experiment RQ3-NS-HOM_5 in natural sediment are lower than the equivalent experiment in glass beads. This is due to the counter electroosmotic flow in the natural sediment matrix (electroosmotic permeability: 1.2×10^{-9} $m^2/V\text{-}s$). Electroosmotic flow is enhanced in the natural sediment / kaolin mix due to the presence of fine grained silts with a high mass-to-charge ratio relative to glass beads (Acar et al., 1995). It was not observed in the glass bead / kaolin mix due to the low proportion of kaolin;

Table 5.3 Nitrate mass flux and velocity through homogeneous settings. The error is the average of values from time points after 100 hours.

Experiment	Nitrate Mass Flux		Velocity ((m/s)/ V_E)
	Observed Values (g/s)	Calculated Values (g/s)	
RQ3-HOM_2	8.5×10^{-7} ($\pm 3.9 \times 10^{-8}$)	7.3×10^{-7} ($\pm 6.1 \times 10^{-8}$)	6.5×10^{-8}
RQ3-HOM_3.1	4.4×10^{-6} ($\pm 5.0 \times 10^{-7}$)	5.3×10^{-6} ($\pm 9.7 \times 10^{-7}$)	6.7×10^{-8}
RQ3-HOM_3.2	4.6×10^{-6} ($\pm 7.4 \times 10^{-7}$)	4.3×10^{-6} ($\pm 4.8 \times 10^{-7}$)	1.0×10^{-7}
RQ3-HOM_4	1.1×10^{-5} ($\pm 1.4 \times 10^{-6}$)	2.1×10^{-5} ($\pm 4.0 \times 10^{-6}$)	7.9×10^{-8}
RQ3-NS-HOM_5	5.3×10^{-6} ($\pm 9.6 \times 10^{-7}$)	5.2×10^{-6} ($\pm 9.7 \times 10^{-7}$)	4.8×10^{-8}

in contrast, an 80:20 mix of glass beads to kaolin in Chapter 4 produced an electroosmotic permeability of $2.7x10^{-9}$ m^2/V-s.

5.3.2.2 Quantifying nitrate flux between layers

The analysis of the nitrate flux between layers of sediment is split into two parts. Firstly, the observed nitrate concentration in homogeneous and heterogeneous settings are compared. Secondly, the predicted nitrate concentrations are compared.

Observed nitrate concentrations within the same material type are higher in heterogeneous experiments than homogeneous experiments, with the exception of RQ3-HET_2 (Figure 5.10). This difference increases as the inlet nitrate concentration at cathode chamber increases (Figure 5.10A-C). Values in Figure 5.10 represent the nitrate concentration across the whole sediment body at an individual time point. They are determined from pore fluid concentrations that are integrated to find the nitrate mass in a particular section of the sediment; these are then summed and divided by the pore volume, accounting for dimensions of the homogeneous or heterogeneous setting. Values are also normalised to the voltage difference between electrodes to provide a more effective comparison between experiments. Nitrate concentrations in all experiments increase over time because the nitrate transport velocity decreases; thus nitrate residence time within the sediment increase. This is a result of applying constant current and allowing the voltage difference between electrodes to drop over time. There is a potential for the pore fluid sampling in heterogeneous systems to raise the concentration in the low-K layer by drawing fluid with a high concentration of the nitrate from the high-K layer. Mass flux per sample event in the non EK controls (RQ3-C-HET_1) in heterogeneous low-K setting is between 4-5% of the mass flux in active EK systems (RQ3-HET_3.1 and RQ3-HET_3.2). Further information is presented in the Appendix K (Table K.2).

A transverse mass flux between layers can be demonstrated by predicting the nitrate concentration at a particular time point; in the homogeneous setting this flux will be into the sediment from the cathode boundary, whereas in the heterogeneous setting it will be from both the cathode boundary and boundary between the high- and low-K layers. The predicted nitrate concentration in homogeneous systems is defined as the product of the mass flux into the sediment from the cathode boundary multiplied by the time before solute

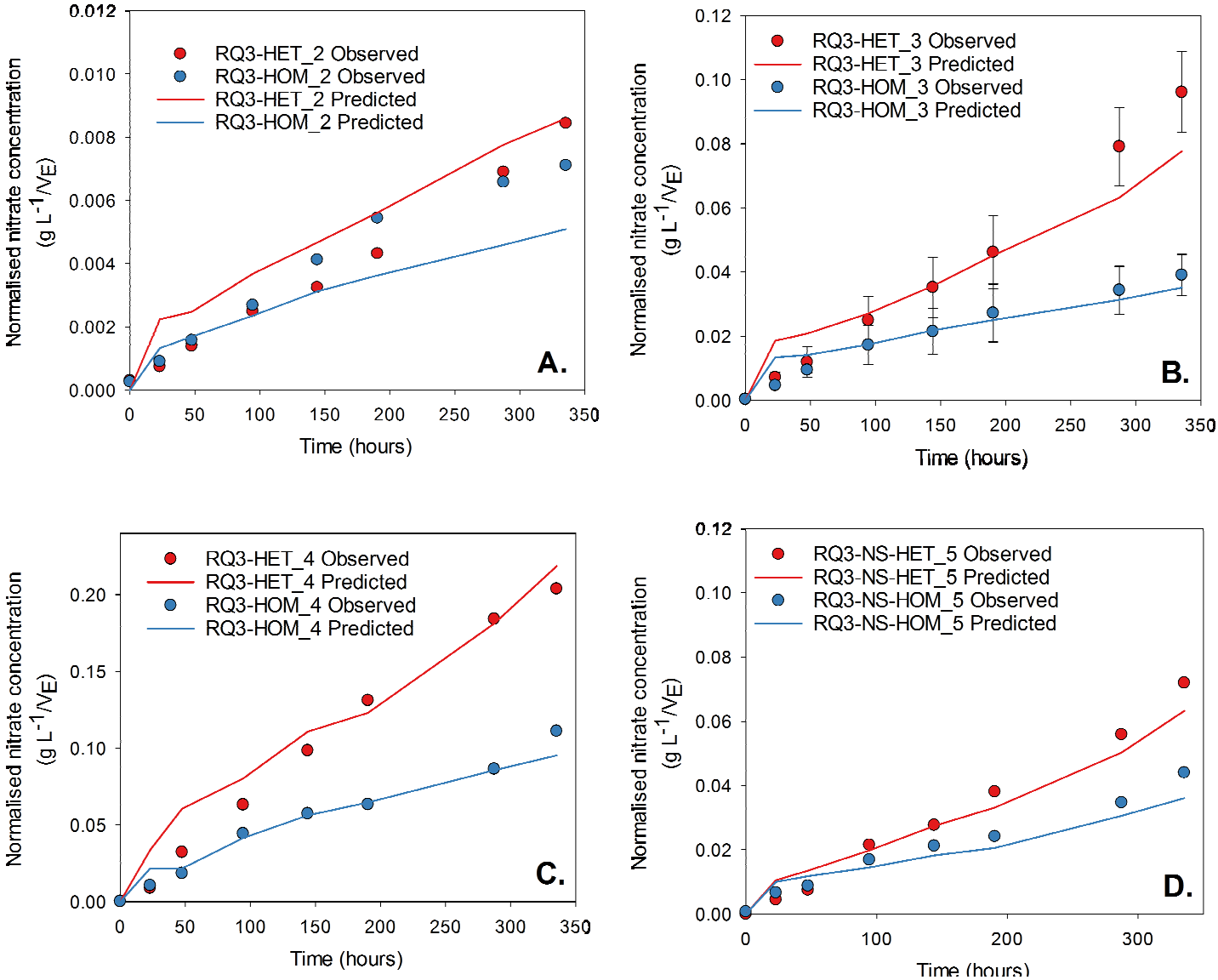

Figure 5.10 Comparison of observed nitrate accumulation within the same material in homogeneous and heterogeneous settings coupled with predicted values for nitrate concentration. Graphs represent experiments with nitrate added at the electrodes: A, RQ3-HET_2 and RQ3-HOM_2 (0.1 g-NO_3/L); B, RQ3-HET_3 and RQ3-HOM_3 (1 g-NO_3/L); C, RQ3-HET_4 and RQ3-HOM_4 (5 g-NO_3/L); D, RQ3-NS-HET_5 and RQ3-NS-HOM_5 (1 g-NO_3/L). Error bars represent one standard deviation from the average of values for experiments RQ3-HET_3.1 and RQ3-HET_3.2, and RQ3-HOM_3.1 and RQ3-HOM_3.2, respectively.

exits the sediment, divided by the domain volume. The time before the solute exits the system is calculated by dividing the domain length by the average electromigration velocity. v_i^{em} (m/s), defined in these experiments as (Wu et al., 2012a):

$$v_i^{em} = \frac{u_i^* - \mathrm{k}_e}{n} \frac{\Delta E}{\Delta x}$$

Equation 5.2

The calculation assumes that mass flux from the cathode chamber is constant, with influx at the cathode equal to efflux at the anode. In homogeneous systems the predicted concentrations are calculated with the observed mass flux values Table 5.3 and velocity values from the relevant bromide tracer tests in Chapter 4 (high-K and low-K velocities: 5.1 and 3.5 $x10^{-8}$ (m/s)/V_E, Chapter 4, Table 4.2).

The predicted nitrate concentration in heterogeneous systems includes an additional mass flux value to that previously defined in homogeneous conditions. This additional flux is described as a transverse mass flux and represents nitrate electromigration between the high- and low-K layers. A value for this phenomenon is obtained using the equation for 1D electromigration mass flux (Eq. 7). Input terms for this equation, such as the nitrate concentration in the high-K layer and effective ionic mobility of the material, are known. The voltage gradient between layers is the voltage difference between probe ports divided by the distance between them. To simplify the calculation, an average of voltage gradient values is taken across the length of the sediment chamber. The transverse flux is then added to the flux across the cathode boundary and incorporated into a nitrate concentration calculation for the heterogeneous setting. In Figure 5.10 the predicted nitrate concentrations are shown as a solid line.

The observed and corresponding calculated nitrate concentration in heterogeneous setting are in good agreement for experiments run at 1 and 5 g-NO_3/L (Figure 5.10B-C). However, in the 0.1 g-NO_3/L run (Figure 5.10A) there appears to be little difference between the homogeneous and heterogeneous systems. This suggests that either there was minimal transverse migration of nitrate or that the effect was masked due to

experimental variability. These results show that transverse electromigration is an important flux of nitrate into the low-K zone at high amendment concentrations. Furthermore, the results are analogous to transverse or lateral diffusion observed in advection-dominated systems, where K is stratified to create high- and low-flow layers (Li and Barry, 1994). In advection-dominated systems contaminant degradation by processes such as chemical oxidation or bioremediation are limited by transverse diffusion at the high/low-K interface where solute mixing and degradation occurs (Li and Barry, 1994; Hønning et al., 2007). Conversely, in EK dominated systems transverse migration is less likely to be a limiting factor. This is despite the EK transverse mass flux between layers being relatively small compared with the flux from electrodes. For example, the transverse flux between layers in RQ3-HET_3 is 8.1×10^{-6} ($\pm 3.0 \times 10^{-6}$) g-NO_3/m^2-s compared with the flux of 2.7×10^{-4} ($\pm 3.1 \times 10^{-5}$) g-NO_3/m^2-s from electrodes in RQ3-HOM_3. However, if the area over which the transverse flux is effective is greater than that at the electrode (such as in these experiments the electrode area is 0.0156 m^2 compared with the 0.06 m^2 area between layers) then a transverse mass flux will be an important consideration at the field scale.

5.3.2.3 Importance of transverse flux at the field-scale

Increasing the flux of nitrate to support and enhance in situ biodegradation is crucial for effective bioremediation of organic contaminants in low-K zones, as the supply of amendment should meet or exceed the microbial capacity to ensure even distribution (Rabbi et al., 2000), but is frequently limiting in these zones. Promoting the transverse flux of nitrate into low-K zones could therefore be an important factor in field applications of in situ bioremediation. A simple electron balance box model, similar to that described in Chapter 2, was developed to explore the importance of transverse migration observed in these experiments in an EK bioremediation scenario. To achieve an electron balance the mass transfer of electrons from electron donors (ED) (represented by organic contaminants) must equal that of electron acceptors (EA) (represented by soluble oxidants, e.g. nitrate or sulphate) for microbial respiration (Thornton et al., 2001). The model simulates the diffusion, advection and electromigration of dissolved oxygen, nitrate

and sulphate (only the latter two in the case of electromigration), as well as the separate addition of nitrate as an amendment at the cathode.

The conceptual scenario created is a contaminated groundwater management issue where the goal is to prevent long-term back-diffusion of sequestered contaminants into a high-K host material. This is achieved by enhancing biodegradation of the contaminants within the low-K lens using EAs delivered by the different transport mechanisms. The model domain comprises a high-K host material and one low-K block (Figure 5.11). Physical and electrokinetic properties for the model are the same as experiment RQ3-HET_4. The low-K zone was simulated as being contaminated with BTEX compounds: benzene 0.07 g/L, toluene 0.065 g/L ethylbenzene 0.05 g/L and xylene 0.06 g/L. Electrokinetic properties include the voltage gradient between the high- and low-K materials derived from experiments RQ3-HET_1 and RQ3-HET_4. These are equivalent to 16.4 and 4.9% of the voltage gradient between electrodes (50 V/m) for scenarios with and without an amendment, added respectively. The model evaluated the presence and absence of a voltage gradient and transverse flux of EAs between high- and low-K materials to determine its influence on remediation timescales. Electroosmotic flow and its influence on the movement of EAs and EDs was excluded from the model.

Several scenarios are evaluated, where the mechanism controlling EA delivery varies. Scenario A, B and C represent diffusion, advection and electromigration by EK, respectively, of EAs in the surrounding groundwater to the low-K zone. In Scenario D, EK was applied and nitrate was added at the cathode (5 g-NO_3/L). In scenario A diffusion occurs at each high-K/low-K interface, scenario B groundwater flow is directly into the low-K block, with flow direction perpendicular to the alignment of the electrodes. The numbers in Figure 5.11 represent the amendment mass flux by electromigration across different boundaries. They include: (1) the nitrate flux across the cathode boundary if amendment is present; (2) the nitrate flux from the high-K host material into the low-K zone with the electric field; (3) the transverse nitrate flux from the high-K host material into the low-K zone as per the observations in these experiments; (4) the flux of nitrate out of the high-K

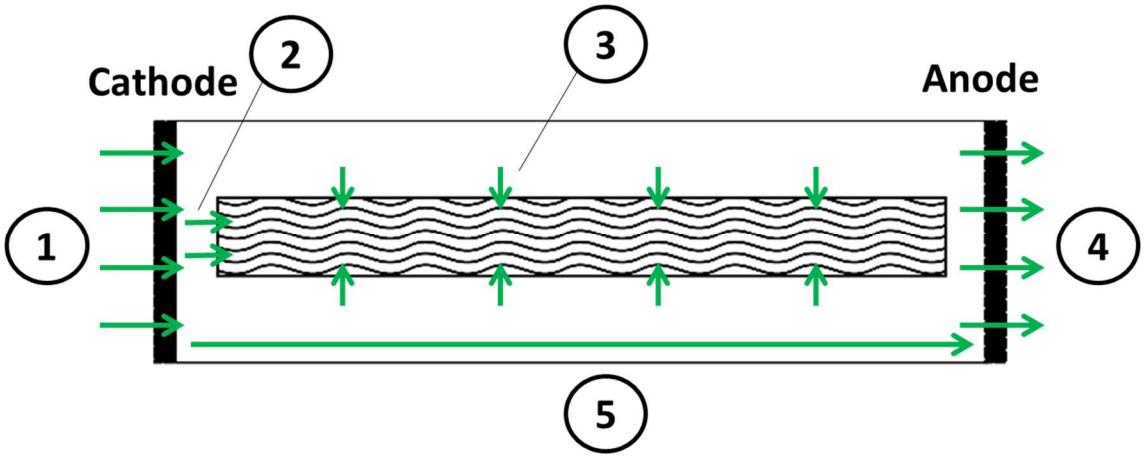

Figure 5.11 Illustration of the model domain (side view) used for the conceptual analysis, showing high-K host material (white) containing a low-K block (waves). Dimensions of host material: 3 x 1 x 10 m; lens: 1 x 1 x 9 m. Green arrows and numbers represent the different nitrate mass flux boundaries under EK.

host material; and (5) the nitrate transport time between the electrodes. The details of these calculations and their input values are in Appendix K (Table K.3 – K.9). Fluxes 1-5 are relevant for scenario D, and flux 2 and 3 are relevant for scenario C. The box model assumes that EAs from the background groundwater and those added as an amendment from the cathode boundary are evenly distributed through the high-K section. In all scenarios, the background groundwater concentration of EAs (see supplementary information) is consistent due to re-supply from groundwater flow.

The results show the time required to balance the ED and EA budgets within the low-K block (Table 5.4). The timescales for delivery of EAs into the low-K block can be significantly reduced by the addition of EK, compared with either diffusion or advection. The presence or absence of the transverse flux had an effect on reducing the timescales. In scenarios C and D the difference was 0.7 and 0.09 years, equivalent to a time saving of 27 and 33%, respectively, over systems where a transverse flux is not developed. In scenario C the presence of a transverse flux had less effect on reducing timescales. This is due to a minimal difference in effective electrical conductivity between the high- and low-K zones compared with scenario D where nitrate is distributed at high concentration through the high-K zone (Figure 5.3). Thus, this phenomenon will be more important at the field-scale when the amendment concentration introduced into the system is higher.

Table 5.4 Results for electron balance model using four scenarios with different transport processes for nitrate amendment. Abbreviations: GW groundwater, EA electron acceptor and ED electron donor.

Scenario	Transport Mechanism	Time (years)	
		EA=ED + Transverse Flux	EA=ED – Transverse Flux
A	Diffusion	48	n/a
B	Advection	38	n/a
C	EK GW EA	1.9	2.6
D	EK NO_3^-	0.18	0.27

5.5 Conclusions

This chapter observes and quantifies, for the first time, a transverse flux of ions arising from voltage differences within a layered heterogeneous setting under an EK applied electric field. This is evaluated in the study using nitrate as an example ion, by considering two hypotheses. The first hypothesis predicts the presence of a voltage difference between layers of material with different effective ionic mobilities. Results show that a greater voltage difference occurs between layers within heterogeneous systems than homogeneous systems and that this difference increases with the addition of nitrate at the cathode. The conceptual model developed to explain this phenomenon links the observed voltage differences and effective resistivity values derived from pore fluid analysis.

The second hypothesis expands the concept of a voltage difference between layers, by proposing an associated mass flux of ions. This is demonstrated using a nitrate amendment and is calculated assuming parameters are known, namely the concentration of the amendment in the host material, the difference in the voltage gradient at the interface between the different materials, effective ionic mobility of the different materials and surface area of the interface. Results show low-K zones within a layered heterogeneous setting relative to the flux predicted for a homogeneous setting of the same material. The importance of this process at the field-scale for an EK-BIO scenario is demonstrated using a simple electron balance model to predict biodegradation timescales in a heterogeneous setting with contaminated low-K zone for electron acceptor transport with, and without, the observed transverse flux. A simulated time saving of up to one third in remediation timescales can be achieved when using EK-BIO, by the enhanced delivery of nitrate into

the low-K zone from this transverse flux, relative to biodegradation supported by advection and diffusion only.

Overall, the findings in this chapter can be combined with Chapter 4 to form a conceptual framework for how EK transport of an amendment is influenced by heterogeneity. This is further developed in Chapter 6 by introducing contaminant and microbial variables.

Chapter 6 Electrokinetic enhanced removal of toluene from physically heterogeneous porous media

6.1 Introduction

At present there are no laboratory based studies in the literature that apply EK-BIO (or other contaminant transformation technologies such as *in situ* chemical oxidation) within heterogeneous settings. This is an important research gap because one of the principle advantages of EK is its effectiveness across a range of K values. Furthermore, EK-BIO is a promising solution to the technical problem posed in Chapter 1 (Figure 6.1). EK can be used to introduce amendments and stimulate bioremediation in low-K zones as well as reduce the contaminant mass by electroosmotic flow. The contamination scenario in Figure 6.1 represent a complex mix of different processes, the contributions of which may influence remediation efficiency. For example, if electromigration of the amendment is too low due to voltage gradient drop (Wu et al., 2012a) or changes in the sediment properties (Chapter 4) then the delivery rate may not be high enough to overcome the demand from biodegradation (Rabbi et al., 2000). Alternatively, the electroosmotic pore fluid flux may be

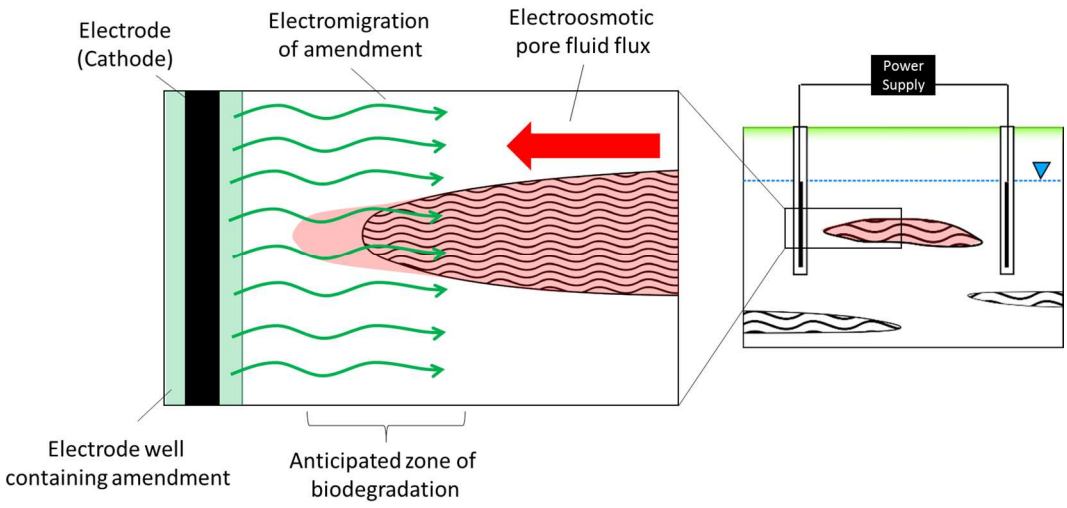

Figure 6.1 Conceptual diagram showing the application of EK-BIO to the technical problem posed in Chapter 1.

too high, shifting the zone of anticipated biodegradation further into the high-K zone (assuming amendment is added at the cathode). More studies are required to understand the mechanisms controlling EK-BIO in heterogeneous settings.

At present all EK-BIO studies have been conducted in homogeneous settings (Hansen et al., 2015; Huang et al., 2013; Mao et al., 2012). However, a range of sediment types and properties have been covered in these references, from high-K sands (Luo et al., 2005b) to low-K clays (Wu et al., 2012). The influence of these materials on biodegradation processes is discussed in Chapter 2. The effectiveness of EK to introduce amendments into heterogeneous aquifer settings has been demonstrated at the laboratory and field-scale (via a modelling study) (Reynolds et al., 2008; Wu et al., 2012b). These findings have been expanded with the studies in Chapters 4 and 5 where the influence of heterogeneous settings is explored in more detail. The findings from these earlier chapters suggest the importance of the effective ionic mobility on amendment delivery. For example, in zones of low effective ionic mobility (such as the low-K sediments in these experiments) there will be an elevated voltage gradient (Chapter 4). This could lead to an increased electroosmotic pore fluid flux and change the dynamics within scenarios such as Figure 6.1. In addition, other studies have demonstrated higher biodegradation rates in these zones due to enhanced contact between microbes, contaminants and other substrates (Li et al., 2010).

6.1.1 Research question and hypothesis

The research question addressed in this chapter is: What is the effect of nitrate migration through physically heterogeneous material by electrokinetics compared with advection on the removal of toluene from a low-K zone containing denitrifying bacteria? This research question is referred to as Research Question 4 (RQ4). The hypothesis is that electrokinetics will enhance the biodegradation of toluene over advection due to the additional mechanisms for nitrate transport created by the electric field.

The objectives were:

1. To conduct bench-scale EK tests to compare toluene removal from low-K zone under EK and advection;
2. To detect presence and movement of the dissolved toluene source by electroosmosis; and
3. To run microcosm tests to determine the biodegradation rate of toluene by the chosen inoculum under ideal conditions.

6.2 Materials and methods

6.2.1 Experimental design

Two types of experiment were used to address RQ4: (1) bench-scale experiments conducted in the rigs developed in Chapter 3; and (2) microcosm experiments. The bench-scale experiments were designed to initiate biodegradation in low-K zones following the addition of nitrate by electromigration. Three different controls were applied that exclude the inoculum, nitrate amendment and EK from the setup (Table 6.1). All bench-scale experiments include a heterogeneous sediment configuration similar to the setup in Chapter 4, a dissolved toluene source and pH control. The bench-scale experiment ran for 14 days (336 hours); sampling of pore fluid samples was every 48 hours and voltage readings were taken every 24 hours when EK was applied. The microcosm experiments ran for 24 days (576 hours); destructive sampling of replicates was every 48 hours after 96 hours and every 120 hours after 336 hours. Raw data for the bench-scale experiments is in Appendix L.

Table 6.1 Experimental variables applied to each rig during the bench-scale experiments.

Rig Designation	Inoculum	Nitrate	EK
A	✗	✓	✓
B	✓	✓	✗
C	✓	✗	✓
D	✓	✓	✓

Microcosm experiments were run to replicate the biodegradation processes in the rigs under ideal conditions. To achieve this, the same setup procedure used in the bench-scale experiments was adapted for the microcosms (this is discussed in more detail in Section 6.2.7). In addition, conditions in the rigs were mimicked in the microcosms. For example, a nitrate solution was added after four days to represent the electromigration of nitrate into the low-K zone. The experiment included an active and blank control microcosm (similar to the bench-scale experiment). These experiments were run for longer than the bench-scale tests to capture any long-term processes associated with biodegradation.

6.2.2 Material properties

Physical heterogeneity in these experiments is represented by a K contrast orientated in series with the electrodes (Figure 6.2). Two types of silica sand were used to represent high- and low-K material: (1) a coarse grained sand (David Ball Group Ltd); and (2) a fine grained sand (Marchington Stone Ltd) mixed 80:20 by weight with kaolin clay (Speswhite, Imerys Performance Materials Ltd) to reduce the K value. Table 6.2 shows the grain size distribution of these materials. Prior to the experiment the sediment was sterilised to minimise biological contamination. The sterilisation method used depended on the material. Coarse-grained sand was autoclaved twice and the fine grained sand and kaolin mix was heat sterilised (3 hours at 150^{o}C). Autoclaving clays can cause aggregation and occlusion of pore spaces, whereas these effects are less pronounced for heat sterilisation (Jenneman et al., 1986). This phenomenon could influence EK migration of substances in the experiment; hence heat sterilisation was applied.

Table 6.2 Physical properties of the sediment used in RQ6 experiments.

Material Property (units)	**High – K**	**Low - K**
Grain Size (mm)	**Fraction (%)**	**Fraction (%)**
<4-2		0
<2-1	1.02	0
<1-0.5	98.75	0.34
<0.5-0.1	0.20	80.65
<0.1-0.05	0.02	3.97
<0.05-0.01		4.24
<0.01-0.005		5.44
<0.005-0.001		3.72
<0.001-0.005		0.42
<0.005-0.0001		1.06
Fraction of organic carbon* (-)	0.0025	0.0027
Porosity (-)	0.39	0.39
Hydraulic conductivity (m/s)	7.0×10^{-4}	6.6×10^{-9}
Electroosmotic permeability (m^2/V-s)	-	3.7×10^{-9}

*Method from the British Standard (BS 1377-3:1990).

The K contrast was created using the method outlined in Chapter 3. Sterilised coarse grained sand was consolidated in the high-K compartment according to the shaker table method outlined in Chapter 3. Once the high-K material was consolidated within the rig it was transferred to an anaerobic chamber along with a tray containing the sterilised fine grained sand and kaolin mix. The anaerobic chamber was sparged with nitrogen for 60 min until O_2 levels were stable at <1%. Oxygen levels within the chamber were measured using an oxygen sensitive sensor (Presens Ltd) fitted to the inside of the anaerobic chamber. The fine grained sand and kaolin mix was then wetted with a volume of synthetic groundwater equivalent to the plastic limit (30% of the kaolin fraction volume). Two different solutions of the same synthetic groundwater were added to the sand kaolin mix: (1) the majority (90%) contained the inoculum (Section 6.2.4); and (2) a concentrated toluene stock (Section 6.2.3). Consolidation of the wetted fine grained sand and kaolin mix was done within the anaerobic chamber using the same method applied for similar mixes in Chapters 4 and 5. The mixture was wet packed into the low-K sediment chamber in the test cell and tamped down using a ceramic pestle (Saichek and Reddy, 2005). This method ensured the inoculum was evenly distributed through the low-K zone.

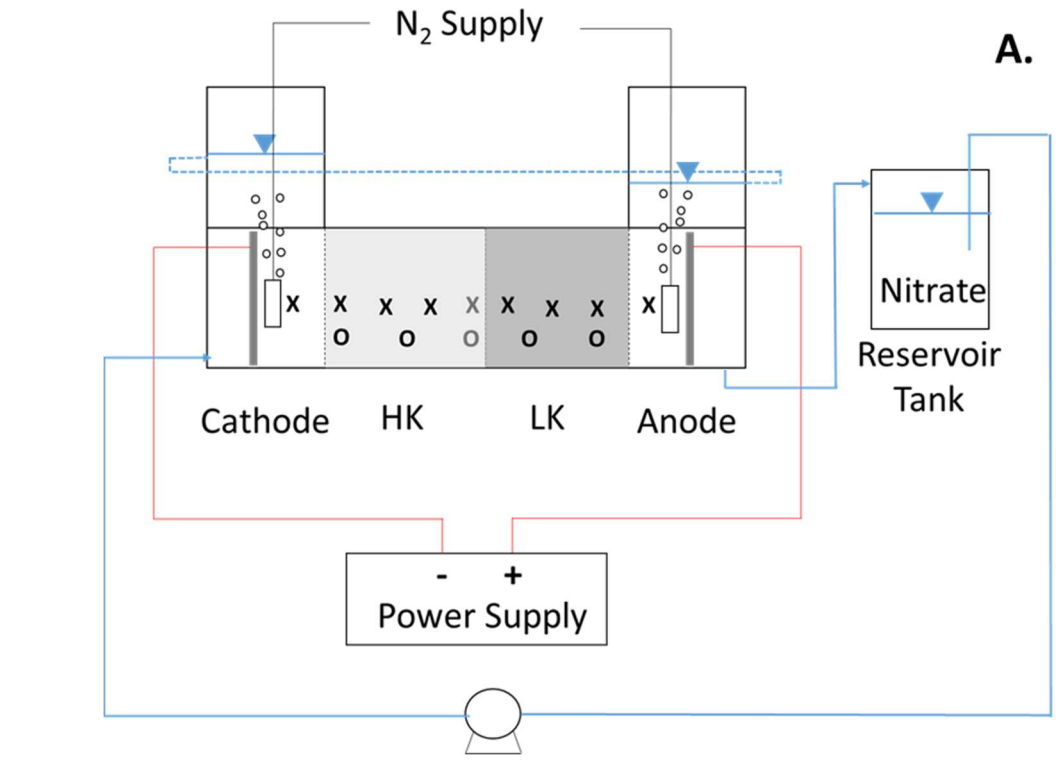

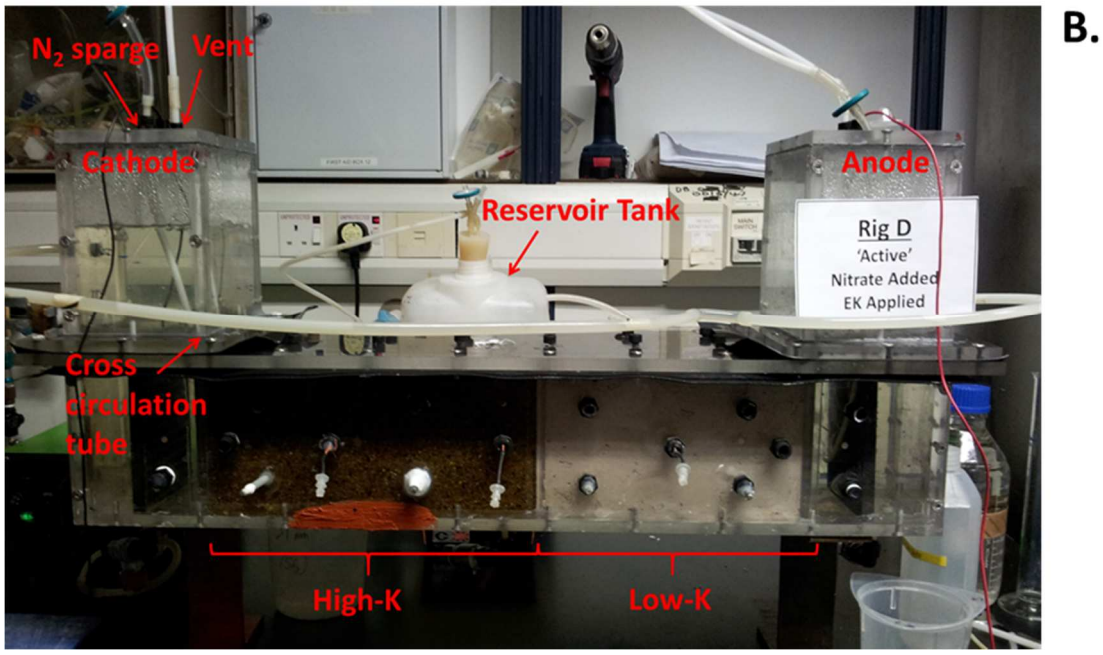

Figure 6.2 Bench scale setup used in RQ4 experiments. A, schematic of experimental setup; HK and LK represent the high and low-K contrast in the sediment, X and O represent sampling and voltage ports respectively; B, annotated digital image of the experimental setup.

Once the material was consolidated and the lid secured, the base unit was removed from the anaerobic chamber. It was then quickly connected to two carboys: (1) a 20 L carboy containing sterile, degassed synthetic groundwater; and (2) a 10 L carboy containing

synthetic groundwater and the inoculum. The 10 L carboy was connected to the valve at the base of the high-K section and the 20 L carboy to the valves in the base of the electrode chambers. Synthetic groundwater was removed from the carboys by displacing it with nitrogen gas, to ensure fluid entering the base unit was anaerobic. Before the addition of synthetic groundwater the carboys were sterilised using bleach and rinsed with sterilised UHQ water. During this process the header tanks were put in place and filled to the desired levels. The high-K section was considered saturated once fluid was observed emerging from threaded ports in the base unit lid, these were then sealed. After saturation the high-K zone is assumed to have inoculum evenly distributed within it.

6.2.3 Contaminant properties

Toluene was selected for these experiments because it is a representative of LNAPL contaminants (CL:AIRE, 2014). It can be degraded by the selected inoculum at concentrations equivalent to 46 mg/L; at higher concentrations toluene has been shown to inhibit growth of the selected inoculum (Lavanchy, 2008). Thus, the optimal starting concentration of toluene in the rigs should be less than or equal to this value.

Toluene was added to the fine-grained sand and kaolin mix as a concentrated stock solution at a ratio of 1:10 with synthetic groundwater. During the mixing and consolidation process the toluene solution is subject to an unknown level of volatilisation. To account for this the starting concentration was designed to be > 46 mg/L. Based on a toluene stock solution concentration of 663 ± 18.6 mg/L, the starting concentration in the rigs should be 66 mg/L. The toluene concentration in pore fluid samples for Rig A-D at the beginning of the experiment were between 5 and 30 mg/L (Figure 6.3). This indicates that approximately 60% of the toluene was lost during the experimental setup. However, it is clear that toluene is retained in the low-K zone at a concentration that will not inhibit biodegradation by the inoculum.

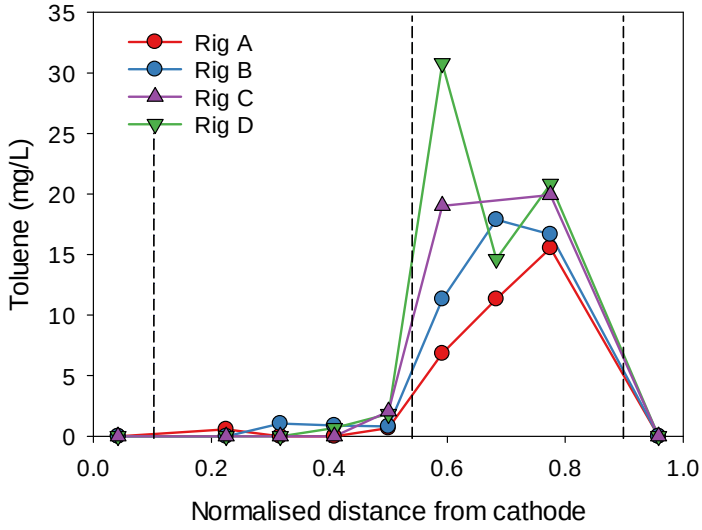

Figure 6.3 Toluene distribution across the length of the sediment chamber for Rig A-D at the beginning of the experiment (t0). Dashed lines represent the boundaries between the sediment and the electrode chambers and the high- and low-K zones.

The concentrated toluene stock was made using a sterilised and degassed sample of synthetic groundwater within a 150 mL capped vial. An aliquot of pure toluene (96.4 µL) was added aseptically through the cap of the vial and allowed to dissolve completely over seven days at 10°C. This was repeated for each rig setup. Samples were taken from the vials for GC analysis before addition to the fine grained sand and kaolin mix (Section 6.2.8).

6.2.4 Microbial growth

To represent the microbiological variable within these experiments a single bacterial strain was identified for the inoculum. *Thauera aromatica* was selected as it is well documented in the literature with the ability to degrade toluene under denitrifying conditions using nitrate as a terminal electron acceptor (Anders et al., 1995). Furthermore, it is a facultative anaerobe, able to grow under both aerobic and anaerobic conditions (Leuthner and Heider, 1998). However, the toluene degrading function of *T. aromatica* is reported to be sensitive to aerobic conditions and will cease when the nutrient medium is saturated with dissolved oxygen (Lavanchy, 2008). Under anaerobic conditions, *T. aromatica* will

degrade toluene to fumarate via benzylsuccinate; this pathway is well documented in the literature (Biegert et al., 1996; Lavanchy, 2008; Winderl et al., 2007).

An R2A slide inoculated with *T. aromatica* strain K172 was obtained from DSMZ Ltd, Germany (DSMZ No. 6984). From this original slide the bacteria was transferred to R2A broth using a sterile loop. It was then grown under aerobic conditions in 100 mL R2A broth at 30ºC to increase cell number (Table 6.4). Aliquots of 1 mL were taken for OD measurements during the incubation. A growth curve for *T. aromatica* is shown in Figure 6.4 showing that the late exponential phase is achieved after 48 hours of incubation.

Table 6.4 Composition of solutions used for *T aromatica* growth.

R2A Broth		**Defined Media**		**Synthetic groundwater**	
0.5 g/L	Yeast Extract		**Solution A**		**Solution A**
0.5 g/L	Meat Peptone	1.63 g/L	KH_2PO_4	0.33 g/L	KH_2PO_4
0.5 g/L	Casamino Acids	11.8 g/L	K_2HPO_4	2.37 g/L	K_2HPO_4
0.5 g/L	Glucose		**Solution B**		**Solution B**
0.5 g/L	Starch	1.06 g/L	NH4Cl	0.21 g/L	NH4Cl
0.3 g/L	K_2HPO_4	0.4 g/L	$MgSO_4x7H_2O$	0.08 g/L	$MgSO_4x7H_2O$
0.05 g/L	$MgSO_4$	4 g/L	KNO_3	0.8 g/L	KNO_3
0.3 g/L	Sodium Pyruvate	0.05 g/L	$CaCl_2x2H_2O$	0.01 g/L	$CaCl_2x2H_2O$
		10 mL/L	**Trace Elements***	2 mL/L	**Trace Elements***
		5 mL/L	**Vitamin Solution***	1 mL/L	**Vitamin Solution***

* See Table 6.3 for component list.

Table 6.3 Composition of supplementary solutions for *T. aromatica* growth.

Trace Elements Solution		**Vitamin Solution***	
10 mL L^{-1}	HCl (25%; 7.7 M)	0.1 g/L	D-Biotin
1.5 g/L	$FeCl_2x4H_2O$	0.1 g/L	Choline Chloride
0.07 g/L	$ZnCl_2$	0.1 g/L	Folic Acid
0.1 g/L	$MnCl_2x4H_2O$	0.2 g/L	myo-Inositol
0.006 g/L	H_3BO_3	0.1 g/L	Niacinamide
0.19 g/L	$CoCl_2x6H_2O$	0.1 g/L	D-Pantothenic Acid•½Ca
0.002 g/L	$CuCl_2x2H_2O$	0.1 g/L	Pyridoxal•HCl
0.024 g/L	$NiCl_2x6H_2O$	0.01 g/L	Riboflavin
0.036 g/L	$NaMoO_4x2H_2O$	0.1 g/L	Thiamine•HCl
		8.5 g/L	NaCl

* Vitamin solution was obtained from Sigma Aldrich, UK No. (B 6891 BME)

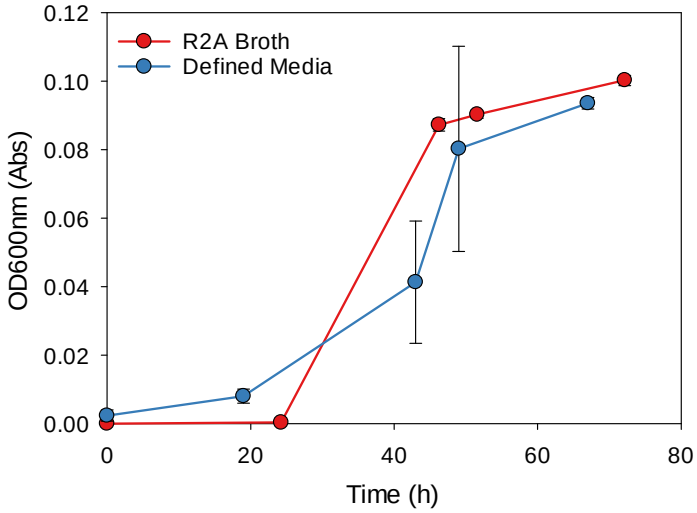

Figure 6.4 Growth curves for *T. aromatica* in R2A broth and defined media (DM). An average value for the control vials was subtracted from the active vials.

The inoculum was grown under anaerobic conditions using toluene as the sole carbon source by taking a 50 mL aliquot of the initial R2A broth. This was centrifuged (10,000 rpm, 15 min) after which the supernatant was decanted and the pellet washed with a sample of the defined *T. aromatica* growth media. The washed re-suspended pellet was then added to a sealable flask containing 140 mL of defined media for anaerobic growth of *T. aromatica*. The defined media is composed of two solutions, A and B, that are adjusted to pH 7.2, autoclaved and then combined after cooling (Table 6.4). A sterile trace element and vitamin solution was added to the media once cooled (Table 6.3). Once the pellet of *T. aromatica* grown under aerobic conditions was transferred to the flask it was capped and degassed using nitrogen. The degassing procedure consisted of inserting two needles aseptically through the vial cap: (1) a long needle (100 mm) that bubbled nitrogen from the base of the vial; and (2) a shorter needle (20-10 mm) to act as a vent. The inoculated flasks were then spiked with 7.4 µL pure toluene that dissolved over several hours equivalent to a concentration of 46 mg/L in the flasks. All ‘Active’ microcosms containing the inoculum were run concurrently with sterile ‘Control’ microcosms. Control microcosms contained sterile growth media prepared according to the same method for the active microcosms but omitting the inoculation step. A visible increase in the turbidity

of the flasks containing the microbe was noted within one month of incubation. After this point a constant growth stock of *T. aromatica* was maintained by transferring 2 mL under anaerobic conditions to a fresh vial every 72 hours.

T. aromatica growth (OD_{600nm}) under anaerobic conditions is shown in Figure 6.4, with the corresponding toluene and nitrate concentration for the same flasks in Figure 6.5. The exponential phase begins after 20 hours and coincides with a decrease in both the toluene and nitrate concentration. Analysis was done on aliquots of 2 mL extracted from the flasks and according to the methods outlined in Section 6.2.8. This demonstrates that the inoculum was actively degrading toluene using nitrate as an electron acceptor.

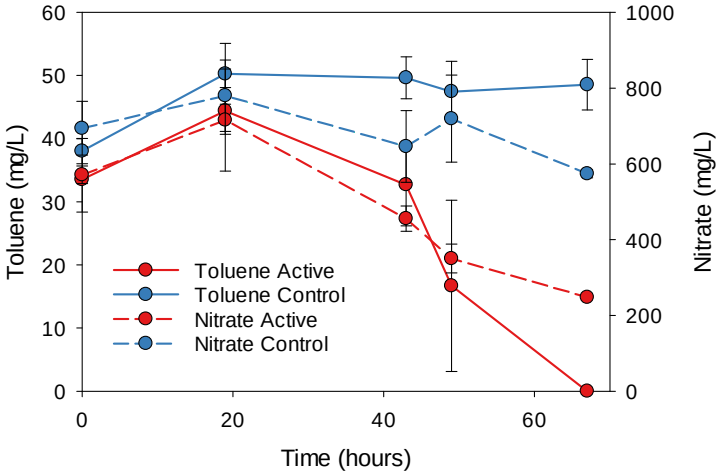

Figure 6.5 Toluene and nitrate concentrations from the defined media growth experiment. Error bars represent one standard deviation from the mean of three replicates.

A dilution factor of five was applied to the defined media to produce a synthetic groundwater for application in the bench-scale experiments (Table 6.4). This is based on electrical conductivity values of the media without potassium nitrate, 3920 µS/cm for the defined media, and 819 µS/cm for the synthetic groundwater. Potassium nitrate is excluded from this test because the objective of the experiment is to add the nitrate by either electrokinetics or advection. The electrical conductivity value for the synthetic groundwater is similar to the starting value in previous experiments (Chapters 4 and 5). The viability of the synthetic groundwater to support *T. aromatica* growth was tested prior

to setting up the bench scale experiment. Growth was observed after 48 hours (from 0.08 to 0.14 A OD_{600nm}) following pelleting of 40 mL anaerobic growth stock under aerobic conditions, transfer to vials that were subsequently degassed, refrigeration at 5°C for 24 hours and incubation at room temperature.

Preparation of an inoculated 10 L volume of synthetic groundwater for the bench-scale experiments included: (1) 17 x 140 mL anaerobic flasks containing degassed DM growth stock inoculated with 2 mL *T. aromatica* solution; (2) incubation of flasks for 48 hours at 30°C to an average of 0.20 Abs OD_{600nm}; (3) transfer of 40 mL to a falcon tube and centrifugation at 5000 rpm for 5 min; (4) decanting of supernatant and re-suspension of the pellet in a degassed 5 mL sample of sterile synthetic groundwater; (5) transfer of 5 mL concentrated *T. aromatica* to a carboy containing 10 L sterile and degassed synthetic groundwater, repeating steps 1-5 for remaining growth stock; and (6) storage of carboy at 5°C until use in the experiments (up to 48 hours). The pelleting process created a dilution factor between the defined media growth stock and the synthetic groundwater of 4.3. Samples of synthetic groundwater with and without *T. aromatica* were analysed for cell counts using epifluorescence microscopy. Samples were stained with Syto 9 (Invitrogen Ltd, UK), filtered and then viewed with an Olympus BX50WI Upright Fluorescence Microscope (Olympus OpticalCo. Ltd, London, UK) fitted with CoolSnap colour camera (Princeton Instruments, Buckinghamshire, UK). The synthetic groundwater containing the inoculum had 9.8×10^5 ($\pm 4.5 \times 10^5$) cells/mL; the control had no observable cells.

6.2.5 Bench scale setup

The same test cell developed in Chapter 3 and applied in Chapters 4 and 5 is used in these experiments. An important consideration is the adsorption of toluene onto rig components. Adsorption tests were conducted on two key materials used in the rig: (1) acrylic, used to construct the base unit and header tanks; and (2) the rubber gasket used to prevent leaks at the interface between the base unit, lid and header tanks. Samples of acrylic and rubber were added to 20 mL vials containing four different concentrations of

toluene. A series of control vials were included that contained no material. Each concentration was run in triplicate; in total 36 vials were used. Vials were sampled immediately after the materials were added and at 72 and 120 hours to determine when toluene distribution was in equilibrium. The surface area of the acrylic and rubber sample was 1032 and 572 mm^2, respectively.

Toluene concentrations were analysed using the GC-MS method specified in Section 6.2.8. Results from the adsorption test indicate that in the no-material control there is little change between the initial concentration and subsequent sampling points (Figure 6.6C). Similarly, the acrylic material appears not to adsorb toluene at the concentration tested (Figure 6.6A). Conversely, the rubber material appears to adsorb more than half the toluene in the vial (Figure 6.6B). The maximum amount of toluene adsorbed is $8.2x10^{-4}$ mg/mm^2. This is equivalent to 21.5 mg of toluene adsorbed on to the rubber gasket in contact with the contaminated sediment in the bench-scale setup (2.6×10^4 mm^2). It is assumed that when the baseline sample is taken, the toluene concentration in the pore fluid is in equilibrium with the rubber gasket in the bench scale experiment.

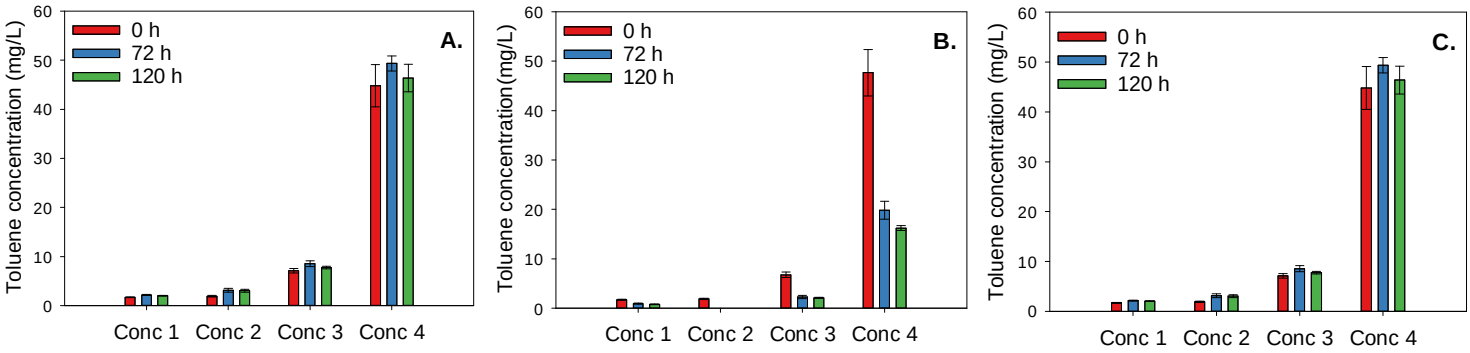

Figure 6.6 Adsorption test for toluene onto materials used in rig construction. A, acrylic; B. rubber gasket; and C, no-material control. Error bars represent the standard deviation from mean of three replicates. Conc 1-4 represent toluene solutions of 2.3, 4.6, 9.2 and 46 mg/L respectively.

Once the material was consolidated, removed from the anaerobic chamber and saturated it was connected to three different systems: (1) nitrogen sparge; (2) electrolyte recirculation; and (3) power supply (Figure 6.2A). The nitrogen sparge consisted of a

nitrogen line into each electrode chamber that bubbled nitrogen through the electrolyte. The objective was to strip out oxygen that could either diffuse into the sediment chamber or be transported by electroosmosis with the electrolyte. The rate at which nitrogen was added varied depending on supply, but was approximately 1.6 mL/s. The function of the electrolyte recirculation is to neutralise pH (described in Section 6.2.6) and distribute the amendment between the RT, cathode and anode. The amendment was added as powdered KNO_3 to the reservoir tank containing 9 L of synthetic groundwater to give a concentration of 10 g-NO_3/L (equivalent to 147.6 g-KNO_3). It was then allowed to dissolve over 3 hours under vigorous stirring. At this point a baseline sample was taken, after which the recirculation system was started (Watson Marlow 505Du peristaltic pump) and the power supply switched on. Similar to previous experiments, a direct current was applied from a power pack (Digimess, PM6003-3) and constant current was established and checked with a multimeter (Digitek, DT-4000ZC).

Once the system was connected, it stood with only the nitrogen sparge active for 24 hours to allow microbial attachment to the sediment as per a similar experiment in the literature (Song and Seagren, 2008). Sampling was conducted using the same method developed in Chapter 3 and applied in Chapters 4 and 5. In these experiments each rig had 7 sample tubes evenly spaced along the sediment chamber, one in each electrode chamber and one sample for the reservoir tank (10 in total, 40 per sample point). Toluene sampling was initially conducted using glass syringes to withdraw pore fluid samples, but these did not provide a sufficient seal to remove samples from the low-K sediment. Hence, disposable plastic syringes were used to quickly withdraw the sample and transfer it to a 2 mL glass vial that was then sealed and stored at -18^{o}C for later analysis. Using plastic syringes increases the potential for toluene loss by adsorption onto the syringe material. An adsorption test was conducted to determine whether this effect was significant over the short timescales associated with sampling (approx. 2 min). Similar to the material adsorption test, four different concentrations were analysed. Vials containing a known

concentration of toluene were then sampled with either a glass or plastic syringe, allowed to stand for one minute and transferred to a glass vial for analysis. This was repeated three times for each concentration. Toluene concentrations were analysed using the GC-MS method specified in Section 6.2.8. Results suggest that at different concentrations the syringe material had minimal effect on the adsorption of toluene (Figure 6.7). Thus, the syringe material is discounted as a removal mechanism of toluene prior to analysis.

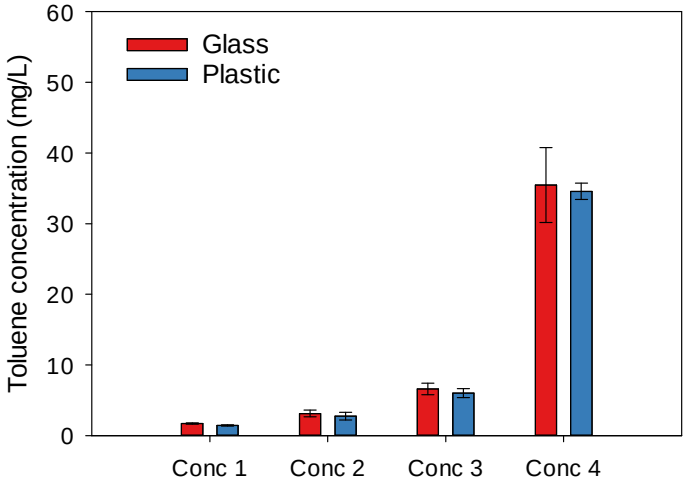

Figure 6.7 Adsorption to material used in sampling procedure. Conc 1-4 is equivalent to 2.3, 4.6, 9.2 and 46 mg/L respectively.

6.2.6 Electrokinetic apparatus

The direct current was applied as a constant current at 25 mA (1.6 A/m^2) similar to experiments in Chapters 3, 4 and 5. However, the pH control method was changed from electrode conditioning to recirculation. This prevented high concentrations of solutes, namely Na and Cl being added to the electrode chambers. Other studies have reported an inhibition effect of chloride in the anode chamber on biodegradation due to electrochlorination (Tiehm et al., 2009). Biodegradation in the anode chamber is expected to be minimal, but electroosmotic flow of anodic chamber fluid could potentially deliver dissolved chlorine into the low-K zone. Hence recirculation is the preferred pH control option.

The configuration of the recirculation system is similar to Wu et al. (2012) and Mao et al. (2012), where a cross circulation tube transfers the catholyte fluid to the anode. However, unlike these methods, the head difference between electrodes allows fluid transfer between electrodes without the need for an additional pump or the risk of short-circuiting the sediment chamber. The head difference is equivalent to a hydraulic gradient of 0.14 between the electrode chambers. Based on the hydraulic conductivity of the low-K zone this is equivalent to a flow rate of 1.2 mL/d and a solute flux (assuming a concentration of 10 g/L) of 0.077 g/d-m^2. This is three orders of magnitude lower than the predicted electromigration solute flux (assuming an effective ionic mobility of $6.5x10^{-9}$ cm^2/s-V and a voltage gradient of 50 V/m) of 28.1 g/d-m^2. Thus, the advective flux of nitrate is considered to be negligible during the experiment.

Calibration of the recirculation system involved varying the rate at which the electrolyte was circulated and observing the pH change at the electrode over 6 time points (Figure 6.8). For each time point direct current is applied for 24 hours and samples taken for pH analysis. After this the fluid circulation rate was reset to 20 mL/min and left to stabilise for 24 hours before EK was applied again and the pump rate set to a new value. Six circulation rates were tested: 0, 5, 14, 18.5 and 25 mL/min. Values for cathode and anode pH are

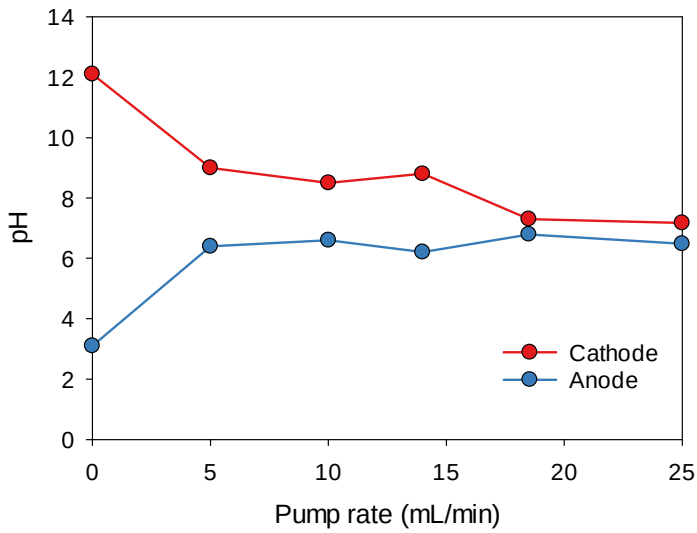

Figure 6.8 pH in the anode and cathode electrode chambers at different pumping rates applied to the recirculation system.

shown in Figure 6.8. As pump rate increases the system is more effective at maintaining neutral pH conditions. After 18 mL/min the pH of each electrode chamber is close to 7. The pH in the electrode chamber at 25 mL/min was continued for seven days to ensure that the pH difference was stable; the cathode pH was 7.2 ± 0.4 and the anode, 6.5 ± 0.2. Thus a pump rate of 25mL/min was applied to neutralise pH in these experiments.

Previous experience applying recirculation systems to these rigs indicated that solute dispersion into the sediment chamber results from the pulsing effect of the peristaltic pump (Chapter 3). This creates an undesired solute flux into the sediment. A fluorescein tracer test was conducted to deduce if this effect occurred in this setup. Fluorescein was added to the reservoir tank and observed moving around the recirculation system. On close inspection no fluorescein migrated into the high-K zone after 5 hours. This was thought to be due to the low-K zone preventing fluid flow through the sediment chamber. However, during the experiment a high nitrate concentration occurred in the high-K zone of the advection control rig. This effect was not due to advection mass transport because the hydraulic conductivity is too low, hence it was concluded that solute dispersion from pumping was occurring these experiments. This was later confirmed in an additional bromide tracer test. This phenomena does not influence the outcome of these experiments because: (1) the toluene, nitrate and microorganisms are located in the low-K zone that is not influence by this dispersion effect; and (2) it does not enhance the removal of toluene from the low-K system.

6.2.7 Microcosm setup

Microcosms were designed to mimic biodegradation processes in the rigs. A blank series of microcosms without the inoculum represented the control. In total 54 sacrificial microcosms (20 mL vials) were prepared that included active and control series over nine time points including the baseline. Preparation of the microcosms included the following steps: (1) sterilisation of vials, caps and other relevant apparatus by autoclave; (2) transfer of apparatus, sterilised sediment and degassed synthetic groundwater to an anaerobic

chamber; (3) transfer a 6.3 mL aliquot of the synthetic groundwater to a vial, synthetic groundwater for control microcosms was filter sterilised before addition; (4) the sediment was added to the vial by pluviation; (5) a 0.1 mL aliquot of 1M NaOH was then added to elevate the pH from 5 to 7 (based on previous tests); (6) the vial was then capped and removed from the anaerobic chamber; (7) the vial was degassed through the cap; (8) a 0.54 mL concentrated toluene solution (600 mg/L) was added to the vial through the cap; and (9) a 0.088 mL concentrated KNO_3 solution (150 g/L) was added through the vial cap after 4 days from the attachment phase.

Fluid samples were taken using a method adapted from the rigs. After the vial cap was removed a sampling tube with the sintered glass block fitted to the end was inserted into the vial. A fluid sample was then extracted using a plastic syringe. Analysis of the sample was for pH, toluene and major ions by methods outlined in Section 6.2.8.

6.2.8 Analytical methods

Major ions and acetate were analyzed using an ion chromatograph (Dionex ICS 3000, Thermo Scientific) with autosampler and eluent regeneration. The anions were separated using a Dionex IonPac AS18 column with an AG18 guard column and 31mM sodium hydroxide as eluent, at a flow rate of 0.25 mL/min. The cations were separated by a Dionex IonPac CS16 column with a CG16 guard column and 48 mM methane sulphonic acid as eluent, at a flow rate of 0.42 mL/min. Selected pore fluid samples from certain time points in the bench-scale experiment were also analysed for pH.

Toluene analysis was conducted on a Varian gas chromatograph (CP-3800) with an attached Varian mass spectrometer (Saturn 2000). Samples were extracted from vials using a solid-phase microextraction (SPME) autosampler. SPME extraction method included inserting a fiber with a polydimethylsiloxane coating (red fiber) and extracting the sample for 5 minutes. The fibre with the adsorbed analyte was inserted into the injection port held at a temperature of 200^{o}C and allowed to desorb for 1 min. The split ratio at the

injection port was 20. The sample is then passed through a 30 m x 0.25 mm x 0.25 µm GC column (HP-5MSUI, Agilent Technologies, Inc). The column oven temperature starts at 40°C then ramps up to 150°C at a rate of 100°C/min, in total the GC run time is 8 min. The MS detector is active between 3 and 4.5 min of the GC run with a scan range between 40-200 m/z. Including the SPME desorption time, the total run time is 13 min.

For both the Dionex and GC-MS method a 5 point calibration was included in each run and quality control standards inserted throughout the samples. A 7.5 µL aliquot of internal standard containing 101.5 mg/L deuterated toluene was added each sample for GC analysis. This allowed more effective quantification of toluene as it compensated for volatilization of toluene over the sample run.

6.3 Results and discussion

6.3.1 Bench-scale experiment conceptual model

Toluene mass removal from the low-K zone in the bench-scale experiments can potentially occur by a number of mechanisms, namely: electroosmosis, diffusion and biodegradation. The influence and characteristics of these processes is shown in a conceptual model (Figure 6.9). Electroosmotic flow is shown moving from the anode to the cathode. Movement of the pore fluid provides a transport vector for dissolved toluene moving it from

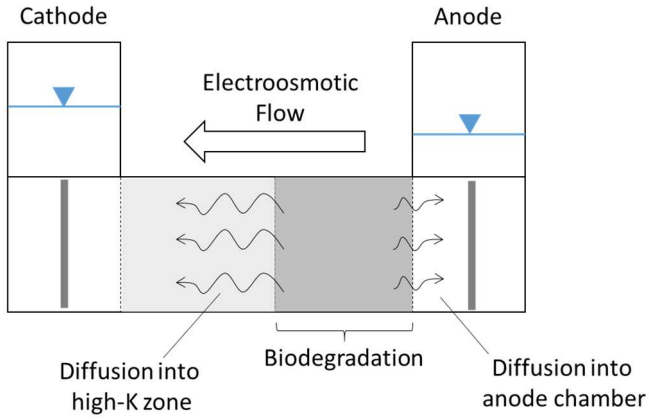

Figure 6.9 Conceptual model for the toluene mass removal processes occurring in the bench-scale experiments.

the low-K to the high-K zone and into the cathode chamber. Solute mass flux by electroosmosis of solute, i is given by (Acar and Alshawabkeh, 1993):

$$J_i^{eo} = C_i v_c^{eo}$$

Equation 6.1

where J_i^{eo}, is the electroosmotic mass flux (mg/m^2-s), C_i is the concentration of the solute (mg/m^3) and v_c^{eo}, is the velocity of a contaminant under the electroosmotic pore fluid flux (m/h). The velocity of toluene transport will be a function of the retardation factor:

$$R_f = \frac{v_w}{v_c} = \frac{v_w^{eo}}{v_c^{eo}}$$

Equation 6.2

where R_f is the retardation factor, v_w is the pore fluid flux (m/s) and v_c is the contaminant velocity (m/s) (Hiscock, 2005). The retardation factor accounts for the adsorption of the contaminant onto the sediment particle surface and will influence the velocity of a contaminant transported by electroosmosis (Bruell et al., 1992). The retardation factor is dependent on the partition coefficient, K_d (mL/g) of the contaminant between the pore fluid and sediment material (Freeze and Cherry, 1979):

$$R = 1 + \frac{\rho_b}{n} K_d$$

Equation 6.3

The K_d value is in turn a function of the fraction of organic carbon in the sediment, f_{OC} and can be determined based on the following relationship for contaminants with a low water solubility (<1x10^{-3} M) (Delle Site, 2001):

$$K_{OC} = \frac{K_d}{f_{OC}}$$

Equation 6.4

Where K_{OC} is the partition coefficient onto organic carbon (mL/g). Due to the presence of organic carbon in these sediments (Table 6.2) it is anticipated that toluene migration by electroosmosis will be retarded to some degree.

Diffusion will be determined by the diffusion mass flux equation:

$$J_i^D = -D_i^* \frac{\Delta C_i}{\Delta x}$$

where J_i^D is the diffusive mass flux (mg/m^2-s). It will occur across the low-K/high-K and low-K/anode chamber interface. The rate of diffusion will be higher at the low-K/anode chamber interface because: (1) toluene is diffusing into a fluid chamber therefore the diffusion coefficient at infinite dilution applies whereas across the low-K/high-K interface it is a function of the porosity and tortuosity of the high-K material; and (2) a higher concentration gradient is observed because toluene is assumed to be removed quickly from the anode chamber based on volatilisation from nitrogen sparging effect and adsorption onto the graphite electrode.

Biodegradation of toluene by *T. aromatica* is expected to be via denitrification as observed in the preliminary growth experiments. The first step is of nitrate reduction to nitrite which is then further reduced to gaseous forms of nitrogen (Anders et al., 1995):

Nitrate reduction to nitrite:

$$C_7H_8 + 18NO_3^- \rightarrow 18NO_2^- + 7CO_2 + 4H_2O$$

Equation 6.5

Nitrite reduction to nitrogen:

$$C_7H_8 + 18NO_2^- \rightarrow 7N_2 + 7CO_2 + 4H_2O$$

Equation 6.6

Based on these relationships toluene biodegradation can be monitored by changes in the nitrate and nitrite concentration. The location where biodegradation is anticipated to occur is in the low-K zone due to high concentration of nitrate, toluene and presence of microbes.

Biodegradation of toluene in the high-K zone is not considered due to the dispersion effect from the recirculation system that will displace toluene over time. Furthermore, microcosm experiments represent biodegradation of toluene under ideal conditions. Results from microcosms can be compared against the rigs to identify biodegradation timescales.

6.3.2 Toluene removal from low-K zone by electroosmosis

A direct current is applied to Rigs A, B and C up to 96 hours. This timescale accounts for: (1) the time required for nitrate to migrate into the sediment chamber and low-K zone by electromigration from the cathode; and (2) electroosmotic pore fluid flux that will flush toluene out of the low-K zone. After 96 hours, based on the lowest voltage gradient observed in Rig A and D between electrodes, nitrate is expected to have migrated across the high-/low-K boundary.

Toluene concentrations within the bench scale tests are derived from the sum of toluene mass in the system divided by the volume. Toluene mass is obtained from pore fluid concentrations and integrated over the dimensions of the bench-scale rig. The toluene mass values are then summed and divided by the volume of either the high- or low-K zone. Toluene concentrations calculated by this method for the low and high-K zone are shown in Figure 6.11A and B. In the low-K zone where the toluene source originates, the concentration for each rig decreases over time indicating that there are removal mechanisms occurring (Figure 6.11A). In the rigs where EK is present there is a noticeable rapid decrease over the period when a direct current is applied. In Rig A this effect is delayed, possibly due to sampling issues. In the advection control (Rig B), a sharp decrease is not observed, implying that the phenomenon is associated with the application of EK. Furthermore, in experiments where EK is applied, toluene is observed in the high-K zone. The conceptual model suggests toluene migration by electroosmotic flow will be predominantly towards the cathode (Figure 6.9), hence toluene should be detected in the high-K zone. This indicates that electroosmotic flow is the principle mechanism by which toluene is removed from the low-K zone during the period EK is applied.

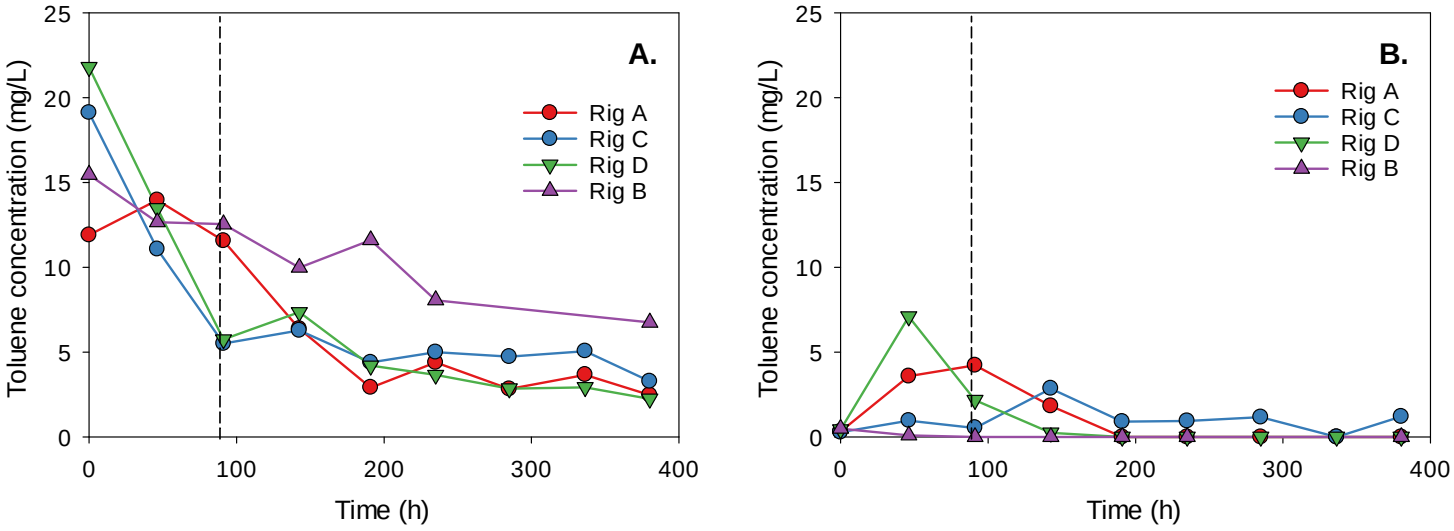

Figure 6.11 Toluene concentrations in different sections of the bench-scale test cell. A, toluene concentration in the low-K zone; B, toluene concentration in the high-K zone. Dashed red line indicates when the direct current is switched off in Rigs A, C and D.

After the bench-scale experiments ended a further test was conducted to demonstrate the influence of electroosmotic flow on the removal of toluene. The application of direct current was swapped between Rig B (advection control, no EK) and Rig C (nitrate control, EK applied). Results show that when a direct current is applied the toluene concentration rapidly decreases compared to a no-EK system where toluene concentrations persist (Figure 6.10).

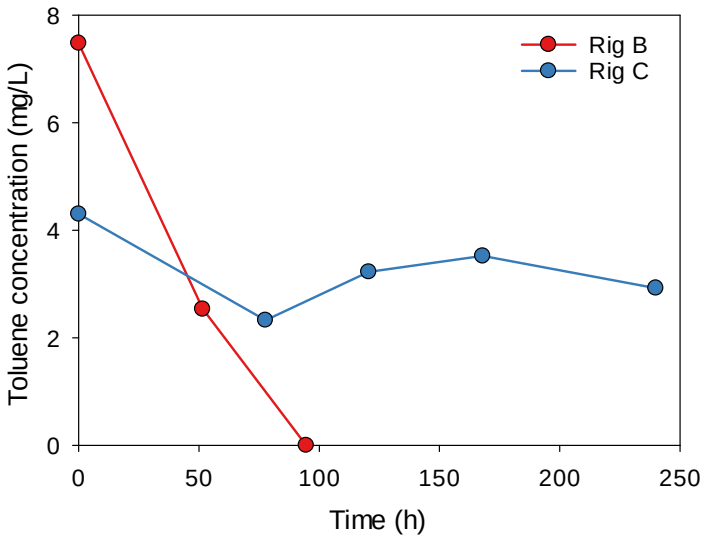

Figure 6.10 Toluene removal from Rig B, EK applied and Rig C EK not applied

6.3.3 Toluene removal from low-K zone by biodegradation

Toluene removal by biodegradation under ideal conditions is observed in the microcosms (Figure 6.12). When the concentrated nitrate solution is added after 100 hours a decrease in the toluene concentration is observed in the active microcosm system. The toluene concentration in the control also decreases, however after 250 hours toluene loss in the active system is more defined. A profile of toluene loss similar to this would be anticipated in the bench-scale experiments following nitrate addition because it is the point in the experiments when the toluene, nitrate and microbes are anticipated to be in the same place. This is in contrast to the observed slow removal of toluene in the rigs following the application of EK (Figure 6.11A). To identify whether toluene was removed by biodegradation in the rigs the indicators of denitrification (nitrate and nitrite) should be examined.

Nitrate concentrations in the rigs and microcosms are presented in Figure 6.13A and B. High nitrate concentrations in Rig A and D demonstrate that EK is effective at delivering the amendment into the low-K zone compared to the no-EK control, Rig-B. This confirms the hypothesis in that EK is more effective at transporting the nitrate into the low-K zone

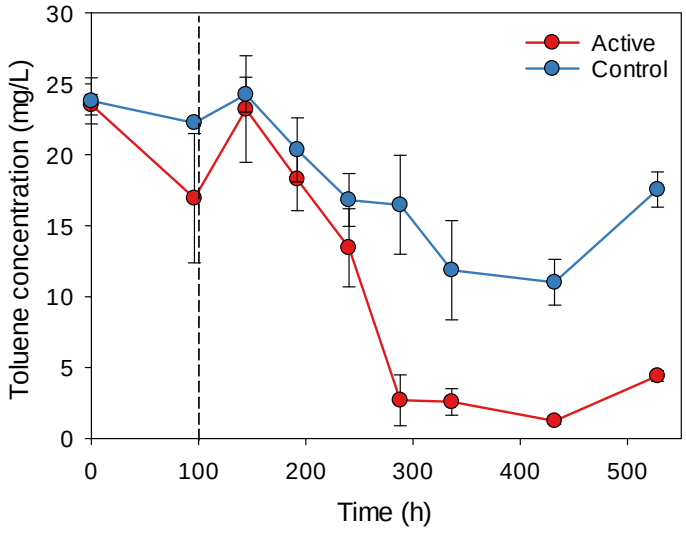

Figure 6.12 Toluene concentration in the active and control microcosm. Dashed red line indicates when nitrate solution is added.

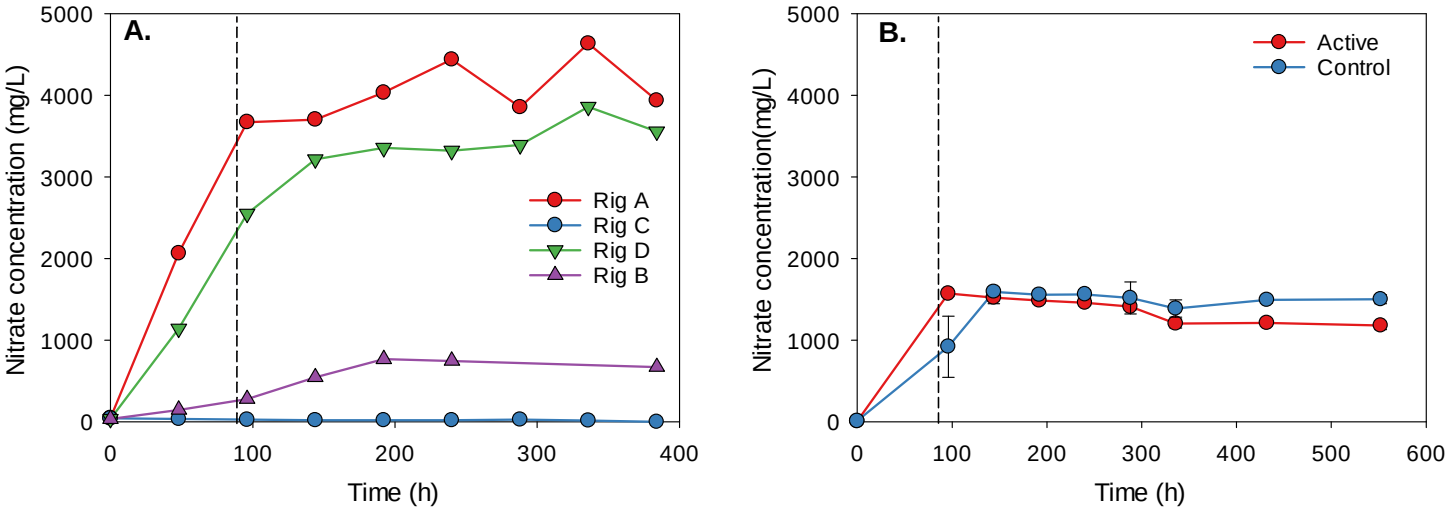

Figure 6.13 Nitrate concentrations in the low-K zone within the bench-scale and microcosm experiment. In A the dashed red line indicates when EK is switched off and B, when nitrate solution is added.

compared to advection. Although, some nitrate is present in Rig B resulting from a draw of high nitrate concentration pore-fluid from the high-K zone due to sampling.

In this instance nitrate is not an effective means to observe toluene degradation in the bench-scale experiments. The predicted nitrate concentration consumed as a result of complete mineralisation of toluene (post electroosmotic flux) is: rig A; 140.1 mg/L; and Rig D; and 69.5 mg/L (based on Equation 6.5). These values are lower than the 5% analytical precision associated with nitrate for the analysis method. Approximate concentrations of 4100 mg/L and 3500 mg/L are equivalent to a 5% analytical precision of 205 and 175 mg/L in Rig A and D respectively. Thus, any drop in the nitrate concentration as a result of toluene biodegradation will be difficult to discern in Rig A and D. In the microcosm experiment a decrease in the nitrate concentration outside the analytical precision boundary (±78.5 mg/L at 1570 mg/L) can be identified for the active microcosm. This indicates that nitrate is being consumed at significant levels compared to the blank control.

Production of nitrite is observed in all bench-scale and microcosm experiments (Figure 6.14A and B). It is observed in Rig A and the microcosm control where no inoculum was included in the experimental setup. This indicates that bacteria are present in the blank

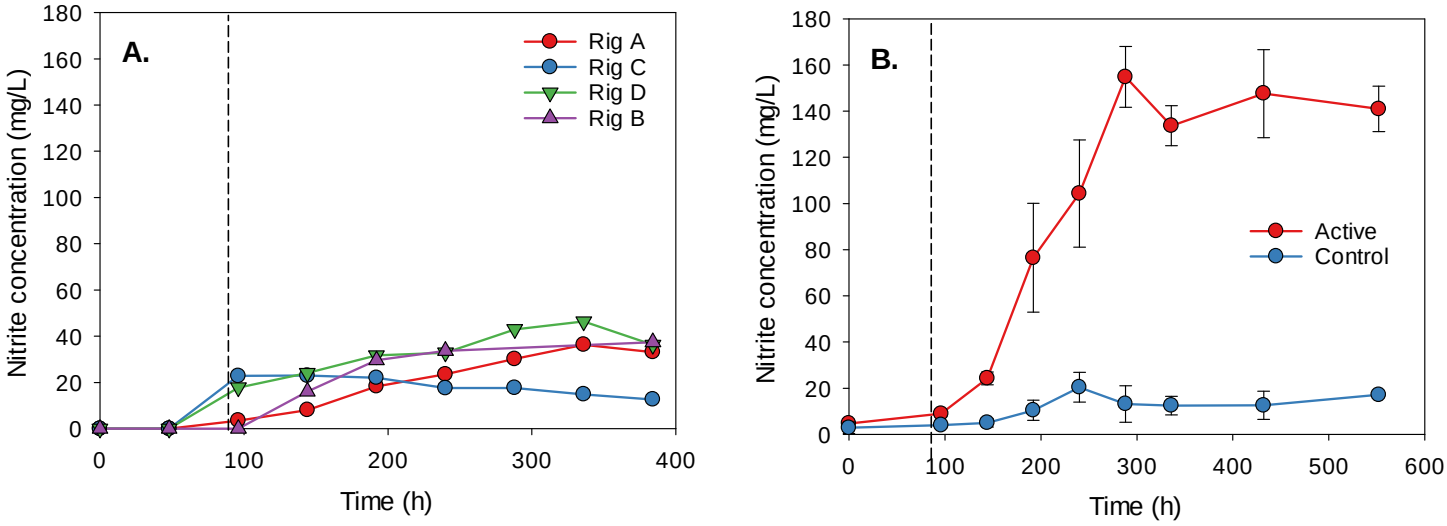

Figure 6.14 Nitrite concentrations in the low-K zone within the bench-scale and microcosm experiment. In A the dashed red line indicates when EK is switched off and B, when nitrate solution is added.

controls and that denitrification is occurring. Bacterial contamination could originate from exposure of the experimental system (e.g. during sampling) or ineffective sterilisation procedure. However, it is not clear whether nitrite production could be the result of toluene degradation. In the microcosm control the increase in the nitrite concentration (max 20.4 mg/L) is equivalent to a toluene concentration of 2.3 mg/L which is less than the 9.5 mg/L decrease observed in Figure 6.12. Further analysis is conducted as part of a toluene mass balance in Section 6.3.5.

In Rig C starting conditions include a low concentration of nitrate (40 mg/L) that is fully consumed over the experiment (not distinguishable in Figure 6.13A). Nitrate is present due to carry over from the pelleting process. Subsequent reduction of this nitrate to nitrite is observed by the presence of nitrite in the low-K zone (Figure 6.14A). It is shown to decrease over time due to nitrate in the low-K zone not being replenished by amendment addition. This was not anticipated to have a significant effect on experimental processes because: (1) the high mass of nitrate added to rig A, B and D by comparison; and (2) growth tests of *T. aromatica* on synthetic groundwater demonstrated no-growth on a toluene substrate when the nitrate concentration was less than 59 mg/L. This suggests

that the nitrite observed in Rig C and potentially other rigs results from denitrification of an alternative carbon source to toluene.

The pH of the pore fluid in EK active systems is not anticipated to hinder biodegradation. Pore fluid pH values are plotted against the distance between electrodes for Rig D (Figure 6.15). At the beginning of the experiment pH in the low-K zone is 5.2 – 5.6 which is lower than the limit of toluene degradation by *T. aromatica* observed in the growth studies (pH 6.6). Over the first 91 hours of EK application the pH is elevated to between 7.2 and 6.4 in the low-K zone. This could be due to the electroosmotic flow of fluid from the anode chamber where the pH over this time ranges from 7.1 – 6.9. The pH is maintained above 6.6 in the low-K zone for the duration of the experiment.

A possible reason for biodegradation not being enhanced in the bench-scale experiment could be a lack of phosphate in the pore fluid. The inorganic phosphate concentration in the synthetic groundwater should be 1290 mg/L. However, at the beginning of the bench-scale experiment the phosphate concentration was below detection limit. Similarly, in the microcosm experiment phosphate concentration was relatively low at 60 mg/L. Phosphate could be consumed as a stress response by the microbes to the experimental conditions

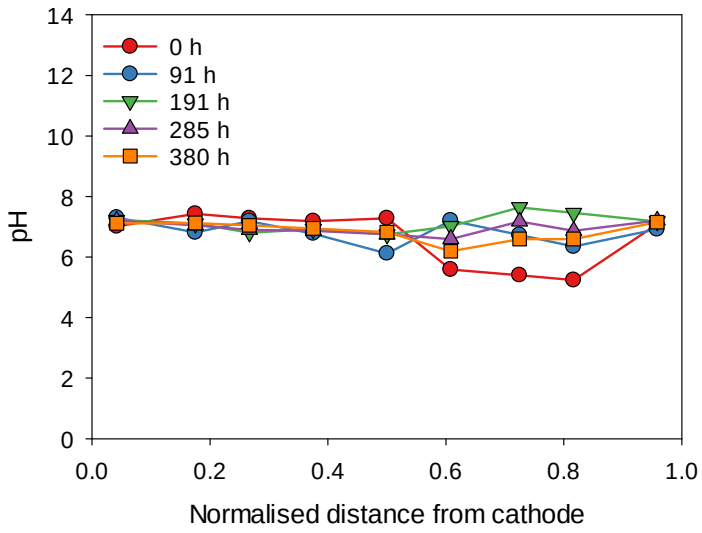

Figure 6.15 pH of pore fluid in the bench-scale experiments for Rig D.

resulting in insufficient quantities being present once the nitrate is added to the system. A secondary microcosm study setup according to Section 6.2.7 confirmed that the inoculum cannot degrade toluene using nitrate when phosphate is absent. Future EK experiments using this inoculum should consider including phosphate as part of the amendment solution.

6.3.4 Toluene removal from low-K zone by diffusion

Diffusion could be a dominant process in the bench-scale experiments. However it is difficult to observe direct evidence because the main diffusion pathway is into the anode chamber. No toluene has been detected in the anode chamber, it is anticipated that any toluene present will have a short residence time due to the recirculation system, volatilisation from the nitrogen sparge and adsorption onto the graphite electrode. Diffusion mass flux across the boundaries observed in the conceptual model (Figure 6.9) can be used to predict toluene mass loss by diffusion. This is applied to Rig B where no EK is applied and mass loss by advection is limited (Figure 6.16). Results demonstrate that a good fit can be obtained between observed and calculated values implying that diffusion is occurring in these systems.

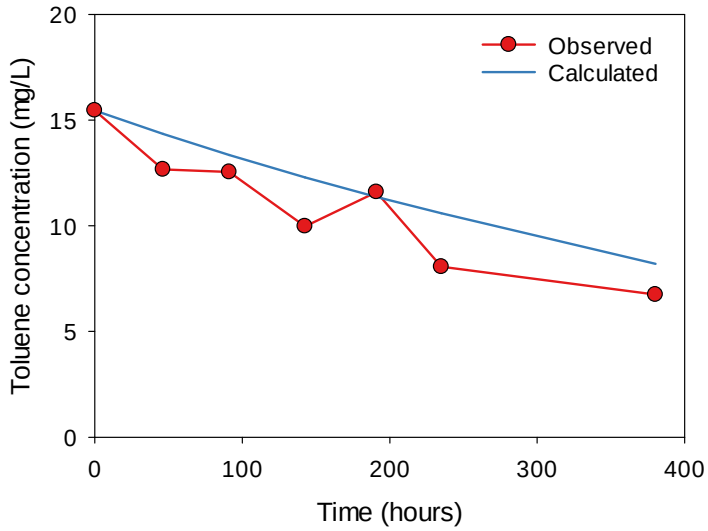

Figure 6.16 Observed and calculated toluene concentrations. Calculated concentrations represent toluene loss by diffusion only.

6.3.5 Toluene mass balance

The hypothesis stated in Section 6.1.1 has not been proven because enhanced biodegradation did not occur in either the EK or advection systems. Therefore, a toluene mass balance was conducted to identify the predominant toluene loss mechanisms from the low-K zone as well as the source of nitrite in the bench-scale experiments. This is done by comparing observed and calculated values of toluene mass loss. Observed values are determined by the difference in toluene mass within the low-K zone over time, whereas calculated values are determined by the equations described in the conceptual model (Section 6.3.1). Toluene loss by electroosmosis is based on the electroosmotic mass flux of toluene out of the low-K zone into the high-K zone towards the cathode (Equation 6.1). The contaminant velocity used in this equation is calculated from the electroosmotic pore fluid flux (based on the electroosmotic permeability, k_e value in Table 6.2 and Equation 1.1). A retardation factor of 1.55 was calculated based on Equation 6.3 and Equation 6.4 using experimental values for the bulk density (2.25 g/mL), porosity and f_{OC} (Table 6.2). A K_{OC} value of 35 mL/g was used because it provided the best fit with observed data. In the literature, K_{OC} values for toluene range from 35 – 165 mL/g (Delle Site, 2001). Toluene loss by diffusion is calculated using the same method as in Section 6.3.1. Toluene loss by biodegradation is based on the observed nitrite production (Figure 6.14) and the stoichiometric relationship with toluene (Equation 6.5). This assumes that nitrite is conserved and not reduced further to gaseous forms of nitrogen.

The toluene mass balance is presented in Table 6.5. It is split into two sections: (1) toluene mass loss from the start of the experiment to 100 hours where the EK is switched off and nitrate is distributed through the low-K zone; and (2) from 100 hours until the end of the experiment. Dividing the experiment in two allows better resolution between EK processes and biodegradation that are anticipated to be present in different parts of the experiment.

Between the start of the experiment and 100 hours, calculated values for electroosmotic flow demonstrate that it is the dominant toluene mass removal process from the low-K

Table 6.5 Toluene loss mass balance for the bench-scale and microcosm experiments.

Experiment		Unit	Rig A	Rig B	Rig C	Rig D	Microcosm Active
Toluene loss <100 hours	**Observed**	mg	9.7	3.7	17.4	16.1	-
	Calculated: electroosmosis	mg	6.2	-	13.9	11.7	-
	Calculated: diffusion	mg	1.7	2.7	2.7	3.2	-
	Mass balance	%	81	72	96	93	-
Toluene loss >100 hours	**Observed**	mg	5.0	7.4	2.8	4.5	0.09
	Calculated: diffusion	mg	1.7	7.9	1.9	3.9	-
	Biodegradation: NO_2 production	mg	42.5	47.9	29.4	46.5	1.09
	Biodegradation: toluene consumption	mg	4.7	5.3	3.3	5.2	0.12
	Mass Balance*	%	34 (129)	106 (178)	66 (181)	86 (202)	- (134)

* Mass balance values in brackets represent toluene loss including biodegradation.

zone. Furthermore, the calculated values provide a good fit with observed data. Similarly, diffusion in Rig B is well represented as previously shown in Figure 6.16.

After 100 hours, biodegradation of toluene is expected to occur due to the presence of nitrate in the low-K zone. Abiotic toluene mass loss by diffusion accounts for >66% in rigs B-D and 34% in Rig A. The calculated mass of toluene lost due to biodegradation based on the nitrite production makes the mass balance exceed 129% for all rigs. This implies that nitrite is produced by denitrification of an alternative carbon source. Additional carbon sources known to be present that could account for the increase in nitrite, include the dilute vitamin solution (3.4 mg/L, Table 6.3) and the organic matter fraction of the sediment (2.7 mg/kg, Table 6.2). To effectively assign a value for excess organic matter it is assumed that the total mass is equivalent to the chemical structure CH_2O; this is equivalent to 20.9 mg and 0.09 mg in the rigs and microcosms respectively. CH_2O can be oxidised to CO_2 via denitrification of nitrate to nitrite by the following:

$$CH_2O + 2NO_3 \rightarrow 2NO_2 + CO_2 + H_2O$$

Equation 6.7

Based on this relationship, the total nitrite production in the rigs is equivalent to less than 100% of the organic matter present in the system (66, 75, 46 and 73% for Rig A-D respectively). This implies that there is sufficient carbon other than toluene that can sustain nitrite production. This is confirmed to some extent by observations of biofilm growth in the reservoir tanks that established after the experiment ended.

Toluene loss is observed in both microcosms (Figure 6.12), in the control microcosm this is potentially due to abiotic factors. It is unlikely due to biodegradation because the stoichiometric relationships between the mass of toluene lost and mass of nitrite produced are different between the active and control microcosms (7.2 and 2.1 mg-NO_2 produced per mg-toluene lost respectively). Abiotic toluene loss mechanisms from the microcosms could arise from the vial cap being compromised during the addition of the concentrated nitrate solution. To account for this in Table 6.5 the toluene loss in the control is subtracted from the toluene loss in the active microcosm. The mass balance shows that >100% toluene can be accounted for by nitrite production, the excess (34%) can be accounted for by consumption of organic matter.

6.3.6 Sensitivity appraisal of toluene removal by electroosmosis

Overall, the data in these experiments suggests that the most effective removal mechanism of toluene from the low-K zone under reported conditions is the electroosmotic mass flux. A comparison of the removal rates is shown in Table 6.6. The toluene removal

Table 6.6 Toluene removal rate observed in bench-scale and microcosm experiments.

Removal Mechanism	Experiment	Observed Removal Rate (mg/L-h)
Electroosmosis (+ diffusion)	Rig A	0.10
	Rig B *	0.079
	Rig C	0.15
	Rig D	0.18
Diffusion	Rig B	0.023
	Rig C *	0.008
Biodegradation	Microcosm	0.066

* Value for toluene mass removal rate from swapping EK application between Rig C and B (Figure 6.10).

rate by biodegradation under ideal conditions in the microcosms accounts for abiotic loss in the controls. It is clear that in these experiments toluene mass removal from the low-K zone is most effective by electroosmosis compared to biodegradation or diffusion.

The observation of enhanced toluene removal by electroosmosis is not new. For example, Bruell et al. (1992) demonstrated the removal of BTEX, PCE and isooctane compounds from clays using water as the purging solution. Furthermore, contaminant removal in heterogeneous settings has been documented by Saichek and Reddy (2005) who observed phenanthrene removal from low-K zones in different low-K/high-K configurations. What is novel about this work is the comparison of electroosmotic and biodegradation contaminant removal rates. Data in Table 6.6 suggests that the point at which it is viable to add an amendment to stimulate biodegradation is when the electroosmotic removal rate is less than that observed for biodegradation.

A sensitivity analysis can highlight the controlling factors for toluene removal by electroosmosis and identify the experimental conditions where stimulating biodegradation would become viable. Electroosmotic removal is controlled by the electroosmotic pore fluid flux and the fraction of organic carbon. The variation in these parameters that decrease the electroosmotic removal rate below 0.066 mg/L-h reflect the conditions where biodegradation would be the most effective toluene removal mechanism in the low-K zone. The sensitivity analysis is shown in Figure 6.17 where toluene removal rate by electroosmosis is plotted against the fraction of organic carbon, f_{OC} in the sediment. The f_{OC} is back calculated using Equations 6.1 – 6.4, the parameters expressed in Table 6.2 and Section 6.3.5 and the range of experimental toluene removal rates (0.008 – 0.18 mg/L-h) that are converted into a mass flux. The different data series represent the toluene removal rate at different electroosmotic pore fluid velocities. These are calculated from Equation 1.1 using the experimental electroosmotic permeability, k_e value (Table 6.2) and a range of voltage gradients (1.5 – 0.5 V/m).

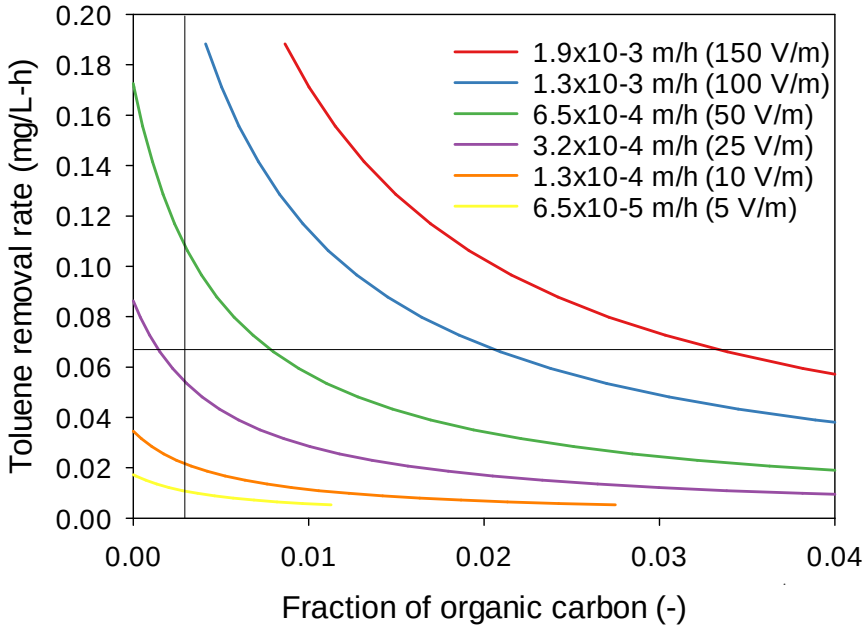

Figure 6.17 Sensitivity analysis of toluene removal by electroosmotic flow to different system variables. The solid black lines intercepting the y and x axis represent the toluene removal rate by biodegradation and the experimental f_{OC} value.

The analysis shows that toluene removal rate decreases as the fraction of organic carbon increases. This is expected due to increased adsorption retarding the contaminant migration velocity out of the low-K zone. Similarly, for a fixed f_{OC} value, the toluene removal rate increases as the electroosmotic pore fluid flux and voltage gradient increases. The experimental values for toluene removal by biodegradation and sediment f_{OC} are shown in the solid black lines intercepting the y and x axis respectively. For biodegradation to be an effective removal mechanism under these experimental conditions, the electroosmotic pore fluid velocity and therefore the voltage gradient would need to decrease. The sensitivity analysis shows that toluene removal by electroosmosis drops below 0.066 mg/L-h when the pore fluid velocity is approximately 3.6×10^{-4} m/h and a voltage gradient around 25 V/m. A low voltage gradient is realistic of systems where a constant current applied and an ionic amendment is added that will increase the electrical conductivity of the sediment (Wu et al., 2012a). This leads to a decrease in the voltage gradient over time. In these experiments the voltage gradient in Rig D dropped from 72 to 19 V/m over 91 hours of EK application. In addition, the findings from Chapter 4 indicate that an elevated

voltage gradient will be observed over the low-K zone. The voltage gradient profile in Rig D for all time points after the baseline and normalised to the voltage between electrodes is shown in Figure 6.18. A similar effect was observed in Rig A but less consistent and in Rig C but only in subsequent tests following the main experiment. This effect of heterogeneity could lead to an enhanced electroosmotic fluid flux across the low-K zone leading to greater contaminant removal compared to homogeneous settings.

Furthermore, the sensitivity analysis highlights sediment characteristics that will determine whether biodegradation is a viable removal mechanism, namely: (1) electroosmotic permeability, k_e; and (2) the fraction of organic carbon, f_{OC}.

A high k_e and subsequent high electroosmotic pore fluid flux is an advantage for contaminant removal but can hinder EK-BIO applications. The k_e in these experiments is 3.7×10^{-9} $m^2/V\text{-}s$ (Table 6.2) and is similar to values in the EK-BIO literature. For example Wu et al. (2007) and Acar et al. (1997) both report k_e values of 2.5×10^{-9} and 4.6×10^{-9} $m^2/V\text{-}s$ respectively. A high k_e can indicate a reduced effectiveness of amendment distribution if the amendment has a negative charge and low effective ionic mobility such as lactate (Wu

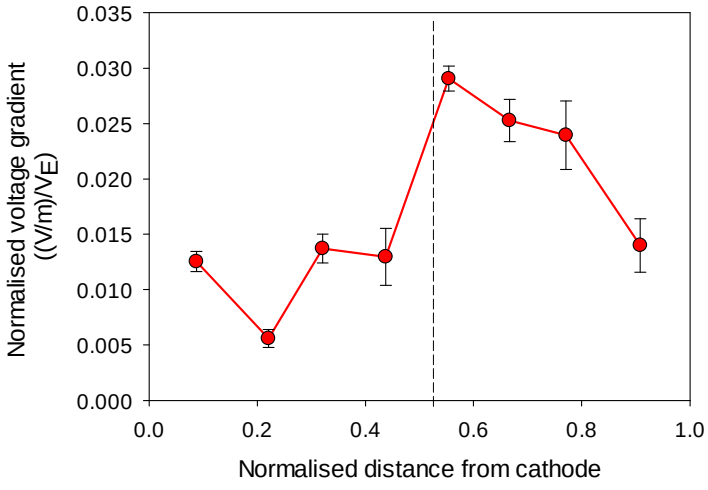

Figure 6.18 Voltage gradient across the sediment section normalised to the voltage between electrodes (V_E) for Rig D. Error bars represent one standard deviation from the mean of four time points after the baseline. Dashed line indicates the location of the high-K/low-K interface.

et al., 2007). Biodegradation and electroosmosis have been coupled to enhance contaminant loss. Pazos et al. (2012) intentionally coupled bioremediation and electroosmosis in a diesel contaminated soil with a k_e value of 5.3-5.5 $x10^{-10}$ m^2/V-s. The coupled treatment resulted in a reduced diesel concentration by 64% compared to 28% for just electroosmosis.

The sensitivity analysis shows that despite the electroosmotic pore fluid velocity, the retardation effect from a high f_{OC} value can decrease the toluene removal rate below the 0.066 mg/L-h threshold to make biodegradation viable. The f_{OC} value ranges from around 0.03 to < 0.01 (Hiscock, 2005). In these experiments the observed f_{OC} value of 0.0027 facilitated the removal of 64, 71 and 57% of the toluene mass over 100 hours in Rig A, C and D respectively. This is in contrast to other EK-BIO studies have f_{OC} values between 0.004-0.008 where the majority of contaminant removal is due to biodegradation (Wu et al., 2012; Mao et al., 2012; Pazos et al., 2012). This is in part due to the toluene partition coefficient for organic carbon (100 ± 65 mL/g) compared to other contaminants such as PAHs, e.g. naphthalene (2930 ± 7250 mL/g) (Delle Site, 2001). This indicates that toluene is more susceptible to electroosmotic transport compared to other contaminants studied in the EK literature that require flushing solutions to mobilise. Saichek and Reddy (2003) compared electroosmotic removal of phenanthrene from two different soils with a ke value of 2.5 and $2.6x10^{-10}$ m^2/V-s and f_{OC} value of 0 and 0.016 for a pure kaolin clay and a glacial till respectively. The authors applied different flushing solutions, deionised water, surfactant (Tween 80) and 40% ethanol and found greater removal rates with the flushing solutions. But the high organic carbon content in the glacial caused more contaminant to adsorb to the sediment.

6.4 Conclusions

Toluene mass isolated in the low-K zone decreased rapidly over the period EK was applied. This was due to the electroosmotic pore fluid flux that transported the dissolved

toluene mass out of the low-K and into the high-K zone. Following EK application and the distribution of nitrate through the sediment, biodegradation was anticipated to be the dominant toluene removal mechanism. However, despite nitrite accumulating in low concentrations in the low-K zone the dominant mass removal mechanisms after EK application was diffusion. This is in contrast to a parallel microcosm study that observed toluene concentrations decrease 200 hours after nitrate was applied by biodegradation.

A comparison of toluene removal rates identified electroosmosis as the dominant mechanism compared to diffusion and biodegradation under ideal conditions (based on microcosm study). Further analysis attempted to identify the extent to which certain experimental variables would need to change to make biodegradation a viable mechanism in these experimental conditions. It identified that within the experimental conditions the voltage gradient would need to drop below 25 V/m to reduce the electroosmotic pore fluid flux. Future experiments should consider the k_e and f_{OC} properties of the sediment to identify whether biodegradation is a viable option. This work raises questions as to the best method to apply EK-BIO at the field-scale. For example, is it better to enhance electroosmotic flow to flush contaminant out of the low-K zone and enhance biodegradation in the high-K zone? This is discussed further in Chapter 8.

Chapter 7 Sustainability assessment of electrokinetic bioremediation compared with alternative remediation options for a petroleum release site

7.1 Introduction

The management of contaminated land is a global challenge. Its restoration is often considered to provide net positive benefits, but if remediation practices are selected and implemented poorly more environmental impact can arise than is associated with the contamination. SuRF-UK has produced a framework which provides a structure for implementing sustainable management practices within a contaminated site project. The framework has two stages: Stage A, plan and project design; and Stage B, remediation option appraisal and implementation. This chapter implemented Stage B of the framework, by applying a sustainability assessment to contaminated site remediation technology selection.

The SuRF-UK sustainable remediation framework describes a tiered approach to sustainability assessments. There are three tiers, each requiring increasing amount of data for the assessment: Tier 1 is qualitative (e.g. simple rankings against ideal criteria); Tier 2 is semi-quantitative (e.g. multi-criteria analysis); and Tier 3 is quantitative (e.g. cost-benefit analysis). The steps associated with an assessment include (Bardos, 2014; Bardos et al., 2011): (1) defining remediation objectives to identify the decision that is being supported; (2) stakeholder engagement; (3) identifying boundaries of the assessment such as system, lifecycle, spatial and temporal; (4) identifying relevant sustainability indicators for the scope of the assessment; (5) defining the assessment methodology, i.e. either Tier 1, 2 or 3 or a combination; (6) conducting the sustainability assessment and (7) verifying and reporting the results.

Several case studies apply the SuRF-UK framework to contaminated sites and demonstrate the economic, environmental and social benefits of the process. For example, a Tier 1 assessment was applied to a fuel storage depot in Madeira, Portugal, concluding enhanced bioremediation to be a more sustainable approach than thermal desorption, based largely on reduced cost and CO_2 emissions, but with an associated longer duration for remediation activity (SuRF-UK, 2013a). Additionally, Tier 2 and 3 assessments were completed at a former airbase site where aviation fuel was thought likely to impact a primary aquifer. It concluded that environmental and social impacts out-weighed the economic, resulting in a more expensive but more sustainable and operationally better solution (SuRF-UK, 2013b).

A novel aspect of this chapter is the inclusion of electrokinetic-enhanced bioremediation (EK-BIO) as a risk management option. The technology is considered a good candidate for sustainable remediation as the principal costs after set up are electricity and the amendment used (Alshawabkeh et al., 1999; Kim et al., 2014). Consequently, there is significant interest in coupling electrokinetics with other remediation technologies and incorporating it as part of remediation options appraisal will further advance the state of knowledge.

7.1.1 Research question and hypothesis

The research question addressed in this chapter is: How does EK-BIO compare with other remediation technologies against a Tier 1 and 2 sustainability assessment for an MTBE contaminated site? This research question is referred to as Research Question 4. The hypothesis is that because the main energy source for EK-BIO technique is electricity it will be more sustainable than the other options. The objectives were to:

1. Perform Tier 1 and Tier 2 sustainability assessments on a site contaminated by an unleaded gasoline release from a petrol filling station and use the findings to inform a management decision;

2. Include EK-BIO in the remediation option appraisal, using an electron balance model to inform operational parameters such as treatment duration, power (electricity) consumption and amendment usage; and
3. Investigate the effect of incorporating photovoltaics and limiting amendment usage on the EK-BIO remediation option using different scenarios relative the base case above.

Currently there are no reported examples of using electrokinetic bioremediation within a sustainability assessment, or how modifications to the treatment design, such as inclusion of photovoltaics, influence the overall sustainability performance. These are important knowledge gaps in the development of electrokinetic remediation.

7.2 Conceptual site model

The focus of this assessment is a petrol filling station (PFS) site located up hydraulic gradient of a water supply well (WSW). There was a fuel release into the subsurface at the PFS resulting in the fuel additive methyl tert butyl ether (MTBE) detection in the WSW. The PFS was decommissioned, the fuel release stopped, and investigation and remediation undertaken. Several groundwater sampling and monitoring events have been completed at the site to assess the risk posed by MTBE to the WSW. Remedial action to date includes the installation of a hydraulic containment system (HCS) to break the source-pathway-receptor (SPR) linkage, and soil vapour extraction (SVE) and multi-phase extraction (MPE) to treat mobile and residual-phase LNAPL near the source zone.

7.2.1 Site geology and hydrogeology

The main hydrogeological units in the shallow subsurface at the site are summarised in Table 7.1 and a cross section in Figure 7.1A. The top of the Cretaceous Chalk aquifer is located at around 20m BGL, and forms a regionally important water supply aquifer. The Chalk is overlain by ca. 20m low permeability clay till, through which a glacial sand channel was cut. The channel sands are a mix of high permeability sands and gravels interspersed

with low permeability silt lenses. Regional groundwater flow is towards the north east, however, the local hydrogeological regime is modified by abstraction at the WSW, which draws Chalk groundwater in an easterly direction. When the WSW is on groundwater flow in the channel sands and chalk is towards the well, creating a downward vertical hydraulic gradient in the channel sands. When the WSW is not pumping the regional groundwater flow is dominant and the hydraulic gradient between the channel sands and chalk aquifer is reversed. The water table fluctuates under the influence of the abstraction and seasonal variations.

Table 7.1 Summary table of the geological units present on site.

Geological Unit	Hydraulic Conductivities (m/s)
Channel Sands	1.5×10^{-5} to 1.2×10^{-9}
Glacial till	1.2×10^{-8} to 1.2×10^{-12}
Chalk	1.2×10^{-3} to 3.5×10^{-4}

7.2.2 Contaminants of potential concern

Numerous petroleum hydrocarbon constituents are present on site. Those exceeding UK drinking water standard or World Health Organisation appearance taste and odour values at the highest number of locations include benzene, toluene, ethyl-benzene, xylene (BTEX) and MTBE. These compounds are considered the main contaminants of potential concern, consistent with other gasoline impacted sites (Bowers and Smith, 2014). Hydrocarbons were present in both free phase and dissolved phases. The free-phase has migrated south-east into the channel sands, with significant smearing due to groundwater fluctuation. The dissolved-phase within the channel sand is drawn down by the vertical hydraulic gradient towards the chalk aquifer (Figure 7.1A) and the WSW, 570 m down gradient. The highest observed concentrations for contaminants of concern are 6 m below groundwater level at: benzene, 52.6; toluene, 63.2; xylene, 18.9; ethylbenzene, 2.8; and MTBE, 23.5 (values in mg/L).

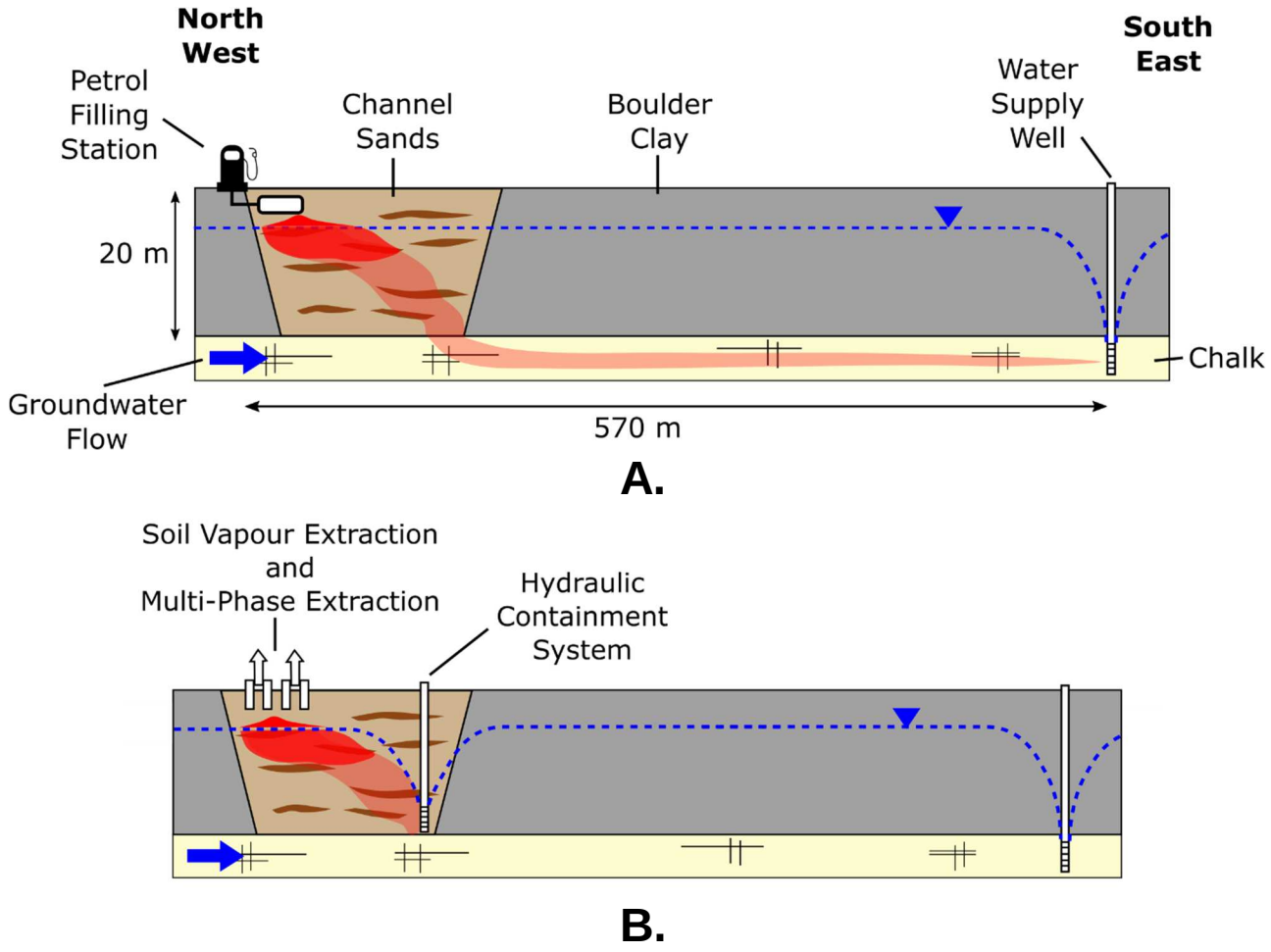

Figure 7.1 Conceptual site model showing A. geological and hydrogeological features and the principle source – pathway – receptor linkage present on site; and B. cross section following the first stage of remedial action.

The distribution of dissolved-phase organic contaminants is influenced by the availability of electron acceptors supporting biodegradation. BTEX and MTBE are present within the channel sands and up to the boundary with the Chalk aquifer. Within the channel sands, BTEX are biodegraded using dissolved oxygen, nitrate, sulphate, and mineral-derived iron and manganese oxides, based on the groundwater quality data. While anaerobic biodegradation of MTBE has been reported (Somsamak et al, 2001, 2005, 2006), it cannot be deduced in the groundwater quality data from the anaerobic biodegradation of BTEX in the channel sands, which is assumed to occur more readily (Wiedemeier et al, 1999). Only MTBE is present in the Chalk aquifer and is biodegraded aerobically, based on observed elevated concentrations of its primary biodegradation product, tert-butyl alcohol (TBA), and the results of microcosm studies.

Based on these observations the principal SPR linkage that drives risk management requirements on site is related to MTBE migration (Table 7.2). Remedial targets for the site consider: (1) MTBE biodegradation rates within the Chalk aquifer; (2) dilution of MTBE at the WSW and during migration between the channel sands and Chalk aquifer; and (3) an agreed remedial objective for MTBE that prevents taste and odour impact at the abstraction well.

Two remedial actions have been implemented to manage the risk of MTBE to the WSW (Figure 7.1B). Firstly, a HCS installed at the boundary between the channel sands and Chalk aquifer to continually extract contaminated water for discharge and treatment. This breaks the SPR linkage, by preventing MTBE from entering the Chalk aquifer, and has been validated by frequent monitoring events over the four years since installation. Secondly, SVE and MPE systems have been installed to remove hydrocarbon mass from the source zone. The sustainability assessment focuses on determining which techniques are appropriate to treat the remaining residual NAPL and dissolved phase contaminants in the source areas.

Table 7.2 The principal SPR linkage present on site and remedial target for MTBE as agreed with the regulator.

Source	**Pathway**	**Receptor**	**Remedial targets**
Dissolved and free-phase MTBE	Dissolution and migration through the saturated channel sand and Chalk aquifer.	Taste and odour impacts resulting from consumption of water extracted from the well.	MTBE: 3.3 mg/L (at source zone, based on achieving taste and odour threshold at point of abstraction)

7.2.3 Identified remediation options

The zone of contamination covers a surface area of 1500 m^2 (75 m x 20 m) and extends 6 m below the water table (ca. 7.5 mbgl). Four *in situ* remediation technologies have been identified for appraisal, all run concurrently with the HCS:

1. *Monitored Natural Attenuation (MNA)* - MNA is the least intensive technique. It is justified on this site as biodegradation of the BTEX and MTBE is observed in the channel sands aquifer and HCS provides protection to the abstraction well.

Treatment design includes utilising existing monitoring wells, with four monitoring events in the first year, followed by one in each subsequent year of operation, adopting a lines-of-evidence approach in line with good practice regulatory guidance (EA, 2000)

2. *Electrokinetic Enhanced Bioremediation (EK-BIO)* - The EK-BIO technique is suitable for application to this site due to the physical heterogeneity over the specified range of hydraulic conductivities in the contaminated channel sands aquifer. The aim is to stimulate anaerobic biodegradation of the BTEX and MTBE compounds by the addition of nitrate. Electrodes are arranged in a bidirectional configuration with a line of cathodes in the centre between two rows of anodes (see Appendix M: Figure M.1, and M.2). The treatment will be conducted in three phases to accommodate optimal electrode distances. A constant voltage gradient of 50 V/m is assumed with a drop of 60% in the zone adjacent to the cathode due to the increase in electrical conductivity from the amendment (Wu et al., 2012a). Subsequently, the voltage gradient drop will control the amendment flux into the system.
3. *Air Sparge / Soil Vapour Extraction (AS/SVE)* – This technique is suitable because of the existing SVE infrastructure and pilot-scale testing of the AS system indicate the treatment could be effective for treating the high-K zones on site. The treatment will be conducted in two phases to accommodate the short AS well radius of influence (ca. 3.3 m) and subsequent high number of treatment wells. The treatment module associated with the AS/SVE system is a catalytic oxidation unit.
4. *Pump and Treat (PT)* - This technique is suitable due to the relatively high hydraulic conductivity of the channel sands and Chalk aquifers. In addition, MTBE is more soluble than other contaminants, with limited retardation by sorption to the aquifer matrix. Two pumping wells with a radius of influence of 20 m are sufficient to cover the treatment area, assuming a drawdown of 5% and hydraulic conductivity of 1.5 x 10^{-5} m/s consistent with the most permeable sections of the channel sands. The

treatment modules associated with the PT system comprise an oil/water separator, air stripper and granulated activated carbon unit.

Realistic treatment durations for each technique have been assigned using sources from site-specific reports and literature values. These include minimum, medium and maximum values (Table 7.3). A simple electron balance model (EBM) was developed (similar to the one in Chapters 2 and 5) to inform EK-BIO treatment durations and other operational parameters as currently no field data exist in the literature for its application to dissolved phase LNAPL contaminants. An EBM determines the length of time required for the number of electron acceptors to equal electron donors (Thornton et al., 2001), in this example, the nitrate amendment and BTEX and MTBE contaminants represent the electron acceptors and electron donors respectively. The number of electrons accepted or donated depends on the stoichiometry of each half reaction (see Appendix M: Table M.1). One-dimensional electromigration mass flux equations were applied to simulate nitrate transport into the treatment domain until a sufficient amount had been added to equalise the electron donor mass (see Appendix M: Table M.2 and M.3) (Acar and Alshawabkeh, 1993). This duration was then added to the length of time required for nitrate to migrate through the treatment domain (Alshawabkeh et al., 1999). The treatment domain was split into three layers to represent the heterogeneity observed on site, material properties were taken from high- and low-K sediments used in Chapter 4. In the electron balance model BTEX in the channel sands aquifer is assumed to be biodegraded anaerobically using nitrate (Wiedemeier et al., 1999). Anaerobic respiration of MTBE using nitrate has been demonstrated (Bradley et al., 2001; Bradley et al., 1999), but cannot be proven at the site from the groundwater quality data. Instead, MTBE is assumed to be aerobically biodegraded to TBA in the Chalk aquifer (Spence et al., 2005). In this way, the EK-BIO treatment is used to enhance the nitrate flux for BTEX biodegradation, allowing aerobic respiration of MTBE further down-gradient in the sand and Chalk aquifers.

The minimum, medium and maximum duration ranges were calculated using a range of sources. For MNA a range of durations is taken from site specific modelling reports; for EK-BIO the transport properties of the materials simulated in the EBM were varied according to different effective ionic mobility values in Chapter 4; for AS/SVE a range of volatile organic carbon extraction rates were taken from pilot trials (see Appendix M: Table M.4 and M.5); and PT a range of attenuation rates from MTBE contaminated sites were used (see Appendix M: Table M.6 and M.7) (McHugh et al., 2013). Further details of treatment design specifications and associated assumptions are given in the supporting information.

Table 7.3 Summary of treatment durations and calculation method used to inform the sustainability assessment.

Option Number	Remediation Option	Treatment Duration Range (years)			Calculation method
		Min	Med	Max	
1	MNA + HCS	15	20	25	Site reports and modelling study
2	EK-BIO + HCS	3.4	6.0	7.3	Electron balance model
3	AS/SVE + HCS	3.8	5.0	7.5	Site reports from pilot test
4	PT + HCS	5.2	6.4	7.0	Literature data based on multiple active MTBE sites (McHugh et al. 2013)

7.3 Sustainability assessment framework

7.3.1 Remediation objectives and stakeholder engagement

The sustainability assessment covers Stage B of the SuRF-UK framework, with the overall task of selecting the most sustainable remedial option to deliver project objectives (SuRF-UK, 2010). The remedial objectives are: (1) to achieve risk-based close out criteria for MTBE in groundwater; and (2) return properties adjacent to the source area back into beneficial use. The stakeholders in this project included the local authority, Environment Agency, water abstraction owner, the site owner and their professional advisors.

7.3.2 Assessment boundaries

This sustainability assessment is constrained by four types of boundary conditions. Firstly, system boundaries; the processes associated with remedial operations to achieve the risk management objectives. An example from the PT option includes establishing site infrastructure, drilling pumping wells, extracting groundwater etc. The assessment boundaries for all remediation technologies are shown in Figure 7.2 which carries over three pages. System boundaries are shown in Figure 7.2 as solid boxes. Secondly, life-cycle boundaries; the materials and energy inputs required for a step in the remediation process, as well as the outputs from that step, such as air emissions from transport or remediation activity. The analysis excludes manufacture of remediation equipment; it is assumed to be rented from a supplier or purchased with the aim of future use. The lifecycles associated with the four options are shown in Figure 7.2 as dashed boxes. Inputs and outputs are shown for each step in the technique. Thirdly, spatial boundaries extend to the area around the site, with the footprint of the dissolved phase plume and transport to and from site. Fourthly, temporal boundaries exist as long as the pollutant linkages and risk management options are required, or as long as the dissolved phase plume in the channel sands aquifer exists. This is shown in Figure 7.2 as the diamond-shaped decision box. Some aspects of remediation techniques are not included in the overall analysis as they are assumed to be in place at the start of the remediation option appraisal. These include drilling monitoring boreholes and establishing site infrastructure and drilling treatment boreholes for the SVE and HCS systems.

Monitored Natural Attenuation

Air Sparge / Soil Vapour Extraction

Electrokinetic Bioremediation

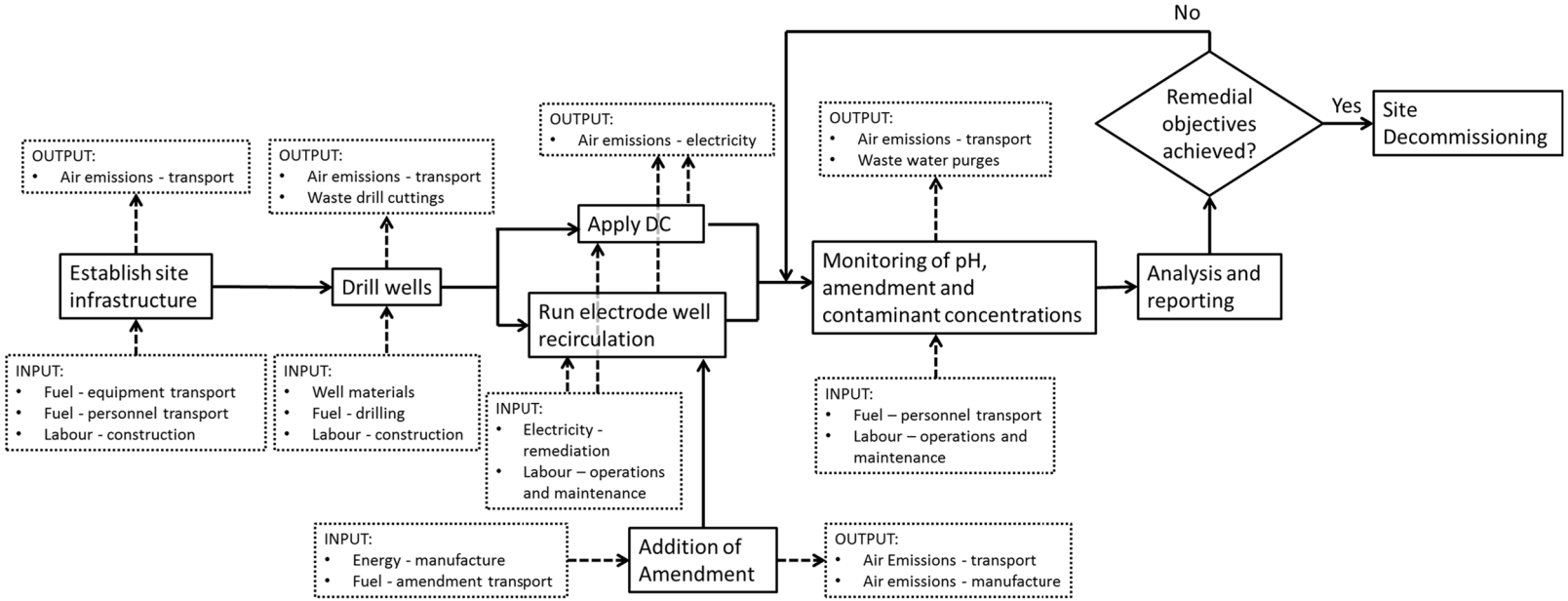

Pump and Treatment

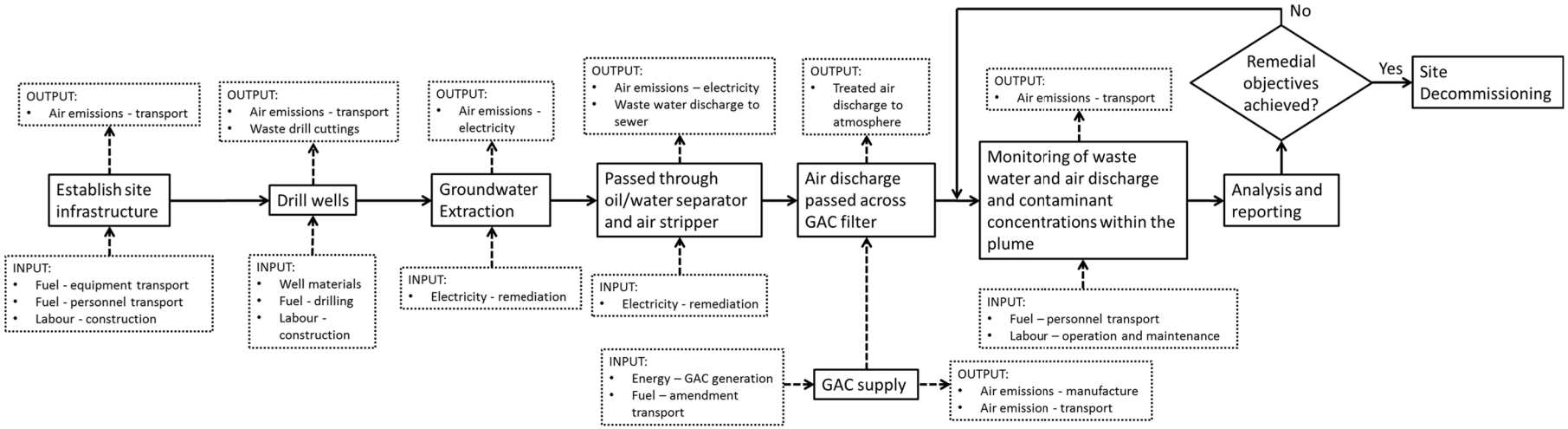

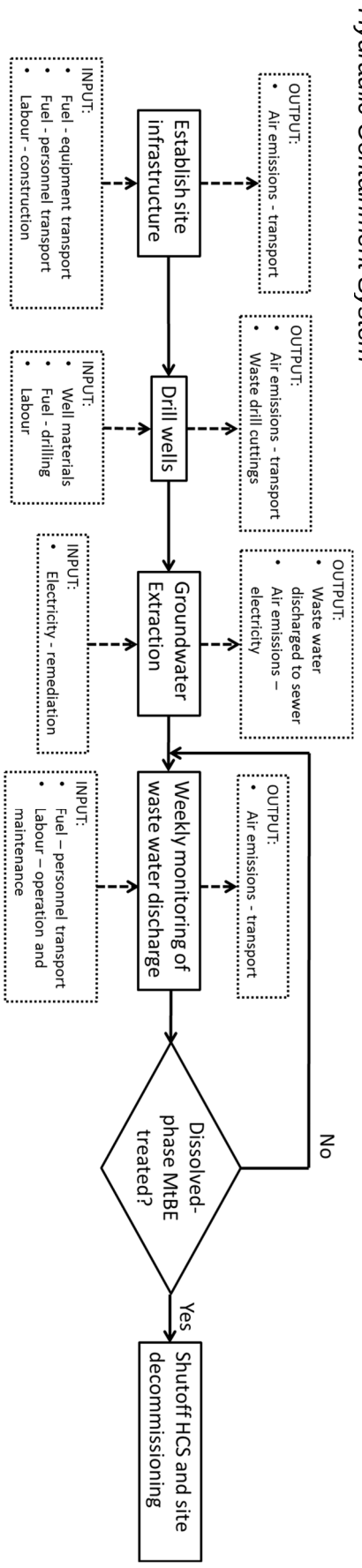

Figure 7.2 Flow diagrams for the four remediation options, showing system boundaries in the solid square boxes, lifecycle boundaries in dashed boxes and the end of remediation activities defined by the decision step in the diamond shaped boxes. GAC, granular activated carbon.

7.3.3 Scope of assessment

The sustainability assessment covers the fifteen indicators described in SuRF-UK documentation across the three 'pillars' of sustainability (SuRF-UK, 2011). The purpose of the indicator set is to make the sustainability assessment more transparent to assessors and stakeholders, as well as facilitating both a Tier 1 and Tier 2 assessment. All fifteen indicators are included to provide the most holistic view. Indicators considered to be a priority were identified by consultation with stakeholders, who selected two priority indicators from each pillar. The two indicators from each pillar with the most number of priority selections are highlighted with an asterisk (*) (Table 7.4). The semi-quantitative Tier 2 assessment required the identification of quantifiable factors within each indicator, subject to data availability. Where no additional factors could be identified the ranking from the qualitative Tier 1 assessment was carried over to the Tier 2 assessment. Care was taken not to replicate scores between indicators. For some indicators more than one metric could be identified, for example, natural resources and waste includes four different metrics: water discharge from treatment, volume of soil material displaced, raw materials used for well construction and volume of fuel consumed. The groundwater quality indicator includes quantitative and qualitative metrics. The quantitative metric is the value of groundwater in the channel sands lost due to abstraction at the HCS that otherwise would have been abstracted at the WSW (Bartlett et al., 2014) and the qualitative metric that considers the broader impacts on groundwater quality, such as groundwater chemistry that are harder to quantify.

7.3.4 Assessment approach

The qualitative Tier 1 assessment comprised a simple ranked comparison of the different remediation options using generic and conservative assumptions against defined sustainability indicators. The semi-quantitative Tier 2 assessment applied a multi-criteria analysis (MCA) using site-specific data to the same sustainability indicators. For the Tier 1 analysis the middle treatment durations from Table 7.3 where used for all treatments. In

Tier 2, treatment durations were subject to an uncertainty analysis that applied the minimum and maximum estimated treatment durations shown in Table 7.3.

Table 7.4 Indicator set with identified priority indicators. Indicators used in the Tier 1 qualitative assessment and Tier 2 semi-quantitative assessment are shown.

Criteria	Sustainability Indicator	Label	Priority	Tier 2 Metric	Unit
Environment	Emissions to air	ENV 1	*	Total CO_2 emissions	kg CO_2-e
	Soil and ground conditions	ENV 2		Qualitative (Tier 1)	n/a
	Groundwater quality	ENV 3	*	Value of water lost to HCS extraction	GBP
				Qualitative (Tier 1)	n/a
	Ecology	ENV 4		Qualitative (Tier 1)	n/a
	Natural resources and waste	ENV 5		Water discharge from remediation treatment only	m^3
				Volume displaced soil material	m^3
				Raw materials used in well construction	kg PVC
				Volume of petrol consumed	m^3
Economic	Direct economic costs	ECON 1	*	Total economic cost	GBP
	Indirect economic costs and benefits	ECON 2		Net present value of housing on site	GBP
	Employment and employment capacity	ECON 3		Qualitative (Tier 1)	n/a
	Induced economic costs and benefits	ECON 4		Net present value of petrol filling station	GBP
	Project lifespan and flexibility	ECON 5	*	Duration of treatment	Years
Social	Human health and safety	SOC 1	*	Time lost due to injury from operation	Hours
				Time lost due to injury from traffic accidents	Hours
	Ethics and equality	SOC 2		Qualitative (Tier 1)	n/a
	Neighborhoods and locality	SOC 3	*	Qualitative (Tier 1)	n/a
	Communities and community involvement	SOC 4		Qualitative (Tier 1)	n/a
	Uncertainty and evidence	SOC 5		Qualitative (Tier 1)	n/a

7.4 Tier 1 sustainability assessment

7.4.1 Tier 1 methodology

A ranked score between 1 and 4 was assigned for the different options framed against an idealised scenario. For example, air emissions (ENV 1*) the ideal scenario is no air

emissions and direct economic cost (ECON 1*) the ideal scenario is minimal capital, operational and management cost (see Appendix M: Table M.8 for descriptions of ideal scenarios for other indicators). A higher rank (i.e., 4) was assigned to the least sustainable option and a low rank (i.e., 1) to the most sustainable option. At Tier 1 all indicators were weighted equally, i.e. a priority indicator such as air emissions had the same weight as a non-priority indicator such as ecology. Qualitative ranking was supported by evidence from different categories and includes qualitative and basic quantitative assessment (see Appendix M: Table M.9 – M.11). Equal rankings were allowed if differences between options were <10%. The treatment durations for the assessment were the middle estimates as defined above. Uncertainty regarding treatment durations was reduced by comparing the individual indicators against an ideal scenario. It was also included as part of the social category of indicators.

7.4.2 Tier 1 results

The rankings and justifications for individual indicators are given in Appendix M: Table M.12. The cumulative rankings of the different options are shown against all indicators and priority indicators (Figure 7.3). The lower the cumulative ranking the more sustainable the

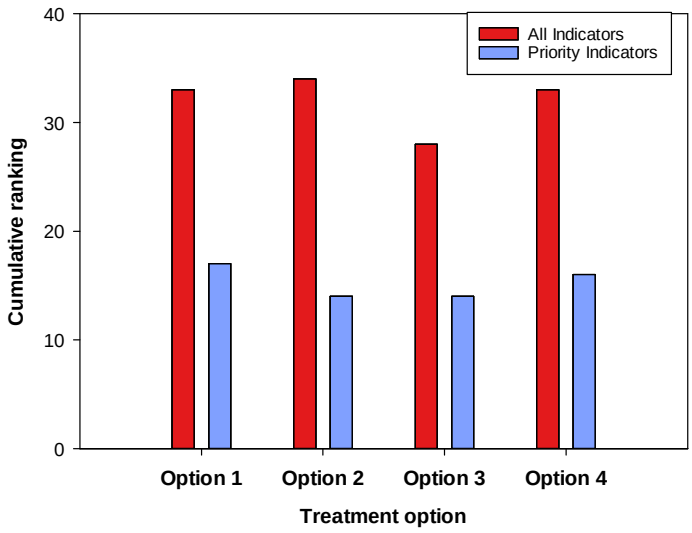

Figure 7.3 Cumulative ranking for the different options investigated as part of the Tier 1 sustainability analysis. Values for all criteria and priority criteria are shown: A lower score represents a more sustainable option.

option. Option 3 (AS/SVE+HCS) appears to be the best option when all indicators are considered. This is due to: 1) shorter treatment duration of indicators that are time-dependent, such as indirect or induced economic benefits; 2) added certainty on treatment performance from pilot-scale study; and 3) a function of the AS/SVE system used to treat both unsaturated strata and groundwater, thus improving soil and groundwater conditions. However, for priority indicators identified during the stakeholder workshop Option 2 (EK-BIO+HCS) and Option 3 are equivalent. This is due to Option 2 scoring well against priority indicators, for example, air emissions and total direct economic cost are lower than Option 3 and Option 4 (PT+HCS) because no treatment plant is used. However, against non-priority indicators Option 2 is less favourable because of high levels of uncertainty compared with other Options and relatively long treatment duration compared to Option 3.

The Tier 1 assessment identifies a choice of two management decisions. Firstly, select Option 3 for the site as it is the most sustainable when all indicators are considered and hence is justified at this level. Secondly that the assessment should progress to Tier 2 and attempt to further differentiate between Options especially against priority indicators. For the purposes of this study the second option will be applied.

7.5 Tier 2 sustainability assessment

7.5.1 Tier 2 scoring method

Both quantitative and qualitative data sources for the individual sustainability indicators were used to inform the MCA (Table 7.4). Further details on how the different metrics were calculated are provided in Appendix M: Table M.12 – M.14. The method of scoring the MCA is similar to that described by Postle et al. (1999) and is shown in Equation 7.1. Numerical values for a particular indicator were normalised against the maximum value across all treatment options and multiplied to provide a score between 0-100. An indicator weighting was then assigned based on stakeholder priorities (Table 7.4). Where more than one metric was an additional normalisation factor was applied to ensure that each sub

indicator contributed an equal amount to the overall indicator score identified. For example, natural resources and waste, ENV 5, there are 4 sub-indicators (Table 7.4) that each contribute 25% to the total indicator score. For indicators where no metrics could be identified, the qualitative ranking from the Tier 1 assessment. The higher the MCA score the lower the sustainability of the option.

$$\text{MCA Score} = \left(\frac{\text{Input Value for Option}}{\text{Maximum Value Across Options}}\right) \times 100 \times \text{Priority Weighting}$$

Equation 7.1

MCA scoring methods for contaminated land options appraisal in the literature include similar components, namely: data for criteria and sub-criteria, a normalisation factor for criteria and sub-criteria and weightings for priority indicators. They differ in how the scores are calculated or presented. For example Harbottle et al. (2008) applies the Postle et al. (1999) method and consider the positive effects of remediation. In the present study, after effects of remediation are not included as it is assumed the benefits of remediation will be the same for all options. Furthermore, Blanc et al. (2004) develop a scoring method that produces a ‘best’ and ‘worst’ ranking of different technologies for a site.

Parameters used to derive the MCA scores are included in Appendix M: Table M.15 – M.17. They include the input values, indicator and sub-indicator weightings and the final weighted MCA score. The same treatment designs are used as for the Tier 1 assessment. In addition, extra scores are compiled for three scenarios that examine the effect of sustainability enhancements applied to Option 2. These include Scenario 1: a photovoltaic array that provides electricity; Scenario 2: constant flushing of electron acceptors in uncontaminated groundwater through the electrode chambers, as opposed to the addition of amendment; and Scenario 3: a combination of scenario 1 and 2. These scenarios were not applied to Options 1, 3 and 4 because their treatment design is unsuitable for the enhancements. For example, Option 3 and 4 include treatment plants that require a regular power supply to ensure treatment efficiency, and neither have an amendment with a low

or no-cost substitute. Option 2 is suitable because effective treatment has been demonstrated with variable amendment fluxes into sediment material that would arise from intermittent power supply (Mao et al., 2012; Wu et al., 2007).

7.5.2 Tier 2 uncertainty analysis

For the Tier 2 assessment uncertainty is represented at the qualitative and quantitative level. Qualitatively uncertainty is represented by the indicator, uncertainty and evidence (SOC 5) that reflects confidence in treatment effectiveness based on quality of available evidence, similar to Tier 1. Quantitatively, the range of duration values shown in Table 7.3 were used to inform other time dependent metrics, i.e. all quantitative metrics with the exception of those specific to site setup (e.g. well drilling), qualitative rankings did not vary.

7.5.3 Tier 2 sensitivity analysis

A sensitivity analysis was conducted to provide insight into which sustainability indicators had the greatest impact on the MCA score for a particular option (Rosen et al., 2015). The analysis requires a Monte Carlo simulation to be performed. This is a stochastic simulation where user defined ranges of uncertainty and probability distribution for different parameters are inputs that are propagated through the model. The output is a forecast that is based on the simulation being run numerous times. The sensitivity analysis is calculated by rank correlation of parameter inputs (independent variable) and the forecast outputs (dependent variable) then performing linear regression on ranked sets. Correlation coefficients are then tallied for each forecast and normalised (McNab and Dooher, 1998).

For this study minimum and maximum values for the different sustainability indicators derived from the uncertainty analysis were used to inform the input range for the simulation. A uniform probability distribution was assumed for all indicators. The output forecast was a range of MCA scores, the simulation was run 10,000 times using Monte Carlo simulation software, Crystal Ball for Microsoft Excel.

7.5.4 Tier 2 results

7.5.4.1 Economic indicators

The MCA scores for economic indicators showed no significant difference between options when the full minimum and maximum range was considered (Figure 7.4A). A breakdown of these values for the middle time estimate showed that the scores were distributed differently (Figure 7.4B). Option 1 scores high against project duration (ECON 5*), direct economic cost (ECON 1*) and employment capacity (ECON 3), but was offset by the timescale that houses and properties can be released to market (ECON 2 and ECON 4). Option 2 scores lowest against ECON 1* compared with Option 3 and Option 4 due to a lack of treatment plant creating a considerable cost saving. Furthermore, Option 2 only requires a relatively cheap amendment and is not power intensive, although a significant expense comes from a high relative setup cost. This is exemplified by the ratio between the setup and operation and management costs, which are 0.01, 0.53, 0.23 and 0.08,

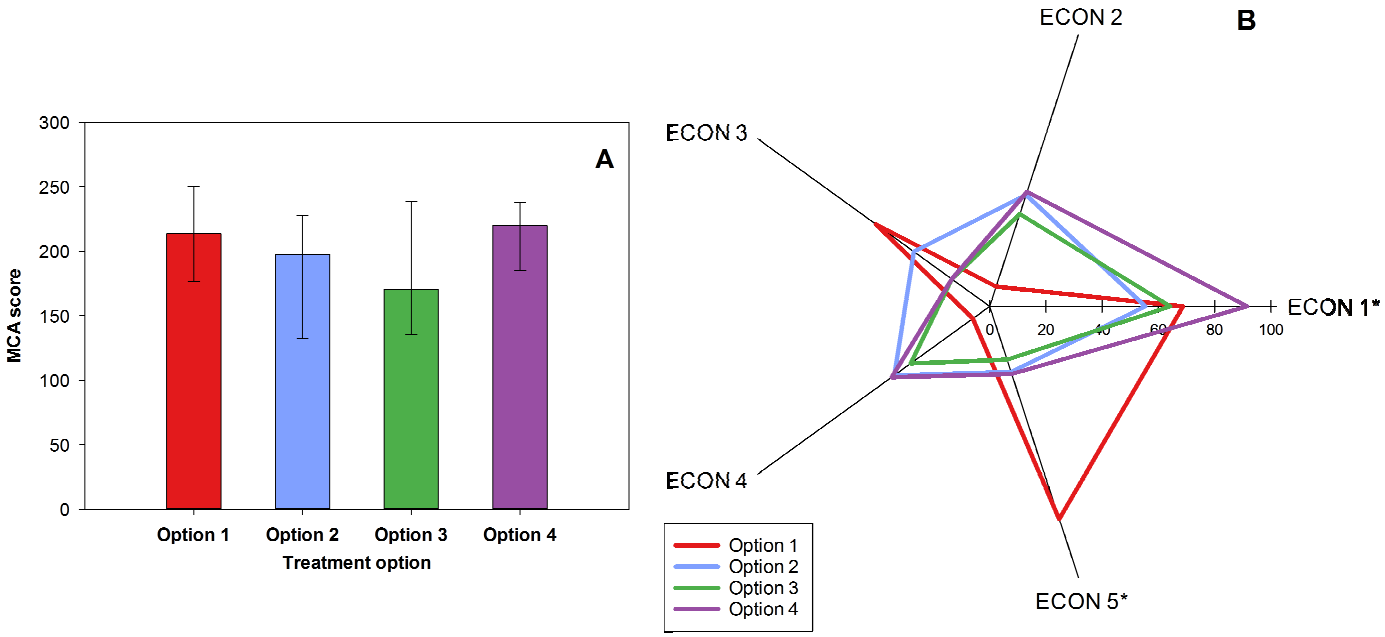

Figure 7.4 Tier 2 sustainability assessment: Economic Indicators. A. is a bar chart showing the cumulative scores for the different indicator categories. B. is a radar plot that shows the distribution of scores in each indicator category for the middle estimate scenario, * represents priority indicators. Error bars on A. represent the minimum and maximum estimated values based on uncertainty analysis. For descriptions of Option 1-4 see Table 7.3 and ECON 1-5 see Table 7.4.

respectively, for Option 1 to 4. These values reflect the fact that while Option 2 does not require treatment plant operation there is a high cost per well due to the initial cost of the electrodes (3x 2m graphite electrodes, ca. £2,000 – £2,500 per well). Option 4 has a low setup cost as only two wells are predicted to effectively capture the dissolved-phase plume. Conversely, Option 3 requires numerous air sparge wells (predicted radius of influence ca. 3.3 m) to cover the site area, but there is a lower cost per well compared with Option 2.

Treatment durations for Option 2-4 are within a similar range based on the quantitative uncertainty analysis. They are relatively short compared with Option 1 and so little difference can be identified between them. This influences ECON 2, 3 and 5*, where treatment duration is a key factor.

7.5.4.2 Environmental indicators

Greater difference between options can be identified using environmental indicators (Figure 7.5A). Option 1 scores noticeably higher than Option 3 due to a difference between the minimum and maximum MCA scores. This is due to the prolonged impact of Option 1 on soil and groundwater conditions (ENV 2 and ENV 3*, respectively). Conversely, Option 3 has a low associated score due to the benefits of AS-SVE treatment used to improve both soil and groundwater conditions by treating residual LNAPL and extracting VOC from the soil zone.

Option 1 scores highly for ENV 3* which considers the value of groundwater abstraction opportunity lost to the water abstractor, based on the volume extracted by the HCS over the treatment period (Bartlett et al. 2014). Option 2 scores high against ENV 3* due to the potential generation of acid and base fronts by uncontrolled electrolysis reactions at the electrodes. However, the effect of adding a large mass of sodium nitrate (6-11 t over treatment) is not considered, because it is assumed that the nitrate will be consumed by biodegradation and thus not impact downgradient receptors.

Atmospheric emission of CO_2 (ENV 1*) is driven by several factors, namely treatment power consumption, transport to and from site, and amendment production. Option 2 scores well due to the low electricity requirement; it has an estimated energy demand range between 14-30 kWh/m^3, which compares well to literature values of 19 kWh/m^3 (Suni et al., 2007). Option 1 and Option 4 have high air emission values due to long-term weekly visits (road transport) to maintain the HCS and high power requirements for an air stripper and granulated activated carbon (GAC) treatment module, respectively.

Option 2 to 4 are not easily distinguishable using the natural resources and waste indicator (ENV 5). ENV 5 combines four categories: water discharged as a result of treatment only (does not include HCS), soil displaced from new well drilling, PVC mass used in new well construction and consumption of fuel. Option 1 scores highly for fuel consumed due to numerous site visits, but low for other values as no new wells are drilled. Option 4 has by far the greatest waste water discharge, compared with other treatments.

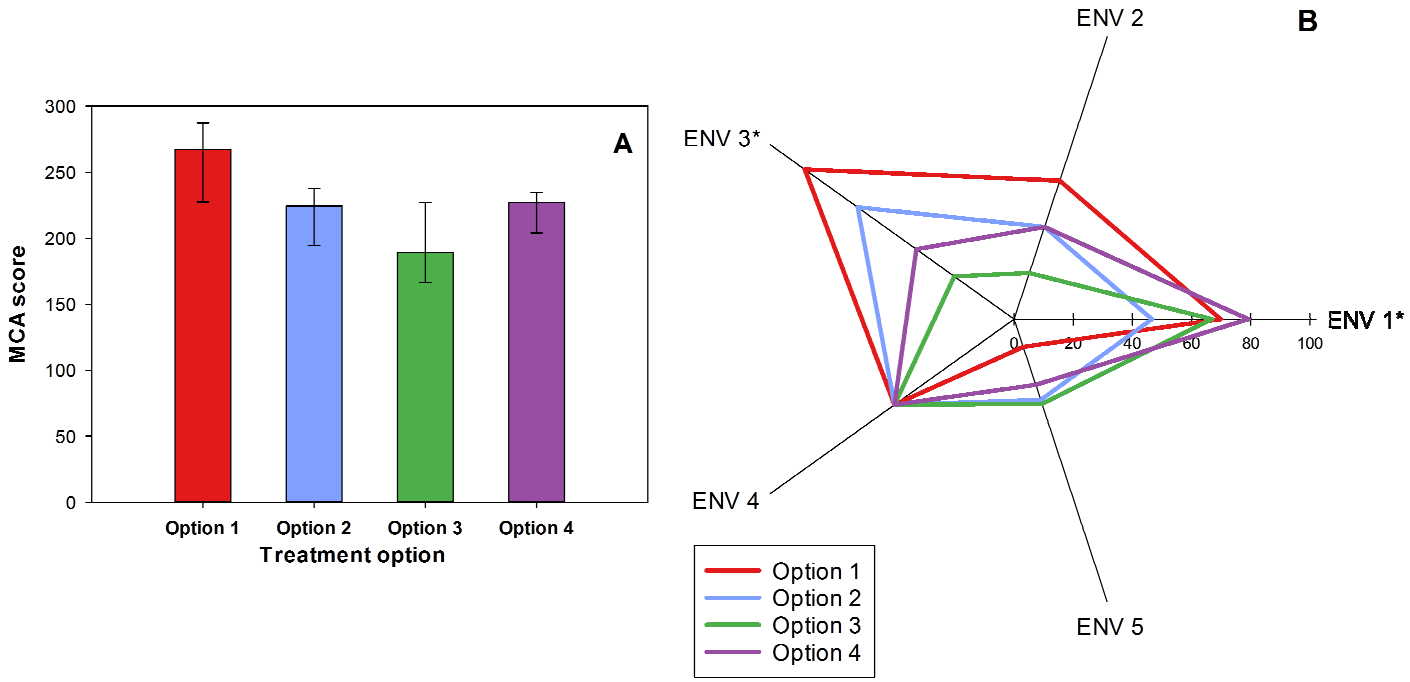

Figure 7.5 Tier 2 sustainability analysis: Environmental Indicators. A. is a bar chart showing the cumulative scores for the different indicator categories. B. is a radar plot showing the distribution of scores in each indicator category for the middle estimate scenario, * represents priority indicators. Error bars on A. represent the minimum and maximum estimated values based on the uncertainty analysis. For descriptions of Option 1-4 see Table 7.3 and ENV 1-5 see Table 7.4.

7.5.4.3 Social indicators

Against social indicators, Option 1 is best because the maximum MCA score is less than the minimum for the other options (Figure 7.6A). This is due to the low level of neighbourhood disturbance associated with this option, as the MNA treatment requires only periodic visiting and sampling (SOC 3*). Also, the current site investigations and modelling reports for MNA suggest a high level of confidence in the predicted treatment duration, and therefore a low score for the uncertainty and evidence indicator (SOC 5). However, a high score is associated with the risk to human health and safety (SOC 1*); this value is calculated using factors for the number of injuries per hour during operations and travel to and from the site. A high score is observed for Option 1 due to the numerous trips to and from site over the treatment period. There is less distinction in the category score between the other options because they have similar treatment duration and there is no safety concern for onsite operations between them if relevant safety procedures are

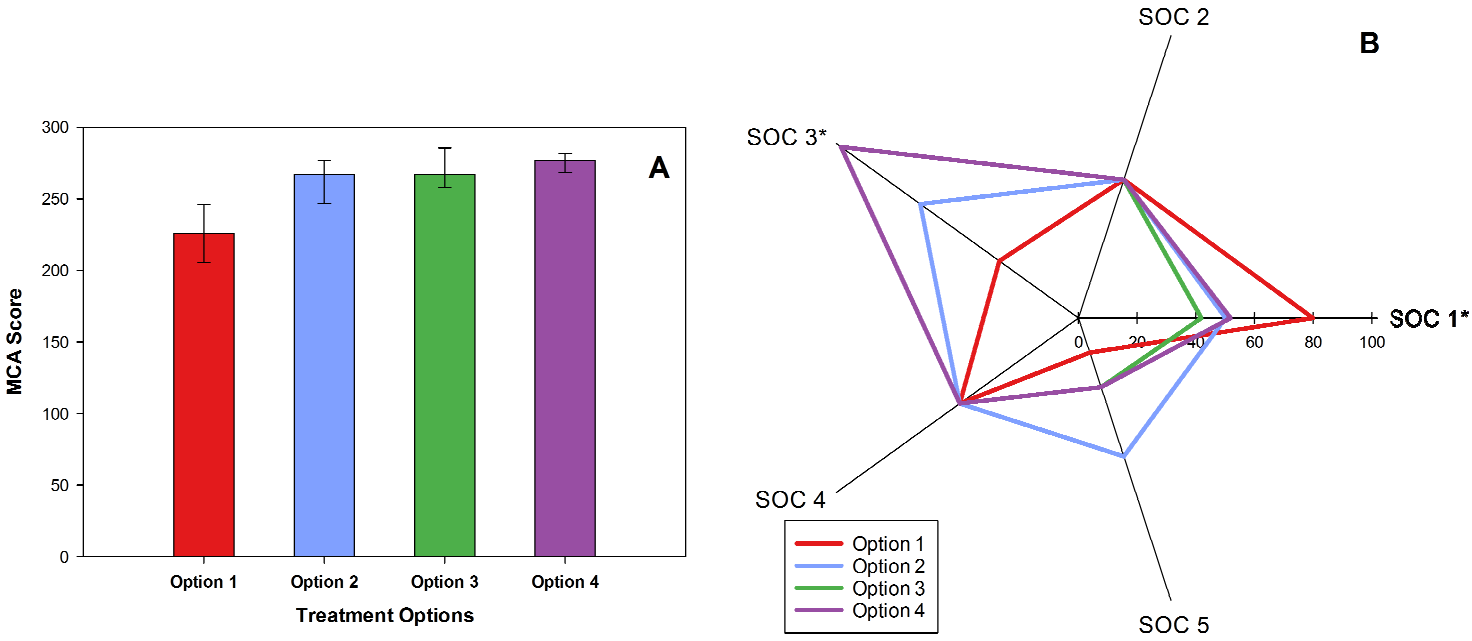

Figure 7.6 Tier 2 sustainability analysis: Social Indicators. A. is a bar chart showing the cumulative scores for the different indicator categories. B. is a radar plot that shows the distribution of scores in each indicator category for the middle estimate scenario, * represents priority indicators. Error bars on A. represent the minimum and maximum estimated values based on uncertainty analysis. For descriptions of Option 1-4 see Table 7.3 and SOC 1-5 see Table 7.4.

followed. However, Option 2 has the highest level of uncertainty but is predicted to cause less disturbance to local community, due to the absence of a treatment plant (Figure 7.6B).

7.5.4.4 Combined assessment

When the sum of MCA scores for all indicators is considered there is no observable difference between treatments (Figure 7.7). For priority indicators, the maximum MCA score for Option 2 is the lowest compared to all other options and overlaps slightly with the minimum score for Option 1 and 4. However, there is an overlap between the minimum and maximum MCA score range for Option 2 and Option 3. Compared against the Tier 1 cumulative rankings for priority indicators, greater differentiation amongst treatments is possible due to the range of uncertainty applied at Tier 2. Similar to the Tier 1 assessment, Option 2 and 3 are indistinguishable; however, there is more clarity between Option 2, 1 and 4.

The sensitivity analysis highlights indicators which have the greatest contribution to the MCA score (Figure 7.8). Indirect and induced economic indicators (ECON 2 and ECON 4) are not included for Option 1 because it is assumed that the sale of properties will be after one year and therefore the value is the same between the minimum and maximum

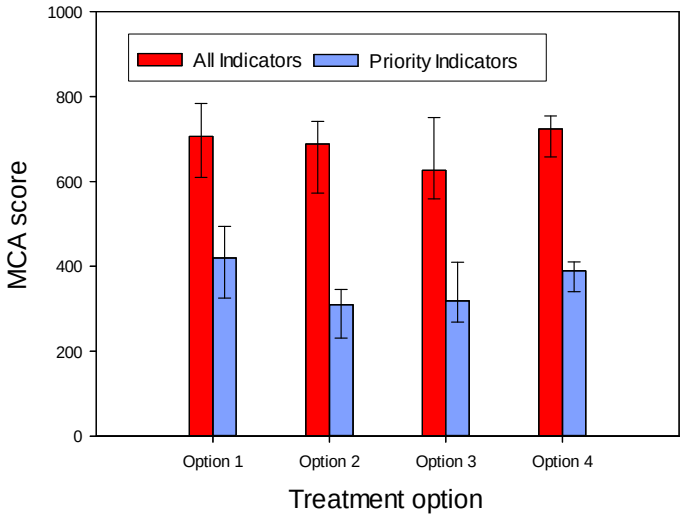

Figure 7.7 Cumulative Tier 2 MCA scores for all and priority indicators. Error bars represent the minimum and maximum estimated values based on uncertainty analysis.

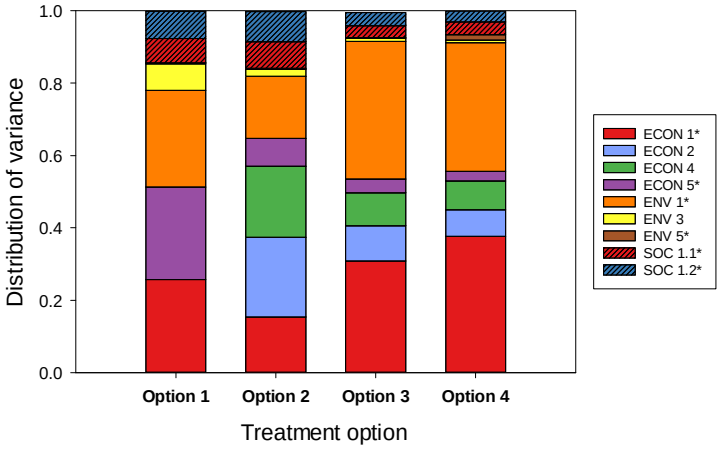

Figure 7.8. Sensitivity analysis of the overall MCA score to individual sustainability indicators. For indicator descriptions see Table 7.4**.**

treatment durations. When an indicator has a low sensitivity it reflects a low range of values relative to other indicators. Thus indicators with the greatest variability will have the greatest effect. The influence of different indicators appears to vary between options. Treatment duration (ECON 5) for example has a greater influence on MCA scores for Option 1 than Options 2-4, whereas air emissions (ENV 1) are less influential than the others.

An analysis of three priority indicators, one from each category, helps identify the role the HCS has in producing the MCA score (Figure 7.9A-C). Overall it is clear that for Option 1 the HCS operation is the driver in terms of cost, emissions and health and safety. A value for the HCS in other options is similar due to the range of treatment durations. The total direct cost and CO_2 emissions from the treatments increase from Options 2 to 4 and is reflected in the MCA analysis. There is less difference between Options 2 to 4 for health and safety due to similar treatment durations.

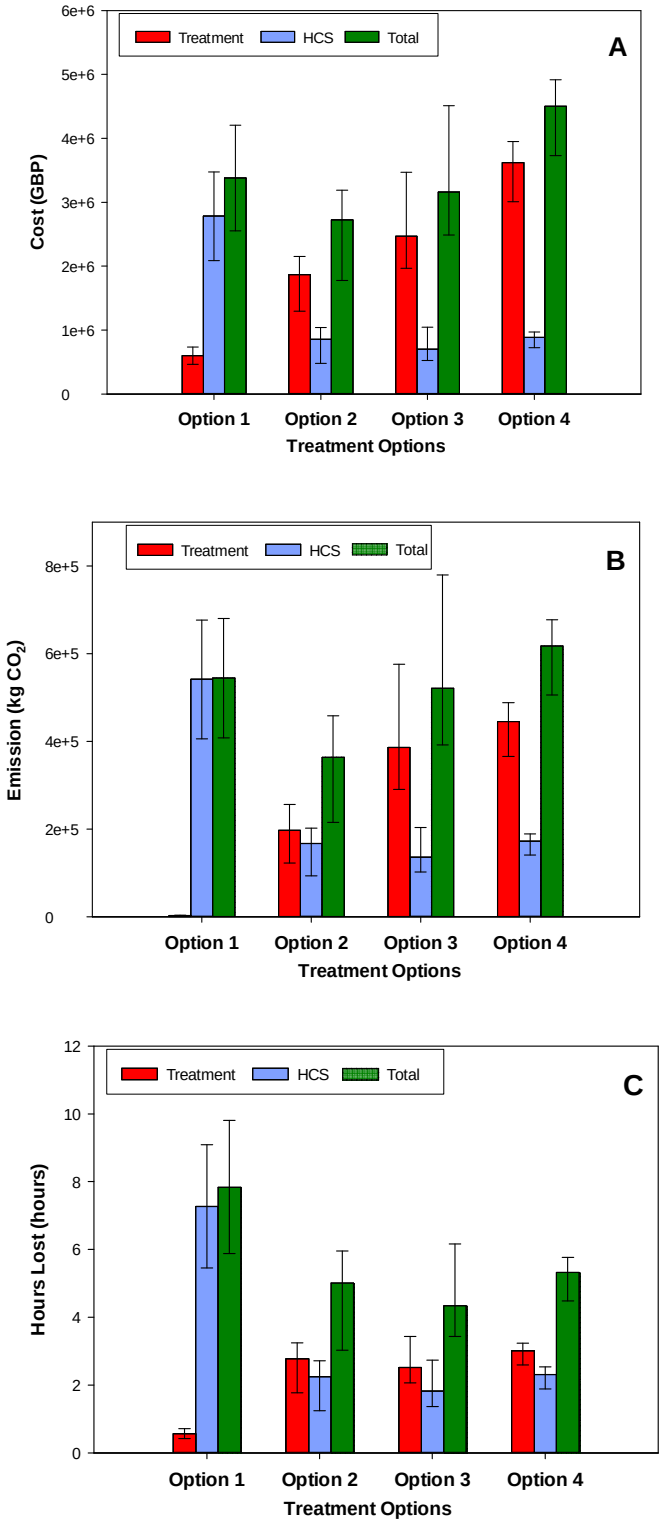

Figure 7.9 Analysis of individual sustainability indicators. A. ECON 1* total direct cost; B. ENV 1* CO_2 emissions; C. SOC 1* hours lost due to accidents. Error bars represent the minimum and maximum estimated values based on uncertainty analysis.

7.5.4.5 Sustainability scenarios

Priority indicator scores from MCA analyses of three different treatment scenarios for Option 2 vary significantly depending on the scenario specifications (Figure 7.10). Input values for these scores are in Table M.19 supporting information. The addition of photovoltaic (PV) panels to Option 2 (scenario 1) does not introduce a significant difference (based on minimum and maximum values) to the base case MCA score (base case and Scenario 1; Scenario 2 and Scenario 3, respectively). The effect is to reduce the total CO_2 emissions and provide a cost saving, however this is lessened by the need to run pumps consistently and the initial set up cost of a PV array equivalent to approximately 48 m^2 (see Appendix M: Table M.13). Conversely, removing the amendment has a significant effect by increasing the MCA score. This is due to an increase in the overall treatment time (e.g. middle estimate rises from 6.2 to 11.3 years) resulting from a decrease in the electron acceptor concentration in electrode wells from amendment to background groundwater supply. As previously highlighted for this CSM, prolonging treatment prolongs HCS operation with subsequent negative effects on sustainability rating. Furthermore, the

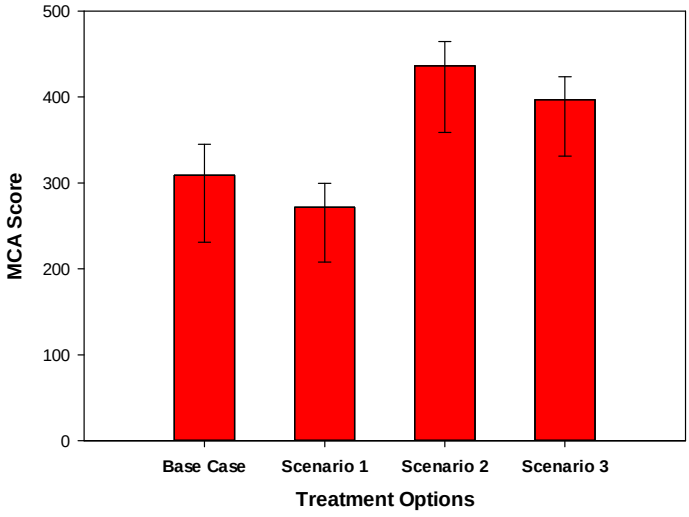

Figure 7.10. MCA score of priority indicators for four different Option 2 scenarios. Base Case: MCA scores from Tier 2 assessment; Scenario 1: solar panels are main source of electricity; Scenario 2: amendment is replaced with re-circulating groundwater; and Scenario 3: a combination of using solar panels and re-circulating groundwater. Error bars represent the minimum and maximum estimated values based on uncertainty analysis.

sodium nitrate amendment is cheap (0.34 GBP/kg), with a relatively low CO_2 footprint compared with other aspects of the treatment process (e.g. base case middle estimate for amendment production versus transport is 5.1 and 15.8 t, respectively).

7.6 Discussion

7.6.1 Tier 1 and Tier 2 assessment outcomes

The SuRF-UK framework is designed to support contaminated land practitioners in identifying the most sustainable remediation option for a site. In this study, similar results are obtained from both the Tier 1 and Tier 2 assessment; Options 2 and 3 performed similarly well against priority indicators, and better than Options 1 and 4. However, the Tier 2 assessment assigns quantitative values for certain indicators and includes an uncertainty analysis that allows more confidence to be placed in the differences between options. This allows the decision maker to eliminate options relative to the lowest priority indicator score, i.e. eliminate Options 1 and 4 based on scores greater than Option 2. Further analysis would be required to differentiate between Options 2 and 3, if it were deemed necessary to show which of these two well-performing options is optimal. This could include a pilot-scale test of Option 2 and using the data to inform a Tier 3 sustainability assessment of the two options. This is contrary to the hypothesis stated in Section 7.1.1 that EK would be the most sustainable technique, this is partly due to the effect of mitigating factors such as HCS.

7.6.2 Comparison of individual treatments

An assessment of remediation options against individual indicators allows the influence of the HCS to be isolated from the treatment (Figure 7.9). It is clear that the HCS makes up a greater proportion of the total value compared to the treatment alone for Option 1. Based on the boundaries of the Tier 2 assessment, MNA has the lowest value for CO_2 emissions, total direct cost and hours lost due to remedial activity and thus could be a very sustainable treatment option in the absence of the HCS. This corresponds to a study by Reddy and

Chirakkara (2013) who identified MNA as the most sustainable option to treat groundwater for a site contaminated with mixed PAH, heavy metal and pesticides. However, in this example there were no immediate down gradient receptors unlike the present study where the CSM and remedial objectives require the WSW to be isolated from MTBE contamination in the channel sands, hence the need for an active containment system, i.e. the HCS.

Furthermore, out of the intensive treatment options EK-BIO has a lower associated cost and greenhouse gas emission footprint. This compares well to an environmental assessment of EK remediation applied to heavy metal contaminated land by Kim et al. (2014). The authors observed during remedial operation that electricity consumption was the highest source of greenhouse gases with little additional extra from transport to and from site. Although overall, the construction stage had the highest associated emissions because the authors included manufacture of consumable materials (e.g. electrodes). The PT option on the other hand has the highest values for total economic cost and CO_2 emissions. Other studies that include PT in the available treatment options often give a poor associated ranking (Cadotte et al., 2007; Reddy and Chirakkara, 2013). This is due to the use of an *ex situ* GAC treatment module and associated manufacture and transport of the GAC to site (Cadotte, et al., 2007).

7.6.3 SuRF-UK framework appraisal

When applying Stage B of the SuRF-UK framework it is important to know the data and time limitations of the project in order to maximise the benefit of the assessment versus the effort expended conducting it. In this study the same management decisions could be reached with a Tier 1 assessment as opposed to a combined Tier 1 and 2 assessment. This is consistent with findings from Smith and Kerrison (2013) where the authors compared the management outcome from Tier 1, 2 and 3 assessments. They found for the same contaminated PFS site that a Tier 2 assessment could differentiate between options ranked equally at Tier 1. Although this did not greatly change the ranking of the

options or the final management decision between assessments. The authors also compared the time and effort required to conduct the assessments and clearly showed it increased between Tier 1, 2 and 3. Overall, the decision to progress between tiers of assessment is highly site and project specific, however it should include consideration of the additional time and data requirements to justify it.

7.6.4 Sustainability scenarios for EK-BIO

Different Option 2 sustainability scenarios were designed to: (1) offset electricity generation required for the EK-BIO treatment using renewable energy sources, i.e. PVs; and (2) reduce natural resources consumption by replacing the electron acceptor source from the amendment with electron acceptors from background groundwater that is pumped through the electrodes. Both techniques individually (scenarios 1 and 2) and combined (scenario 3) demonstrated limited improvement in the overall sustainability of the treatment. These findings demonstrate that introducing such techniques provide a benefit against green remediation objectives (US EPA, 2008). However when considered as part of a holistic approach, such as the SurF-UK framework, these techniques do not always result in a more sustainable solution.

With regards to the PV scenario, there was a small decrease in the score (i.e., improved sustainability), but not significant over the minimum and maximum ranges. Other EK remediation studies have successfully applied PV in their setups at the laboratory- and field-scale (Godschalk and Lageman, 2005; Jeon et al., 2015; Yuan et al., 2009). The noted benefits to using PVs include reduced operational cost and reduced pH changes and corrosion at the electrodes due to the intermittent power supply (Jeon et al., 2015). Furthermore, the remediation efficiency is comparable although slightly lower than systems with a mains direct current supply (Yuan et al., 2009; Jeon et al., 2015). PVs did not significantly reduce the MCA score in this study because: Option 2 is already a comparatively energy efficient option; the HCS contributes half of the CO_2 emissions; and the sensitivity of the influenced indicator is relatively low compared to other indicators (air

emissions, ENV 1*, Figure 7.8). Hence, any decrease in cost or CO_2 emissions from incorporating PVs would have a decreased effect on the overall MCA score.

7.7 Conclusions

This chapter applies Stage B of the SuRF-UK sustainable remediation framework to inform a management decision for LNAPL and dissolved phase remediation on a complex petroleum fuel-contaminated site. Both a Tier 1 and Tier 2 sustainability assessment are performed using a sustainable indicator set with priority indicators selected through a stakeholder workshop. These assessments identified Options 2 and 3 (EK-BIO+HCS and AS/SVE+HCS) as the most sustainable options, whereas Options 1 and 4 (MNA+HCS and PT+HCS) were least sustainable under the conditions of the assessment.

In addition to aiding the management decision on site there are wider implications:

- A comparison of individual treatments without the HCS against certain individual indicators highlighted EK-BIO as having lower CO_2 emissions and total cost compared to AS/SVE and PT. This is the first time EK-BIO has been compared to other remediation technologies and shows that it could be a competitive remediation technology in similar assessments in the future;
- The effectiveness of the SurF-UK approach is appraised by comparing the outcome of both the Tier 1 and 2 assessments. Both produced a joint ranking for AS/SVE and EK-BIO treatments, but the uncertainty analysis in Tier 2 gives more confidence in the decision to eliminate the MNA and PT technologies from future analyses, however only proceeding with the Tier 1 assessment could result in time and cost savings; and
- Treatment design modifications intended to make the EK-BIO option more sustainable actually had relatively little effect in changing the sustainability score compared with the other options.

Chapter 8 Thesis conclusion

8.1 Introduction

The aim of this research was to investigate the influence of physical heterogeneity on the electromigration of amendments for the enhancement of bioremediation of petroleum hydrocarbons in granular porous media. This aim is set within the wider context of the technical problem posed in the introduction, which is the mass transfer limitations for bioremediation of contaminants. An example of this is contaminant mass sequestered within low-K zones of physically heterogeneous aquifer settings. These scenarios pose two mass transfer limitations on bioremediation: (1) reduced bioaccessibility of contaminants due to their slow back-diffusion into the high-K host material; and (2) reduced bioavailability/bioaccessibility of electron acceptors within the low-K zone due to both consumption and limited resupply from the high-K zone across the K boundary. Furthermore, this scenario represents a significant site management issue. A sequestered contaminant mass can prolong remediation efforts by creating a rebound of contaminant concentrations following the initial stage of remediation.

To address the research aim, research objectives were posed. This chapter summarises the findings from all previous chapters to address the thesis research aim and objectives. The wider implications of this research with regards to field scale applications are also discussed by considering the research findings against a conceptual model that details the different aspects of EK-BIO application.

8.2 Summary of thesis findings

8.2.1 Summarise the state of knowledge for EK-BIO application in the natural environment

There are a number of existing reviews into EK and EK-BIO that cover a range of topics, such as EK enhancement techniques (Yeung and Gu, 2011) and EK-BIO processes at the micro-scale (Wick et al., 2007). The objective of the literature review presented in Chapter 2 was to summarise the current scientific literature with a focus on the practical aspects of applying EK-BIO. This included covering a range of topics: EK-BIO processes at the micro and macro scale, influence of subsurface environmental processes on EK-BIO and methods for enhancing EK-BIO at field-scale. The review also includes a simple electron balance model that re-creates a contaminant plume scenario. The model compares the electron acceptor mass flux from background groundwater into a plume by both advection-dispersion and electromigration; the latter also includes electron acceptor migration from an amendment added at the electrode wells.

Overall, there are two main findings from the review. Firstly, that the natural environment will impart a significant influence on EK-BIO with a range of implications. At the microscale the application of EK-BIO in different material types will result in different mechanisms of substance mixing. In clays there is likely to be a counter electroosmotic flow thus mixing will occur from substances travelling in opposite directions, whereas for sands longitudinal mixing could arise from overlapping migration paths. Also, different subsurface phenomena will alter how EK-BIO is applied. For example, groundwater flow will present an additional transport vector that is likely to exceed migration rates of EK in high-K material. The second finding is that there is a range of EK application methods that have the potential to negate the variability observed in natural environments. For example, if the pH buffering capacity of the soil or sediment is variable between the electrodes creating uneven pH control, different electrode configurations could be applied to better control pH (e.g. polarity reversals or radial configuration). This highlights the need for a detailed

understanding of the physiochemical properties of the subsurface on site to best inform treatment design.

Chapter 2 justifies the aim of the thesis within the wider context of the current literature. Experiments within physically heterogeneous material are limited, yet they are more representative of the natural environment which is an area of EK literature that needs to be developed. Furthermore, while EK-biostimulation has been demonstrated at the lab scale in low-K material it has not been applied in heterogeneous settings. Moreover, this chapter forms a basis for wider EK-BIO applications which can be drawn upon for implications of this research to field scale applications.

8.2.2 Development of laboratory apparatus that conceptually represents the technical problem expressed in the introduction

Chapter 3 focused on the development, construction and testing of bespoke laboratory apparatus. The design process consisted of using a conceptual model to determine a series of requirements for the setup. Existing laboratory-scale designs in the literature were then considered with respect to these design requirements. The final design carried forward to construction was a refinement of existing designs (such as Harbottle et al. (2009) and Mao et al. (2012)).

Once constructed, preliminary experiments were conducted to optimise the experimental setup and ensure it produced reproducible results. These included refining the construction, sampling and sediment consolidation protocols. It also involved a series of experiments to determine the most suitable pH control and nitrate addition method. The pH control experiments looked at two different methods: (1) electrode fluid recirculation, but this generated advection through the sediment chamber due to pumping; and (2) electrode conditioning with hydrogen chloride and sodium hydroxide. The latter method provided the most consistent pH values across the sediment without influencing nitrate migration. The nitrate addition method determined that a constant concentration of nitrate

should be added to the cathode opposed to only adding nitrate at the start of the experiment. This was in order to prolong experiments and observe a continual nitrate breakthrough at the anode. Results from these initial tests have provided interesting results; in systems where no pH control is applied there was an inverse spatial correlation between the voltage gradient and the nitrate concentration as well as a reduced nitrate migration rate between electrodes.

The results from preliminary experiments demonstrate that the laboratory apparatus and the construction protocols can generate reproducible experiments. It is therefore, fit for purpose to apply in the amendment migration experiments conducted in Chapters 4 and 5. Chapter 6 included a lot of new methods such as a different recirculation system and GC and microscopy analysis; these are addressed in the materials and methods section of that chapter.

8.2.3 Define the controlling mechanisms of physical heterogeneity on the electromigration of an amendment

This research objective was addressed over two chapters. Each chapter represents a different arrangement of physical heterogeneity. For Chapter 4, two different material types with high- and low-K properties were arranged in series; for Chapter 5 these materials were arranged in layers. All experiments were conducted in the laboratory apparatus developed in Chapter 3. Analysis for these experiments was based on major ion analysis of pore fluid samples and voltage readings.

Spatial changes in material type are equivalent to changes in the effective ionic mobility which is a function of the porosity and tortuosity of the material. In Chapter 4, bromide electromigration experiments through homogeneous material demonstrated that the effective ionic mobility decreased as K decreased in the materials used. This is suggested to be due to an increase in the tortuosity of the migration path the ion must take through the material. The K value of a material in these experiments was lowered by mixing glass

beads with powdered kaolin. Thus, the tortuosity factor can be influenced by occlusion of pore spaces in low-K material where there is a greater proportion of clay added to the glass bead mix. The results showed that in heterogeneous settings where the effective ionic mobility varied spatial, the following controls on nitrate migration were observed: (1) a spatial change in nitrate migration rate due to changes in effective ionic mobility and subsequent accumulation of nitrate at the interface between these materials; and (2) a spatial change in the voltage gradient distribution across the hydraulic conductivity contrast, due to the inverse relationship with effective ionic mobility. The latter finding led to the observation that mass transport was higher through the same material in the heterogeneous compared to the homogenous setting due to the elevated voltage gradient.

In Chapter 5, material with different effective ionic mobilities were arranged in layers to represent a different form of physical heterogeneity. This configuration led to a voltage difference between layers in the heterogeneous compared to homogenous experiments. This observation is expanded further by linking it to values of pore fluid effective resistivity. The phenomenon can be explained by higher resistivity values in the low-K layer that increase between the anode and cathode, this initiates a transfer in the electric current between layers and distorts the voltage field accordingly. Furthermore, nitrate concentrations are elevated in the low-K material in heterogeneous compared with homogeneous systems. Using predicted concentrations, this is shown to be a function of a transverse flux associated with the voltage difference between layers. This is the first time this phenomenon has been quantified. The importance of this phenomena at field scale for delivery of an amendment (i.e., electron acceptor, donor or nutrient) by EK for bioremediation is presented in an electron balance model.

Overall, Chapters 4 and 5 develop the fundamentals of EK applications to physically heterogeneous settings. In Chapter 4 amendment migration is quantified and demonstrated not to be hindered within heterogeneous settings. Chapter 5, identifies a previously unreported phenomenon in the electrokinetic transport literature.

8.2.4 Enhanced removal of a sequestered organic contaminant by the electromigration of an amendment

In Chapter 6, a heterogeneous configuration similar to the K contrast in Chapter 4 was generated within the laboratory apparatus developed in Chapter 3. A single species inoculum was distributed within the high- and low-K zones and a dissolved contaminant (toluene) was added to the low-K zone. The experimental design for bench-scale tests compared EK and advection based migration of nitrate through the sediment chamber; three different controls were incorporated where EK, the inoculum and nitrate amendment were absent. In addition, microcosm experiments were conducted to determine the biodegradation rate of toluene by the inoculum under ideal conditions. Analysis of these experiments was based on toluene and major ion concentrations in the pore fluid and voltage readings.

Toluene removal from the low-K zone was predicted to be by three mechanisms: (1) electroosmotic flow from the anode to the cathode; (2) diffusion across the low-K/high-K interface; and (3) denitrification by the inoculum. Electroosmosis was shown to be the most prominent removal mechanism in the bench-scale experiments. This is based on analysis of toluene concentrations in the rigs and a mass balance that accounted for toluene loss from the low-K zone. Biodegradation was not enhanced by the electromigration of nitrate in these experiments. However in the microcosms, upon the addition of nitrate the inoculum successfully degraded toluene, hence a biodegradation rate under ideal conditions could be obtained. A comparison of toluene removal rates by electroosmotic flow and biodegradation showed electroosmosis to the most effective removal mechanism under these experimental settings. A sensitivity analysis was conducted to determine the experimental conditions where the electroosmotic removal rate would be equivalent to that of biodegradation. The key variables analysed include electroosmotic permeability, fraction of organic carbon (f_{OC}) and the voltage gradient. The findings provide an insight into the type of conditions in which enhanced biodegradation should be attempted over

enhanced electroosmotic flow, for example where the material has a low electroosmotic permeability, a high f_{OC} or a lower voltage gradient.

Overall, this chapter expands current knowledge of EK applications to heterogeneous settings to enhance the transformation of contaminants sequestered within low-K zones. It highlights the competing removal mechanisms and discusses the conditions under which electroosmosis or bioremediation would be more effective.

8.2.5 Compare EK-BIO against other remediation technologies using the SuRF-UK framework

Chapter 7 considers EK-BIO application at the field scale by comparing it against other remediation technologies using a sustainability assessment. Metrics for EK-BIO application are derived from a simple electron balance model. This is the first time EK-BIO has been compared against other technologies in this way. Sustainable management practices can be applied to the remediation of contaminated land to maximise the economic, environmental and social benefits of the process. The Sustainable Remediation Forum-UK (SuRF-UK) have developed a framework to support the implementation of sustainable practices within contaminated land management and decision making. This chapter applies this framework, including a qualitative (Tier 1) and quantitative (Tier 2) sustainability assessments, to a complex contaminated site where the principal contaminant source is unleaded gasoline, giving rise to a dissolved phase BTEX and MTBE plume. The pathway is groundwater migration through a Chalk aquifer and the receptor is a water supply borehole. A hydraulic containment system (HCS) has been installed to manage the MTBE plume migration.

In addition to EK-BIO, the following options were considered: monitored natural attenuation (MNA), air sparging / soil vapour extraction (AS/SVE) and pump and treat (PT). The sustainability assessment uses an indicator set from the SuRF-UK framework and includes priority indicators that were identified through consultation with the primary

stakeholders. At Tier 1 the options are ranked based on qualitative supporting information, whereas in Tier 2 a multi-criteria analysis is applied. Furthermore, the multi-criteria analysis was refined for scenarios where photovoltaics (PVs) are included and amendments are excluded from the EK-BIO option.

Overall, the analysis identified AS/SVE and EK-BIO as more sustainable remediation options at this site than either PT or MNA. The wider implications of this study include: (1) an appraisal of the management decision from each Tier of the assessment with the aim to highlight areas for time and cost savings for similar assessments in the future; (2) the observation that EK-BIO performed well against key indicators compared to the other intensive treatments; and (3) introducing methods to improve the sustainability of the EK-BIO treatment design (such as PVs) did not have a significant effect in this instance.

8.2.6 Addressing the overall aim of the thesis

This thesis has successfully demonstrated amendment migration through physically heterogeneous porous media and developed understanding of EK-BIO applications in these settings. This has been achieved by: (1) developing a conceptual framework for how EK transport processes behave in physically heterogeneous conditions and linking spatial changes in sediment properties to controlling factors on EK transport; and (2) discussing the effectiveness of EK-BIO in physically heterogeneous settings with regards to competing removal mechanisms on contaminants from low-K zones (i.e. electroosmosis). In addition, desk based studies further developed understanding on EK-BIO: (1) a literature review on the practical aspects of EK-BIO detailed the different applications and suggested how aspects of the natural environment could influence the technology; and (2) a sustainability assessment compared EK-BIO with other technologies and expanded on literature that has applied EK-BIO with renewable energy technologies such as solar power.

8.3 Implications for EK-BIO applications at the field-scale

The findings of this thesis have wider implications for field-scale applications of EK-BIO. They primarily apply to the following aspects: amendment properties, high-K material properties, low-K material properties, contaminant properties and EK field design. These are discussed with reference to the scenario shown in Figure 8.1. It assumes that contamination is localised to the low-K zone and an amendment is added at the cathode and migrated towards the anode. Groundwater flow direction is illustrated on Figure 8.1 and will only impact transport within the high-K material. Figure 8.1 is representative of scenarios where EK is applied to a heterogeneous subsurface. It has been chosen for the purposes of demonstration, the research presented herein will have similar implications for other scenarios.

8.3.1 Amendment properties

8.3.1.1 How does increasing the amendment concentration influence the electromigration of an amendment?

Selecting the right amendment concentration for a treatment requires consideration of several factors and the trade-offs between them. The results from these experiments impact on two aspects of field application: (1) the migration of amendment into the sediment from the electrode and the associated voltage drop; and (2) the migration of amendment through layered systems.

If amendment concentration is too high, migration will stall adjacent to the electrode (Wu et al., 2012a), however if it is too low insufficient amendment mass will be delivered to the contaminated zone (Rabbi et al., 2000). Experiments from Chapter 4 demonstrate that, where heterogeneity is defined as a single contrast between high- and low-K materials, the voltage gradient is highest across the low-K zone (assuming it has a lower effective ionic mobility value). If an amendment was added into these low-K zones via electrode or amendment wells, the higher voltage gradient would counter the effect of the voltage

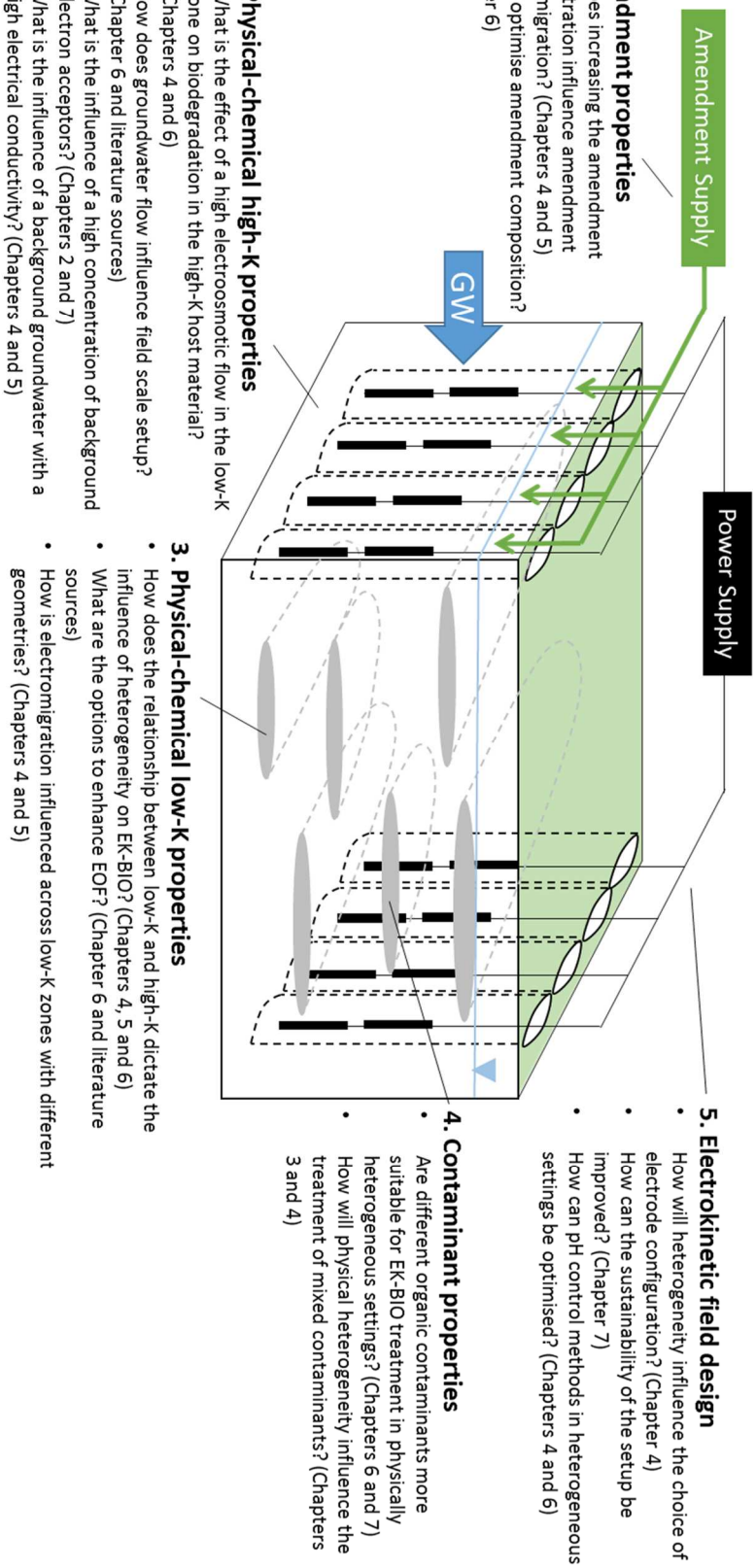

Figure 8.1 Conceptual diagram showing key aspects of a typical EK field setup with associated implications from this research. The blue arrow signifies to the direction of groundwater flow.

gradient drop associated with adding high amendment concentrations. Thus, a higher amendment mass flux into the sediment from the electrode or amendment well could be maintained compared to a homogenous setting. For example, in clay an amendment concentration equivalent to 0.2 S/m at an electrode spacing of 1 m results in a 60% drop in the voltage gradient next to the cathode compared to a system where the voltage gradient is fixed (Wu et al., 2012a). Assuming a system where 100 V is applied between electrodes 1 m apart and homogeneous conditions where voltage is distributed uniformly the inlet voltage gradient decreases from 100 V/m to 40 V/m. In a heterogeneous setting where an increase of 30% relative to a fixed voltage gradient is observed across a low-K zone equivalent to half the sediment section (Chapter 4, Table 4.4), the voltage gradient would drop from 130 V/m to 52 V/m when the amendment is added.

In layered heterogeneous settings the voltage difference appeared more pronounced between layers with different K values when an amendment was added at a higher concentration (0.1 to 5 g/L). Experiments from Chapter 5 showed this phenomenon led to a subsequent increase in the transverse amendment mass flux of a negatively charged amendment from the high to the low-K layer. In these experiments the effective ionic mobility was lower in the low-K than the high-K zone. Ensuring a high amendment mass flux into a low-K zone with a sequestered contaminant be relevant in certain scenarios. Under the right conditions, a transverse mass flux may be an important pathway for the amendment into these contaminated zones (such as Figure 8.1). An electron balance model in Chapter 5 illustrates the importance of a transverse flux in reducing remediation times. For conventional remediation technologies, a transverse mass flux across K boundaries is limited by dispersion and/or diffusion of substances. Song and Seagren (2008) identified dispersion as the rate limiting factor for biodegradation in a layered heterogeneous setting. Similarly, Hønning et al. (2007) observed diffusion as the limiting transport mechanism to deliver permanganate into a clay contaminated with PCE.

8.3.1.2 How can the amendment composition be optimised?

The function of EK-Biostimulation is to introduce a limiting substance that is required to enhance bioremediation. This is applied in laboratory-scale experiments in Chapter 6. It is important when designing the amendment that one limiting substance is not exchanged for another. In Chapter 6 a possible reason for biodegradation not being observed in the experiments was insufficient supply of phosphate from the background synthetic groundwater. This could be rectified in future attempts by including phosphate in the amendment composition. Other authors have excluded phosphate or other nutrients from their amendment composition based on the experimental design including it within the minimal media. For example, Tiehm et al. (2010) enhanced toluene degradation by adding a nitrate amendment by electromigration within a minimal media that contained a phosphate concentration of 0.55 g-PO_4/L. Alternatively, mixed amendments can contain a primary active compound plus small concentrations of other nutrients (e.g. lactate with minimal media as in Mao et al. (2012)); or a more equally mixed amendment (e.g. ammonium nitrate and potassium di-hydrogen phosphate as in Xu et al. (2010)). Having multiple components within the amendment may reduce migration rates due to competitive transport from the ion mix (Lohner et al., 2008a). It may also increase the chance of biofouling in the sediment preventing the amendment reaching its target location (Rabbi et al., 2000). Overall, it is important to design a balanced amendment because it is difficult to predict the potential stresses exerted by EK on biodegradation.

8.3.2 Physical-chemical high-K properties

8.3.2.1 What is the effect of a high electroosmotic flow in the low-K zone on biodegradation the high-K host material?

The findings in Chapter 6 suggest that in situations where the contaminant removal rate from the low-K zone by electroosmosis is high there will be an increased concentration of contaminants in the high-K material. Therefore, in these scenarios, it would be more effective to focus bioremediation efforts within the high-K zone. This could be beneficial to

the bioremediation process. Firstly, mixing by advection-dispersion between bacteria, contaminants and electron acceptors will be greater in high-K material. This reduces the mass transfer limitations on biodegradation of contaminants (Simoni et al., 2001). Secondly, microbial abundance in fine grained sediments is limited due to narrow pore sizes (Rebata-Landa and Santamarina, 2006). In these settings without the application of EK, microbes are less motile and mass transfer is controlled by diffusion. Thus, in high-K zones where the pore spaces are not as confined, microbial abundance may be greater and therefore more conducive to bioremediation. Thirdly, the presence of low-K zones facilitates greater mixing in the high-K host material due to a disruption in the advective flowlines down gradient of the low-K zone (Bauer et al., 2009).

The method of bioremediation applied within the high-K zone could include either natural attenuation or biostimulation. Natural attenuation would be suitable if no immediate intensive remediation action was required and the background concentration of electron acceptors was sufficient. Alternatively, biostimulation could be applied where amendments are introduced to aid biodegradation. A similar concept was applied at field scale by Godschalk and Lageman (2005). The authors developed an EK-biofence to disperse nutrients from amendment wells to initiate degradation of PCE downgradient of the contaminant source. If there was a sensitive receptor downgradient, a pump and treat system could be installed to extract the contaminants released into the high-K zone. This is similar to the field scale problem discussed in Chapter 7. Typically, the amount of contaminant recovered in these systems decreases over time but is not representative of the reduction in contaminant mass in the aquifer (US EPA, 1994). EK could therefore be used to enhance extraction of contaminants from pump and treat systems.

8.3.2.2 How does groundwater flow influence field scale setup?

An advective flow field will have an important control on the configuration of an EK field setup within a heterogeneous setting that covers zones of high-K material (such as Figure 8.1). Advection will be more dominant in high-K material, whereas EK will be more

important in low-K material. For example, the calculated advective bromide mass flux (hydraulic gradient: 0.1; concentration: 1g/L) for the high-K and low-K materials in Chapter 4 (RQ2-Tracer_1 and RQ2-Tracer_4) is $2.2x10^{-2}$ and $4.5x10^{-7}$ g/m^2-s, respectively. This is compared with an observed bromide electromigration mass flux in the same high-K and low-K material of $1.2x10^{-4}$ and $7.4x10^{-5}$ g/m^2-s, respectively (based on values from Table 4.2 and accounting for observed voltage gradient). In high-K material solute transport by EK cannot easily override advection in the opposite direction (Eid et al., 1999). However, for treatments to be effective in scenarios such as Figure 8.1, an amendment must first migrate through the high-K section to reach the target low-K zone. The solution is to position the electric field so that it complements the existing advective flow field (Figure 8.1). Wu et al. (2012b) showed a similar approach in modelling simulations of EK-ISCO. Each simulation included a step where the oxidant, permanganate was first distributed through the high-K zones of a model heterogeneous aquifer and then EK applied. An alternative approach is to place the amendment injection well/ electrode within the low-K zone, thus eliminating the influence of the advective flow field.

8.3.2.3 What is the influence of a high concentration of electron acceptors in the background groundwater?

This section considers high background concentrations of electron acceptors in relation to the mass of electron donors presented by the contaminant mass. The implications of a high concentration of electron acceptors in background groundwater are considered in the context of the scenario presented in Figure 8.1. It is assumed that electron acceptors are depleted in low-K zones compared to high-K zones due to the presence of contamination and low advective replenishment. A high concentration in the high-K zone indicates there is capacity for biodegradation. Thus, enhancing bioremediation by initiating an electroosmotic pore fluid flux to move the contaminant from the low-K to the high-K zone is more viable. Alternatively, if the electron acceptors are primarily in the form of dissolved ions (nitrate and sulphate) these can be manipulated for electromigration and used to

influence treatment design. The electron balance models in Chapters 2 and 7 both include background electron acceptors as an alternative to the amendment. It is considered a sustainable approach because the environmental impact and economic cost of the amendment is avoided. However, in both Chapters 4 and 7 using only background electron acceptors results in extended remediation timescales. A more in-depth MCA analysis in Chapter 7 shows that increasing the timescale of remediation offsets the benefit of avoiding the amendment. Under different scenarios there could be a sustainability benefit from using this method in conjunction with, for example, solar panels.

8.3.2.4 What is the influence of a background groundwater with a high electrical conductivity?

A high concentration of ions within the electrolyte will increase the electrical conductivity of the fluid with implications for the impact of the amendment. This has been shown in Chapters 4 and 5 to impact on how the amendment behaves within the heterogeneous setting. The more amendment added the greater the proportion of the total electrolyte. For example in Chapter 5 an amendment concentration of 0.1, 1 and 5 was equivalent to 3.4, 22.6 and 67.2% of the electrical conductivity of the electrolyte. It follows that if the electrical conductivity of the background electrolyte was higher, the amendment would make up a lower proportion. This would lead to a reduced impact on the voltage gradient (Wu et al., 2012a). An implication for amendment migration in heterogeneous settings include a reduced transverse mass flux.

8.3.3 Physical-chemical low-K properties

8.3.3.1 How will a variation in low-K properties influence the effect of heterogeneity?

The material used in experiments for Chapters 4, 5 and 6 show a decrease in K as equivalent to a decrease in the effective ionic mobility. However, the properties that dictate the effective ionic mobility will vary in the natural environment and exhibit different values

compared to the materials used in these experiments. For example, the nitrate effective ionic mobility for low-K material in Chapter 4 was $6.5x10^{-9}$ m^2/s-V compared to reported values for kaolin (representative of clays with high water content, 67% (Mitchell, 1993)) which are typically higher (1.55 -$1.65x10^{-8}$ m^2/s-V) due to higher porosity and tortuosity values (Acar and Alshawabkeh, 1993; Thevanayagam and Rishindran, 1998). Therefore, it is important to consider the findings of the thesis within the context of a subsurface where the effective ionic mobility in low-K material may be elevated equivalent to or above the value for high-K material.

In Chapter 4 the influence of a higher effective ionic mobility for the low-K zone needs to be considered in two scenarios. Firstly, if the effective ionic mobility is equivalent between the two materials then a minimal voltage difference would be expected. This is similar to experiments RQ1-HET_2A and RQ1-HET_2B where the voltage difference was ± <1% compared to a linear voltage gradient (Table 4.4). However, the influence of electroosmotic flow could still lead to an accumulation of nitrate at the high-K/low-K interface and reduce migration times compared to homogeneous settings. Secondly, if the effective ionic mobility is higher in the low-K than the high-K material. For example, assume an effective ionic mobility of $1.3x10^{-8}$ and $1.65x10^{-8}$ for the high- and low-K materials respectively (values from Chapter 4, Table 4.2 and Thevanayagam and Rishindran (1998)). The difference in value is equivalent to that observed for experiment RQ2-HET_3 ($1.3x10^{-8}$ and $1.0x10^{-8}$ m^2/s-V, high- and low-K respectively). Hence, it could be anticipated that an elevated voltage gradient could be observed over the high-K compared to the low-K zone under these circumstances.

In Chapter 5 the implications of a higher effective ionic mobility in the low-K zone can be discussed with reference to the conceptual model, Figure 5.4. If the low-K layer exhibited a higher effective ionic mobility and therefore lower effective resistivity the current transfer between layers would alter. This is demonstrated in Figure 8.2 which shows the pore fluid resistivity of high- and low-K layers and the transfer of current and voltage difference

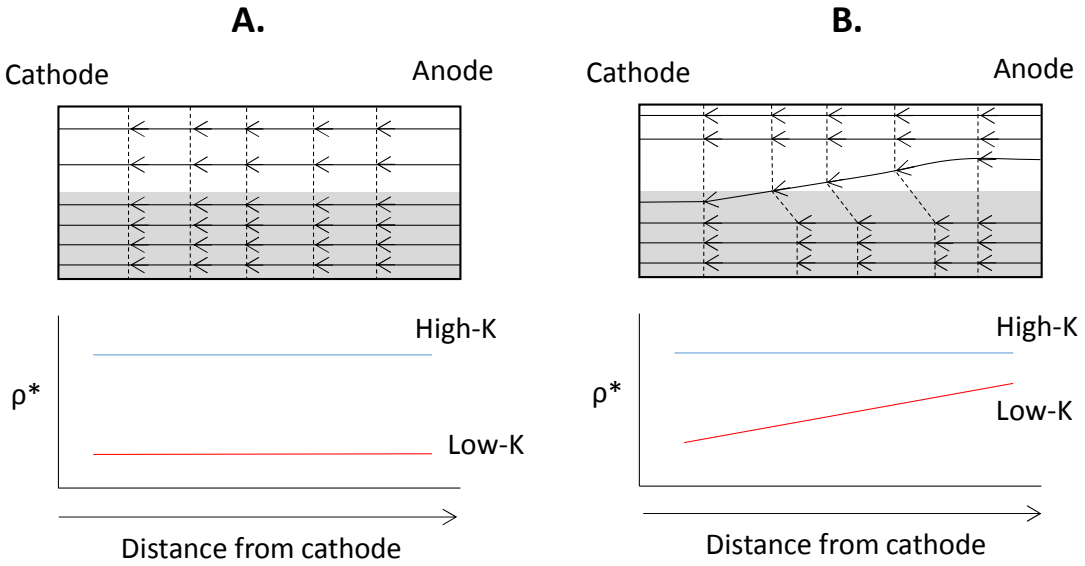

Figure 8.2 Diagrams showing the influence of an increased effective ionic mobility value in the low-K layer based on the conceptual model in Chapter 5, Figure 5.4. A represents resistivity gradient in the low-K layer increasing from anode to cathode, B the gradient increases from cathode to anode.

between layers. For simplicity, the resistivity values in the high-K layer are assumed constant through the sediment. Figure 8.2A shows lower resistivity values throughout the low-K layer. There is expected to be minimal current transfer and voltage difference between layers in this scenario. This is due to a consistently lower resistivity in the low-K layer compared to the high-K layer. Figure 8.2B shows low-K resistivity decreasing toward the cathode that could arise from amendment accumulation. In this scenario the current will transfer from the high-K layer to the low-K layer leading to a higher voltage gradient in the high-K layer. The subsequent electromigration mass flux will be in the opposite direction to that observed in Chapter 5.

The findings from Chapter 6 depend on the influence of the electroosmotic flow as a removal mechanism for toluene. A high effective ionic mobility in the low-K zone will not influence this phenomenon directly. It would result in a greater mass flux of substances into the low-K zone, reducing the time in which nitrate is distributed within it. This would have implications for the pore fluid electrical conductivity and subsequently the

electroosmotic permeability. Furthermore, it would lessen any potential voltage gradient difference observed between high- and low-K zones (Figure 6.18).

8.3.3.2 What are the methods to enhance contaminant removal by electroosmotic flow?

If bioremediation would be more effective in the high-K zone and subsurface conditions were conducive to a high electroosmotic flow, then options to enhance contaminant removal by electroosmotic flow and their impact on biodegradation should be considered. These broadly involve increasing the electroosmotic flow rate or the solubility of the contaminant via surfactants and/or co-solvents (Cameselle and Reddy, 2012).

Based on Equation 1.1 there are two key variables that can be controlled to enhance the electroosmotic pore fluid flux, namely the zeta potential and the voltage gradient. The zeta potential is highly sensitive to changes in pH and electrical conductivity. Changes in pH within the sediment can alter the zeta potential by changing the charge on the clay particle surface, e.g. an excess of H^+ ions will move this charge closer to zero (Vane and Zang, 1997). Thus, enhancing electroosmotic flow rate can be achieved by controlling pH changes at the electrodes which is compatible with maintaining microbial activity (Lear et al., 2004). Organic acids are a good example of an electrode conditioning fluids to control pH. Cameselle (2015) noted citric acid was particularly effective at maintaining a consistent high electroosmotic flow rate compared to oxalic or tartaric acid. They have also been successfully used in conjunction with bioremediation experiments (e.g. citric acid used to enhance removal and biodegradation of diesel in Pazos et al. (2012)). Increasing the electrical conductivity has also been shown to influence the zeta potential. Typically, increasing the electrolyte concentration will move the zeta potential closer to zero, reducing electroosmotic flow (Vane and Zang, 1997). This is due to the reduction in the diffuse double layer thickness resulting from the increase in ion concentration (Yukselen-Aksoy and Kaya, 2010). A potential barrier to future field applications of EK-BIO where the

goal is to enhance both electroosmotic flow and bioremediation is the influence of a high concentration amendment on the zeta potential and sustaining electroosmotic flow.

Furthermore, the voltage gradient is proportional to the electroosmotic flow. However it is not a clear linear relationship because there are complex chemical processes that can vary over the course of EK application. Cameselle (2015) showed that a voltage field strength of 150 V/m produced a lower cumulative electroosmotic flow compared to 100 V/m. This is partly due to the increased electrical current required for the high voltage test and subsequent increased generation of hydrogen and hydroxyl ions at the electrode. Maintaining a low intensity electric current is also beneficial for bioremediation applications. At high electric current intensities there can be negative effects on the cell structure of microorganisms and impair their ability to sustain biodegradation (Luo et al., 2005c).

The addition of solubilising agents do not enhance electroosmotic flow, rather they enhance desorption of contaminants from the sediment matrix and thus increase contaminant removal. Surfactants or co-solvents has been widely used to enhance the removal of contaminants from low-K material. Saichek and Reddy (2005) demonstrated enhanced contaminant removal from a low-K zone within heterogeneous settings. They showed high mass recovery of the contaminant, phenanthrene using 5% Igepal CA-720 when EK was applied at 200 V/m. Soil properties can influence the effectiveness of the surfactant. For example, soils with a high buffering capacity are more suitable for non-ionic surfactants because pH changes are buffered preventing adsorption of the surfactants to particle surfaces (Reddy and Saichek, 2003). Additionally, different surfactants can influence the viscosity and dielectric constant of the pore fluid which are generally considered constant (Page and Page, 2002). The surfactant, Tween 80 was shown to increase the viscosity, whereas a 40% ethanol co-solvent flushing fluid lowered the dielectric constant of the fluid (Cameselle and Reddy, 2012). Furthermore, if the aim of remediation methods is to enhance bioremediation in the high-K zone, it is important that

the surfactant used can be degraded by microorganisms, therefore biodegradable surfactants should be considered (Mulligan, 2009).

8.3.3.3 How is electromigration influenced across low-K zones with different geometries?

Findings from Chapter 4 demonstrated that when heterogeneity was represented by a contrast of materials with different K (and effective ionic mobility) values, there were subsequent spatial controls on the voltage gradient and the rate of electromigration. These findings can be expanded to different heterogeneous settings. For example, a graduated K contrast where the K value of material decreases in series from high to low could generate a step-like increase in the voltage gradient; and a high-K/low-K/high-K configuration would create an increase in the voltage gradient specifically over the central low-K zone. Furthermore, it is important to maximise current density into the low-K zone to enhance the amendment mass flux and increase treatment efficiency. For example, in Figure 8.1 there are multiple narrow, low-K lenses with a reduced surface area exposed to the amendment flux. This could lead to a drop in treatment efficiency because less amendment reaches the target location, with implications for treatment costs (Wu et al., 2012b). However in these scenarios the importance of a transverse flux demonstrated in Chapter 5 is highlighted because it could be an important route for amendment into low-K zones.

8.3.4 Contaminant properties

8.3.4.1 Are different organic contaminants more suitable for EK-BIO treatment in physically heterogeneous settings?

The susceptibility of contaminants to electroosmosis will be an important factor for their treatment in heterogeneous settings. It determines the location of the contaminant during remediation and therefore helps inform treatment design. Contaminant properties were discussed in Chapter 6. One of the key properties is the partition coefficient, K_d;

contaminants with a high value will adsorb more strongly to sediment organic matter (Delle Site, 2001). PAHs are a good example of contaminants that adsorb strongly to sediment or organic matter particle surfaces. Numerous studies look at coupling surfactants with EK removal of PAHs (e.g. Reddy and Saichek, 2003; Saichek and Reddy, 2003; Cameselle and Reddy, 2012). There is also evidence that EK can enhance the bioremediation of PAHs either by the addition of nutrients (Xu et al., 2010) or through enhanced desorption and subsequent bioaccessibility (Niqui-Arroyo et al., 2006). Other examples from the literature where contaminants are subject to prolonged EK application for the purposes of enhanced bioremediation include PCE (Wu et al., 2012; Mao et al., 2012) and pentachlorophenol (Harbottle et al., 2009). This suggests minimal electroosmotic migration of these contaminants by EK, thus bioremediation would be an effective transformation mechanism within these materials.

8.3.4.2 How will physical heterogeneity influence the treatment of mixed contaminants?

A mixture of organic and inorganic contaminants is common at contaminated sites. These types of sediments have been tested for EK remediation typically involving the addition of surfactants and chelating agents such as EDTA (Alcántara et al., 2012). In a heterogeneous setting the distribution of surfactants within low-K zones is unlikely to be a limiting factor because effective treatment by this method in these settings has been demonstrated by Saichek and Reddy (2005). However, removal of mixed contaminants can include generating acidic conditions across the sediment to facilitate metal removal. High removal rates of metals have been observed when organic acids are added at the cathode to suppress the base front (Maturi et al., 2008; Ammami et al., 2013). Heterogeneity has been shown in Chapter 3 to influence the migration of acid and base fronts. In these preliminary experiments, the pH front met closer to the anode compared to homogeneous settings implying that migration of the acid front was mitigated by the

effects of the heterogeneous settings. When applied to removing mixed contaminants in heterogeneous settings there could be implications for the rate of acid front migration.

8.3.5 Electrokinetic field-design

8.3.5.1 How will heterogeneity influence the choice of electrode configuration?

Results from Chapters 4 and 5 show that physical heterogeneity influences the electric field, and therefore will directly affect the choice of electrode configuration. There are numerous types of electrode configuration (see Figure 2.2), the three considered here are unidirectional (Figure 8.1), radial and radial-pair arrangements. Unidirectional configurations are representative of a large number of EK experiments within the literature as well as bidirectional configurations to some extent. Under a unidirectional configuration with a simple K contrast at the field-scale, similar phenomena to those observed in Chapter 4 will occur, e.g. controls on the voltage gradient. However, if the variety and orientation of low-K zones vary (such as shown in Figure 8.1) there will be corresponding perturbations to the applied electric field. A nonlinear electric field results in nonlinear ion flow paths, decreasing migration rates between electrodes (Segall and Bruell, 1992). However this could be beneficial based on experiments in Chapter 5 that showed a negatively charged amendment directed toward the low-K zone based on a non-uniform electric field.

A radial configuration consists of a central electrode surrounded by electrodes of the opposite polarity and can be used to enhance the distribution of an amendment (Wu et al., 2013). In these configurations the voltage gradient tends to be highest adjacent to the central electrode (Alshawabkeh et al., 1999). This could be enhanced in heterogeneous settings by placing this central electrode within a low-K zone and the surrounding electrodes within the high-K host material. A uniform distribution of amendments could be limited in heterogeneous settings due to the variation in migration rates.

A radial-pairs configuration involves arranging electrodes to encompass the perimeter of the contaminated zone. A voltage is then applied between an individual electrode pair across the sediment mass which is periodically swapped with other electrodes (Fan et al., 2007). The benefit of this configuration is to enhance mixing within the soil between microbes, contaminants and nutrients (Luo et al., 2006). Chapter 2 discusses the different mechanisms of substance mixing within different sediments such as sands and clays. The effectiveness of this electrode configuration could be reduced in heterogeneous settings. For example, electrophoretic migration of microbes will be reduced in low permeability sediments due to occlusion.

8.3.5.2 How can the sustainability of the field-scale be improved?

The sustainability assessment in Chapter 7 demonstrated different options for enhancing the sustainability of the EK-BIO treatment. The results showed that techniques, namely using background electron acceptors instead of an amendment, and/or solar panels did not improve the outcome of the sustainability assessment. However, this does not mean that these techniques would not be effective at other sites. Such sites would need to exhibit: (1) a high concentration of electron acceptors in the background groundwater; and (2) the absence of a containment system running for the duration of the treatment, such as the hydraulic containment system in Chapter 7.

The sustainability of an EK-BIO treatment could also be improved if the remediation goal is to couple electroosmotic removal of contaminants from the low-K zone with natural attenuation in the high-K zone. This is based on findings from Chapter 6. If an intensive bioremediation element can be removed then there are potentially time and cost savings. These result from a reduced complexity of the remediation design that excludes amendments and the need to maintain favourable conditions for biodegradation within the EK treatment area. This assumes that degradation will occur down-gradient of the contaminated zone where the pH changes at the electrodes will be reduced (Tiehm et al., 2010). However, there is a trade-off because enhancement techniques for electroosmotic

flow can be applied that will reduce the sustainability of this option. They include electrode conditioning with organic acids such as citric acid, or the addition of surfactants (Cameselle and Reddy, 2012).

8.3.5.3 How can pH control methods in heterogeneous settings be optimised?

Two pH control methods have been applied in these experiments: (1) recirculation of electrode fluid, Chapter 6; and (2) electrode conditioning where concentrated HCl and NaOH were added to the electrode chambers, Chapters 4 and 5. The effectiveness of the recirculation system has been demonstrated in Chapter 6, however there was un-intended dispersion of the amendment into the high-K zone. This would be beneficial at the field scale because it would reduce the migration time between the amendment and the low-K zone similar to the effect form a hydraulic gradient between electrodes (Wu et al., 2012b).

8.4 Future research needs

How is microbial activity distributed spatially within a physically heterogeneous setting?

Following on from the findings in Chapter 6, more research is required on the mechanisms by which EK can overcome mass transfer limitations in heterogeneous settings. Chapter 6 identified the importance of electroosmosis as a removal mechanism of contaminants from a low-K zone. Further understanding is required on the fate of the contaminant once it is in the high-K zone and efficacy of techniques to enhance electroosmotic flow. A conceptual model for a potential laboratory scale experiment is presented in Figure 8.3. Electroosmosis initiates the release of contaminants from the low-K zone that is then transported by advection into the high-K zone. Nitrate amendment is added at the inflow section and will be subject to electromigration once it passes through the electric field. The objective of these experiments is to enhance bioremediation and observe where microbial activity is occurring, either in the high- or low-K zone. This depends on electroosmotic flow

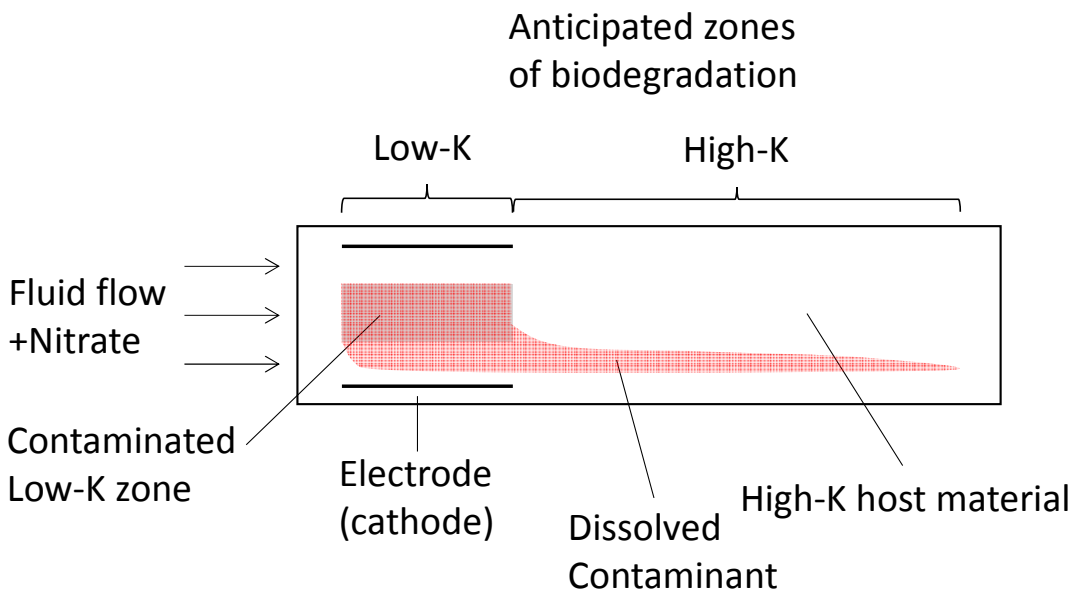

Figure 8.3 Conceptual diagram of a laboratory scale experiment to test electroosmotic removal of contaminants from a low-K zone with subsequent biodegradation within the high-K zone down-gradient.

which could be enhanced using different techniques such as increasing the voltage gradient or electrode configuration. The setup in Figure 8.3 suggests a unidirectional electric field which could skew the distribution of contaminants in the high-K zone; applying a bidirectional setup or polarity reversals may make to the contaminants more evenly distributed in the high-K zone. If contaminants were detected in the high-K zone, the setup could be modified to test a 2 stage application of EK. Firstly, contaminants are released from low-K zone by EOF and then additional electrodes arranged in a similar array down gradient could enhance mixing and biodegradation within the high-K zone.

These experiments will need to: (1) maintain electroosmotic flow in the presence of a high concentration amendments; (2) maintain suitable biodegradation conditions down-gradient of the contaminated low-K zone, specifically pH changes however this could be reduced with polarity reversals; and (3) build and design a laboratory setup that can sample pore fluid to a high enough resolution to determine where biodegradation is occurring. The outcome of this research would be to demonstrate the effectiveness of EK

as a coupled technology to remove contaminants from a low-K zone for either enhanced biodegradation or removal.

What are the controls on EK-BIO treatment within a layered heterogeneous setting?

The objective of this question is to observe the influence of a transverse mass flux of amendment (identified in Chapter 5) into a contaminated low-K zone to enhance biodegradation. It is anticipated that an experimental setup similar to that in Chapter 5 will be applied. It will also be relevant for observing whether the voltage difference that drives the transverse electromigration mass flux will also initiate a transverse electroosmotic pore fluid flux. This could be identified by the presence of contaminants within the high-K zone. There are a number of barriers the experimental setup will need to address. Firstly, the electroosmotic flow of the contaminant within the low-K layer toward the cathode, this could lead to rapid depletion of contaminant mass in the low-K zone. To overcome this a material similar to that used Chapter 5 could be used where the electroosmotic permeability of the material was very low. Secondly, a high resolution of pore fluid sampling at the high-K / low-K interface would be required. It would also allow the identification of the presence of microbiological activity within the experiment. Overall, this question will develop the importance of the transverse flux identified in this thesis to EK-BIO processes.

Is EK-BIO a viable remediation technology at the field-scale when applied with various enhancements to improve the sustainability of the setup?

This future work combines the sustainability aspects of EK-BIO application (Chapter 7) with further development of the technology at the field-scale. The chosen site should fulfil certain criteria such as: represent a mass transfer limitation on biodegradation where EK can be applied (e.g. electron acceptor mass flux limited by transverse dispersion or physical heterogeneity) and be well characterised. The stages of this research are:

1. An initial sustainability assessment that details how EK-BIO would be applied to the site and identifies it as a favourable option to continue to the pilot or field scale.

In addition, methods to enhance the sustainability of the technology could be included. In Chapter 7 this was using background electron acceptors and solar panels, which may be valid at this field site. Additional techniques could include using the natural buffering capacity of the sediment to reduce pH changes (e.g. calcareous soils or sediments) and therefore the intensity of the pH control system.

2. Laboratory-scale testing of the method of EK-BIO application. For example, if the site exhibited physical heterogeneity, then experiments similar to those in Chapter 6 could be replicated with materials from site. Once the application of EK-BIO has been verified, the sustainability enhancements could also be tested. Replicating the use of solar panels at the laboratory-scale has been done for metal removal studies (Yuan et al., 2009; Jeon et al., 2015), but never for EK-BIO applications. A potential method for repeatable application of solar panels at the laboratory scale experiment could include a power supply linked to a timer that applied current in a diurnal cycle.
3. Field-scale application of the EK-BIO technology according to the technique described in the sustainability assessment and using the methods verified at the laboratory-scale. This will require intensive monitoring to ensure that issues such as heat or pH generation do not compromise the treatment. Frequent sampling events from monitoring and electrode wells will also be required.

The main outcome of this research will be to further the application of EK-BIO at the field scale and develop a niche for the technology as a sustainable option compared to conventional techniques. In addition to publications at the different stages of research, a technical guidance document could be compiled to assist practitioners applying the technology. The main challenge to implementing this future research is the cost associated with desk, laboratory and field scale tests, but also the high level of collaboration that would be required between academic institutions, consultancies and industry.

8.5 Summary of key conclusions

- Physical heterogeneity corresponded to spatial changes in the effective ionic mobility with subsequent controls on amendment migration and the voltage gradient.
- In settings where heterogeneity is represented by a contrast in material type with different K values, the following was observed:
    - At the interface between the high-K and low-K zones there was an increase in the amendment concentration as the contrast in K increased
    - A higher voltage gradient was observed across zones with a low effective ionic mobility, this increased as the ratio of effective ionic mobility increased between the high- and low-K zones
    - Mass transport through the same low-K material in homogeneous settings is lower than heterogeneous setting (effect of high-K accounted for) due to the higher voltage gradient observed across the low-K zone.
    - An elevated voltage gradient across the low-K zone could be manipulated at field scale to reduce the voltage gradient drop associated with adding a high concentration amendment within the low-K zone.
- In settings where heterogeneity is represented by two layers of material with different K values, the following was observed:
    - A difference in the voltage readings between layers was observed in heterogeneous but not homogenous settings. This implies that the heterogeneous setting is driving non-uniformities in the electric field.
    - The voltage difference between layers can be attributed to differences in the pore fluid properties of the layers. It was shown to be more pronounced in experiments where more nitrate was added at the cathode.
    - The voltage difference was shown to be equivalent to a transverse mass flux between layers. This was demonstrated by calculating the mass flux at

the electrode / sediment and high-K / low-K boundary to provide a predicted concentration of nitrate that was then compared against observed values.

  - The implication of a transverse flux in a field scale scenario was demonstrated using an electron balance model, it is shown to be an important mass transfer process at this scale.

- In experiments that include both a sequestered contaminant (toluene) within the low-K zone and toluene degrading bacteria distributed through the whole sediment chamber, the following was observed:
  - Toluene mass decreased in all EK systems compared to advection due to electroosmosis. Biodegradation of toluene is assumed to be minimal in these experiments based on findings from a mass balance analysis
  - A parallel microcosm study demonstrated biodegradation of toluene following the addition of nitrate, thus toluene biodegradation potential was demonstrated and degradation rates under optimal conditions could be obtained.
  - The microcosm study also highlights that a possible reason for biodegradation not occurring is due to a lack of phosphate in the pore fluid.
  - A comparison of removal rates showed electroosmosis as the most effective removal mechanism. This prompted a sensitivity analysis to determine the conditions under which biodegradation would be viable in these experimental settings; the experimental variables analysed include electroosmotic permeability, voltage gradient and fraction of organic carbon.
- A Tier 1 and Tier 2 sustainability assessment (based on the SuRF-UK framework) compared EK-BIO and other remediation technologies for application to a BTEX and MTBE contaminated site, it observed:
  - That the sustainability assessment identified EK-BIO and air sparge / soil vapour extraction as the most sustainable options.

- The requirement for a hydraulic containment system on site to protect a sensitive down gradient receptor was the main driver for the monitored natural attenuation option being unsustainable.
- Enhancements to EK-BIO technique designed to improve the sustainability assessment score has little effect. These techniques included only using electron acceptors in the background groundwater avoiding the need for an amendment and using solar panels as an energy source.
- An appraisal of the SuRF-UK framework showed that both Tier 1 and Tier 2 arrived at same conclusion; this finding could save time and money in future assessments.

Chapter 9 References

Abraham, W.-R., Nogales, B., Golyshin, P.N., Pieper, D.H. and Timmis, K.N. (2002), Polychlorinated Biphenyl-Degrading Microbial Communities in Soils and Sediments. *Current Opinion in Microbiology*, 5(3): 246–253.

Acar, Y.B., Alshawabkeh, A. N. and Gale, R.J. (1993), Fundamentals of Extracting Species from Soils by Electrokinetics. *Waste Management*, 13(2): 141–151.

Acar, Y.B., Gale, R.J., Alshawabkeh, A.N., Marks, R.E., Puppala, S., Bricka, M. and Parker, R. (1995), Electrokinetic Remediation: Basics and Technology Status. *Journal of Hazardous Materials*, 40(2): 117–137.

Acar, Y.B., Rabbi, M.F. and Ozsu, E.E. (1997), Electrokinetic Injection of Ammonium and Sulfate Ions into Sand and Kaolinite Beds. *Journal of Geotechnical and Geoenvironmental Engineering*, 123(3): 239–249.

Acar, Y.B. and Alshawabkeh, A.N. (1993), Principles of Electrokinetic Remediation. *Environmental Science and Technology*, 27(13): 2638–2647.

Acuňa, A.J., Tonin, N., Pucci, G.N., Wick, L. and Pucci, O.H. (2010), Electrobioremediation of an Unsaturated Soil Contaminated with Hydrocarbon after Landfarming Treatment. *Portugaliae Electrochimica Acta*, 28(4): 253–263.

Aksu, Z. and Bülbül, G. (1998), Investigation of the Combined Effects of External Mass Transfer and Biodegradation Rates on Phenol Removal Using Immobilized P. Putida in a Packed-Bed Column Reactor. *Enzyme and Microbial Technology*, 22(5): 397–403.

Alcántara, M.T., Gómez, J., Pazos, M. and Sanromán, M.A. (2012), Electrokinetic Remediation of Lead and Phenanthrene Polluted Soils. *Geoderma*, 173-174: 128–133.

Alshawabkeh, A.N., Bricka, M.R. and Gent, D.B. (2005), Pilot-Scale Electrokinetic Cleanup of Lead-Contaminated Soils. *Journal of Geotechnical and Geoenvironmental Engineering*, 131(3): 283–291.

Alshawabkeh, A.N. and Acar, Y.B. (1996), Electrokinetic Remediation. II: Theoretical Model. *Journal of Geotechnical Engineering*, 122(3): 186–196.

Alshawabkeh, A.N., Yeung, A.T. and Bricka, M.R. (1999), Practical Aspects of In-Situ Electrokinetic Extraction. *Journal of Environmental Engineering*, 125(1): 27–35.

Ammami, M.T., Benamar, A., Wang, H., Bailleul, C., Legras, M., Le Derf, F. and Portet-Koltalo, F. (2013), Simultaneous Electrokinetic Removal of Polycyclic Aromatic Hydrocarbons and Metals from a Sediment Using Mixed Enhancing Agents. *International Journal of Environmental Science and Technology*, 11(7): 1801–1816.

Anders, H. J., Kaetzke, A., Kämpfer, P., Ludwig, W. and Fuchs, G. (1995), Taxonomic Position of Aromatic-Degrading Denitrifying Pseudomonad Strains K 172 and KB 740 and Their Description as New Members of the Genera *Thauera*, as *Thauera aromatica* Sp. Nov., and *Azoarcus*, as *Azoarcus evansii* Sp. Nov. *International Journal of Systematic Bacteriology*, 45(2): 327–333.

Andrews, J.E., Brimblecombe, P., Jickells, T.D., Liss, P.S. and Reid, B.J. (2005), An Introduction to Environmental Science, 68–140, in: Oxford: Blackwell Publishing.

Bardos, P. (2014), Progress in Sustainable Remediation. *Remediation Journal*, 25(1): 23–32. .

Bardos, P., Bone, B., Boyle, R., Ellis, D., Evans, F., Harries, N.D. and Smith, J.W.N. (2011), Applying Sustainable Development Principles to Contaminated Land Management Using the SuRF-UK Framework. *Remediation Journal*, 21(2): 77–100.

Bartlett, T.W., Smith, J.W.N. and Hardisty, P.E. (2014), Quantifying the Loss of Available Groundwater Resource Associated with Point-Source Contamination in Unused Aquifers. *Hydrogeology Journal*, 22(4): 749–759.

Bass, D.H., Hastings, N.A. and Brown, R.A. (2000), Performance of Air Sparging Systems: A Review of Case Studies. *Journal of Hazardous Materials*, 72(2-3): 101–119.

Bauer, R.D., Maloszewski, P., Zhang, Y., Meckenstock, R.U. and Griebler, C. (2008), Mixing-Controlled Biodegradation in a Toluene Plume--Results from Two-Dimensional Laboratory Experiments. *Journal of Contaminant Hydrology*, 96(1-4): 150–68.

Bauer, R.D., Rolle, M., Bauer, S., Eberhardt, C., Grathwohl, P., Kolditz, O., Meckenstock, R.U. and Griebler, C. (2009), Enhanced Biodegradation by Hydraulic Heterogeneities in Petroleum Hydrocarbon Plumes. *Journal of Contaminant Hydrology*, 105(1-2): 56–68.

Bi, R., Schlaak, M., Siefert, E., Lord, R. and Connolly, H. (2010), Alternating Current Electrical Field Effects on Lettuce (Lactuca Sativa) Growing in Hydroponic Culture with and without Cadmium Contamination. *Journal of Applied Electrochemistry*, 40(6): 1217–1223.

Bi, R., Schlaak, M., Siefert, E., Lord, R. and Connolly, H. (2011), Influence of Electrical Fields (AC and DC) on Phytoremediation of Metal Polluted Soils with Rapeseed (Brassica Napus) and Tobacco (Nicotiana Tabacum). *Chemosphere*, 83(3): 318–26.

Biegert, T., Fuchs, G. and Heider, J. (1996), Evidence That Anaerobic Oxidation of Toluene in the Denitrifying Bacterium Thauera Aromatica Is Initiated by Formation of Benzylsuccinate from Toluene and Fumarate. *European Journal of Biochemistry*, 238(3): 661–8.

Blanc, A., Métivier-Pignon, H., Gourdon, R. and Rousseaux, P. (2004), Life Cycle Assessment as a Tool for Controlling the Development of Technical Activities: Application to the Remediation of a Site Contaminated by Sulfur. *Advances in Environmental Research*, 8(3-4): 613–627.

Boopathy, R. (2000), Factors Limiting Bioremediation Technologies. *Bioresource Technology*, 74(1): 63–67.

Bowers, R.L. and Smith, J.W.N. (2014), Constituents of Potential Concern for Human Health Risk Assessment of Petroleum Fuel Releases. *Quarterly Journal of Engineering Geology and Hydrogeology*, 47(4): 363–372.

Bradley, P.M., Chapelle, F.H. and Landmeyer, J.E. (2001), Effect of Redox Conditions on MTBE Biodegradation in Surface Water Sediments. *Environmental Science and Technology*, 35(23): 4643–4647.

Bradley, P.M., Landmeyer, J.E. and Chapelle, F.H. (1999), Aerobic Mineralization of

MTBE and Tert-Butyl Alcohol by Stream-Bed Sediment Microorganisms. *Environmental Science and Technology*, 33(11): 1877–1879.

Bruell, C.J., Segall, B.A. and Walsh, M.T. (1992), Electroosomotic Removal of Gasoline Hydrocarbons and TCE from Clay. *Journal of Environmental Engineering*, 118(1): 68–83.

Cadotte, M., Deschênes, L. and Samson, R. (2007), Selection of a Remediation Scenario for a Diesel-Contaminated Site Using LCA. *The International Journal of Life Cycle Assessment*, 12(4): 239–251.

Cameselle, C. (2015), Enhancement Of Electro-Osmotic Flow During The Electrokinetic Treatment Of A Contaminated Soil. *Electrochimica Acta*, 181: 4–11.

Cameselle, C., Chirakkara, R.A. and Reddy, K.R. (2013), Electrokinetic-Enhanced Phytoremediation of Soils: Status and Opportunities. *Chemosphere*, 93(4): 626–36.

Cameselle, C. and Reddy, K.R. (2012), Development and Enhancement of Electro-Osmotic Flow for the Removal of Contaminants from Soils. *Electrochimica Acta*, 86: 10–22.

Cang, L., Wang, Q.–Y., Zhou, D.–M. and Xu, H. (2011), Effects of Electrokinetic-Assisted Phytoremediation of a Multiple-Metal Contaminated Soil on Soil Metal Bioavailability and Uptake by Indian Mustard. *Separation and Purification Technology*, 79(2): 246–253.

Cang, L., Zhou, D.-M., Alshawabkeh, A.N. and Chen, H.-F. (2007), Effects of Sodium Hypochlorite and High pH Buffer Solution in Electrokinetic Soil Treatment on Soil Chromium Removal and the Functional Diversity of Soil Microbial Community. *Journal of Hazardous Materials*, 142(1-2): 111–7.

Cang, L., Zhou, D.-M., Wang, Q.-Y. and Fan, G.-P. (2012), Impact of Electrokinetic-Assisted Phytoremediation of Heavy Metal Contaminated Soil on Its Physicochemical Properties, Enzymatic and Microbial Activities. *Electrochimica Acta*, 86: 41–48.

Carey, M.A., Finnamore, J.R., Morrey, M.J. and Marsland, P.A. (2000), *Guidance on the Assessment and Monitoring of Natural Attentuation of Contaminants in Groundwater*. Bristol.

Chapman, S.W., Parker, B.L., Sale, T.C. and Doner, L.A. (2012), Testing High Resolution Numerical Models for Analysis of Contaminant Storage and Release from Low Permeability Zones. *Journal of Contaminant Hydrology*, 136-137: 106–116.

Chirakkara, R.A.., Reddy, K.R. and Cameselle, C. (2015), Electrokinetic Amendment in Phytoremediation of Mixed Contaminated Soil. *Electrochimica Acta*: 1–13.

Chung, H.I. and Lee, M.H. (2007), A New Method for Remedial Treatment of Contaminated Clayey Soils by Electrokinetics Coupled with Permeable Reactive Barriers. *Electrochimica Acta*, 52(10): 3427–3431.

CIRIA (2002), *Biological Methods Fo Assessment and Remediation of Contaminated Land: Case Studies* (D. Barr, J. R. Finnamore, R. P. Bardos, J. M. Weeks, and C. P. Nathanail, Eds.). London: CIRIA.

CL:AIRE (2014), *An Illustrated Handbook of LNAPL Transport and Fate in the Subsurface* (M. O. Rivett, Ed.). London: CL:AIRE.

Colacicco, A., De Gioannis, G., Muntoni, A., Pettinao, E., Polettini, A. and Pomi, R. (2010),

Enhanced Electrokinetic Treatment of Marine Sediments Contaminated by Heavy Metals and PAHs. *Chemosphere*, 81(1): 46–56.

Coulon, F., Brassington, K.J., Bazin, R., Linnet, P.E., Thomas, K.A., Mitchell, T. R., Lethbridge, G., Smith, J.W.N. and Pollard, S.J.T. (2012), Effect of Fertilizer Formulation and Bioaugmentation on Biodegradation and Leaching of Crude Oils and Refined Products in Soils. *Environmental Technology*, 33(16): 1879–1893.

CRC (2002), *Handbook of Chemistry and Physics* (D. R. Lide, Ed.). Boca Raton: CRC Press.

DeFlaun, M.F. and Condee, C.W. (1997), Electrokinetic Transport of Bacteria. *Journal of Hazardous Materials*, 55(1-3): 263–277.

DEFRA (2008), *Guidance on the Legal Definition of Guidance on the Legal Definition of Contaminated Land*. Department for Environment, Food and Rural Affairs.

Delle Site, A. (2001), Factors Affecting Sorption of Organic Compounds in Natural Sorbent/water Systems and Sorption Coefficients for Selected Pollutants. A Review. *Journal of Physical and Chemical Reference Data*, 30(1): 187–439.

Delgado, A. V., González-Caballero, F., Hunter, R.J., Koopal, L.K., Lyklema, J., 2007. Measurement and interpretation of electrokinetic phenomena. *Journal of Colloid Interface Science*. 309, 194–224.

Department of Environment (1995a), Industry Profile: Gas Works, Cokes Works and Other Coal Carbonisation Plants.

Department of Environment (1995b), *Industry Profile: Oil Refineries and Bulk Storage of Crude Oil and Petroleum Products*.

Dzenitis, J.M. (1997), Steady State and Limiting Current in Electroremediation of Soil. *Journal of The Electrochemical Society*, 144(4): 1317.

Eid, N., Larson, D., Slack, D. and Kiousis, P. (1999), Nitrate Electromigration in Sandy Soil in the Presence of Hydraulic Flow. *Journal of Irrigation and Drainage Engineering*, 125(1): 7–11.

Elektorowicz, M. and Boeva, V. (1996), Electrokinetic Supply of Nutrients in Soil Bioremediation. *Environmental Technology*, 17(12): 1339–1349.

Environment Agency (2005), *Indicators for Land Contamination*. Bristol.

Environment Agency (2009), *Dealing with Contaminated Land in England and Wales*. Bristol: Environment Agency.

Eykholt, G.R. (1997), Development of Pore Pressures by Nonuniform Electroosmosis in Clays. *Journal of Hazardous Materials*, 55(1-3): 171–186.

Fan, X., Wang, H., Luo, Q., Ma, J. and Zhang, X. (2007), The Use of 2D Non-Uniform Electric Field to Enhance in Situ Bioremediation of 2,4-Dichlorophenol-Contaminated Soil. *Journal of Hazardous Materials*, 148(1-2): 29–37.

Faulkner, D.W.S., Hopkinson, L. and Cundy, A.B. (2005), Electrokinetic Generation of Reactive Iron-Rich Barriers in Wet Sediments: Implications for Contaminated Land Management. *Mineralogical Magazine*, 69(5): 749–757.

Fetter, C. (1993), *Contaminant Hydrogeology*. New York: Macmillan Publishing Company.

Fetter, C., 2001. Applied Hydrogeology: Fourth Edition. Prentice Hall, New Jersey.

Fonseca, B., Pazos, M., Tavares, T. and Sanromán, M.A. (2012), Removal of Hexavalent Chromium of Contaminated Soil by Coupling Electrokinetic Remediation and Permeable Reactive Biobarriers. *Environmental Science and Pollution Research International*, 19(5): 1800–8.

Freeze, R.A. and Cherry, J.A. (1979), *Groundwater*. Uppersaddle River: Pearson Education.

Gill, R.T., Rolfe, S.A., Harbottle, M.J., Smith, J.W.N. and Thornton, S.F. (2013), Stimulating in Situ Bioremediation in Electron Acceptro-Limited Zones by Nitrate Delivery Using Electrokineticsin a Model Scale Aquifer, , in: *AquaConSoil Barcelona 2013: Theme D1.15 New methods for enhanced bioremediation of organic compounds*.

Gill, R.T., Harbottle M.J., Smith J.W.N. and Thornton S.F. (2014), Electrokinetic-enhanced Bioremediation of Organic Contaminants: A Review of Processes and Environmental Applications. *Chemosphere, 107: 31-42.*

Gill, R.T., Thornton, S.F., Harbottle, M.J. and Smith, J.W.N., (2015), Electrokinetic Migration of Nitrate through Heterogeneous Granular Porous Media. *Ground Water Monitoring and Remediation*, 35 (3): 46–56.

Gill, R.T., Thornton S.F., Harbottle M.J. and Smith J.W.N., (2016a), The Effects of Physical Heterogeneity on the Electromigration of Nitrate in Layered Granular Porous Media. *Electrochimica Acta* (under review)

Gill, R.T., Thornton S.F., Harbottle M.J. and J.W.N. Smith. (2016b). Sustainability Assessment of Electrokinetic Bioremediation Compared with Alternative Remediation Options for a Petroleum Release Site. *Journal of Environmental Management* (under review)

Godschalk, M.S. and Lageman, R. (2005), Electrokinetic Biofence, Remediation of VOCs with Solar Energy and Bacteria. *Engineering Geology*, 77(3-4): 225–231.

Goi, A., Kulik, N. and Trapido, M. (2006), Combined Chemical and Biological Treatment of Oil Contaminated Soil. *Chemosphere*, 63(10): 1754–63.

Goldscheider, N., Hunkeler, D. and Rossi, P. (2006), Review: Microbial Biocenoses in Pristine Aquifers and an Assessment of Investigative Methods. *Hydrogeology Journal*, 14(6): 926–941.

Gómez, J., Alcántara, M.T., Pazos, M. and Sanromán, M.A. (2009), A Two-Stage Process Using Electrokinetic Remediation and Electrochemical Degradation for Treating Benzo[a]pyrene Spiked Kaolin. *Chemosphere*, 74(11): 1516–1521.

Gonzini, O., Plaza, A., Di Palma, L. and Lobo, M.C. (2010), Electrokinetic Remediation of Gasoil Contaminated Soil Enhanced by Rhamnolipid. *Journal of Applied Electrochemistry*, 40(6): 1239–1248.

Hansen, B.H., Nedergaard, L.W., Ottosen, L.M., Riis, C. and Broholm, M.M. (2015), Experimental Design for Assessment of Electrokinetically Enhanced Delivery of Lactate and Bacteria in 1,2-Cis-Dichloroethylene Contaminated Limestone. *Environmental Technology and Innovation*, 4: 73–81.

Harbottle, M.J., Al-Tabbaa, A. and Evans, C.W. (2008), Sustainability of Land

Remediation. Part 1: Overall Analysis. *Proceedings of the ICE - Geotechnical Engineering*, 161(2): 75–92.

Harbottle, M.J., Lear, G., Sills, G.C. and Thompson, I.P. (2009), Enhanced Biodegradation of Pentachlorophenol in Unsaturated Soil Using Reversed Field Electrokinetics. *Journal of Environmental Management*, 90(5): 1893–900.

Hiscock, K. (2005), Hydrogeology: Principles and Practice, 74–121, in: Oxford: Blackwell Publishing.

Hodges, Daniel (2010), Permanganate Electromigration in Low Permeability Media. Unpublished MSc Thesis, Universtiy of Western Australia.

Hodges, D., Fourie, A., Thomas, D. and Reynolds, D. (2013), Overcoming Permanganate Stalling during Electromigration. *Journal of Environmental Engineering*, 139(5): 677–684.

Hønning, J., Broholm, M.M. and Bjerg, P.L. (2007), Role of Diffusion in Chemical Oxidation of PCE in a Dual Permeability System. *Environmental Science and Technology*, 41(24): 8426–8432.

Huang, D., Guo, S., Li, T. and Wu, B. (2013), Coupling Interactions between Electrokinetics and Bioremediation for Pyrene Removal from Soil under Polarity Reversal Conditions. *CLEAN - Soil, Air, Water*, 41(4): 383–389.

Huang, W.E., Oswald, S.E., Lerner, D.N., Smith, C.C. and Zheng, C. (2003), Dissolved Oxygen Imaging in a Porous Medium to Investigate Biodegradation in a Plume with Limited Electron Acceptor Supply. *Environmental Science and Technology*, 37(9): 1905–1911.

Jenneman, G.E., McInerney, M.J., Crocker, M.E. and Knapp, R.M. (1986), Effect of Sterilization by Dry Heat or Autoclaving on Bacterial Penetration through Berea Sandstone Effect of Sterilization by Dry Heat or Autoclaving Penetration through Berea Sandstone. *Applied and Environmenal Microbiology*, 51(1): 39–43.

Jeon, E.-K., Ryu, S.-R. and Baek, K. (2015), Application of Solar-Cells in the Electrokinetic Remediation of As-Contaminated Soil. *Electrochimica Acta*.

Jones, C.J.F.P., Lamont-Black, J. and Glendinning, S. (2011), Electrokinetic Geosynthetics in Hydraulic Applications. *Geotextiles and Geomembranes*, 29(4): 381–390.

Jones, E.H., Reynolds, D.A., Wood, A.L. and Thomas, D.G. (2011), Use of Electrophoresis for Transporting Nano-Iron in Porous Media. *Ground Water*, 49(2): 172–183.

Karagunduz, A., Gezer, A. and Karasuloglu, G. (2007), Surfactant Enhanced Electrokinetic Remediation of DDT from Soils. *The Science of the Total Environment*, 385(1-3): 1–11.

Khan, F.I., Husain, T. and Hejazi, R. (2004), An Overview and Analysis of Site Remediation Technologies. *Journal of Environmental Management*, 71(2): 95–122.

Killham, K. (1994), *Soil Ecology*. Cambridge: Cambridge University Press.

Kim, D. H., Yoo, J.C., Hwang, B.R., Yang, J.S. and Baek, K. (2014), Environmental Assessment on Electrokinetic Remediation of Multimetal-Contaminated Site: A Case Study. *Environmental Science and Pollution Research*, 21(10): 6751–6758.

Kim, S.S. and Han, S.J. (2003), Application of an Enhanced Electrokinetic Ion Injection System to Bioremediation. *Water, Air, and Soil Pollution*, 146: 365–377.

Kim, S.-H., Han, H.-Y., Lee, Y.-J., Kim, C.W. and Yang, J.-W. (2010), Effect of Electrokinetic Remediation on Indigenous Microbial Activity and Community within Diesel Contaminated Soil. *The Science of the Total Environment*, 408(16): 3162–8.

Kim, S.-S., Kim, J.-H. and Han, S.-J. (2005), Application of the Electrokinetic-Fenton Process for the Remediation of Kaolinite Contaminated with Phenanthrene. *Journal of Hazardous Materials*, 118(1-3): 121–31.

Kim, W.-S., Park, G.-Y., Kim, D.-H., Jung, H.-B., Ko, S.-H. and Baek, K. (2012), In Situ Field Scale Electrokinetic Remediation of Multi-Metals Contaminated Paddy Soil: Influence of Electrode Configuration. *Electrochimica Acta*, 86: 89–95.

Kleinsteuber, S., Schleinitz, K.M. and Vogt, C. (2012), Key Players and Team Play: Anaerobic Microbial Communities in Hydrocarbon-Contaminated Aquifers. *Applied Microbiology and Biotechnology*, 94(4): 851–73.

Ko, S.-O., Schlautman, M.A. and Carraway, E.R. (2000), Cyclodextrin-Enhanced Electrokinetic Removal of Phenanthrene from a Model Clay Soil. *Environmental Science and Technology*, 34(8): 1535–1541.

Lavanchy, P.M. (2008), Microbial Community Metabolic Concurrence Involved in Toluene Degradation: Effect of Oxygen Availability on Catabolic Gene Expression of Aerobic and Anaerobic Toluene Degrading Bacteria. PhD Thesis, Helholtz Centre for Environmental Research - UFZ

Lear, G., Harbottle, M.J., Sills, G., Knowles, C.J., Semple, K.T. and Thompson, I.P. (2007), Impact of Electrokinetic Remediation on Microbial Communities within PCP Contaminated Soil. *Environmental Pollution*, 146(1): 139–46.

Lear, G., Harbottle, M.J., van der Gast, C.J., Jackman, S.A., Knowles, C.J., Sills, G. and Thompson, I.P. (2004), The Effect of Electrokinetics on Soil Microbial Communities. *Soil Biology and Biochemistry*, 36(11): 1751–1760.

Lee, G.T., Ro, H.M. and Lee, S.M. (2007), Effects of Triethyl Phosphate and Nitrate on Electrokinetically Enhanced Biodegradation of Diesel in Low Permeability Soils. *Environmental Technology*, 28(8): 853–60.

Lee, H.-S. and Lee, K. (2001), Bioremediation of Diesel-Contaminated Soil by Bacterial Cells Transported by Electrokinetics. *Journal of Microbial Biotechnology*, 11(6): 1038–1045.

Lee, K.-Y. and Kim, K.-W. (2010), Heavy Metal Removal from Shooting Range Soil by Hybrid Electrokinetics with Bacteria and Enhancing Agents. *Environmental Science and Technology*, 44(24): 9482–7.

Leuthner, B. and Heider, J. (1998), A Two-Component System Involved in Regulation of Anaerobic Toluene Metabolism in Thauera Aromatica. *FEMS Microbiology Letters*, 166(1): 35–41.

Li, D., Niu, Y.-Y., Fan, M, Xu, D.-L. and Xu, P. (2013), Focusing Phenomenon Caused by Soil Conductance Heterogeneity in the Electrokinetic Remediation of Chromium (VI)-Contaminated Soil. *Separation and Purification Technology*, 120: 52–58.

Li, F., Guo, S. and Hartog, N. (2012), Electrokinetics-Enhanced Biodegradation of Heavy Polycyclic Aromatic Hydrocarbons in Soil around Iron and Steel Industries.

Electrochimica Acta, 85: 228–234.

Li, L. and Barry, D.A. (1994), Mass Transfer in Soils with Local Stratification of Hydraulic Conductivity Diffusion. *Water Resources Research*, 30(11): 2891–2900.

Li, T., Guo, S., Wu, B., Li, F. and Niu, Z. (2010), Effect of Electric Intensity on the Microbial Degradation of Petroleum Pollutants in Soil. *Journal of Environmental Sciences*, 22(9): 1381–1386.

Li, X.Y., Ding, F., Lo, P.S.Y. and Sin, S.H.P. (2002), Electrochemical Disinfection of Saline Wastewater Effluent. *Journal of Environmental Engineering*, 128(8): 697–704.

Li, Z., Yuan, S., Wan, J., Long, H. and Tong, M. (2011), A Combination of Electrokinetics and Pd/Fe PRB for the Remediation of Pentachlorophenol-Contaminated Soil. *Journal of Contaminant Hydrology*, 124(1-4): 99–107.

Lohner, S.T., Becker, D., Mangold, K.-M. and Tiehm, A. (2011), Sequential Reductive and Oxidative Biodegradation of Chloroethenes Stimulated in a Coupled Bioelectro-Process. *Environmental Science and Technology*, 45(15): 6491–7.

Lohner, S.T., Katzoreck, D. and Tiehm, A. (2008a), Electromigration of Microbial Electron Acceptors and Nutrients: (I) Transport in Synthetic Media. *Journal of Environmental Science and Health. Part A, Toxic/hazardous Substances and Environmental Engineering*, 43(8): 913–21.

Lohner, S.T., Katzoreck, D. and Tiehm, A. (2008b), Electromigration of Microbial Electron Acceptors and Nutrients: (II) Transport in Groundwater. *Journal of Environmental Science and Health. Part A, Toxic/hazardous Substances and Environmental Engineering*, 43(8): 922–5.

Lohner, S.T., Tiehm, A., Jackman, S. and Carter, P. (2009), Coupled Electrokinetic Bioremediation: Applied Aspects, 389–416, in: Reddy, K. and Cameselle, C. (Eds.), *Electrochemical Remediation Technologies for Polluted Soils, Sediments and Groundwater*. New Jersey: John Wiley & Sons.

Lohner, S.T. and Tiehm, A. (2009), Application of Electrolysis to Stimulate Microbial Reductive PCE Dechlorination and Oxidative VC Biodegradation. *Environmental Science and Technology*, 43(18): 7098–7104.

Luo, Q., Wang, H., Zhang, X., Fan, X. and Qian, Y. (2006), In Situ Bioelectrokinetic Remediation of Phenol-Contaminated Soil by Use of an Electrode Matrix and a Rotational Operation Mode. *Chemosphere*, 64(3): 415–22.

Luo, Q., Zhang, X., Wang, H. and Qian, Y. (2005a), Mobilization of Phenol and Dichlorophenol in Unsaturated Soils by Non-Uniform Electrokinetics. *Chemosphere*, 59(9): 1289–98.

Luo, Q., Zhang, X., Wang, H. and Qian, Y. (2005b), The Use of Non-Uniform Electrokinetics to Enhance in Situ Bioremediation of Phenol-Contaminated Soil. *Journal of Hazardous Materials*, 121(1-3): 187–94.

Luo, Q., Wang, H., Zhang, X. and Qian, Y. (2005c), Effect of Direct Electric Current on the Cell Surface Properties of Phenol-Degrading Bacteria. *Applied and Environmental Microbiology*, 71(1): 423–7.

Lyklema, J., 2003. Electrokinetics after Smoluchowski. *Colloids and Surfaces A: Physicochemical and Engineering Aspects*, 222, 5–14.

Ma, J.W., Wang, F.Y., Huang, Z.H. and Wang, H. (2010), Simultaneous Removal of 2,4-Dichlorophenol and Cd from Soils by Electrokinetic Remediation Combined with Activated Bamboo Charcoal. *Journal of Hazardous Materials*, 176(1-3): 715–20.

Mackay, D.M., Cherry, J.A., (1989) Groundwater contamination: Pump-and-treat remediation. Environmental Science and Technology, 23(6): 630–636.

Maillacheruvu, K.Y. and Chinchoud, P.R. (2011), Electrokinetic Transport of Aerobic Microorganisms under Low-Strength Electric Fields. *Journal of Environmental Science and Health. Part A, Toxic/hazardous Substances & Environmental Engineering*, 46(6): 589–95.

Maini, G., Sharman, A.K., Knowles, C.J., Sunderland, G. and Jackman, S.A. (2000), Electrokinetic Remediation of Metals and Organics from Historically Contaminated Soil. *Journal of Chemical Technology and Biotechnology*, 75(8): 657–664.

Mao, X., Wang, J., Ciblak, A., Cox, E.E., Riis, C., Terkelsen, M., Gent, D.B. and Alshawabkeh, A.N. (2012), Electrokinetic-Enhanced Bioaugmentation for Remediation of Chlorinated Solvents Contaminated Clay. *Journal of Hazardous Materials*, 213-214: 311–7.

Mattson, E.D., Bowman, R.S. and Lindgren, E.R. (2002), Electrokinetic Ion Transport through Unsaturated Soil: 2. Application to a Heterogeneous Field Site. *Journal of Contaminant Hydrology*, 54(1-2): 121–140.

Maturi, K., Khodadoust, A.P. and Reddy, K.R. (2008), Comparison of Extractants for Removal of Lead, Zinc, and Phenanthrene from Manufactured Gas Plant Field Soil. *Practice Periodical of Hazardous, Toxic, and Radioactive Waste Management*, 12(4): 230–238.

Maturi, K. and Reddy, K.R. (2006), Simultaneous Removal of Organic Compounds and Heavy Metals from Soils by Electrokinetic Remediation with a Modified Cyclodextrin. *Chemosphere*, 63(6): 1022–31.

McCray, J.E., Tick, G.R., Jawitz, J.W., Gierke, J.S., Brusseau, M.L., Falta, R.W., Knox, R.C., Sabatini, D.A., Annable, M.D., Harwell, J.H. and Wood, A.L. (2011), Remediation of NAPL Source Zones: Lessons Learned from Field Studies at Hill and Dover AFB. *Ground Water*, 49(5): 727–44.

McNab, W.W., and Dooher, B.P. (1998), Uncertainty Analyses of Fuel Hydrocarbon Biodegradation Signatures in Ground Water by Probabilistic Modeling. *Ground Water*, 36(4): 69–698.

Meckenstock, R.U., Elsner, M., Griebler, C., Lueders, T., Stumpp, C., Aamand, J., Agathos, S.N., Albrechtsen, H.-J., Bastiaens, L., Bjerg, P.L., Boon, N., Dejonghe, W., Huang, W.E., Schmidt, S.I., Smolders, E., Sørensen, S.R., Springael, D. and van Breukelen, B.M. (2015), Biodegradation: Updating the Concepts of Control for Microbial Cleanup in Contaminated Aquifers. *Environmental Science and Technology*, 49(12): 7073–7081.

Megharaj, M., Ramakrishnan, B., Venkateswarlu, K., Sethunathan, N. and Naidu, R. (2011), Bioremediation Approaches for Organic Pollutants: A Critical Perspective. *Environment International*, 37(8): 1362–75.

Mena, E., Rubio, P., Cañizares, P., Villaseñor, J. and Rodrigo, M.A. (2012), Electrokinetic Transport of Diesel-Degrading Microorganisms through Soils of Different Textures Using Electric Fields. *Journal of Environmental Science and Health. Part A,*

Toxic/hazardous Substances and Environmental Engineering, 47(2): 274–9.

Mitchell, J.K. (1993), *Fundamentals of Soil Behavior Second Edition*. New York: John Wiley & Sons.

Mohamedelhassan, E. and Shang, J.Q. (2001), Effects of Electrode Materials and Current Intermittence in Electro-Osmosis. *Ground Improvement*, 5(1): 3–11.

Moon, J.-W., Moon, H.-S., Kim, H. and Roh, Y. (2005), Remediation of TCE-Contaminated Groundwater Using Zero Valent Iron and Direct Current: Experimental Results and Electron Competition Model. *Environmental Geology*, 48(6): 805–817.

Mrozik, A. and Piotrowska-Seget, Z. (2010), Bioaugmentation as a Strategy for Cleaning up of Soils Contaminated with Aromatic Compounds. *Microbiological research*, 165(5): 363–75.

Mulligan, C.N. (2005), Environmental Applications for Biosurfactants. *Environmental Pollution (Barking, Essex : 1987)*, 133(2): 183–98.

Mulligan, C.N. (2009), Recent Advances in the Environmental Applications of Biosurfactants. *Current Opinion in Colloid & Interface Science*, 14(5): 372–378.

NICOLE (2010), *NICOLE Road Map and Guidance: Considering Sustainability in Remediation*.

Niqui-Arroyo, J.-L., Bueno-Montes, M., Posada-Baquero, R. and Ortega-Calvo, J.-J. (2006), Electrokinetic Enhancement of Phenanthrene Biodegradation in Creosote-Polluted Clay Soil. *Environmental Pollution*, 142(2): 326–32.

Niqui-Arroyo, J.-L. and Ortega-Calvo, J.-J. (2010), Effect of Electrokinetics on the Bioaccessibility of Polycyclic Aromatic Hydrocarbons in Polluted Soils. *Journal of Environment Quality*, 39(6): 1993.

Obiri-Nyarko, F., Grajales-Mesa, S.J., Malina, G., 2014. An overview of permeable reactive barriers for in situ sustainable groundwater remediation. *Chemosphere,* 111: 243–259.

Ouhadi, V.R., Yong, R.N., Shariatmadari, N., Saeidijam, S., Goodarzi, A.R. and Safari-Zanjani, M. (2010), Impact of Carbonate on the Efficiency of Heavy Metal Removal from Kaolinite Soil by the Electrokinetic Soil Remediation Method. *Journal of Hazardous Materials*, 173(1-3): 87–94.

Page, M.M. and Page, C.L. (2002), Electroremediation of Contaminated Soils. *Journal of Environmental Engineering*, 128(3): 208–219.

Paillat, T., Moreau, E. and Touchard, G. (2000), Electrokinetic Phenomena in Porous Media Applied to Soil Decontamination. *IEEE Transactions on Dielectrics and Electrical Insulation*, 7(5): 693–704.

Paillat, T., Moreau, E. and Touchard, G. (2001), Flow Electrification through Porous Media. *Journal of Loss Prevention in the Process Industries*, 14(2): 91–93.

Paliwal, V., Puranik, S. and Purohit, H.J. (2012), Integrated Perspective for Effective Bioremediation. *Applied Biochemistry and Biotechnology*, 166(4): 903–24.

Palmroth, M.R.T., Langwaldt, J.H., Aunola, T.A., Goi, A., Münster, U., Puhakka, J.A. and Tuhkanen, T.A. (2006), Effect of Modified Fenton's Reaction on Microbial Activity and

Removal of PAHs in Creosote Oil Contaminated Soil. *Biodegradation*, 17(2): 131–41.

Pamukcu, S. (2009). Electrochemical Transport and Transformations, 29-63, in: Reddy, K., Cameselle, C. (Eds.), *Electrochemical Remediation Technologies for Polluted Soils, Sediments and Groundwater*. New Jersey: John Wiley & Sons.

Pazos, M., Plaza, A., Martín, M. and Lobo, M.C. (2012), The Impact of Electrokinetic Treatment on a Loamy-Sand Soil Properties. *Chemical Engineering Journal*, 183: 231–237.

Postle, M., Fenn, T., Grosso, A. and Steeds, J. (1999), *Cost-Benefit Analysis for Remediation of Land Contamination*. Bristol: Environment Agency.

Pucci, G.N., Acuna, A.J., Wick, L.Y. and Pucci, O.H. (2012), Electrobioremediation of Patagonian Soils Contaminated with Hydrocarbons. *Portugaliae Electrochimica Acta*, 30(5): 361–370.

Pulkka, S., Martikainen, M., Bhatnagar, A. and Sillanpää, M. (2014), Electrochemical Methods for the Removal of Anionic Contaminants from Water - A Review. *Separation and Purification Technology*, 132: 252–271.

Rabbi, M.F., Clark, B., Gale, R.J., Ozsu-Acar, E., Pardue, J. and Jackson, A. (2000), In Situ TCE Bioremediation Study Using Electrokinetic Cometabolite Injection. *Waste Management*, 20(4): 279–286.

Rahman, Md.A., Jose, S.C., Nowak, W. and Cirpka, O.A. (2005), Experiments on Vertical Transverse Mixing in a Large-Scale Heterogeneous Model Aquifer. *Journal of Contaminant Hydrology*, 80(3-4): 130–48.

Ramírez, E.M., Camacho, J.V., Rodrigo, M.A., Cañizares, P., 2015. Combination of bioremediation and electrokinetics for the in-situ treatment of diesel polluted soil: A comparison of strategies. Science of the Total Environment, 533: 307–316.

Rebata-Landa, V. and Santamarina, J.C. (2006), Mechanical Limits to Microbial Activity in Deep Sediments. *Geochemistry, Geophysics, Geosystems*, 7(11): 1-12.

Reddy, K.R. and Chandhuri, K.S. (2009), Fenton-Like Oxidation of Polycyclic Aromatic Hydrocarbons in Soils Using Electrokinetics. *Journal of Geotechnical and Geoenvironmental Engineering*, 135(10): 1429–1439.

Reddy, K.R. and Saichek, R.E. (2003), Effect of Soil Type on Electrokinetic Removal of Phenanthrene Using Surfactants and Cosolvents. *Journal of Environmental Engineering*, 129(4): 336–346.

Reddy, K.R. and Chirakkara, R.A. (2013), Green and Sustainable Remedial Strategy for Contaminated Site: Case Study. *Geotechnical and Geological Engineering*, 31(6): 1653–1661.

Reynolds, D.A. and Kueper, B.H. (2002), Numerical Examination of the Factors Controlling DNAPL Migration through a Single Fracture. *Ground Water*, 40(4): 368–377.

Reynolds, D.A., Jones, E.H., Gillen, M., Yusoff, I. and Thomas, D.G. (2008), Electrokinetic Migration of Permanganate through Low-Permeability Media. *Ground Water*, 46(4): 629–37.

Da Rocha, U.N., Tótola, M.R., Pessoa, D.M.M, Júnior, J.T.A., Neves, J.C.L. and Borges, A.C. (2009), Mobilisation of Bacteria in a Fine-Grained Residual Soil by

Electrophoresis. *Journal of Hazardous Materials*, 161(1): 485–91.

Rowe, R. K. and Badv, K. (1996), Chloride Migration through Clayey Silt Underlain by Fine Sand or Silt. *Journal of Geotechnical Engineering*, 122(1): 60–68.

Saichek, R.E. and Reddy, K.R. (2005), Surfactant-Enhanced Electrokinetic Remediation of Polycyclic Aromatic Hydrocarbons in Heterogeneous Subsurface Environments. *Journal of Environmental Engineering and Science*, 4(5): 327–339.

Saichek, R.E. and Reddy, K.R. (2003), Effect of pH Control at the Anode for the Electrokinetic Removal of Phenanthrene from Kaolin Soil. *Chemosphere*, 51(4): 273–87.

Segall, B.A. and Bruell, C.J. (1992), Electroosmotic Contaminant-Removal Processes. *Journal of Environmental Engineering*, 118(1): 84–100.

Semple, K.T., Doick, K.J., Jones, K.C., Burauel, P., Craven, A. and Harms, H. (2004), Defining Ioavailability and Bioaccessibility of Contaminated Soil and Sediment Is Complicated. *Environmental Science and Technology*, 38(12): 228A–231A.

Shi, L., Harms, H. and Wick, L.Y. (2008), Electroosmotic Flow Stimulates the Release of Alginate-Bound Phenanthrene. *Environmental Science and Technology*, 42(6): 2105–2110.

Shi, L., Müller, S., Harms, H. and Wick, L.Y. (2008), Effect of Electrokinetic Transport on the Vulnerability of PAH-Degrading Bacteria in a Model Aquifer. *Environmental Geochemistry and Health*, 30(2): 177–82.

Shi, L., Müller, S., Loffhagen, N., Harms, H. and Wick, L.Y. (2008), Activity and Viability of Polycyclic Aromatic Hydrocarbon-Degrading Sphingomonas Sp. LB126 in a DC-Electrical Field Typical for Electrobioremediation Measures. *Microbial Biotechnology*, 1(1): 53–61.

Simoni, S.F., Schäfer, A., Harms, H. and Zehnder, A.J.B. (2001), Factors Affecting Mass Transfer Limited Biodegradation in Saturated Porous Media. *Journal of Contaminant Hydrology*, 50(1-2): 99–120.

Smith, J.W.N., Boshoff, G. and Bone, B.D. (2003), Good Practice Guidance on Permeable Reactive Barriers for Remediating Polluted Groundwater, and a Review of Their Use in the UK. *Land Contamination and Reclamation*, 11(4): 411–418.

Smith, J.W.N. and Kerrison, G. (2013), Benchmarking of Decision-Support Tools Used for Tiered Sustainable Remediation Appraisal. *Water, Air, and Soil Pollution*, 224(12): 1–11.

Song, X., Hong, E. and Seagren, E.A. (2014), Laboratory-Scale in Situ Bioremediation in Heterogeneous Porous Media: Biokinetics-Limited Scenario. *Journal of Contaminant Hydrology*, 158: 78–92.

Song, X. and Seagren, E.A. (2008), In Situ Bioremediation in Heterogeneous Porous Media: Dispersion-Limited Scenario. *Environmental Science and Technology*, 42(16): 6131–6140.

Spence, M.J., Bottrell, S.H., Higgo, J.J., Harrison, I. and Fallick, A.E. (2001), Denitrification and Phenol Degradation in a Contaminated Aquifer. *Journal of Contaminant Hydrology*, 53(3-4): 305–18.

Spence, M.J., Bottrell, S.H., Thornton, S.F., Richnow, H.H. and Spence, K.H. (2005),

Hydrochemical and Isotopic Effects Associated with Petroleum Fuel Biodegradation Pathways in a Chalk Aquifer. *Journal of Contaminant Hydrology*, 79(1-2): 67–88.

Sturman, P.J., Stewart, P.S., Cunningham, A.B., Bouwer, E.J. and Wolfram, J.H. (1995), Engineering Scale-up of in Situ Bioremediation Processes: A Review. *Journal of Contaminant Hydrology*, 19(3): 171–203.

Suni, S., Malinen, E., Kosonen, J., Silvennoinen, H. and Romantschuk, M. (2007), Electrokinetically Enhanced Bioremediation of Creosote-Contaminated Soil: Laboratory and Field Studies. *Journal of Environmental Science and Health. Part A, Toxic/hazardous Substances and Environmental Engineering*, 42(3): 277–87.

Suni, S. and Romantschuk, M. (2004), Mobilisation of Bacteria in Soils by Electro-Osmosis. *FEMS Microbiology Ecology*, 49(1): 51–7.

SuRF-UK (2010), *A Framework for Assessing the Sustainability of Soil and Groundwater Remediation*. London.

SuRF-UK (2011), *Annex 1: The SuRF-UK Inicator Set for Sutainable Remediation Assessment*.

SuRF-UK (2013a), Sustainability Assessment: Shell Terminal Facility, Madeira. *SuRF-UK Bulletin*: 1–9.

SuRF-UK (2013b), Upper Heyford - Remediation Options Appraisal. *SuRF-UK Bulletin*, September: 1–7.

Teerakun, M., Reungsang, A., Lin, C.-J. and Liao, C.-H. (2011), Coupling of Zero Valent Iron and Biobarriers for Remediation of Trichloroethylene in Groundwater. *Journal of Environmental Sciences*, 23(4): 560–567.

Teng, Y., Shen, Y., Luo, Y., Sun, X., Sun, M., Fu, D., Li, Z. and Christie, P. (2011), Influence of Rhizobium Meliloti on Phytoremediation of Polycyclic Aromatic Hydrocarbons by Alfalfa in an Aged Contaminated Soil. *Journal of Hazardous Materials*, 186(2-3): 1271–6.

Thepsithar, P. and Roberts, E.P.L. (2006), Removal of Phenol from Contaminated Kaolin Using Electrokinetically Enhanced in Situ Chemical Oxidation. *Environmental Science and Technology*, 40(19): 6098–6103.

Thevanayagam, S. and Rishindran, T. (1998), Injection of Nutrients and TEAs in Clayey Soils Using Electrokinetics. *Journal of Geotechnical and Geoenvironmental Engineering*, 124(4): 330–338.

Thornton, S.F. and Rivett, M.O. (2008), Monitored Natural Attenuation of Organic Contaminants in Groundwater: Principles and Application. *Proceedings of the ICE - Water Management*, 161(6): 381–392.

Thornton, S.F., Lerner, D.N. and Banwart, S.A. (2001), Assessing the Natural Attenuation of Organic Contaminants in Aquifers Using Plume-Scale Electron and Carbon Balances: Model Development with Analysis of Uncertainty and Parameter Sensitivity. *Journal of Contaminant Hydrology*, 53(3-4): 199–232.

Thornton, S.F., Lerner, D.N. and Tellham, J.H. (1995), *The Technical Aspects of Controlled Waste Management: Laboratory Studies of Landfill Leachate-Triassic Sandstone Interactions*. London.

Thornton, S.F., Quigley, S., Spence, M.J., Banwart, S.A., Bottrell, S. and Lerner, D.N.

(2001), Processes Controlling the Distribution and Natural Attenuation of Dissolved Phenolic Compounds in a Deep Sandstone Aquifer. *Journal of Contaminant Hydrology*, 53(3-4): 233–267.

Thrash, J.C. and Coates, J.D. (2008), Review: Direct and Indirect Electrical Stimulation of Microbial Metabolism. *Environmental Science and Technology*, 42(11): 3921–3931.

Tiehm, A., Augenstein, T., Ilieva, D., Schell, H., Weidlich, C. and Mangold, K.-M. (2010), Bio-Electro-Remediation: Electrokinetic Transport of Nitrate in a Flow-through System for Enhanced Toluene Biodegradation. *Journal of Applied Electrochemistry*, 40(6): 1263–1268.

Tiehm, A., Lohner, S.T. and Augenstein, T. (2009), Effects of Direct Electric Current and Electrode Reactions on Vinyl Chloride Degrading Microorganisms. *Electrochimica Acta*, 54(12): 3453–3459.

US EPA (1994), Methods for Monitoring Pump and Treat Performance. Oklahoma.

US EPA, 1996. Pump-and-Treat Ground-Water Remediation: A Guide for Decision Makers and Practitioners. Washington DC.

US EPA (2008), Incorporating Sustainable Environmental Practices into Remediation of Contaminated Sites Technology Primer Green Remediation : Incorporating Sustainable Environmental Practices into Remediation of Contaminated Sites. Cincinnati.

US EPA (2013), Protecting and Restoring Land: Making a Visible Difference in Communities. OSWER FY13 End of Year Accomplishments Report.

Vane, L.M. and Zang, G.M. (1997), Effect of Aqueous Phase Properties on Clay Particle Zeta Potential and Electro-Osmotic Permeability: Implications for Electro-Kinetic Soil Remediation Processes. *Journal of Hazardous Materials*, 55(1-3): 1–22.

Velasco-Alvarez, N., González, I., Damian-Matsumura, P. and Gutiérrez-Rojas, M. (2011), Enhanced Hexadecane Degradation and Low Biomass Production by Aspergillus Niger Exposed to an Electric Current in a Model System. *Bioresource Technology*, 102(2): 1509–15.

Virkutyte, J., Sillanpää, M. and Latostenmaa, P. (2002), Electrokinetic Soil Remediation — Critical Overview. *Science of the Total Environment*, 289(1-3): 97–121.

Wada, S. and Umegaki, Y. (2001), Major Ion and Electrical Potential Distribution in Soil under Electrokinetic Remediation. *Environmental Science and Technology*, 35(11): 2151–5.

Wang, Q.-Y., Zhou, D.-M., Cang, L. and Sun, T.-R. (2009), Application of Bioassays to Evaluate a Copper Contaminated Soil before and after a Pilot-Scale Electrokinetic Remediation. *Environmental Pollution*, 157(2): 410–6.

Wick, L.Y., Buchholz, F., Fetzer, I., Kleinsteuber, S., Härtig, C., Shi, L., Miltner, A., Harms, H. and Pucci, G.N. (2010), Responses of Soil Microbial Communities to Weak Electric Fields. *The Science of the Total Environment*, 408(20): 4886–93.

Wick, L.Y., Mattle, P.A., Wattiau, P. and Harms, H. (2004), Electrokinetic Transport of PAH-Degrading Bacteria in Model Aquifers and Soil. *Environmental Science and Technology*, 38(17): 4596–4602.

Wick, L.Y. (2009), Coupling Electrokinetics to the Bioremediation of Organic Contaminants: Principles and Fundamental Interactions, 369–387, in: Reddy, K. R. and Cameselle, C. (Eds.), *Electrochemical Remediation Technologies for Polluted Soils, Sediments and Groundwater*. New Jersey: John Wiley & Sons.

Wick, L.Y., Shi, L. and Harms, H. (2007), Electro-Bioremediation of Hydrophobic Organic Soil-Contaminants: A Review of Fundamental Interactions. *Electrochimica Acta*, 52(10): 3441–3448.

Wiedemeier, T.H., Rifai, H.S., Newell, C.J. and Wilson, J.T. (1999), *Natural Attenuation of Fuels and Chlorinated Solvents in the Subsurface*. New York: John Wiley & Sons.

Winderl, C., Schaefer, S. and Lueders, T. (2007), Detection of Anaerobic Toluene and Hydrocarbon Degraders in Contaminated Aquifers Using Benzylsuccinate Synthase (bssA) Genes as a Functional Marker. *Environmental Microbiology*, 9(4): 1035–46.

Wu, M.Z., Reynolds, D.A.., Prommer, H., Fourie, A. and Thomas, D.G. (2012a), Numerical Evaluation of Voltage Gradient Constraints on Electrokinetic Injection of Amendments. *Advances in Water Resources*, 38: 60–69.

Wu, M.Z., Reynolds, D.A., Fourie, A., Prommer, H. and Thomas, D.G. (2012b), Electrokinetic in Situ Oxidation Remediation: Assessment of Parameter Sensitivities and the Influence of Aquifer Heterogeneity on Remediation Efficiency. *Journal of Contaminant Hydrology*, 136-137: 72–85.

Wu, M.Z., Reynolds, D.A., Fourie, A. and Thomas, D.G. (2013), Optimal Field Approaches for Electrokinetic in Situ Oxidation Remediation. *Ground Water Monitoring and Remediation*, 33(1): 62–74.

Wu, X., Alshawabkeh, A.N., Gent, D.B., Larson, S.L. and Davis, J.L. (2007), Lactate Transport in Soil by DC Fields. *Journal of Geotechnical and Geoenvironmental Engineering*, 133(12): 1587–1596.

Wu, X., Gent, D.B., Davis, J.L. and Alshawabkeh, A.N. (2012), Lactate Injection by Electric Currents for Bioremediation of Tetrachloroethylene in Clay. *Electrochimica Acta*, 86: 157–163.

Xu, W., Wang, C., Liu, H., Zhang, Z. and Sun, H. (2010), A Laboratory Feasibility Study on a New Electrokinetic Nutrient Injection Pattern and Bioremediation of Phenanthrene in a Clayey Soil. *Journal of Hazardous Materials*, 184(1-3): 798–804.

Yang, M., Annable, M.D. and Jawitz, J.W. (2015), Back Diffusion from Thin Low Permeability Zones. *Environmental Science and Technology*, 49(1): 415–422.

Yeh, C.-H., Lin, C.-W. and Wu, C.-H. (2010), A Permeable Reactive Barrier for the Bioremediation of BTEX-Contaminated Groundwater: Microbial Community Distribution and Removal Efficiencies. *Journal of Hazardous Materials*, 178(1-3): 74–80.

Yeung, A.T. (2006), Fundamental Aspects of Prolonged Electrokinetic Flows in Kaolinites. *Geomechanics and Geoengineering*, 1(1): 13–25.

Yeung, A.T. and Gu, Y.-Y. (2011), A Review on Techniques to Enhance Electrochemical Remediation of Contaminated Soils. *Journal of Hazardous Materials*, 195: 11–29.

Yuan, S., Zheng, Z., Chen, J. and Lu, X. (2009), Use of Solar Cell in Electrokinetic Remediation of Cadmium-Contaminated Soil. *Journal of Hazardous Materials*, 162(2-3): 1583–1587.

Yuan, Y., Guo, S.-H., Li, F.-M. and Li, T.-T. (2013), Effect of an Electric Field on N-Hexadecane Microbial Degradation in Contaminated Soil. *International Biodeterioration and Biodegradation*, 77: 78–84.

Yukselen-Aksoy, Y. and Kaya, A. (2010), A Study of Factors Affecting on the Zeta Potential of Kaolinite and Quartz Powder. *Environmental Earth Sciences*, 62(4): 697–705.

Zhou, D.-M., Cang, L., Alshawabkeh, A.N., Wang, Y.-J. and Hao, X.-Z. (2006), Pilot-Scale Electrokinetic Treatment of a Cu Contaminated Red Soil. *Chemosphere*, 63(6): 964–71.

Appendix A: Review paper

Document title: Electrokinetic-bioremediation of organic contaminants: A review of processes and environmental applications

A pdf document containing the article is provided on the attached CD, filename: ‘Appendix A – EK-BIO review paper.pdf’.

Appendix B: Conference paper manuscript

Document title: Stimulating *in situ* bioremediation in electron acceptor limited zones by nitrate delivery using electrokinetics in a model scale aquifer

A Microsoft Word document containing the manuscript is provided on the attached CD, filename: ‘Appendix B – AQS paper.docx’.

Appendix C: Research article

Document title: Electrokinetic migration of nitrate through heterogeneous granular porous media

A pdf document containing the article is provided on the attached CD, filename: ‘Appendix C – Chp4 experimental paper.pdf’.

Appendix D: Research article

Document title: Effect of physical heterogeneity on the electromigration of nitrate in layered granular porous media

A pdf document containing the article is provided on the attached CD, filename: ‘Appendix D – Chp5 experimental paper.pdf’.

Appendix E: Research article manuscript (accepted)

Document title: Sustainability assessment of electrokinetic bioremediation compared with alternative remediation options for a petroleum release site

A pdf document containing the article is provided on the attached CD, filename: ‘Appendix E – Chp7 accepted experimental paper manuscript.pdf’.

Appendix F: Chapter 2 - Supporting information

A Microsoft Word document that provides additional information on the electron balance model, filename: ‘Appendix F – Chp2 Supporting information.docx’.

Appendix G: FT experiments

A Microsoft Word document that details the results from initial experiments conducted in an old fish tank (FT), filename: ‘Appendix G – FT experiments.docx’.

Appendix H: Chapter 3 - Raw data

A Microsoft Excel spreadsheet that contains raw data for the preliminary experiments in Chapter 3, filename: ‘Appendix H – Chp3 Raw Data.xls’.

Appendix I: Chapter 4 - Raw data

A Microsoft Excel spreadsheet that contains raw data for the experiments in Chapter 4 and results from the clay surface adhered salts dissolution test, filename: ‘Appendix I – Chp4 Raw Data.xls’.

Appendix J: Chapter 5 - Raw data

A Microsoft Excel spreadsheet that contains raw data for the experiments in Chapter 5, filename: ‘Appendix J – Chp5 Raw Data.xls’.

Appendix K: Chapter 5 - Supporting information

A Microsoft Word document that provides additional information on the electron balance model in Chapter 5, filename: ‘Appendix K – Chp5 Supporting Information.docx’.

Appendix L: Chapter 6 - Raw data

A Microsoft Excel spreadsheet that contains raw data for the experiments in Chapter 6, filename: ‘Appendix L – Chp6 Raw Data.xls’.

Appendix M: Chapter 7 - Supporting information

A Microsoft Word document that provides additional information on:

- Assumptions and methods used to calculate treatment times for the different remediation options (including the electron balance model for the EK-BIO scenario);
- Input values for the different calculations;
- Tier 1 assessment information and weighting justifications;
- Tier 2 assessment information, justifications and MCA scores; and
- Sustainability scenario MCA scores.

Filename: ‘Appendix M – Chp7 Supporting information.docx’.